Chemical Safety of Drinking Water Networks

Mónica Sofia Freitas dos Santos

Dissertation presented to obtain the degree of

DOCTOR IN ENVIRONMENTAL ENGINEERING

by

UNIVERSITY OF PORTO

SUPERVISION

DOCTOR MARIA ARMINDA COSTA ALVES

DOCTOR LUÍS MIGUEL PALMA MADEIRA

PORTO, 2013

I dedicate this thesis to
my parents Aurora and Américo
my brother, Américo

Acknowledgements

I wish to thank the Faculty of Engineering of the University of Porto (FEUP), the Chemical Engineering Department (DEQ) and the Laboratory for Process, Environmental and Energy Engineering (LEPAE) for the facilities that allowed me to conduct the scientific experiments.

I am also grateful to "Fundação para a Ciência e a Tecnologia" (FCT) for my PhD grant (SFRH/BD/61302/2009) and for the financial support through the project Acquasafe (PTDC/AAC-AMB/101687/2008).

I also wish to thank to the European commission within the 7th Framework Programme FP7-SEC-2007-1 - "Security; Increasing the security of Citizen; Water distribution surveillance" for the financial support of the European Research Project SecurEau (http://www.secureau.eu/ – Contract no. 217976).

I would like to express my deep sense of gratitude to my supervisor Professor Arminda Alves and co-supervisor Professor Luís Miguel Madeira for believing in me and for giving me the opportunity to participate in this interesting and challenging work. Thank you for your continuous support and availability, as well as, for the scientific suggestions and recommendations. It has been a great honor and privilege to work and learn with them.

My special thanks to Professor Luís Melo, head of the SecurEau research team in Portugal, for accepting me as member of such great group, for helping me every time I needed and for giving me the opportunity to participate in all SecurEau meetings.

I would like also to thank Professor Lúcia Santos for advising me to the SecurEau project. I have no doubt that I am also writing this thesis today because of her.

My acknowledgement also go to Dr. Gabriela Schaule from the IWW Water Centre (Rheinisch-Westfälisches Institut für Wasserforschung gemeinnützige GmbH – Mülheim an der Ruhr, Germany) for kindly supplying the deposits from drinking water networks.

I wish to thank Syngenta Crop Protection, Lda, particularly Eng. Mónica Teixeira, for supplying Gramoxone.

I am also grateful to *Águas do Douro e Paiva* company (AdDP), specially to Dr. João Vilaça e Engª Rita Reis for supplying the detailed information about drinking water distribution systems of the South Oporto metropolitan area.

My special thanks to Carmen Rodrigues (from FEUP) for being always available for helping me in the respirometry technique and actinometry experiments.

To Cátia Oliveira (from FEUP), with whom I worked during this period, I wish to thank the availability and all dedication.

I am grateful to Dina Martins (from FEUP) for supplying cells of *Pseudomonas fluorescens* and clay for my scientific experiments, as well as, the respective composition/characterization of the materials.

My gratitude is also towards my lab colleagues for the company, friendship and support during these years: José, Vera, Raquel, Leandro, Nuno, Patrícia and Marzieh. I also thank the joy and cheerfulness of our "pitufos": Vera, Rúben, Carina, Sara, Eduardo and Mariana. My special thanks to the technicians Sr. Serafim, Fátima, José Luís, Liliana and Luís Carlos.

Thank you to all my friends for their support, encouragement and for the good times we shared.

I am grateful to my family, especially to my parents and my brother, for their love, patience, endless support and encouragement. Thank you for helping me to build a future that I think is always better. I am indebted to you forever. Special thanks also to Jorge, for his love, friendship, infinite patience and for helping and understanding me during the past few years. Simão, my godson, you are still a child but I would like you to know that your smile cheered me up in the less easy moments and was an inspiration for me. I hope you will be very proud of your godmother.

Preface

This PhD thesis was developed at LEPAE (Laboratory for Process, Environmental and Energy Engineering), in the Chemical Engineering Department of the Faculty of Engineering-University of Porto (DEQ-FEUP), throughout the period between 2009 and 2013 and under the scholarship SFRH/BD/61302/2009 and the European Project SecurEau (FP7-SEC-2007-1, www.secureau.eu).

The main objective of SecurEau project was to limit the impact on the population due to safe water privation in a contamination event and to launch an appropriate response for rapidly restoring the use of the drinking water networks, particularly after a deliberate contamination. For defining a general strategy of rehabilitation of the distribution network after a terrorist attack, SecurEau consortium proposed to work with representative chemical (paraquat, chlorfenvinphos, carbofuran, BDE-100 and mercury), biological (*Bacillus anthracis*, *E. Coli.* O157, *Francisella tularensis*) and radiological (radionuclides such as Co, Sr, Cs, U, Po, Ir and Am) agents and surrogates. The CBRN (Chemical, Biological and Radionuclides) listed above were selected based on several criteria and represent strong candidates to be used in deliberate contamination activities. SecurEau, acting as a demonstration project for designing and implementing an effective and timely response upon a CBRN attack, was built with the aim to address the following points:

1) detection of unexpected changes in water quality which could be in relation with a deliberate contamination event, by applying commercially available or recently developed generic sensors placed throughout the distribution systems;

2) adaptation of known analytical methods to rapidly detect specific CBRN contaminants in water and in biofilms/deposits and to control the cleaning procedures;

3) localization of the point source (s) of contamination and subsequently the contaminated area (*via* modeling reactive transport) allowing delimitation of the corrective actions;

4) implement decontamination procedures of the distribution system including the treatment of water extracted and used for flushing the pipe walls;

5) controlling the efficacy of the corrective actions by analyzing the water bulk and specially the pipe walls and the deposits.

The present work was centered in the second and fourth topics of SecurEau project and two key chemicals: paraquat dichloride (PQ) and a polybrominated diphenyl ether (BDE-100).

The dissertation is organized in nine chapters. The first one (which constitutes Part I) corresponds to a general introduction, including a review on the state of the art of the topics of interest: analytical methods for detection and quantification of the key chemicals in waters and soils (because no studies were found for deposits from drinking water networks); adsorption/desorption studies of such chemicals on solid matrices and degradation technologies for the treatment of waters contaminated with the considered chemicals. The Chapters 2 to 5 and 6 to 7 were organized in Part II (paraquat) and Part III (BDE-100), respectively.

In Chapter 2, three analytical methodologies are described for the quantification of PQ in waters in response to different scenarios: in case of a deliberate contamination event (higher concentrations); for drinking water quality control in accordance with the European Union legislation (lower concentrations), and for PQ confirmation purposes and identification of PQ degradation by-products. All methods were validated and the global uncertainty associated to the results was determined.

The analytical methodology for PQ quantification in deposits from drinking water networks is reported in Chapter 3. The method was validated and its applicability to the quantification of diquat in the same matrix was also tested.

Chapter 4 is mostly addressed to the interaction between PQ and three deposits representative of those found in drinking water networks. The effect of some parameters such as stirring speed, particle size, initial PQ concentration and temperature on the adsorption kinetics was evaluated. Herein, the adsorption isotherms at two different temperatures were also obtained and some desorption experiments were conducted.

The treatment of PQ-contaminated waters by oxidation with Fenton's reagent was examined in the last chapter of Part II (Chapter 5), where a parametric study was carried out to study the effect of some variables on the PQ degradation. A semi-empirical kinetic model is proposed to describe the PQ concentration histories under such a wide range of conditions, and the biodegradability of the final effluent was assessed. Additionally, the PQ degradation performance by the classic Fenton process is compared to the photo-Fenton one.

In Chapter 6 (Part III), a dispersive liquid-liquid microextraction – gas chromatography – mass spectrometry method was developed and validated for BDE-100 identification and quantification in water matrices. The effect of the extraction and dispersive solvents, extraction solvent volume, dispersive solvent volume, extraction time and salt addition on the extraction efficiency was studied. Moreover, the suitability of the developed method for the quantification of other environmental abundant polybrominated diphenyl ethers in waters was evaluated.

Chapter 7 is a preliminary study about degradation of BDE-100 in waters by photolysis and photo-Fenton. Concerning the photolysis process, the degradation efficiency was examined for different UV-Vis light intensities. The applicability of photo-Fenton methodology for the treatment of BDE-100 contaminated waters is a completely new research topic, for which preliminary results were reached by now.

Finally, Chapters 8 and 9 (Part IV) compile the main conclusions and the suggestions for future work, respectively.

Contents

Part II – Paraquat

Part III – BDE-100

Abstract

This work is part of a larger research project – SecurEau – which intended to contribute to the suppression of some gaps related to the restoring of the normal function of a drinking water distribution system after a deliberate contamination event. In particular, this thesis aims to develop appropriate analytical methodologies to quantify and identify chemical contaminants in water and deposits from drinking water networks, to evaluate the sorption and affinity of the chemical contaminants to the walls/deposits/biofilms of the pipelines and to develop cleaning/decontamination techniques able to efficiently remove the threat.

Two chemical compounds, of the five target ones selected by SecurEau consortium, were explored herein: paraquat dichloride (PQ) and a polybrominated diphenyl ether (BDE-100).

In case of a suspicion of contamination, there is an urgent need to identify the specific cause of the threat and the definition of a minimum response time is essential to mitigate the impact of an attack. For PQ, analytical methods in water were developed and validated for screening purposes (to detect high concentrations as those predictable in emergency situations) by direct injection-liquid chromatography-diode array detector (DI-LC-DAD), for trace analyses by solid phase extraction-liquid chromatography-diode array detector (SPE-LC-DAD) and for confirmation purposes and identification of degradation by-products by direct injection-liquid chromatography-mass spectrometry detector (DI-LC-MS). Limits of detection of 10 μg/L, 0.04 μg/L and 20 μg/L were achieved for DI-LC-DAD, SPE-LC-DAD and DI-LC-MS methods, respectively. Moreover, global uncertainties below 13, 11 and 6% were found for the most part of the calibration ranges of the same methods, respectively. Different demands were recognized for BDE-100, whose quantification in water was only accounted for a dispersive liquid-liquid microextraction-gas chromatography-mass spectrometry detector (DLLME-GC-MS) method due to its extremely low water solubility. The same method could be applied for the quantification of other PBDEs (BDEs 28, 47, 85, 99, 153, 154 and 183) in waters with limits of quantification ranging from 2 ng/L (BDE-100) to 113 ng/L (BDE-183). All these methods proved to be suitable for the purpose that they were designed.

Concerning the deposits, one simple and fast analytical methodology was successfully implemented for PQ quantification in this matrix. For such purpose, three deposits representative of those found in drinking water networks were considered: herein called S2 and S3 (iron rich deposits) and S4 (calcium rich deposit). A limit of detection of 0.1 μgPQ/gS3 was obtained for PQ-S3 system with the expanded uncertainty ranging from 10-54% for concentrations between 193 and 5 μgPQ/gS3, respectively. The method proved to be reliable for the quantification of PQ in all of the above mentioned deposits. Additionally, it was demonstrated that this method is also suitable for the screening of diquat in these samples.

The PQ adsorption on those deposits follows a pseudo-second order kinetic model and Langmuir adsorption capacities of 5.7, 11 and 0.40 mg/g were achieved at 20 °C for S2, S3 and S4 deposits, respectively. The adsorption studies indicated that, in case of a contamination event, it is unlikely that PQ would adsorb on such materials, unless there is a stagnancy of the fluid for a very long period of time (closer to batch conditions). However, adsorption of PQ in loose deposits that are transported with the flowing water is much more insidious and cannot be neglected. On the other hand, S2 (brown) and S3 (tubercle) deposits can be used as low-cost adsorbents (often discarded upon pipes cleaning/maintenance operations) for the treatment of PQ-contaminated waters.

Finally, the degradation of both chemicals in water was studied using procedures based on advanced oxidation processes. Complete PQ degradation is reached after 4 h of classic dark Fenton reaction in batch mode (T =30 °C, $[Fe^{2+}]_0$ = 5.0×10^{-4} M, $[H_2O_2]_0$ = 1.6×10^{-2} M, and pH_0 = 3.0, for $[PQ]_0$ = 100 mg/L). Although only 40% of mineralization was recorded after these 4 h of reaction, it was proved that the final effluent is less toxic than the original one. The photo-Fenton process represents an attractive alternative for classic dark Fenton in off-line applications because higher mineralization degrees were reached (96% after 1 h of reaction). Concerning BDE-100, nearly 68% of the initial concentration of this chemical in water was degraded after 5 min of exposition to UV-Vis light ($[BDE\text{-}100]_0$ = 50 μg/L and 1.6×10^{-6} Einstein/s).

Resumo

O presente trabalho enquadra-se no âmbito de um projeto mais abrangente – SecurEau – que pretende contribuir para a supressão de algumas lacunas relacionadas com o restabelecimento do funcionamento normal de um sistema de distribuição de água potável após um episódio de contaminação deliberada. Em particular, esta tese tem como objetivo desenvolver metodologias analíticas apropriadas para a quantificação e identificação de contaminantes químicos em águas e depósitos de uma rede de água potável, avaliar a sorção e afinidade dos contaminantes químicos para as paredes/depósitos/biofilmes das tubagens e desenvolver técnicas de limpeza/descontaminação capazes de remover eficazmente a ameaça.

Esta tese focou-se em dois compostos químicos, dos cinco selecionados pelo grupo SecurEau: dicloreto de paraquato (PQ) e um éter difenílico polibromado (BDE-100).

Em caso de suspeição de contaminação, há uma urgente necessidade de identificar a causa específica da ameaça e a definição de um tempo mínimo de resposta é essencial para atenuar o impacto de um ataque. Para o PQ, desenvolveram-se e validaram-se métodos analíticos em águas para fins de rastreio (para detetar elevadas concentrações como as previstas em situações de emergência) por injeção direta- cromatografia líquida-deteção por arranjo de díodos (DI-LC-DAD), para análises vestigiais por extração em fase sólida-cromatografia líquida-deteção por arranjo de díodos (SPE-LC-DAD) e para fins de confirmação e identificação de sub-produtos de degradação por injeção direta-cromatografia líquida-deteção por espectrometria de massa (DI-LC-MS). Obtiveram-se limites de deteção de 10 μg/L, 0.04 μg/L and 20 μg/L para os métodos DI-LC-DAD, SPE-LC-DAD e DI-LC-MS, respetivamente. Para além disso, encontraram-se incertezas globais abaixo de 13, 11 e 6% para a maior parte da gama de linearidade dos mesmos métodos, respetivamente. Diferentes necessidades foram reconhecidas para o BDE-100, cuja quantificação em água foi apenas assegurada pelo método de microextracção dispersiva líquido-líquido-cromatografia gasosa-deteção por espectrometria de massa devido à sua solubilidade em água ser extremamente baixa. O mesmo método poderá ser aplicado para a quantificação de outros PBDEs (BDEs 28, 47, 85, 99, 153, 154 e 183) em águas com limites de quantificação que variam de 2 ng/L (BDE-100) a 113 ng/L (BDE-183). Todos os métodos provaram ser adequados para o fim a que foram desenvolvidos.

Relativamente aos depósitos, implementou-se uma metodologia analítica simples e rápida para a quantificação de PQ nesta matriz. Para tal, consideraram-se três depósitos representativos dos encontrados em redes de distribuição de água potável: aqui designados por S2 e S3 (depósitos ricos em ferro) e S4 (depósito rico em cálcio). O método provou ser adequado para a quantificação de PQ em todos os depósitos acima mencionados. Adicionalmente, foi demonstrado que o método é também apropriado para a quantificação de diquato nestas amostras.

A adsorção de PQ nestes depósitos segue um modelo cinético de pseudo-segunda ordem e alcançaram-se capacidades de adsorção de Langmuir de 5.7, 11, 0.40 mg/g a 20 °C para os depósitos S2, S3 and S4, respetivamente. Os estudos de adsorção indicaram que, em caso de contaminação, é improvável que o PQ possa adsorver em tais depósitos, a menos que haja uma estagnação do fluído por um longo período de tempo (próximo das condições *batch*). Contudo, a adsorção de PQ nos depósitos que são transportados com a corrente de água é muito mais insidiosa e não pode ser negligenciada. Por outro lado, os depósitos S2 (castanho) e S3 (tubérculo) podem ser usados como adsorventes de baixo custo (frequentemente descartados nas operações de manutenção e limpeza de condutas) para o tratamento de águas contaminadas com PQ.

Finalmente, a degradação de ambos os químicos em água foi estudada usando procedimentos baseados em processos de oxidação avançados. Atingiu-se completa degradação de PQ após 4 h de reação por Fenton clássico em modo *batch* (T =30 °C, $[Fe^{2+}]_0 = 5.0\times10^{-4}$ M, $[H_2O_2]_0 = 1.6\times10^{-2}$ M, e $pH_0 = 3.0$, para $[PQ]_0 = 100$ mg/L). Apesar de serem registados níveis de mineralização de apenas 40% após 4 h de reação, provou-se que o efluente final é menos tóxico que o original. O processo de foto-Fenton constitui uma alternativa atrativa ao Fenton clássico em aplicações *off-line* porque permite alcançar maiores níveis de mineralização (96% após 1 h de reação). No que diz respeito ao BDE-100, aproximadamente 68% da concentração inicial deste químico em água foi degradada após 5 min de exposição à luz UV-Vis (($[BDE\text{-}100]_0$ = 50 μg/L e 1.6×10^{-6} Einstein/s).

Figure captions

Table captions

Nomenclature

Abbreviations

AC – acetone

ACN – acetonitrile

AO – anodic oxidation

API – atmospheric pressure ionization

BFRs – brominated flame retardants

BiFE – bismuth-film electrode

CAC – activated carbon F300

CB – chlorobenzene

CCG – chemically converted graphene

CDPV – cathodic differential pulse voltammetry

CF – chloroform

CFe – classic Fenton

CPE – cloud point extraction

CTC – carbon tetrachloride

CV% – coefficient of variation

CZE-DAD – capillary zone electrophoresis with diode array detector

DAD – diode array detector

DCM – dichloromethane

DI-LC-DAD – direct injection-liquid chromatography-diode array detector

DI-LC-MS – direct injection-liquid chromatography-mass spectrometry detector

DLLME – dispersive liquid-liquid microextraction

DLLME-GC-MS – dispersive liquid-liquid microextraction-gas chromatography-mass spectrometry detector

DNA/CILE – carbon ionic liquid electrode modified by a deoxyribonucleic acid film

DPV – differential pulse voltammetry

DQ – diquat

DWDS – drinking water distribution system

ECD – electron capture detector

EDTA – ethylenediaminetetraacetic acid

EFe – electro-Fenton

EF – enrichment factor

EI – electronic impact ionization

EPS – extracellular polymeric substances

%ER – extraction recovery in percentage

ESI – electrospray ionization

FAP-CPE – carbon paste electrode impregnated with fluoroapatite

FR – flame retardants

GA-MSPD – graphene-assisted matrix solid-phase dispersion

GC – gas chromatography

GC-MS – gas chromatography-mass spectrometry

GE/AuNPs – gold electrode modified with gold nanoparticles

GE/AuNPs/DNA – gold electrode modified with gold nanoparticles and deoxyribonucleic acid

GMX – gramoxone

GPC – gel permeation chromatography

HAP/CPE – carbon paste electrode modified by hydroxyapatite

HFBA – heptafluorobutyric acid

HF-LPME – hollow-fiber liquid phase microextraction

HF-MMLLE – hollow-fiber microporous membrane liquid-liquid extraction

HRGC-HRMS – high resolution gas chromatography and mass spectrometry

HS-SPME – headspace solid-phase microextraction

IDMS – isotope dilution mass spectrometry

ISO – International Organization for Standardization

ISP – ionspray ionization

LC – liquid chromatography

LC-DAD – liquid chromatography-diode array detector

LC-MS – liquid chromatography-mass spectrometry detector

LC-MS-MS – liquid chromatography-tandem mass spectrometry

LC-TSP-MS – liquid chromatography thermospray mass spectrometry

LC-UV – liquid chromatography-ultraviolet detector

LLE – liquid-liquid extraction

LLE-LC-MS/MS – liquid-liquid extraction–liquid chromatography–tandem mass spectrometry

LOD – limit of detection

LOQ – limit of quantification

LR – linearity range

MAE – microwave-assisted extraction

MeOH – methanol

MS –mass spectrometry detector

MSWV – multiple square-wave voltammetry

MTBE – methyl tert-butyl ether

MWCNTs-DHP/CG electrode – glassy carbon electrode modified with multiwalled carbon nanotubes within a dihexadecylhydrogen phosphate film

NCGCE – nafion coated glassy carbon electrode

NCME – nafion/clay modified electrode

NFGCE – nafion film coated glassy carbon electrode

NP-CPE – carbon paste electrode modified with natural phosphate

OPG/CoPc – ordinary pyrolitic graphite electrode modified by cobalt phthalocyanine

OUR – oxygen uptake rate

PBDEs – polybrominated diphenyl ethers

PBDFs – polybrominated dibenzofurans

PCBs – polychlorinated biphenyls

PDMS – polydimethylsiloxane

PEF – photoelectro-Fenton;

PLE – pressurized liquid extraction

PM-β-CD/OH-TSO – permethylated-β-cyclodextrin/hydroxyl-termination silicon oil

POPs – persistent Organic Pollutants

PP – polypropylene

PQ – paraquat dichloride

QA – quaternary ammonium

Rec% – recovery in percentage

RSD% – relative standard deviation

SBSE – stir bar sorptive extraction

SDME – single-drop microextraction

SFOME – solidification of floating organic drop microextraction

SIA – sequential injection analysis

SIM – selected ion-monitoring

SIMS – static secondary ion mass spectrometry

SOM – soil organic matter

SP – solid phase

SPE – solid phase extraction

SPE-LC-DAD – solid phase extraction-liquid chromatography-diode array detector

SRM – selected reaction monitoring

SWV – square-wave voltammetry

TAC – tire-derived adsorbent

TA-IL-DLLME – temperature-assisted–ionic liquid–dispersive liquid-liquid microextraction

TCE – 1,1,2,2-Tetrachloroethane

TD-GC-MS – thermal desorption-gas chromatography-mass spectrometry

THF – tetrahydrofuran

UABE – ultrasound assisted back extraction

UAE – ultrasound-assisted extraction

USAEME – ultrasound-assisted emulsification-microextraction

UV – ultraviolet

WWTP - waste water treatment plant

μECD – micro-cell electron capture detector

μSPE – micro-solid-phase extraction

Notation

K_{oc} – organic carbon-normalized sorption coefficient

$q_{\max}$ – maximum adsorption capacity of Langmuir isotherm (mg/g)

K_L – adsorption equilibrium constant of Langmuir isotherm (L/mg)

MSC – mathematic/model selection criterion

K_f – adsorption equilibrium constant of Freundlich isotherm (mg/g/(mg/L)$^{1/n}$)

n – constant of Freundlich isotherm

A – constant of Temkin isotherm (L/mol)

B – constant of Temkin isotherm (Jg/mol^2)

R – correlation coefficient

T – temperature (K or °C)

Ea – apparent activation energy (kJ/mol)

q_e – paraquat concentration in the solid in the equilibrium(mg/g)

q – paraquat concentration in the solid at time t (mg/g)

t – time (min or h)

k_1 – adsorption kinetic constant of pseudo-first order model (L/g/min)

k_2 – adsorption kinetic constant of pseudo-second order model (L^2/min/g/mg)

Greek symbols

φ – photonic flux (Einstein/s)

PART I. GENERAL INTRODUCTION

1 Introduction

Although our planet is called “blue planet” (once 70% of it is covered with water), only 2% is freshwater for human use, because the major part corresponds to oceans, where the water is too salty to drink and inadequate for many applications. Of the freshwater available on Earth, about 99% is in ice and groundwater (water underground in aquifers). Although groundwater resources exceed salt-free surface water on earth, typically only individual households and small towns may be served sufficiently by groundwater from wells or springs. Large cities tend to use surface water and centralize water treatment and distributions systems. The amount of surface water available to drink is dramatically affected by the seasons, weather patterns and long-term shifts in climate. Additionally, surface water is more likely to suffer anthropogenic contamination than groundwater due to its proximity. Surface, and in some cases groundwater, could be polluted by exposition to acid rain, storm water runoff, sewage overflow, agricultural runoff and industrial waste. Microbial pollution of drinking water has been considered the most threat for human health for many years [1] but there are well established and robust methods for protecting drinking water from that [2]. On the other hand, while the consequences of microbial contamination are quickly and fairly easily identified, chemical contamination is usually much more insidious with effects not seen until the source has been in use for a considerable period, usually many years.

Water plays an important role in our life being imperative to human and ecosystem health and is the base for an economic welfare. Due to the extreme importance of this source, water and particularly drinking water has been often a political or military target [3]. For that also contribute the several points of vulnerability of a water distribution system: the catchment, the raw water transport system, the treatment facilities, the water reservoirs and the distribution systems. In this perspective, Peter H. Gleick reports a lot of situations where water or systems were used as delivery vehicles to cause violence to a human population [4]. A great concern about this issue has been generated and a lot of measures have been taken to limit the impact that these kind of attacks could represent for human life. Protection and surveillance of water infrastructures, the detection of water quality deterioration in drinking water distribution systems and operational procedures for decontamination of water infrastructures are needed to

prevent or to restore quickly the functionality of the distribution system after a deliberate (or accidental) contamination. In this context, and with some experience gained in the past with other related projects, SecurEau, an European project (FP7-SEC-2007-1), entitled “Security and decontamination of drinking water distribution systems following a deliberate contamination”, was established [5]. As mentioned before, the intent of SecurEau was to serve as a demonstration project for designing and implementing an effective and timely response on CBRN (chemical, biological and radionuclide) agents. The work done during the four years of the project duration and now presented in this thesis had the intention to minimize some gaps related to the feasibility of the detection and remediation methods, to quickly detect and eliminate the contamination, especially that originated by emergent chemicals. The work done in this thesis was focused in two chemicals (an herbicide and a flame retardant) among the five ones selected by SecurEau team. Paraquat (herbicide) and BDE-100 (flame retardant) were chosen to be target compounds due to their different physical-chemical characteristics which determine the final effects in consumers as well as in sorption, dispersion and the accumulation patterns in case of a deliberate contamination of drinking water distribution systems. Paraquat is included in the “old” toxicants that may be easily acquired and manipulated, despite of the effective control measures, and BDE-100 represents the “new” ones with lethal effects at extremely low doses.

A state of the art concerning the topics covered during the thesis period is set out below. First, a literature review about analytical methods for identification and quantification of each chemical in water and soils (because no studies were found for deposits from drinking water networks) was made. Indeed, in case of a deliberate or accidental contamination event, appropriate analytical methodologies should be used to rapidly detect and quantify the contaminants in these matrices. Water should be the first matrix of being contaminated but, depending on the affinity of such compounds for the pipe walls, deposits and/or biofilms could also be crucial zones of contaminants accumulation. So, it has to be made sure that the deposits are not long-term reservoirs from which the contaminants leach into the system, possibly with patches release from the surfaces.

Since the adsorption/desorption of the contaminants on deposits from drinking water networks dictates the dispersion and accumulation of them throughout the network, the interaction of the target chemicals on solids was other topic well reviewed (again no

published data was found concerning interactions with pipe deposits). Finally, an overview of the existing degradation methodologies for the treatment of waters contaminated with the target chemicals was performed. Actually, the implementation of efficient cleaning procedures is one of the main goals of this study.

1.1 Paraquat

Paraquat was first synthesized in 1882 [6]. Since 1933, it has been used as redox indicator (under the name methyl viologen) in chemical laboratories [6]. Its herbicidal properties were discovered in 1957 and one year later paraquat was introduced by Imperial Chemical Industries [6]. In 1962, paraquat began to be marketed as a highly effective contact herbicide [6]. Nowadays, this bipyridylium compound is widely used as herbicide around the world (nearly 90 countries), despite of being prohibited in Europe [7]. Its popularity is related to its quick and non-selective action to kill green plant tissue upon contact. Some studies proved that paraquat is one of the few herbicides capable of controlling the growth of weeds that became resistant as a result of over-use of non-selective glyphosate herbicides [8, 9]. Paraquat is denoted as a class I toxicological agent, being considered as possible carcinogenic and mutagenic molecule [10-12]. Its toxicity is associated with the reduction of the bivalent cation (PQ^{2+}) to a free radical ($PQ^{\bullet+}$), which reacts with oxygen to form a superoxide radical ($O_2^{-\bullet}$), hydrogen peroxide (H_2O_2) and hydroxyl radical ($OH^{\bullet}$) [12]. Since the produced radicals are unstable and reactive, they cause lesions in the cellular membrane, protein and DNA [13]. Paraquat is often encountered in cases of poisoning [14-16]. Chronic and acute exposition effects caused by casual ingestion or poisoning with paraquat are well known and have been documented in the literature [17-19]. Some of these studies report respiratory distress [16, 20], neurodegenerative disorder of the nervous system (such as Parkinson's disease) [21, 22] and effects on the kidneys [20].

The uncontrolled and abusive use of paraquat has generated a great concern related to the potential risk that it represents to humans, animals and the environment [23]. For such feelings have contributed the long residence time of paraquat in the environment (it is a non-biodegradable and highly persistent molecule), its elevated toxicity, even at low doses, its large availability and its relatively low cost [10, 11, 24].

The main physical-chemical characteristics of paraquat are indicated in Table 1.1, where it can be seen that this chemical has extremely high water solubility.

Table 1.1. Physical and chemical properties of paraquat[a].

Chemical structure Common Name CAS n.º Molecular formula Molecular weight	Solubility in water at 25 °C (g/L)	Melting point (°C)	Boiling point (°C)	Vapor pressure (mmHg)	Henry's constant (atm. m^3/mol)	Log K_{ow}
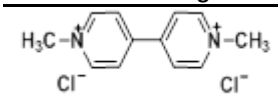 Paraquat 1910-42-5 $C_{12}H_{14}N_2Cl_2$ 257.18 g/moL	620	108.59	351.92	1.01×10^{-7}	3.22×10^{-13}	-4.5

[a]Values were extracted from EPI Suite TM, copyright 2000-2012 Environmental Protection Agency, United States.

This property together with those presented before, such as availability, low cost and high toxicity, support the idea that it could be a strong candidate to be used in a deliberate contamination; that's why it was selected as model compound in SecurEau project. Additionally, this polar herbicide is positively charged, non-volatile, thermally stable and stable in acidic conditions [25]. Paraquat hydrolyzes at pH levels above 12 [26]. Concerning the European Union drinking water legislation, there are no established values specifically for paraquat, but a maximum individual pesticide concentration in drinking water was set at 0.1 μg/L [27].

1.1.1 Analytical methods for paraquat detection and quantification in waters

Due to the intensive use of paraquat and other pesticides on agriculture, and because the interaction between such compounds with soils determines their biological activity, mobility and degradation, the sorption of pesticides on soil has been subject of numerous studies [28-36]. Indeed, the inaccessibility of micropores to microbes, the surface stabilization against desorption of the pesticide and the reduction of aqueous-phase concentrations to levels below those necessary for microbial utilization, compromise the microbial attack of the compounds that are sorbed to inorganic/organic surfaces [37]. In the particular case of paraquat, the interaction with clays, which are the main components of the mineral fraction of soils, and organic matter, is very rapid and strong [34, 38, 39]. In some cases, this non-selective herbicide is inactivated by irreversible

adsorption on clays [40, 41]. Although this fact may induce the conclusion that paraquat could be considered as safe for many agricultural uses, it has been detected in waters. Watercourse contamination may result from a vertical transport through the soil profile promoted by the dissolved colloids such as dissolved organic matter and dispersed colloidal clay [29]. Fernández et al. analyzed water samples from irrigation channels, rivers and lagoons taken from three different marsh areas of the Valencian community (Spain) and a paraquat concentration of 3.95 μg/L was detected [42]. More recently (2006), paraquat concentrations between 1.5 and 18.9 μg/L and 9.3 and 87.0 μg/L were found in ground and surface water of Thailand, respectively [36]. Even at very low doses, this herbicide can pass some treatment steps and reach the water distribution systems, posing a threat to human health. Beyond the natural occurrence of paraquat in drinking water due to its large usage in some countries, its presence may be the result of a deliberate or accidental contamination [43, 44], which is the main focus of this thesis [5]. In those circumstances, the paraquat concentration in water could be very high, partially due to its high solubility in water. Thus, effective analytical methods for paraquat quantification in waters are required.

Paraquat is a cationic compound extremely soluble in water and non-volatile, which makes its analysis rather difficult [45-47]. Many analytical approaches have been proposed for paraquat determination in water matrices: liquid chromatography, gas chromatography, voltammetry, capillary electrophoresis, spectrophotometry and sensors. The number of publications found in the literature about the application of each technique for such purpose is depicted in Figure 1.1.

As shown, the two most used techniques for paraquat quantification in water matrices are liquid chromatography and electrochemical processes, followed by spectrophotometry and capillary electrophoresis. Sensors represent the less popular alternative (5% of the studies). Gas chromatography was not accounted for this list because its applicability is quite difficult under this context, unless an extensive sample preparation and derivatization procedures were programmed before the analysis [48]. Sensors offer some advantages over the conventional chromatographic and electrophoretic based methods, such as lower cost and higher simplicity of use, ability to measure pollutants in complex matrices with minimal sample preparation and possibility of miniaturization and portability, which allows their use as field devices working on-site

[49]. Nevertheless, they are not the preferred technique, as demonstrated by Figure 1.1, which may be due to the higher detection limits attained [50, 51] and the necessity of confirmation methods, even if the contaminant is detected. Although eleven percent of the all studies are related with capillary electrophoresis, the application of this technique combined with ultraviolet (UV), diode array (DAD) or even mass spectrometry (MS) detectors generally leads to limits of detection higher than the EU legislated level (0.1 μg/L) [47].

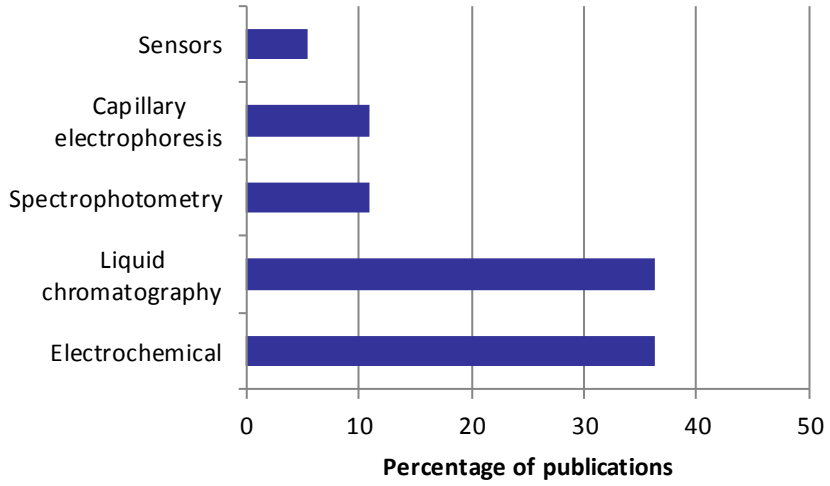

Figure 1.1. Relative contribution of the different analytical methodologies used for paraquat quantification in water matrices (search in data base Scopus, from 1993 to 2013).

On the other hand, capillary electrophoresis suffers from the instability of reagents, interferences, extensive sample treatment and high cost *per* analysis [23, 24]. Spectrophotometry contributes with the same percentage as capillary electrophoretic methods for the overall studies reported in the literature.

The two most popular methodologies (liquid chromatography and voltammetry) are explored in detail below.

1.1.1.1 The particular case of electrochemical methods

Electrochemical methods offer countless advantages in time and cost savings, as well as simplicity. They present many of the requirements for field chemical analysis due to the

speed in the acquisition of the results, portability and good sensitivity [52]. Table 1.2 compiles all developed electrochemical methods for paraquat quantification in waters. Generally, voltammetric analytical techniques are based on processes occurring at Hg based-surfaces because they allow a well-known and defined electrochemical behavior, high hydrogen overpotential, good stability, reproducibility and sensitivity [53, 54]. However, the high toxicity of mercury has triggered the search for safer alternative electrodes [54-56]. In this context, different electrode materials have been used for paraquat quantification in waters such as gold [10, 53, 57-59], platinum [57] and carbon-based composites [23, 53, 57, 60]. Nevertheless, in the last few years, the development of different types of chemically-modified electrodes has been one of the most promising areas [11]. Chemically-modified electrodes are electrodes made of a conducting or semiconducting material, coated or mixed with a chemical modifier by charge-transfer reactions or interfacial contact [11]. The great advantage of using these electrodes is related to their capacity to act as redox mediators, increasing the charge transfer between the electrode and the redox species, thus promoting an improvement in the analytical sensitivity [11]. With this purpose in mind, different compounds have been studied as chemical modifiers in some electrode types. Concerning paraquat analysis in water, different chemically-modified electrodes are listed in Table 1.2., which exhibit similar (1.9 and 3 μg/L) [23, 61] or higher sensitivity (0.1-0.7 μg/L) [12, 20, 24, 62-64] than mercury electrodes (2 and 3 μg/L) [65, 66]. Although some of these modified electrodes have attractive limits of detection, serious interferences from surfactants and humic substances are sometimes reported [24].

Beyond the electrode surface composition, the size of this device is another factor that may influence the sensitivity of the method. Microelectrodes [53, 58, 59] and ultramicroelectrodes [57] proved to provide lower limits of detection (4-20 μg/L) than the others of the same material (20-820 μg/L) [10, 60, 67]. The ultramicroelectrodes promote a significant improvement of the quality of the results by increasing the resolution and the current density and decreasing the resistance effects of the solution [68].

Table 1.2. Studies found in the literature concerning the determination of paraquat in waters by electrochemical methods.

Electrode	**Instrumental technique**	**Analytical parameters**	**Ref**
MWCNTs-DHP/CG electrode (glassy carbon electrode modified by multiwalled carbon nanotubes within a dihexadecylhydrogen phosphate film)	SWV	LR – 9-279 μg/L RSD – 3.5-6.3% LOD – 1.9 μg/L	[61]
DNA/CILE (carbon ionic liquid electrode modified by a deoxyribonucleic acid film)	DPV	LR – 9-13,038 μg/L RSD – 3.8% (reproducibility), 2.0% (repeatability) LOD – 0.7 μg/L Rec – 97-100%	[12]
BiFE (bismuth-film electrode)	DPV	LR – 123-8,940 μg/L RSD – 5.1% (reproducibility), 3.7% (repeatability) LOD – 17 μg/L Rec – 97-105%	[52]
OPG/CoPc (ordinary pyrolitic graphite electrode modified by cobalt phthalocyanine)	SWV	LR – 93-5,420 μg/L RSD – 1.58% (reproducibility), 0.58% (repeatability) LOD – 27 μg/L Rec – 93-119%	[11]
HAP/CPE (carbon paste electrode modified by hydroxyapatite)	SWV	LR – 149-3,725 μg/L RSD – 1.60% LOD – 3 μg/L	[23]
Hanging mercury drop electrode	SWV	LR – 10-250 μg/L RSD – 1.0-8.3% (repeatability) LOD – 2.0 μg/L	[65]
Au-ME (gold micro-electrode)	MSWV	LR – 93-1,937 μg/L RSD – 1.8% for peak 1 and 2.0% for peak 2 (reproducibility), 1.2% for peak 1 and 1.98% for peak 2 (repeatability) LOD – 0.044 μg/L (peak 1); 0.146 μg/L (peak 2) Rec – 79-99%	[58]
Gold and carbon fiber microelectrodes	SWV	RSD – 1.20% (peak 1) and 1.70% (peak 2) LOD – 4.51 μg/L (peak 1); 9.82 μg/L (peak 2) Rec – 89.5-95.0% (peak 1); 91.0-95.0% (peak 2)	[53]

Table 1.2. Studies found in the literature concerning the determination of paraquat in waters by electrochemical methods (continued).

Electrode	Instrumental technique	Analytical parameters	Ref
Gold microelectrodes	SWV	LR – 186-30,919 μg/L RSD – 1.70% for peak 1 and 1.20% for peak 2 (reproducibility), 1.60% for peak 1 and 1.20% for peak 2 (repeatability) LOD – 4.51 μg/L (peak 1) Rec – 89.5-95.0% (peak 1)	[59]
Gold electrodes	SWV	RSD – 2% LOD – 21 μg/L (pure water); 76.4 μg/L (polluted water) Rec – 90.5% (pure water); 101.0% (polluted water)	[10]
NCGCE (Nafion coated glassy carbon electrode)	DPV	LR – up to 12 μg/L RSD – 2.2% LOD – 0.7 μg/L Rec – 94-106%	[24]
Pt, Au or carbon fiber ultramicroelectrodes	SWV	LR – 800-30,919 μg/L LOD – 3.9 μg/L (Pt); 6.2 μg/L (Au); 20.3 μg/L (carbon)	[57]
NCME (Nafion/clay modified electrode)	SWV	LR – up to 80 μg/L RSD – 1-3% LOD – 0.5 μg/L Rec – 98.3%	[62]
Glassy carbon electrode	SWV and DPV	LR – 1000-8000 μg/L LOD – 820 μg/L (DPV); 820 μg/L (SWV) Rec – 96%	[60]
Mercury electrode	SWV	LR – 9-1,860 μg/L LOD – 3 μg/L	[66]
NP-CPE (carbon paste electrode modified with natural phosphate)	SWV	LR –4-559 μg/L RSD – 2% LOD – 0.1 μg/L	[20]
Gold electrode	SWV and DPV	LR – up to 2×10^5 μg/L (DPV), up to 2×10^4 μg/L (SWV) LOD – 261 μg/L (DPV), 186 μg/L (SWV)	[67]

Table 1.2. Studies found in the literature concerning the determination of paraquat in waters by electrochemical methods (continued).

Electrode	Instrumental technique	Analytical parameters	Ref
GE/AuNPs (gold electrode modified with gold nanoparticles)	SWV and DPV	LR – up to 2×10^5 μg/L (DPV), up to 6×10^4 μg/L (SWV) LOD – 279 μg/L (DPV), 428 μg/L (SWV)	[67]
GE/AuNPs/DNA (gold electrode modified with gold nanoparticles and deoxyribonucleic acid)	SWV and DPV	LR – up to 2×10^5 μg/L (DPV), up to 6×10^4 μg/L (SWV) LOD – 242 μg/L (DPV), 354 μg/L (SWV)	[67]
FAP-CPE (carbon paste electrode impregnated with fluoroapatite)	SWV	LR – 9-1×10^4 μg/L RSD – 1.4% (peak 1), 1.8% (peak 2) LOD – 0.6 μg/L (paek 1), 1.4 μg/L (peak 2)	[63]
NFGCE (nafion film coated glassy carbon electrode)	CDPV	LR – 1-100 μg/L LOD – 0.5 μg/L Rec – 101%	[64]

Notes: CDPV – cathodic differential pulse voltammetry; DPV – differential pulse voltammetry; LOD – limit of detection; LR – linearity range; Rec – Recovery; RSD – relative standard deviation; SWV – square wave voltammetry.

Concerning the voltammetric techniques implemented for the paraquat quantification in water matrices, differential pulse (DPV) and square wave voltammetry (SWV) are the most applied but, the need to obtain lower detection limits, justifies the use of an extremely sensitive electroanalytical methodology named multiple square-wave voltammetry (MSWV) [58]. The MSWV is a multipulse technique whose perturbation mode is similar to the SWV [69-72], but with the difference that onto each step of the staircase it can be applied more than one pair of potential pulses of opposing sign [73-75]. The response obtained by MSWV is produced in few seconds and it allows the improvement of the analytical sensitivity to about 2-3 orders of magnitude (related to SWV), even in complex samples [58, 75-78].

The automation of SWV by flow methods, proposed for the first time by Simões and co-workers [79], is an interesting option since improves the sensitivity and reproducibility of the analysis, as a consequence of the highly controllable conditions of mass transport provided by the flowing solutions [65]. Sequential injection analysis (SIA) introduced by dos Santos et al. for quantification of paraquat in natural waters, has advantages over the flow methods [65]. By in-line dilution of a single standard stock solution, as well as sample conditioning before the measuring step, SIA facilitates the automation for construction of calibration and standard addition curves [65, 80, 81].

1.1.1.2 The particular case of liquid chromatography methods

All analytical methods found in the literature about paraquat quantification in waters by liquid chromatography are compiled in Table 1.3. As can be seen, direct determination of paraquat by liquid chromatography leads to limits of detection ranging from 5 to 2000 μg/L and above the EU legislated value (0.1 μg/L) [46-48, 82-84]. Typically, liquid chromatography (LC) requires an enrichment and isolation procedure of paraquat prior to its determination, if compliance with the legislation is a priority issue [25]. Liquid-liquid extraction (LLE) is not suitable for preconcentration of this herbicide because it is highly soluble in water [85]. Solid phase extraction (SPE) is the most widely used preconcentration procedure for such purpose and because of that, alternative extraction methodologies were excluded from this review.

Table 1.3. Studies found in the literature concerning the determination of paraquat in waters by liquid chromatography.

Analytical method	Sample volume	Extraction/Treatment	Mass Detector	Analytical parameters	Ref.
LC-UV		----------	----------	LR – 4-100 mg/L LOD – 2 mg/L	[82]
Off-line SPE-LC-UV	250 mL	Addition of humic acids (20 mg/L), lauryl sulphate (300 μg/L), NaCl (100 mg/L) and phenols (4 μg/L) to distilled water Off-line SPE Column – silica; Conditioning – 0.5 M H_2SO_4,H_2O, 2% (v/v) ammonium hydroxide; Load – 250 mL; Elution – 5 mL A:B (10:90, v/v) (A: MeOH and B: 2 g tetramethylammonium hydroxide +30 g ammonium sulphate in 1 L H_2O, pH 3)	----------	RSD – 4.3-10.4% LOD – 0.08 μg/L Rec – 85-91%	[25]
	25 mL	Off-line SPE Column – silica; Conditioning – 0.5 M H_2SO_4 (2.5 mL), H_2O (5 mL), 2% (v,v) ammonium hydroxide (2.5 mL), H_2O (5 mL); Load – 25 mL sample at 4 mL/min; Elution – 2.5 mL of 0.1 M sodium sulphate solution in water: MeOH (1:1, v/v) at pH 2	----------	RSD – 6-11% LOD – 0.06 μg/L Rec – 95-98%	[86]
	250 mL	adjust pH of the H_2O to 9 Off-line SPE Column – silica; Load – 250 mL sample at 3-5 mL/min; Elution – 2 mL of 8% MeOH in 6.0 M HCl	----------	LOD – 0.4 μg/L Rec – 80%	[85]
	250 mL	adjust pH of the H_2O to 9 Off-line SPE Column – porous graphitic carbon; Conditioning – MeOH (2 mL), H_2O (2 mL); Load – 250 mL sample at 2-3 mL/min; Elution – 2 mL trifluoroacetic acid:acetonitrile (2:8, v/v)	----------	RSD – 4-10% LOD – 0.2 μg/L Rec – 88%	[85]

Table 1.3. Studies found in the literature concerning the determination of paraquat in waters by liquid chromatography (continued).

Analytical method	Sample volume	Extraction/Treatment	Mass Detector	Analytical parameters	Ref.
Off-line SPE-LC-UV	1000 mL	Off-line SPE Column – ultra quat SPE; Conditioning – ACN (4 mL), H_2O (4 mL); Load – 1000 mL sample at 20-25 mL/min; Elution – 2 mL + 2×2 mL of a 0.1% H_3PO_4 aqueous solution	----------	RSD – 5% LOD – 0.006 μg/L Rec – 97%	[87]
	1000 mL	Off-line SPE Column – silica; Conditioning – H_2O (5 mL), concentrated ammonium hydroxide in H_2O (2.5 mL), H_2O (5 mL); Load – 1000 mL; Elution – 1 mL of a mixture of A:B (90:10, v/v) (A: 1 g tetramethylammonium hydroxide +15 g ammonium sulphate in 1 L H_2O, pH 3 and B: MeOH)	----------	LR – 0.1-25 μg/L LOD – 0.025 μg/L Rec – 91%	[88]
Off-line SPE-LC-DAD	250 mL	adjust pH of the H_2O to 9 Off-line SPE Column – C_8; Conditioning – H_2O (5 mL), MeOH (5 mL), H_2O (5 mL), solution A (5 mL), H_2O (5 mL), MeOH (5 mL), H_2O (5 mL), solution B (20 mL); Load – 250 mL sample at 3-6 mL/min; Elution – 4.5 mL of solution C (solution A – 0.5 g of acetyl trimethyl ammonium bromide and 5 mL of concentrated ammonium hydroxide in 1 L H_2O; solution B – 10 g of 1-hexanesulfonic acid, sodium salt and 10 mL of concentrated ammonium hydroxide in 500 mL H_2O; solution C – 13.5 mL of orthophosphoric acid and 10.3 mL of diethylamine in 1 L H_2O.)	----------	RSD – 5% LOD – 0.68 μg/L Rec – 91%	[89]

Table 1.3. Studies found in the literature concerning the determination of paraquat in waters by liquid chromatography (continued).

Analytical method	Sample volume	Extraction/Treatment	Mass Detector	Analytical parameters	Ref.
On-line SPE-LC-UV	50 mL	On-line SPE Column – silica; Load – 50 mL; Elution – linear gradient from 100-50% A in 15 min and maintained for 10 min (A: 2 g tetramethylammonium hydroxide +30 g ammonium sulphate in 1 L H_2O, pH 3 and B: MeOH)	----------	RSD – 1.8-8.0% LOD – 0.1 μg/L Rec – 25-103%	[90]
	50 mL	On-line SPE Column – graphitized carbon black; Conditioning – 5 mL MeOH, 5 mL H_2O; Load – 50 mL at 2.5 mL/min; Elution – linear gradient from 90-20% A in 15 min and maintained for 5 min (A: 1 g tetramethylammonium hydroxide +15 g ammonium sulphate in 1 L H_2O, pH 3 and B: MeOH)	----------	LOD – 0.04 μg/L Rec – 94-98%	[91]
LC-MS	----------	----------	ESI/ion trap	LOD – 25 μg/L	[83]
		Addition of 0.1 M nonafluoropentanoic acid to H_2O	ESI/single quadrupole	RSD – 2.1% (repeatability), 7.4% (reproducibility) LOD – 0.1 μg/L Rec – 105%	[92]
		----------	ESI/single quadrupole	LOD – 11 μg/L	[46]
		----------	ESI/Ion trap	LOD – 7 μg/L	[84]

Table 1.3. Studies found in the literature concerning the determination of paraquat in waters by liquid chromatography (continued).

Analytical method	Sample volume	Extraction/Treatment	Mass Detector	Analytical parameters	Ref.
Off-line SPE-LC-MS	200 mL	Off-line SPE Column – resin; Conditioning – H_2O (5 mL), MeOH (5 mL), H_2O (5 mL); Load – 200 mL at 3 mL/min; Elution – 5 mL of 1 M ammonium chloride solution in MeOH:H_2O (50:50, v/v)	ESI/IDMS	LR – 10-1000 μg/L RSD – 3% LOD – 0.2 μg/L Rec – 98%	[93]
	250 mL	Off-line SPE Column – silica; Load – 250 mL sample pH 9 at 2-3 mL/min; Elution – 2 mL of 6 M HCl in 8% MeOH	API/single quadrupole	RSD – 7.4-13.5% LOD – 1.8-3.8 μg/L Rec – 91.6%	[94]
	250 mL	Off-line SPE Column – silica; Load – 250 mL sample pH 9 at 2-3 mL/min; Elution – 2 mL of 6 M HCl in 8% MeOH	ESI/single quadrupole	RSD – 6.5-9.4% LOD – 4.7-11.0 μg/L Rec –89.1%	[94]
	250 mL	Off-line SPE Column – silica; Load – 250 mL sample pH 9 at 3-4 mL/min; Elution – 5 mL of 6 M HCl :MeOH (9:1, v/v)	ESI/single quadrupole	RSD – 5.9% LOD – 0.40 μg/L Rec – 92.8%	[95]
	500 mL	Addition of 3 mL MeOH to 500 mL H_2O Off-line SPE Column – ENVI-8 DSK; Conditioning – MeOH (10 mL); Load – 500 mL sample; Elution – 5 M trifluoroacetic acid (2×6 mL)	ESI/IDMS	RSD – 12% LOD – 0.2 μg/L Rec – 46-85%	[96]
On-line SPE-LC-MS	25 mL	Addition of 1.6×10^{-3} M of surfactant to H_2O On-line SPE Column – alumina; Conditioning – 25 mL solution containing 16 mg of sodium dodecyl sulfate; Load – 50 mL sample at 2.5 mL/min; Elution – 0.1 M HFBA in MeOH at 2.5 mL/min	ESI/ion trap	RSD – 4-10% LOD – 0.020-0.030 μg/L Rec – 93-104%	[97]

Table 1.3. Studies found in the literature concerning the determination of paraquat in waters by liquid chromatography (continued).

Analytical method	Sample volume	Extraction/Treatment	Mass Detector	Analytical parameters	Ref.
On-line SPE-LC-MS	50 mL	Add HFBA to obtain a 15 mM solution Adjust pH of the H_2O to 9 On-line SPE Column – C_8; Conditioning – MeOH (10 mL); Load – 50 mL sample at 2 mL/min; Elution — linear gradient from 12-40% B in 7 min and stepwise elution from 40-60% B. (A: 15 mM HFBA solution, pH 3.3; B: ACN)	ESI/single quadrupole	RSD – 6-14% LOD – 0.06 μg/L Rec – 87%	[46]
	50 mL	Add HFBA to obtain a 15 mM solution Adjust pH of the H_2O to 9 On-line SPE Column – C_8; Conditioning – MeOH (10 mL); Load – 50 mL sample at 2 mL/min; Elution — linear gradient from 12-40% B in 7 min and stepwise elution from 40-60% B. (A: 15 mM HFBA solution, pH 3.3; B: ACN)	ESI/ion trap	RSD – 7-13% LOD – 0.05 μg/L Rec – 112%	[84]
LC-MS-MS	----------	----------	ESI/ion trap	LOD – 5 μg/L	[83]
		----------	ISP/triple quadrupole	RSD – <10% LOD – 5 μg/L Rec – 90-110%	[48]
		----------	Turbo ionspay™/triple quadrupole	RSD – 7% (SRM) LOD – 7 μg/L (SIM), 0.2 μg/L (SRM)	[47]
		----------	Z-spray/time-of-flight	RSD – 7% (SRM) LOD – 8.6 μg/L	[47]

Table 1.3. Studies found in the literature concerning the determination of paraquat in waters by liquid chromatography (continued).

Analytical method	Sample volume	Extraction/Treatment	Mass Detector	Analytical parameters	Ref.
On-line SPE-LC-MS-MS	10 mL	On-line SPE Column – Hysphere-Resin GP (polydivinylbenzene); Load – 10 mL at 150 μL/min; Elution – linear gradient from 7-15% B and a stepwise to 60% B (A: 20 mM HFBA in H_2O, pH 2.0 and B: 20 mM HFBA in ACN)	ESI/ion trap	RSD – 7.9% (repeatability); 10.1 (reproducibility) LOD – 0.03 μg/L Rec – 90%	[83]
	30 mL	Add HFBA to obtain a 20 mM solution Adjust pH of the H_2O to 9 On-line SPE Column – polydivinylbenzene; Conditioning – MeOH (10 mL), H_2O (10 mL), 20 mM HFBA in H_2O (10 mL); Load – 30 mL sample at 2 mL/min; Elution — isocratic step of 2 min at 10% B, a linear gradient from 10-40% in 7.5 min, an isocratic step of 4 min at 40% and a stepwise elution from 40-70% in 11.5 min (A: 20 mM HFBA aqueous solution in 100 mM formic acid/ammonium formate buffer, pH 3.3; B: ACN)	Turbo ionspay™/triple quadrupole	RSD – 7% (SRM) LOD – 0.04 μg/L (SIM), 0.002 μg/L (SRM)	[47]
			Z-spray/time-of-flight	RSD – 8% (SRM) LOD – 0.02 μg/L	[47]

Notes: API – atmospheric pressure ionization; DAD – diode array detection; ESI – electrospray ionization; IDMS – isotope dilution mass spectrometry; ISP – ionspray ionization; LC – liquid chromatography; LOD – limit of detection; LR – linearity range; MS – mass spectrometry detection; MS-MS – tandem mass spectrometry detection; Rec – Recovery; RSD – relative standard deviation; SPE – solid phase extraction; UV – ultraviolet detection.

The most used packing materials for SPE extraction of paraquat contaminated water samples are: silica [25, 85, 86, 88, 90, 94, 95], cation-exchange resins [47, 83, 93] and apolar phases such as C_8 [46, 84, 89, 96] and graphitized carbon black [85, 91]. During the extraction procedure by SPE, competitive interaction processes occur between the target analyte and the active sites on the solid phase or the components of the sample matrix [88]. For the particular case of paraquat quantification in waters, the efficiency of the preconcentration SPE procedure can be significantly affected, among other factors, by the dissolved organic matter (as humic substances) and surfactants present in water samples [88]. The dissolved organic matter is composed by humic substances (50%) and small molecules (50%), such as carboxylic acids, amino acids, carbohydrates and other trace elements [88]. Indeed, paraquat, with its divalent cationic character can react with two negatively charged sites of humic substances, which are the most abundant components in non-living organic materials of aquatic environments [88]. Cationic, anionic, zwitterionic and non-ionic surfactants can also be found in water as ubiquitous pollutants [88]. Beyond the surfactants and humic acids, it has been also observed that the presence of other contaminants in the water matrix (such as inorganic salts, phenols, polycyclic aromatic hydrocarbons, other pesticides or related compounds) may compromise the analysis performance, significantly diminishing the recovery efficacy or significantly interfering in the posterior determination [25]. Ibánez and co-workers (1996), demonstrated that both humic substances and surfactants have a negative influence in the extraction procedure of paraquat from waters, except cationic surfactants that maintain, or even improve, the extraction efficiency [88]. This behaviour has been attributed to their displacement capacity, avoiding the bound of pesticides with other molecules [25]. In 1998, the same authors proved that cationic surfactants have the ability to eliminate interferences associated with a diminution in the efficacy of SPE [25]. Recovery percentages above 80% were achieved when waters with high levels of humic acids and anionic surfactants were extracted by SPE in a silica cartridge [25]. The presence of other organic compounds in water samples did not also affect the paraquat extraction efficiency [25].

Solid phase extraction can be operated in on-line or off-line mode. Under on-line configuration, the concentrated analyte is directly desorbed and transferred to the analytical column at the same time it is separated [90]. On-line coupling to LC has many

advantages over off-line SPE configuration: lower risk of sample contamination; elimination of analyte losses by evaporation or by degradation during sample preconcentration; lower solvent consumption requirements (thereby decreasing the cost for organic solvents waste disposal); higher sensitivity due to the transfer and analysis of the totality of the extracted species to the analytical system; and improvement of precision and accuracy [49]. On the other hand, using off-line SPE mode, the limits of detection ranging between 0.06 and 11 μg/L [25, 85, 86, 89, 93-96], except for two studies where lower limits of detection are reported (0.006 and 0.025 μg/L) [87, 88]. However, such lower limits of detection were achieved by using 1000 mL of sample, which may be a limiting factor in the choice of the method. On-line coupling SPE to LC can be performed by commercially available devices [90] and led to limits of detection ranging from 0.02 to 0.1 μg/L of PQ, using only up to 50 mL of sample [46, 47, 83, 84, 90, 91, 97].

The chromatographic separation of paraquat is frequently achieved by ion-pairing reagents, which improve the paraquat affinity to some column stationary phases, once applied to the mobile phase. Since non-volatile ion-pairing reagents are typically employed in chromatographic conditions of LC-UV methods, the development of a LC-MS method from the existing one may be not possible [92]. The utilization of conventional non-volatile ion-pairing reagents in LC-MS systems may contribute to the contamination of the interface by alkylsulfonate salts [92].

Mass spectrometry based methods offer superior sensitivity, mass specific data and allow the use of isotopically labelled surrogates [93]. The use of isotopically labelled surrogates as reference masses allows a closely monitoring and compensation for any errors during the analysis [47, 98]. Even so, the use of LC-MS as confirmatory tool is not always possible due to the low mass resolution of some mass analysers (quadrupole and ion-trap) in single MS mode and due to the lack of structural information provided by the atmospheric pressure ionization techniques [47, 83]. For this reason, selected reaction monitoring (SRM) performed on triple quadrupole has gained advantage over other tools [83]. The presence of the target analyte can be confirmed by time-of-flight mass analyser in a single MS mode because it has high selectivity and mass accuracy [47, 99].

To overcome some ambiguity problems, tandem mass spectrometry is often applied; however, this is only possible at low concentration levels when the MS-MS spectrum of the target compounds has more than one abundant product ion [47].

In sum, electrochemical methods benefit from the possibility of working on-site, conferred by the simplicity and portability of the equipment, and offer relatively good sensitivities when traditional electrodes, as mercury ones, are used (2-3 μg/L). However, a great investment must be done to reach limits of detection comparable to that offered by liquid chromatography methodologies (0.006-0.1 μg/L using SPE prior to analysis): investment in specific electrodes such as the chemical modified ones, small size devices (microelectrodes and ultramicroelectrodes) and in extremely sensitive electroanalytical methodologies (as MSWV). Taking all these points in consideration and, once the laboratory is provided with equipment like LC-DAD and LC-MS, it was decided to use liquid chromatography methods for the development of analytical methodologies for the identification and quantification of PQ in water matrices and in different scenarios (Chapter 2).

1.1.2 Analytical methods for paraquat quantification in deposits from drinking water networks

Other important matrices susceptible of being contaminated by a deliberate or accidental chemical contamination front are the surfaces of the pipelines and/or the deposits/biofilms formed along them, as well as those in suspension. Hence, it is of crucial importance to develop analytical methodologies able to determine the amount of chemicals in deposits/biofilms. Concerning biofilms, it was not possible to accomplish this task because difficulty was encountered on the achievement of sufficient amounts of biofilm to perform the experiments. So, methods were only developed for deposits (mainly inorganic materials).

The definition of the best analytical methodology to extract paraquat from deposits has to account the main properties of such materials. The formation and the composition of deposits is dependent of several factors as the age of the pipeline, fluid dynamics, temperature, water contents (particularly dissolved solids and organic contents), water characteristics, the chemical composition of the pipes and joints and the treatments applied to the water supply.

1.1.2.1 Characterization of deposits from drinking water distribution systems

Presently water distribution pipelines are made of materials that may be classified in three groups:

(1) Metallic pipes, as cast iron, steel and galvanized-iron pipes – are alloys of iron, carbon, and silicon, contain carbon as graphite (pure carbon), as iron carbide (Fe_3C) in cementite, or as solid solution in austenite (γ phase iron) [100].

(2) Cement pipes, as cement and concrete pipes – are constituted by lime, silica and alumina, aggregated in complex compounds. Their basic composition is tricalcium silicate ($3CaO.SiO_2$ – 50% wt.); dicalcium silicate ($2CaO.SiO_2$ – 25% wt.), tricalcium aluminate ($3CaO.Al_2O_3$ – 10% wt.), tetracalcium aluminoferrite ($4CaO.Al_2O_3.Fe_2O_3$ – 5% wt.) [101].

(3) Plastic pipes, such as PVC and low-density polyethylene pipes – have different compositions. PVC, polyvinyl chloride, is a thermoplastic polymer constructed of repeating vinyl groups having one hydrogen replaced by chloride and unlike most of other plastics it contains about 56.8% (wt.%) of chlorine [102]. Polyethylene is also a thermoplastic polymer consisting of long chains produced by combining the monomer ethylene. High density polyethylene (HDPE) has an average density of 0.940-0.970 g/cm^3 and a melting temperature of 128-136 ^oC [103].

Águas do Douro e Paiva (AdDP) is a private company which is responsible for the distribution of the treated water to the local public drinking water facilities in South Oporto metropolitan area. This company integrates three subsystems of distribution: *Lever Norte*, *Lever Sul* and V*ale do Sousa e Baixo Tâmega*. The number of pipelines, the length of the distribution systems, as well as the materials which compose them, are summarized in Table 1.4. As indicated in Table 1.4, concrete pipelines only exist in the Lever Norte subsystem. The pipelines made of this material were built in the 70s of the last century and are at the end of its life cycle. All the other pipelines (including the ones of the other subsystems) were built in the last 15 years. It is evident that the material most used for pipeline construction is the cast iron (93% of the all 489 Km of length). Lower contributions were registered for the other two materials: steel (5%) and concrete

(2%). However it is important to highlight that the water networks that deliver water from local public drinking water facilities to the intended end point or user may be substantially different. However it is important to highlight that the water networks that deliver water from local public drinking water facilities to the intended end point or user may be substantially different.

Table 1.4. Constitution of the water supply network of the South Oporto metropolitan area, Portugal (information supplied by AdDP)

Subsystem	Municipalities	Materials	Number of pipelines	Pipeline length (m)
Lever Norte	Porto, Matosinhos, Gondomar, Valongo, Maia and Paredes oeste	Steel	1	5,383
		Concrete	3	12,106
		Cast iron	17	113,557
Lever Sul	Vila Nova de Gaia, Santa Maria da Feira, Espinho, Ovar, São João da Madeira, Oliveira de Azeméis, Arouca and Vale de Cambra norte	Steel	3	18,100
		Cast iron	30	148,757
Vale do Sousa e Baixo Tâmega	Castelo de Paiva, Cinfães, Paredes este, Lousada, Felgueiras, Paços de Ferreira, Amarante oeste and Baião	Cast iron	40	191,399

Echeverría et al. analyzed deposit samples from several sites of the three major subsystems of the Medellin city (Colombia) [104], where the pipelines were composed by reinforced concrete (about 54%), ductile iron (about 27%) and steel (10%). They found three predominant deposits across the water distribution systems that were classified in three categories: brown, tubercle and white deposits.

According to these authors, brown deposits, formed everywhere in the studied system, are mainly composed by aluminosilicates and humic acids. Tubercle deposits, which are mostly mixtures of magnetite (Fe_3O_4), goethite (α-FeO(OH)) and in some cases lepidocrocite (γ-FeO(OH)), are formed on metallic pipelines (steel and ductile iron). White deposits were less abundant since they were found only at some places and are formed by calcite, aluminosilicates and quartz [104].

Despite of the large heterogeneity of deposits formed along drinking water networks, due to the different conditions experienced during their growth, deposits with similar constitution have been reported in other studies [104]. Indeed, deposits with similar

characteristics to tubercle and brown deposits (so that may be categorized according to this nomenclature) were found around the world, namely in: old galvanized steel pipes from Champaign (Illinois, USA) [105]; old cast iron pipes from Boston (Massachusetts, USA) [105]; old cast iron pipes from midwest, west and northeast of USA [106]; cast iron and polyethylene pipes from 16 towns of Finland (EU) [107]; old cast iron, ductile iron and asbestos cement pipes from east central of New Jersey (USA) [108]; cast iron pipes from Ulhasnagar (Maharashtra, India) [109] and on cast iron, galvanized steel and ductile iron pilot-scale pipes [110]. Therefore, it is assumed that deposits from drinking water networks may be classified in accordance with the three categories proposed by Echeverría and co-workers [104].

In sum, it can be concluded that the analytical method to be developed for the detection of paraquat on deposits will have to deal with the problem of a great heterogeneity of the matrix of interest (containing iron oxides, aluminum silicate hydroxides, calcium salts and hydroxides, etc).

Up to the author's knowledge, no studies exist in the literature about quantification of paraquat, or even other chemicals, in deposits from drinking water networks. Due to the lack of information concerning this topic, it was decided to check which methodologies have been implemented for paraquat determination in soils and to use some strategies as starting points for the development of the new methodology in deposit samples. Even for soil samples, a relatively low number of studies was found in the literature (Table 1.5). Indeed, the analysis of paraquat in soils is a challenging task as a result of the strong affinity of this herbicide to them [93, 111]. As evidenced in Table 1.5, procedures involving refluxing or digestion of the sample (in sulfuric or hydrochloric acids, or even under milder solvents such as in an acidified mixture of MeOH/EDTA) are the ones most reported for extraction of paraquat from soils [29, 30, 33, 112-115]. Such drastic extraction conditions with strong acids induce the releasing of chemicals by matrix structure destruction [33]. This extraction step is required due to the strong interaction between paraquat and soils, as referred before. Although digestion and refluxing extraction techniques do not demand sophisticated equipment, they demand time (taken hours), large solvent quantities (25-100 mL) and high sample amounts (5-100 g) [29, 30, 33, 112, 113, 115].

Table 1.5. Studies found in the literature concerning the analytical methods for paraquat quantification in soils.

Sample amount	Extraction/treatment	Clean-up	Instrumental technique	Analytical parameters	Year	Ref
10 g	Reflux with 18 N H_2SO_4; 5 h	SP – Dowex 50 W-X8 (H^+ form) Eluent – Saturated ammonium chloride solution	Spectrophotometry	----------	1967	[33]
100 g	Reflux with H_2SO_4	SP – Dowex 50-X8 (Na^+ form) Eluent – Ammonium chloride solution	Spectrophotometry	LR – 2.98-6.25 μg/g Rec – 95%	1988	[112]
10 g	freeze-dried; extracted with DCM	----------	LC-TSP-MS	LOD – 0.17 μg/g	1993	[116]
10 g	Digestion with 6 M HCl; adjust to pH 9	SP – Adsorbex silica cartridges (400 mg) Eluent – 0.1 M HCl in MeOH	CZE-DAD	RSD – 4% LOD – 0.008 μg/g Rec – 92%	1996	[114]
5 mg	----------	----------	SIMS	LOD – 6 μg/g	1997	[117]
50 g	Digestion with 25 mL H_2SO_4 5 M; adjust to pH 9	SP – silica gel column (25 cm × 1 cm i.d.); Conditioning – 2×20 mL H_2O Elution – 50 mL saturated ammonium chloride solution	Spectrofluorimetric	LR – 0.3-4.5 μg/g RSD – 1% LOD – 0.1 μg/g Rec – 101%	1998	[115]
3 g	MAE – 15 mL H_2SO_4 9 M; 1120 W; 15 cycles; 30 s/cycle	----------	----------	Rec – 22.1-105.3%	2001	[118]

Table 1.5. Studies found in the literature concerning the analytical methods for paraquat quantification in soils (continued).

Sample amount	Extraction/treatment	Clean-up	Instrumental technique	Analytical parameters	Year	Ref
1 g	Shaking with 10 mL of a 0.02 M EDTA/0.5 M ammonium acetate after acidification to a pH 4.7; adjust pH to 9-10	SP – silica cartridge	LC-UV	Not recovery	2008	[113]
1 g	MAE – 200 μL benzalkonium chloride+8 mL HNO_3 (65%)+ 2mL HCl (37%)+2 mL HF (48%); 30 min ramp time to reach 200 °C and hold there for 20 min; 800 W MAE – 20 mL 4% boric acid aqueous solution; 15 min ramp time to reach 180 °C and hold there for 15 min; 800 W; pH adjustment to 9-10	SP – silica cartridge	LC-UV	RSD – 10% LOD – 0.050 μg/g Rec – 102%	2008	[113]
5 g	Digestion with 30 mL of a mixture 70:30 (v/v) MeOH:5%(w/v) EDTA acidified with 2% (v/v) formic acid ; 3 h; adjust to pH 9	SP – silica cartridge Elution – 10 mL 70:30 (v/v) MeOH: 6.5 M HCl	LC-UV	RSD – <15% LOD – 0.020 μg/g Rec – 98-102%	2009	[29] [30] [113]

Notes: CZE-DAD – capillary zone electrophoresis-diode array detection; DAD – diode array detection; DCM – dichloromethane; EDTA – ethylenediaminetetraacetic acid; LC – liquid chromatography; LC-TSP-MS – liquid chromatography-thermospray-mass spectrometry; LOD – limit of detection; LR – linearity range; MAE – microwave-assisted extraction; MeOH – methanol; Rec – recovery; RSD – relative standard deviation; SP – solid phase; UV – ultraviolet detection.

Pateiro-Moure et al. tested the ability of a mechanical shaking methodology to extract paraquat from a contaminated soil and no recovery was attained under the conditions employed [113]. Generally, similar limits of detection (0.008-0.1 μg/g) were achieved by microwave-assisted extraction (MAE) and the traditional refluxing or digestion techniques (see Table 1.5). MAE has the advantages over the others of requiring shorter extraction times (10-50 min), less solvent quantities (10-20 mL) and lower sample amounts (1-3 g) [113, 118, 119]. On the other hand, MAE involves sophisticated equipment, especially when *aqua regia* (nitro-hydrochloric acid) is employed as extraction solvent [113]. Despite of the differences observed on the extraction time for the different techniques and approaches referred above, generally the corresponding methods are globally time-consuming (taken hours) since they require clean-up steps after the extraction (see Table 1.5). A substantial reduction of the sample preparation time by extraction and clean-up steps elimination can be obtained by direct surface analysis [117]. Paraquat is easily detected by static secondary ion mass spectrometry (SIMS), which is a direct surface analysis technique, and offers fast analysis times, on the order of 10 min/sample [117]. On the other hand, it can be observed from Table 1.5 that the limit of detection obtained by SIMS (6 μg/g) is higher than that achieved by the other methods (0.008-0.17 μg/g). Additionally, chromatographic methods allow obtaining higher quantitative information than surface [117].

In short, the search for an easy and fast extraction methodology for the extraction of PQ from deposits, preserving matrix structure, justifies the procedure adopted in Chapter 3 by using an aqueous saturated ammonium chloride solution. Indeed, the matrix structure destruction, as occurs in digestion and refluxing procedures, typically conducts to complex extracts that require clean-up procedures which increase the time of analysis.

1.1.3 Sorption of paraquat on deposits from drinking water networks

The study of pesticides adsorption on deposits from drinking water networks is of paramount importance, particularly in case of an accidental or deliberate contamination event, where high paraquat concentrations may be involved; it would be also of relevance the use of such materials in applications like wastewater treatment, thus adding value to those solid residues that result from water networks cleaning and maintenance

operations. As occurred for methods of paraquat quantification in deposits, no studies exist about paraquat adsorption on the same matrices. Again, the paraquat adsorption studies on other materials were picked up from literature for comparison purposes. There are several studies about paraquat adsorption on clays and soils (Table 1.6 – [28-36, 38, 39, 120-126]). The interaction of pesticides, as paraquat, with soils may involve either their mineral and/or organic components. For soils that have higher organic matter levels (>5%), the pesticide sorption process depends on the total organic matter content, being the nature of the organic matter an insignificant aspect. On the other hand, for soils with low organic matter content, the active components of the inorganic fraction (namely the content and composition of the clay and identity of the major cations) are responsible for the mobility of the pesticides. Concerning the particular case of paraquat adsorption on soils, the interaction is frequently reported as rapid and very strong [28-30, 32, 36]. Hence, the mechanism involves ionic and charge transfer bonds [127]. Bipyridylium herbicides such as paraquat form highly stable and unreactive bonds with the carboxyl groups of the humic substances by ion-exchange via their cationic group [28]. In some cases, paraquat has high affinity for clay surfaces in relation to soil organic matter, especially as compared with inorganic cations [29]. The interaction between paraquat and clay particles depends on the particular type of clay [29, 30]. Weber and Scott demonstrated that paraquat binds to interlayer spacings in montmorillonites via Coulombic and Van der Waals forces and to kaolinite via Coulombic forces alone [29].

Concerning the adsorption isotherms, Langmuir and Freundlich are the ones that better describe the adsorption of PQ on clays, soils and the other materials (Table 1.6). For Langmuir isotherms, maximum adsorption capacities (q_{max}) vary from 0.5 mg/g for crystalline iron oxide coated quartz particles [31] to 171.48 mg/g for calcium alginate gel beads [121]. The shapes of isotherms have been classified as L-type [31, 36, 123] and H-type [29, 39, 126] isotherms according to the Giles classification [128]. The L-type isotherm corresponds to a decrease of sites availability as the solution concentration increases, which indicates saturation of the surfaces. On the other hand, H-type adsorption isotherms are an extreme version of the L-type ones, being its adsorption in many instances close to 100%, particularly for the lowest concentrations.

Concerning the desorption of paraquat from soils/clays, the extent of the process is typically very small, also due to the strong interaction between both [30, 32, 34, 36].

Table 1.6. Studies found in the literature about paraquat adsorption on soils, clays and other solids.

Adsorbent type	Kind of interaction	Sorption capacity/model parameters	Ref.
Soils	Very rapid sorption (equilibrium time of minutes) Adsorption is sensitive to pH and paraquat concentration levels	----------	[28]
	Paraquat is strongly adsorbed to the soils: little amount desorbed from them that ranged in 2.1 – 2.4% and 10.5-14.3% at 100 and 200 mg/L, respectively. Sorption of PQ is clearly increased with the organic matter removal from soil. Adsorption isotherms fitted with the Freundlich equation	- Freundlich isotherm: K_f = 4148-4456 L^n $\mu mol^{(1-n)}$/kg for all soils studied, $1/n$ = 0.22-0.31	[29]
	PQ is strongly adsorbed by both soils: the extent of desorption of PQ from both soils with $CaCl_2$ was very small <1%. The addition of cooper at concentrations from 0 to 3.15 mM resulted in no significant increase in the PQ adsorption.	- Linear isotherm: K_D =1.28×10^3 L/kg for soil 1; K_D = 429 L/kg (q≤4) or 24 L/kg (q>4) for soil 2	[30]
	Paraquat strongly adsorbed: only 0.42% of the paraquat adsorbed on sandy loam soil is removed with CaCl2 and none extraction was observed for muck soil. Adsorption is not affected by T, pH or addition of a pesticide mixture (lindane, paraquat and glyphosate).	- Freundlich isotherm: K_f = 28.7 L/kg and $1/n$ = 0.60 for sandy loam soil K_f =1419 L/kg and $1/n$ = 1.01 for muck soil	[32]
	At low concentrations, paraquat desorption requires refluxing with 18 N sulfuric acid. As the concentration in soil increases, a portion of paraquat can be desorbed by leaching with saturated ammonium chloride. At high levels, the unbounded paraquat can be leached with water.	----------	[33]
	It seems that paraquat interacts strongly with soil components being the most favorable mechanism the ionic bonding. Negligible desorption of paraquat from the soils (in the absence or presence of increased content of soluble fluvic).	----------	[34]
	Paraquat adsorption capacity depends on the clay content. Lower desorption percentages were achieved 0.04-0.17% and 0.80-5.83% for clay and sandy loam soils, respectively.	- Freundlich isotherm: K_f = 787 (mg/kg)(L/μg)$^{1/n}$ and $1/n$ = 0.247 for clay; K_f = 18 (mg/kg)(L/μg)$^{1/n}$ and $1/n$ = 0.412 for sandy loam soils	[36]

Table1.6. Studies found in the literature about paraquat adsorption on soils, clays and other solids (continued).

Adsorbent type	Kind of interaction	Sorption capacity/model parameters	Ref.
Clays	The bond strength of paraquat with respect to an exterior surface is much smaller than to the interlayer. There are indications that adsorption on inorganic oxides is very weak. Montmorillonite has strong PQ adsorption capacity	- Langmuir isotherm: q_{max} = 41×10^{-6} mol/g for illite; q_{max} = 20×10^{-6} mol/g for kaolinite	[38]
	The adsorption is governed by electrostatic interactions.	- Langmuir isotherm: q_{max} = 0.18×10^{-6} moL/m^2 for silica; 1.5×10^{-6} moL/m^2 for kaolinite; 4×10^{-6} moL/m^2 for illite; 0.6×10^{-6} moL/m^2 for montmorillonite	[39]
	It seems that the initial pH does not influence the kinetic constant but, the paraquat adsorption capacity increase with the pH. The adsorbed paraquat amount increased as temperature decreased –endothermic. The rate constant decrease with increasing temperature.	----------	[122]
	The rate of adsorption of paraquat onto clay is very fast. The intra-particle diffusion mechanism plays a significant role in the adsorption.	- Freundlich isotherm: K_f = 36.02 (mg/g)(L/mg)$^{1/n}$ and 1/n = 0.0294	[125]
	Illite and illite modified with nonylammonium chloride are the most effective adsorbents.	- Langmuir isotherm: q_{max} = 12.3 mg/g for sepiolite, 42.4 mg/g for bentonite, 54.5 mg/g for illite, 9.8 mg/g for sepiolite modified with dodecylammonium chlorides, 23.1 mg/g for bentonite modified with dodecylammonium chlorides, 24.4 mg/g for illite modified with dodecylammonium chlorides, 12.3 mg/g for sepiolite modified with nonylammonium chlorides, 49.9 mg/g for bentonite modified with nonylammonium chlorides and 57.3 mg/g for illite modified with nonylammonium chlorides	[123]
	Adsorption rate very fast pH and salinity were found to be considerable significance in the ion exchange process. Sorption of paraquat may occur in two steps: transfer sorbate and chemical complexation/ ion exchange at adsorbent sites	----------	[126]

Table 1.6. Studies found in the literature about paraquat adsorption on soils, clays and other solids (continued).

Adsorbent type	Kind of interaction	Sorption capacity/model parameters	Ref.
Tire-derived adsorbent (TAC) Activated carbon F300 (CAC)	The adsorption of paraquat is weakly pH dependent. The rate of sorption of PQ onto CAC is very fast (almost 90% of the maximum possible adsorption taking place in the first 5 min)	- Langmuir isotherm: q_{max} = 33.7 mg/g for TAC q_{max} = 75.8 mg/g for CAC	[120]
Quartz and quartz iron oxide	PQ has higher sorption strength on crystalline iron oxide coated quartz particles than on amorphous ones. The maximum sorption capacity for PQ can be found, instead on amorphous iron-oxides coated quartz. The higher addition of phosphates (P) contributes to the increase of PQ maximum sorption on iron oxide coated quartz particles.	- Langmuir isotherm: q_{max} = 0.7 mg/g for amorphous iron oxide coated quartz particles q_{max} = 0.5 mg/g for crystalline iron oxide coated quartz particles	[31]
Calcium alginate gel beads	Sorption of paraquat onto the calcium alginate gel beads is pH-dependent (increase with increasing pH). Equilibrium time is 120 min Calcium compete with paraquat for the available binding sites	- Langmuir isotherm: q_{max} = 149.71 mg/g at pH 3 and 20 °C q_{max} = 171.48 mg/g at pH 7 and 20 °C	[121]
Spent diatomaceous earth from the beer brewery activated by sodium hydroxide	The kinetic adsorption is rapid (the equilibrium is reached approximately in 30 min). It seems that the rate constant is not influenced by the initial pH. The adsorption should be a physical process, which is an exothermic process and the amount of adsorbate adsorbed onto adsorbent increases with the lowering of adsorption temperature.	- Freundlich isotherm: K_f = 3.37 (mg/g)(L/mg)$^{1/n}$ and 1/n = 1.89 for spent diatomaceous earth K_f= 12.80 (mg/g)(L/mg)$^{1/n}$ and 1/n = 13.51 for treated diatomaceous earth	[124]

Notes: Isotherm equations: Linear ($q = K_D C$; q is the amount of PQ adsorbed, K_D is the linear coefficient of distribution and C is the concentration of PQ in the liquid phase), Langmuir ($q = K_L C q_{max} / (1 + CK_L)$; q is the amount of PQ adsorbed, K_L is the Langmuir adsorption equilibrium constant, C is the concentration of PQ in the liquid phase and q_{max} is the maximum adsorption capacity) and Freundlich ($q = CK_f^{1/n}$; q is the amount of PQ adsorbed, K_f is the Freundlich adsorption equilibrium constant, C is the concentration of PQ in the liquid phase and n is the Freundlich constant)

1.1.4 Degradation technologies for paraquat in waters

To reduce the paraquat (and other pesticides) impact, powerful and practical treatment processes for its (their) degradation in water matrices are needed. The traditional chemical and biological treatments are not sufficiently effective for most pesticides [129]. On the other hand, in some physical processes there is a simple transfer of the pollutants from one phase to another, not being destroyed. The advanced oxidation processes (AOPs) are clean technologies based on the generation of extremely reactive and non-selective hydroxyl radicals, with very high oxidative power (E_0 = 2.8 V). Due to their powerful capability to oxidize numerous organic compounds into CO_2 and H_2O, AOPs have been selected for various applications. Among them, the Fenton's reaction is a promising process, which appeared in 1894 when Fenton strongly improved tartaric acid oxidation by the use of ferrous ion and hydrogen peroxide [130]. Fenton's reaction is a non-expensive and environmental friendly oxidation method, widely used in wastewater treatment. The process has a complex mechanism, which can even though be simplified by the following equations [131, 132]:

$$H_2O_2 + Fe^{2+} \rightarrow Fe^{3+} + OH^- + HO^\bullet, \quad k_1 = 76\ M^{-1}s^{-1} \qquad 1.1$$

$$Org. + HO^\bullet \rightarrow Org.^\bullet \rightarrow ... \rightarrow CO_2 + H_2O, \quad k_2 \approx 10^7 - 10^{10} M^{-1}s^{-1} \qquad 1.2$$

$$H_2O_2 + OH^\bullet \rightarrow H_2O + HO_2^\bullet, \quad k_3 = (1.2 - 4.5) \times 10^7 M^{-1}s^{-1} \qquad 1.3$$

$$Fe^{2+} + HO^\bullet \rightarrow Fe^{3+} + OH^-, \quad k_4 = 4.3 \times 10^8 M^{-1}s^{-1} \qquad 1.4$$

$$HO^\bullet + HO^\bullet \rightarrow H_2O_2, \quad k_5 = 5.3 \times 10^9 M^{-1}s^{-1} \qquad 1.5$$

$$Fe^{3+} + H_2O_2 \leftrightarrow Fe^{III}(HO_2)^{2+} + H^+, \quad k_6 = 3.1 \times 10^{-3} \qquad 1.6$$

$$Fe^{III}(HO_2)^{2+} \rightarrow Fe^{2+} + HO_2^\bullet, \quad k_7 = 2.7 \times 10^{-3} s^{-1} \qquad 1.7$$

Briefly, the reaction between iron and hydrogen peroxide produces hydroxyl radicals with high oxidative power (eq. 1.1), which attack the organic matter present in the water (eq. 1.2). Unfortunately, some parallel reactions occur (eqs. 1.3-1.5), and so the hydroxyl radicals are not only consumed to degrade the organic matter but also to produce other radicals, with less oxidative power, or other species (so-called scavenging effect of $HO^\bullet$). Besides, this leads to the undesired consumption of hydrogen peroxide (eq. 1.3). On the

other hand, eqs. 1.6 and 1.7 indicate the generation of Fe^{2+} by the reaction between H_2O_2 and Fe^{3+} (Fenton-like process); this way ferrous ion is restored, acting as catalyst in the overall process.

Few studies about paraquat degradation by AOPs in water were published and are hereby compiled in Table 1.7. As can be seen, most of them refer to photocatalytic processes by the action of TiO_2 [133-138]. In these cases, high paraquat degradation values were achieved for a wide range of initial parent compound concentrations (7.5 to 1000 mg/L). Nevertheless, it is important to emphasize that this kind of treatment could import excessive electricity costs. The ozonation was also tested to degrade PQ in water [139, 140]. Relatively low PQ degradation by ozonation in the presence of light was obtained by Kearney et al. [139] (only 32.8% of paraquat was destroyed after 7 h). More recently, Dhaouadi and Adhoum [141] used four different activated carbons as catalysts in paraquat degradation by the heterogeneous Fenton's process. The same researchers also tested and compared four different advanced oxidation methods in the degradation of paraquat: anodic oxidation (AO), electro-Fenton (EFe), photoelectro-Fenton (PEF) and classic Fenton (CFe) [142]. All but one treatment method (CFe) was optimized. The CFe treatment was not optimized as only one experiment was done for comparison purposes. The paraquat concentration versus time plot indicated that the fastest initial degradation rate was attained for the CFe method, but after 20 min no paraquat degradation was observed. Dhaouadi and Adhoum [142] concluded that CFe has a significantly lower oxidative ability as compared to other systems. However, this may be due to the insufficient peroxide quantity used in the operation. Therefore, an optimized classic Fenton process could potentially lead to comparable paraquat degradation efficiencies. Up to the author's knowledge, there are no other studies reported concerning paraquat degradation by the homogeneous Fenton's process, which was addressed in this thesis (Chapter 5).

Table 1.7. Studies reported in the literature about paraquat degradation in water by AOPs.

Treatment	Operating conditions	Analytical method for PQ monitoring	Results and Comments	Ref.
UV light over TiO_2-coated polythene or polypropylene films	$[PQ]_0$ = 50 mg/L T = 26 °C 15 mL O_2/min 8.8×10^{-5} g TiO_2/cm^2 for polythene and 3.1×10^{-5} g TiO_2/cm^2 for polypropylene	UV spectrophotometer	Complete degradation to CO_2, NH_3, HCl and small quantities of NO_2^-/NO_3^- within ca. 6 h.	[133]
UV light over commercial TiO_2	$[PQ]_0$ = 10, 20 and 40 mg/L UV (365 nm) 50 mL O_2/min 200 mg TiO_2 /L pH = 4, 6.6, 7 and 9	LC	Paraquat is slowly degraded by direct photolysis in the presence of dissolved oxygen ($[PQ]_0$ = 20 and 40 mg/L; pH_0 6.6). Direct photolysis with UV light destroyed 60% of paraquat in less than three hours of reaction ($[PQ]_0$ = 10 mg/L; pH_0 6.6). In the presence of TiO_2, all species were consumed after three hours of reaction at high pH values.	[134]
UV light over TiO_2	$[PQ]_0$ =1000 mg/L 0.5 L air/min TiO_2 film (three-time coating) attained from the hydrothermal method UV-light intensity: 36 W/m^2	Potassium ferric-oxalate actinometrical method	About 100% of paraquat was degraded after 15 h of reaction.	[135]
UV light and/ or air-sparging over TiO_2	$[PQ]_0$ = 100 mg/L 1 L air/min 0.1 g TiO_2/L UV-light intensity: 4, 8, 12, 24 and 36 W/m^2	UV – spectrophotometer	Paraquat removal rate was 0.54 mg/L/h with only air-sparging. In the presence of UV-light, the removal rate with air-sparging was 50% higher in 24 h than that without it. In the presence of TiO_2, the removal rates in 40 h were 1.4, 1.6 and 2.2 mg/L/h at the UV light intensities of 4, 8 and 12 W/m^2, respectively. In the presence of TiO_2 with air-sparging, the required times for 90% removal of PQ were 18, 12 and 3 h at the UV light intensities of 12, 24 and 36 W/m^2, respectively.	[143]

Table 1.7. Studies reported in the literature about paraquat degradation in water by AOPs (continued).

Treatment	Operating conditions	Analytical method for PQ monitoring	Results and Comments	Ref.
UV light over TiO_2 (commercial and "home prepared")	$[PQ]_0$ = 7.5 mg/L 200 mg TiO_2 /L pH = 4, 7 or 9	UV-visible spectrophotometer	Under alkaline medium, paraquat degradation is almost complete after 30 min of reaction. Five compounds structures were proposed for intermediate degradation products of paraquat oxidation	[136]
UV light over commercial TiO_2	$[PQ]_0$ = 20 mg/L 0.04 and 0.4 g TiO_2/L UV-light intensity: 140 W/m^2	UV spectroscopy	Near complete mineralization of paraquat was achieved after ca. 3 h of irradiation by using 0.4 g/L of catalyst amount at neutral pH (ca. 5.8).	[137]
Xenon lamp over $1C_{60}$/ 1 V-TiO_2 (composition in wt%)	$[PQ]_0$ = 15 – 50 mg/L 1 g catalyst/L pH=6.5	UV-visible spectrophotometer	70% degradation within 4 h.	[138]
UV light in the presence of O_2 or O_3	$[PQ]_0$ = 1500 mg/L 32 g O_3 /h 66 low-pressure mercury vapor lamps (254 nm)	GC	Significant oxidation of PQ did not occur in the presence of oxygen during 7 h. When O_3 was fed 32.8% of PQ was destroyed during 7 h. 4-carboxy-1-methylpyridinium ion, monoquat, monopyridone, 4,4'-bipyridyl, 4-picolinic acid, oxalate, malate, succinate and N-formylglycine were proposed for intermediate compounds of PQ oxidation.	[139]
O_3	$[PQ]_0$ = 231 – 2057 mg/L 38.6 L O_3 /h pH = 4.2 to 8.0	LC	Paraquat was degraded after 120 min of reaction at pH 8.0. N-methylisonicotinic acid, N-formyloxamic acid, ammonia, oxamic acid and nitrate were proposed for intermediate compounds of PQ oxidation.	[140]

Table 1.7. Studies reported in the literature about paraquat degradation in water by AOPs (continued).

Treatment	Operating conditions	Analytical method for PQ monitoring	Results and Comments	Ref.
Heterogeneous Fenton (AC-Fe as catalyst)	$[PQ]_0$ = 20 mg/L 1 g catalyst/L T=70 °C $[H_2O_2]_0$ = 12.5 mM	LC	71.4% of chemical oxygen demand abatement was obtained under the conditions indicated.	[141]
Anodic oxidation (AO); Electro-Fenton (EFe); Photoelectro-Fenton (PEF)	$[PQ]_0$ = 10 – 50 mg/L T = 25 °C pH = 3 $[Fe^{2+}]_0$ = 0.1 – 2 mM $[H_2O_2]_0$ = 20 mM Current intensity: 50, 100 and 200 mA	LC	The PEF is the most efficient treatment. Classic dark Fenton under the same conditions leads to a high removal rate at the initial stage of the experiment but poor degradation efficiency was obtained maybe due to the insufficient H_2O_2.	[142]
Homogeneous Fenton	$[PQ]_0$ = 50 – 200 mg/L T = 10 – 70 °C pH = 2 – 5 $[Fe^{2+}]_0 = 1.0\times10^{-4} – 5.0\times10^{-4}$ M $[H_2O_2]_0 = 1.6\times10^{-3} – 5.7\times10^{-2}$ M	LC	Under selected conditions (T =70.0 °C, $[Fe^{2+}] = 5.0\times10^{-4}$ M, $[H_2O_2] = 3.4\times10^{-2}$ M, and pH = 3.0) nearly all the initial paraquat dichloride was degraded after 1 h and 60% of the organic matter was mineralized after 4 h. At 30 °C, complete paraquat degradation and 40 % of mineralization were reached after 4 h of reaction.	[144] (Chapter 5)

Notes: AO – anodic oxidation; EFe – electro-Fenton; GC – gas chromatography; LC – liquid chromatography; PEF – photoelectro-Fenton; UV – ultraviolet.

1.2 Polybrominated diphenyl ethers (PBDEs)

Accidental fires inflict a heavy toll in terms of economic loss, human suffering and, in the extreme, death. As a response to this challenge, there was a need to produce and use flame retardants (FR), as a mean to reduce the likelihood of ignition, to hind the fire spread and to provide some extra time in the early stages of a fire when it is much easier to escape [145]. For a long time, flame retardants were associated to safe and protection and were used in a widespread number of applications such as: industries of plastics, textiles, electronic equipment and in building materials. Among the organohalogenated flame retardants the bromine-based ones are the most effective and applied [146]. Their popularity on fire prevention is related in part to the weak bond between bromine and the carbon atoms, which enables the bromine atom to interfere at a more favorable point in the combustion process [145]. Brominated flame retardants (BFRs) can be classified in reactive or additive, depending on the manner they are incorporated in the polymer. Reactive flame retardants are chemically bonded to the material while additive flame retardants are not covalently bonded and are often applied to the substrate surface as a spray in a coating formulation [147]. For that reason, additive BFRs are easily leached out from the surface of the material and thus released into the environment during their natural operational life and also during processing, recycling or combustion [145, 148]. Polybrominated diphenyl ethers (PBDEs) are an example of additive flame retardants [149]. As observed in Figure 1.2, they have structures similar to polychlorinated biphenyls (PCBs) with an oxygen atom between the aromatic rings [149].

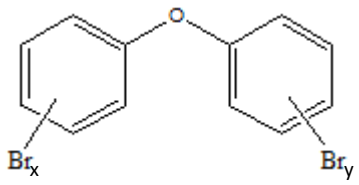

x+y = 1–10

x+y = 1 Mono-BDEs	x+y = 6 Hexa-BDEs
x+y = 2 Di-BDEs	x+y = 7 Hepta-BDEs
x+y = 3 Tri-BDEs	x+y = 8 Octa-BDEs
x+y = 4 Tetra-BDEs	x+y = 9 Nona-BDEs
x+y = 5 Penta-BDEs	x+y = 10 Deca-BDEs

Figure 1.2. Chemical structure of PBDEs (adapted from [150]).

Theoretically, there are 209 PBDEs congeners differing in the number and/or position of the bromine atoms in the aromatic ring. Commercial PBDEs are typically prepared by bromination of diphenyl ether in the presence of a catalyst. As a consequence, mixtures of PBDEs with various bromination degrees are produced. There are three main PBDEs commercial mixtures: penta-BDE, octa-BDE and deca-BDE. Commercial Penta-BDE is a mixture of tetra (24-38%), penta (50-60%) and hexa (4-8%) congeners [151]. The Octa-BDE mixture is composed by hexa (10-12%), hepta (44%), octa (31-35%) and nona (10-11%) congeners [151]. Commercial Deca-BDE formulation contains octa (0.8%), nona (22%) and deca (77%) congeners [152]. The main properties of technical PBDE mixtures are indicated in Table 1.8. The uses of penta-BDE and octa-BDE commercial mixtures were completely banned by the European Union (EU) since 2004, after a comprehensive risk assessment analysis under the Existing Substances Regulation 793/93/EEC [153]. In May 2009, at the 4th meeting of the parties of the Stockholm Convention for Persistent Organic Pollutants (POPs), the penta-BDE and octa-BDE commercial mixtures were officially classified as POPs substances and were included in the Annex A (elimination of production and use of all intentionally produced POPs) [154, 155]. In the United States, several states have adopted legislation to ban the penta-BDE and octa-BDE mixtures and, owing to growing apprehension, the main US chemical producer voluntarily agreed to stop its manufacturing [156]. Deca-BDE commercial mixture has been current explored without any restriction which, in part, has contributed to the increase on the lower PBDEs environmental findings as a consequence of congeners debromination [156]. Indeed, the major PBDEs findings in environmental matrices correspond to lower brominated flame retardants, which have been considered more dangerous for humans and wildlife than the higher brominated ones due to their high efficiency to be bioaccumulated [152, 157-159]. The larger molecules, specially the fully brominated deca-BDE, are poorly absorbed due to their lower ability to cross biological membranes, rapidly eliminated and thus, they are unlikely to be bioaccumulative [145, 149]. Due to their persistence, bioaccumulation and toxicity, ubiquity and long-range atmospheric transport, PBDEs have even been found in the remote arctic environment [160]. Estimated half-lives in the environment between 2 and 10 years were reported for these chemicals [161]. Toxicity information about PBDEs is scarce and the toxicity assessment of each congener in particular has not been finished yet [148, 156].

Table 1.8. Physical and chemical properties of technical PBDE mixtures (adapted from [162]).

Property	Penta-BDE	Octa-BDE	Deca-BDE
Color	Clear, amber to pale yellow	Off-white	Off-white
Physical state	Highly viscous liquid	Powder	Powder
Melting point	-7 to -3 °C (commercial)	85-89 °C (commercial)	290-306 °C
Boiling point	>300 °C (decomposition starts above 200 °C)	decomposes at >330 °C (commercial)	decomposes at >320 °C
Density (g/mL)	2.28 at 25 °C	2.8 (commercial)	3.0
Solubility in water (μg/L)	13.3 (commercial)	1 at 25 °C (commercial)	<0.1
Log Kow	6.57 (commercial)	6.29 (commercial)	6.265
Log Koc	4.89-5.10	5.92-6.22	6.80
Vapor pressure (mmHg)	3.5×10^{-7} (commercial)	4.9×10^{-8} (commercial)	3.2×10^{-8}

Table 1.9. Some physical and chemical properties of BDE-100.

Common Name CAS n.º Molecular formula Molecular weight (g/moL)	Chemical Structure	Solubility in water (μg/L) [a]	Vapor pressure (mmHg) [a]	Henry's law constant (atm. m^3/mol) [a]	Log K_{ow} [b]
BDE-100 **189084-64-8** **564.7** **2,2´,4,4´,6-pentabromodiphenyl ether**	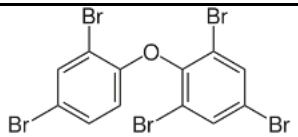	40 (at 25 °C)	2.15×10^{-7}	6.80977×10^{-7}	7.24

Notes:. [a] – [163]; [b] – [164]

Some studies have pointed out their potential to act as hormone disruptors, neurodevelopmental toxic and carcinogenic agents [148, 149]. However, it is inappropriate to make generalized statements about PBDEs toxicology because their physicochemical properties vary considerably from congener to congener [145]. As referred in the beginning of this chapter, the thesis work was mainly focused in BDE-100 congener because it was the one selected by SecurEau team to represent the "new" chemicals. The main properties of this specific congener are presented in Table 1.9.

1.2.1 Analytical Methods for PBDEs in waters

Analytical methods for PBDEs in waters are complex and laborious, due to the necessity of using a pre-concentration step in the extraction procedure. This pre-concentration step is always needed in order to reach LODs low enough to determine the ultra-trace levels at which PBDEs are present in water (normally within the ng/L or low μg/L range) [165-167]. The analytical methods found in the literature for PBDEs in waters are compiled in Table 1.10. It is organized by decreasing order of the year of publication. Concerning the chromatographic techniques, gas chromatography with electron-capture [168] or mass spectrometry detection [147, 149, 169-173] are the most widely used for the determination of PBDEs in water samples, but high-performance liquid chromatography with diode array, ultraviolet or mass spectrometry detectors may be also applied [156, 174-178].

Methods that use liquid chromatography generally lead to higher LODs (10-700 ng/L) [174-178]. The liquid-liquid extraction–liquid chromatography–tandem mass spectrometric (LLE-LC-MS/MS) method conducts to lower LODs (0.004-0.1 ng/L) but the equipment is rather expensive, extremely high sample volume is required (1 L) and significant amounts of organic solvents (non-environmental friendly) are typically used, which limits this method for monitoring a large number of samples [156].

SPE plus dispersive liquid-liquid microextraction (DLLME) is another method used for the extraction of PBDEs from water and plant samples, presenting low LOD (0.03-0.15 ng/L), but with the disadvantages of requiring high sample volume and laborious experimental procedure [168]. On the other hand, the electron-capture detector used does not allow the identification of the compounds, which may represent a problem if any undesired interference co-elutes with target analytes.

Table 1.10. Studies found in the literature about the analytical methods for PBDEs quantification in waters.

Analytes	Extraction	Determination	Analytical parameters	Ref.
BDEs 47,99,154,183	TA-IL-DLLME Sample volume – 5 mL; Dispersive solvent – MeOH (1 mL); Extraction solvent – [C8MIM] [PF6] (40 μL)	LC-DAD	LR – 500-500,000 ng/L RSD – 1.0-3.8% LOD – 100-400 ng/L Rec – 81.0-127.1%	[174]
BDEs 28,47,99,154,183,209	SFOME Sample volume – 40 mL; Extraction solvent – 2-dodecanol (25 μL); Temperature – 60 °C; Stirring speed – 900 rpm; Extraction time – 25 min; Salt addition – no	LC-DAD	LR – 5000-500,000 ng/L (BDE-209) 500-75,000 ng/L (others) LOD – 10-40 ng/L Rec – 92-118%	[175]
BDEs 28,47,85,99,100,153,154	SPE Column – Supelclean LC-C18; Conditioning – DCM (2 mL), MeOH (5 mL), H_2O (5 mL); Load – 100 mL at 10 mL/min; Elution – n-hexane (2 mL) + DLLME Sample volume – 5 mL; Disperser solvent – ACN (1 mL); Extraction solvent – 1,1,2,2-tetrachloroethane (22 μL); Salt addition – no	GC-ECD	LR – 0.1-100 ng/L (BDEs 28, 47) 0.5-500 ng/L (others) RSD – 4.2-7.9% LOD – 0.030-0.15 ng/L Rec – 66.8-94.1%	[168]
BDEs 47,99,100,153,154	LLE Sample volume – 1 L; Extraction solvent – n-hexane (100 mL); Salt addition – 20 g	LC-MS-MS	LR – 0.025-10 ng/L LOD – 0.004-0.1 ng/L Rec – 43-99%	[156]
BDEs 47,99,100,153	USAEME Sample volume – 10 mL; Temperature – 35 °C; Extraction solvent – chloroform (100 μL); Extraction time – 5 min	GC-MS	LR – 5-5000 ng/L (BDEs 47,100) 5-10 000 ng/L (BDEs 99,153) RSD – <10.3% LOD – 1-2 ng/L Rec – ≥96%	[169]
BDEs 47,99,100,153	CPE Sample volume – 10 mL; Non-ionic surfactant – Triton X-100 (0.4 g/L); Salt addition – 400 μL of 6.15 mol/L; Temperature – 80 °C; Equilibrium time – 7 min + UABE Extraction solvent – isooctane (50 μL); Extraction time – 5 min	GC-MS	LR – 4-150 ng/L RSD – ≤8.5% LOD – 1-2 ng/L Rec – 96-106%	[170]
BDE-209	DLLME Sample volume – 5 mL; Disperser solvent – THF (1 mL); Extraction solvent – tetrachloroethane (22 μL); Salt addition – no	LC-UV	LR – 1000-500,000 ng/L RSD – 2.1% LOD – 200 ng/L Rec – 89.9-95.8%	[177]

Table 1.10. Studies found in the literature about the analytical methods for PBDEs quantification in waters (continued).

Analytes	Extraction	Determination	Analytical parameters	Ref.
BDEs 28,47,99,209	DLLME Sample volume – 5 mL; Disperser solvent – ACN (1 mL); Extraction solvent – tetrachloroethane (20 μL); Salt addition – no	LC-DAD	LR – 50-50,000 ng/L (BDEs 28, 99) 100-100,000 ng/L (others) RSD – 3.8-6.3% LOD – 12.4-55.6 ng/L Rec – 87.0-114.3%	[176]
BDE-209	SDME Sample volume – 5 mL; Extraction solvent – toluene; Solvent drop volume – 3 μL; Extraction time – 15 min; Stirring speed – 600 rpm; Salt addition – no	LC-DAD	LR – 1,000-1,000,000 ng/L RSD – 4.8% LOD – 700 ng/L Rec – 91.5-102.8%	[178]
BDEs 28,47,99,100	HF-LPME Sample volume – 3 mL; Temperature – 40 °C; Extraction solvent – decane; Stirring speed – 1000 rpm; Extraction time – 20 min; Salt addition – no	GC-MS	LR – 200-20,000 ng/L RSD – 5.1-9.1% LOD – 15.2-40.5 ng/L Rec – 85-110%	[147]
BDEs 28,47,99,100,153,154,183	HF-MMLLE Sample volume – 100 mL; Extraction solvent – n-undecane; Stirring speed – 1200 rpm; Extraction time – 60 min; Salt addition – no	GC-MS	LR – 1-100 ng/L RSD – 16.9% LOD – 1.1 ng/L Rec – 85-110%	[171]
BDEs 28,47,66,85,99,100,138,153,154	MAE Sample volume – 1.5 L; Extraction solvent – hexane-acetone, 1:1 (v/v) (60 mL); Temperature – 85 °C; Extraction time – 1 min; Two cycles	GC-MS-MS	LR –500-100,000 ng/L LOD –0.02-0.1 ng/membrane Rec – 72-91%	[172]
BDEs 28,47,66,85,99,100,138,153,154	SBSE Sample volume – 100 mL; PDMS commercial stir bars; Temperature – ambient; Extraction time – 25 h; Methanol addition – 20%	TD-GC-MS	LR – 20-600 ng/L RSD – ≤20% LOD – 0.3-9.6 ng/L Rec – 94-106%	[173]
BDEs 3,47,85,99,100,153,154	HS-SPME Sample volume – 10 mL; Fiber – PDMS; Extraction temperature – 100 °C; Extraction time – 30 min; Desorption temperature – 280 °C; Desorption time – 2 min; Salt addition – no	GC-MS-MS	LR – 0.12-503 ng/L RSD – 1.2-26% LOD – 0.0075-0.190 ng/L Rec – 74-117%	[149]

Notes: ACN – acetonitrile; CPE – cloud point extraction; DAD – diode array detection; DCM – dichloromethane; DLLME – dispersive liquid-liquid microextraction; ECD – electron capture detector; GC – gas chromatography; HF-LPME – hollow-fiber liquid phase microextraction; HF-MMLLE – hollow-fiber microporous membrane liquid-liquid extraction; HS-SPME – headspace solid phase microextraction; LC – liquid chromatography; LLE – liquid-liquid extraction; LOD – limit of detection; LR – linearity range; MAE – microwave-assisted extraction; MeOH – methanol; MS – mass spectrometry detector; MS-MS – tandem mass spectrometry detector; PDMS – polydimethylsiloxane; Rec – recovery; RSD – relative standard deviation; SBSE – stir bar sorptive extraction; SDME – single-drop microextraction; SFOME – solidification of floating organic drop microextraction; SPE – solid phase extraction; TA-IL-DLLME – temperature-assisted–ionic liquid–dispersive liquid-liquid microextraction; TD-GC-MS - thermal desorption-gas chromatography-mass spectrometry; THF – tetrahydrofuran; UABE – ultrasound assisted back extraction; USAEME – ultrasound-assisted emulsification-microextraction; UV – ultraviolet detection

A great variety of recent extraction techniques has been applied prior to GC-MS: ultrasound-assisted emulsification-microextraction (USAEME) [169], cloud point extraction (CPE) with ultrasound assisted back extraction (UABE) [170], hollow-fiber liquid phase microextraction (HF-LPME) [147], hollow-fiber microporous membrane liquid-liquid extraction (HF-MMLLE) [171], microwave assisted extraction (MAE) [172], stir bar sorptive extraction (SBSE) [173] and headspace solid phase microextraction (HS-SPME) [149]. Almost all extraction techniques use low sample volume (up to 10 mL) [147, 149, 169, 170]. This is particularly important if the analytical method is designed to be applied, for instance, to degradation or sorption experiments (which is the case of the present thesis), where several samples are taken along the time. Although advantages are recognized to each of the described methods, some drawbacks are also pointed out. Some of them are rather laborious, increasing the time of analysis [170, 173], other present lower precision [147, 171], as reported by Fontana et al. [169] and Zang et al. [179], or require higher sample volumes (up to 1.5 L) [172]. Finally, carry-over phenomena have also been pointed as a disadvantage for SBSE and HS-SPME [149, 173].

Therefore, the search for a simple and inexpensive method, capable of being applied either to environmental monitoring or to degradation/sorption studies of PBDEs in aqueous samples (which require small volumes of sample and quick response) justified the choice of DLLME in this thesis (Chapter 6).

DLLME technique has gained a great popularity due to the easiness of operation, rapidity, low time and cost, high recovery and enrichment factor [176]. The application of this promising technique for PBDEs determination in water samples is still very limited. Up to the author's knowledge, only three analytical methodologies, based exclusively on DLLME as extraction technique, were found in the literature for such purpose [174, 176, 177]. All of them use detectors (DAD and UV) that do not allow an unequivocal compound confirmation. Furthermore, the LODs obtained by these methods (12-400 ng/L) are in general not compatible with the requirements for monitoring purposes. The most recent DLLME method uses ionic liquid as extraction solvent, but the use of such ionic liquids, with too high viscosity, represents an important trouble for the direct injection in the liquid chromatograph [174].

1.2.2 Analytical methods for PBDEs in deposits from drinking water networks

Up to the author knowledge, there is no published data concerning analytical methodologies for PBDEs quantification in deposits from drinking water networks. As for paraquat, the strategy was to understand which methodologies have been implemented for PBDEs determination in soils and take them as first analytical approaches for deposits analysis. Unfortunately, it was not possible to work in this field during the thesis period due to time scarcity but, here are compiled some aspects that should be taken into account in a future work related to this matter.

In Table 1.11, it is compiled all analytical methodologies found in the literature for PBDEs quantification in soils. Pressurized liquid extraction (PLE) is the most frequently used extraction technique. Accordingly to Table 1.11 and for PLE procedure, the soil sample is put in contact with the extraction solvent, typically dichloromethane (DCM), mixtures of hexane/DCM, acetone/hexane or ethyl acetate:MeOH, at 60-120 °C and 2500-2031 psi during a maximum of 20 min [180-184]. In this technique, the dispersion of the sample is promoted by the addition of sand [183], diatomaceous earth [180, 182] or Spe-ed^{TM} (a type of cleaned and sieved diatomaceous earth) [184], which also act as drying agents. Using PLE, PBDEs recoveries are similar to those achieved with conventional Soxhlet extraction with the advantage of using reduced solvent volumes (10-30 mL) in shorter extraction times (5-20 min). Although widely accepted as a robust liquid-solid extraction technique, Soxhlet has been pointed out as a time consumer method (12-24 h), which requires high solvent volumes [185-187]. Additionally, PLE procedure typically conducts to low standard deviations because of being an automated system. Less common, is the ultrasonication with ethyl acetate [188] or hexane:MTBE [189]. This technique is relatively quick when compared to Soxhlet methodology (30-60 min) and similar detection limits were obtained (0.002-0.09 ng/g) [185-189].

As observed from Table 1.11, Soxhlet, PLE and ultrasonication extractions involve clean-up steps before instrumental analysis due to the soil matrix complexity and the need of extract purification in order to prevent chromatographic systems contamination. The SPME has a great advantage over the last extraction techniques because typically does not require the mentioned time consuming multi-step purification methods.

Table 1.11. Studies found in the literature about the analytical methods for PBDEs quantification in soils.

Analytes	Extraction	Clean-up	Instrumental technique	Analytical parameters	Year	Ref.
BDEs 17, 47, 66, 100, 153, 183	PLE 1 g soil+ 7 g Spe-ed™ PSE matrix; ethyl acetate:MeOH (90:10, v/v); 80 °C; 120 bar (1740 psi); 10 min; 2 cycles; concentration to 1 mL	not applicable	GC-MS-MS	LR – 10-200 μg/L RSD – <12-17% LOD – 0.2-2.5 ng/g Rec – 75-102%	2012	[184]
BDEs 28, 47, 99, 100, 153, 154, 183	μ-SPE 1 g soil; 25 mL ultrapure water; μ-SPE device (copper (II) isonicotinate coordination polymer into a porous polypropylene envelope) immerged into the water; 90 °C; 60 min; rinsing μ-SPE device with ultrapure water; drying using a cheese cloth; extraction with 1 mL hexane by sonication during 20 min	not applicable .	GC-μECD	LR – 0.1-200 ng/g RSD – 1.3-10.1% LOD – 0.026-0.066 ng/g Rec – 70-90%	2012	[190]
BDEs 28, 47, 66, 68, 85, 99, 138, 153, 154, 183	Ultrasonication 1 g soil; 5 mL hexane:MTBE (1:1, v/v); 20 min; 3 cycles	• Treatment with 2 g copper powder • Acid silica gel column – elution with 40 mL DCM; evaporation; concentration to 1 mL	GC-MS	RSD –5-10% LOD – 0.047-0.094 ng/g Rec – 76-109%	2012	[189]
BDEs 17, 28, 47, 66, 85	GA-MSPD SPE column with 100 mg soil+ 10 mg CCG+ 50 mg anhydrous sodium sulfate+ 50 mg florisil; elution with 2×500 μL hexane:DCM (1:1); concentration to 50 μL hexane	not applicable	GC-ECD	LR – 0.1-50.0 ng/g RSD – 5.7-15.7% LOD – 0.006-0.029 ng/g Rec – 69.4-104.6%	2011	[191]
BDEs 41 different congeners	PLE 10 g soil+copper powder; hexane:DCM (1:1, v/v); 1508 psi; 100 °C; 10 min; two cycles	• Concentrated H_2SO_4 (60 mL) treatment • Florisil – elution with hexane:methylene chloride (1:2, v/v) (240 mL) • Concentration to 200 μL	GC-MS	RSD – 2.9-21.8% LOD – 0.01-0.03 ng/g (mono- to hepta-BDEs), 1.43 ng/g (nona-BDE) and 0.20 ng/g (deca-BDE) Rec –24-133%	2011	[181]

Table 1.11. Studies found in the literature about the analytical methods for PBDEs quantification in soils (continued).

Analytes	Extraction	Clean-up	Instrumental technique	Analytical parameters	Year	Ref.
BDEs 28, 47, 99, 100, 153, 154, 183	PLE 1 g soil+ 0.5 g sand; DCM; 1500 psi; 100 °C; 5 min; 1 cycle	• Acid silica:silica (10:5 or 15:0) – elution with isohexane • Concentration to 100 μL	GC-MS	LR – 0.10-30 ng/L (for BDE-183); 0.05-30 ng/g (for others) RSD – ≤3% LOD – 0.011-0.054 ng/g Rec – 81-103%	2010	[183]
BDEs 3, 17, 28, 71, 47, 66, 100, 99, 85, 154, 153, 138, 183, 190, 209	PLE 20 g soil+ 3-4 g diatomaceous earth+ 1 g Cu; DCM; 2031 psi; 120 °C; 6 min; two cycles	• GPC column – elution with hexane:DCM (1:1, v/v) (90+70+50 mL) • SPE columns with neutral aluminum oxide and deactivated silica gel – elution with 15 mL hexane, 5 mL hexane:DCM (9:1, v/v) and 20 mL hexane: DCM (4:1, v/v) • Concentration to 500 μL	GC-MS	RSD – <20% LOD – 0.003-0.110 ng/g Rec – >88%	2010	[182]
BDEs 3, 7, 15, 17, 28, 47, 49, 66, 71, 77, 85, 99, 100, 119, 126, 138, 153, 154, 156, 183, 184, 191, 196, 197	PLE 10 g soil+ 2 g diatomaceous earth+ 2 g copper powder; acetone:hexane (1:1, v/v); 1500 psi; 60 °C; 5 min; 1 cycle	• Florisil:silica gel (1:1, v/v) column – elution with acetone:hexane (1:1, v/v)	GC-MS	LR – 20-200 ng/g RSD – 2.2-11.5% LOD – 0.1-1.0 ng/g Rec – 94-109%	2009	[180]
BDEs 47, 77, 99, 100, 118, 153, 154, 181, 183, 190	Soxhlet 2 g soil; 200 mL hexane:acetone (1:1); 24 h;	• Concentrated H_2SO_4 treatment (2 mL) • Alumina column – elution with 8 mL hexane and 8 mL DCM:hexane (2:3, v/v) • Concentration to 50 μL	GC-MS	RSD – <10% LOD – 0.01-0.34 ng/g Rec – 87.6% (BDE-77)	2008	[187]
BDEs 17, 47, 66, 100, 99, 85, 154, 153, 138	HS-SPME 1 g soil; PM-β-CD/OH-TSO fiber; adsorption (95 °C, 60 min); desorption (300 °C, 12 min)	not applicable	GC-MS	LR – 0.1-10 ng/g RSD – 6.9-9.9% LOD – 0.013-0.078 ng/g Rec – 78.2-99.2%	2007	[192]

Table 1.11. Studies found in the literature about the analytical methods for PBDEs quantification in soils (continued).

Analytes	Extraction	Clean-up	Instrumental technique	Analytical parameters	Year	Ref.
BDEs 28, 47, 99, 100	HF-LPME 0.5 g soil + 10 mL H_2O with (30% MeOH); decane; 40 °C; 1000 rpm; 20 min	not applicable	GC-MS	LR – 0.2-20 μg/L RSD – <10% LOD – 15.2-40.5 ng/L Rec –84.5-111.7%	2007	[147]
BDEs 3, 15, 28, 47, 99, 139, 153, 154, 183	Soxhlet 1 g soil+ 10 g anhydrous sodium sulfate+ 5 g copper powder; hexane:acetone (1:1, v/v); 12 h	• Multi-step columns of silica gel and activated neutral alumina	GC-MS	RSD – <10% LOD – 0.008-0.1 ng/g (10 g soil) Rec – >60%	2006	[186]
BDEs 15, 47, 49, 85, 99, 100, 153, 154	UAE 2 g sample+ 0.25 g florisil; 8 mL hexane; 360 W; 15 min + HS-SPME PDMS; 5 mL Milli-Q water; adsorption (100 °C, 60 min); desorption (280 °C, 3 min)	not applicable	GC-MS-MS	LR – 1.25-100 ng/g (for BDE-153); 0.5-100 ng/g (for others) RSD – 0.8-14% LOD – 0.01-1.20 ng/g Rec – 92-138%	2006	[193]
BDEs 15, 49, 47, 100, 99, 85, 154, 153	HS-SPME 0.5 g soil+2 mL water; PDMS; adsorption (100 °C, 60 min); desorption (280 °C, 3 min)	not applicable	GC-MS-MS	LR – 0.1-10 ng/g RSD – 1.0-16% LOD – 0.014-0.625 ng/g Rec – 95.7-105.1%	2006	[194]
BDEs 17, 47, 66, 100, 153, 183	Ultrasonication 10 g soil+ 3 g anhydrous sodium sulfate, 5 mL ethyl acetate; 15 min; 2 cycles	• Florisil column – elution with 10 mL of hexane:DCM (1:2, v/v); concentration to 1 mL	GC-MS	LR – 0.01-10 ng/g RSD – 1-9% LOD – 0.002-0.030 ng/g Rec – 81-104%	2006	[188]
BDEs 3, 7, 17, 47, 66, 100, 153, 183	Soxhlet 4 g soil+ 20 g anhydrous sodium sulfate+ 15 g copper powder; hexane:acetone (1:1, v/v); 18 h; concentration to 1 mL	• 2 columns: acidic silica gel (30%, w/w) and activated neutral alumina	GC-MS	RSD – 11-26% LOD – 0.013-0.25 ng/g Rec – 61-118%	2005	[185]

Notes: CCG – chemically converted grapheme; DCM – dichloromethane; ECD – electron capture detector; μECD – micro-cell electron capture detector; GA-MSPD – graphene-assisted matrix solid-phase dispersion; GC – gas chromatography; HF-LPME – hollow-fiber liquid phase microextraction; HS-SPME – headspace solid phase microextraction; LOD – limit of detection; LR – linearity range; MeOH – methanol; MS – mass spectrometry detector; MS-MS – tandem mass spectrometry detector; PDMS – polydimethylsiloxane; PLE – pressurized liquid extraction; Rec – recovery; RSD – relative standard deviation; SPE – solid phase extraction; μ-SPE – micro-solid-phase extraction; UAE – ultrasound-assisted extraction.

However, specific fibers may be needed (copper (II) isonicotinate coordination polymer into a porous polypropylene envelope [190] and PM-β-CD/OH-TSO fiber [192]) and some problems concerning carry-over phenomena have been pointed out. Concerning the purification techniques, soil extracts contain relatively large amounts of elemental sulphur, which would disturb the GC analysis and must be removed [150]. Sulphur removal methodologies comprise the treatment with copper powder, silica modified with $AgNO_3$ in a multi-layer silica column or desulfuration with mercury [150]. Sulphur may be also removed during the extraction by addition of copper powder to a Soxhlet beaker [185, 186] or a PLE cell [180-182]. Another point that should be taken into account, when a soil matrix is extracted, is the organic matter content. Soil samples have high levels of organic matter that compromises the purification via column chromatography [150]. For that reason, the treatment with concentrated sulfuric acid is sometimes required prior to the subsequent purification steps [181, 187]. The purification and fractionation of the extract is performed using a great variety of adsorbents: silica [182, 183, 185, 186, 189], florisil [180, 181, 188], GPC [182] and alumina [182, 185-187]. Finally, the extract is concentrated before the analysis.

The general problem in the analysis of complex samples like soils is linked to the large number of matrix components, still after exhaustive extraction techniques, which may coelute with the analytes, disturbing the quantitative analysis. Concerning the instrumental analysis, gas chromatography with mass spectrometry detection is the method of choice for PBDEs quantification in soils. The tandem mass spectrometry technique may surpasses others in analytical specificity but it is not widely used due to its relatively poor sensitivity and reproducibility [150].

1.2.3 Sorption of PBDEs on deposits from drinking water networks

As occurred in the last section, no studies about PBDEs adsorption/desorption on deposits from drinking water distribution systems were found in the literature. This topic may have particular relevance in the context of a deliberate or accidental contamination of drinking water networks because the sorption processes may determine the fate, mobility and bioaccessibility or bioavailability of PBDEs in this field. Again, due to the lack of information concerning this topic, the soil sorption studies were checked for

comparison purposes. Even so, few studies on this matrix were found in the open scientific literature. A brief description of the available studies is presented below.

Mueller et al. (2006) monitored the extractability of BDE-47, 99 and 100 from soils contaminated with an environmentally relevant level of a commercial penta-BDE mixture. Additionally, they studied the influence of plants (radish and zucchini) on penta-BDE behavior in soil [195]. They demonstrated that the reduced recovery of PBDEs from soils (less than 7%) is attributed to abiotic sorption processes [195]. Monoculture plantings did not affect the recovery of PBDEs from soil but, interspecific plant interactions may enhance their bioavailability in soil and increase the human exposure risk [195].

Liu et al. (2010) focused on the sorption dynamics of BDE-28 and BDE-47 on soils [196]. They show that the two-compartment first-order kinetic model is the one that better describes the experimental results. This model is characterized by a fast sorption at the beginning (0-5 h) and a subsequent phase of slow sorption (9-265 h) [196]. They assumed that the first stage of sorption may correspond to the adsorption on soil organic matter (SOM) fractions with loose structure and mostly located in the outer sphere of SOM, while the slow sorption may be associated to the sorption of BDE-28 and BDE-47 to the SOM fractions with condensed conformation and mostly distributed in inner sphere of SOM [196]. One year later, they characterized BDE-28 and -47 sorption isotherms using the same set of soil samples [197]. They reported satisfactory fittings of isothermal data with both linear distribution and non-linear Freundlich models [197]. Afterwards, the same research group published another study about BDE-28 and -47 focusing, at this time, on the desorption kinetics and isothermal characteristics of these two PBDEs in soils [198]. They found an appropriate description of the BDE-28 and -47 desorption results by the two (rapid and slow)-compartment first-order kinetic model and concluded that the SOM constituents are once again the main responsible for these findings [198]. Concerning the desorption isotherms, both linear distribution and nonlinear Freundlich models were identified as being the most suitable for description of their results [198].

Olshansky et al. 2011 studied the adsorption and desorption behaviors of BDE-15 in soils. The authors concluded that the amount and the structure/properties of the SOM affect BDE-15 sorption to soils [199]. The sorptive capacities obtained for humin are higher than that obtained for the corresponding soil. They advanced that a possible reason for that observation is the fact that during the isolation of humin, by humic and fulvic fractions

removal, the non-polar polyethylene domains are exposed enhancing the adsorption efficiency for hydrophobic organic compounds [200, 201]. Concerning the desorption phenomenon, negligible or no desorption was reported for soil samples in contrast to humin, where desorption isotherm hysteresis was not pronounced [199]. Pronounced desorption isotherm hysteresis attained for soil samples may be induced by irreversible chemical binding, physical entrapment of molecules within the SOM matrix and/or by deformation of the sorbent matrix [199]. In sum, PBDEs sequestration from soils is probably governed by other SOM constituents and not by humin [199].

More recently, Xin and co-workers investigated the adsorption and desorption behaviors of BDE-47 in single system and in binary system (in the presence of BDE-209) [202]. They also concluded that the adsorption/desorption of BDE-47 on/from soils are really affected not only by the amount but also by the structure and properties of the SOM. It seems that condensed SOM (including kerogen, BC and humic acid in glassy state) exhibits higher capacities [202]. They verified that BDE-209 can suppress the sorption of BDE-47, but the latest caused no effect on BDE-209 sorption, which can be attributed to the higher accessibility of more hydrophobic molecules to adsorption sites [202]. Once again, irreversible surface adsorption between sorbent and sorbate was reported, which is supported by the desorption hysteresis obtained [202]. More hysteretic BDE-47 desorption isotherms were achieved in the presence of BDE-209 may be due to the accelerated sorbent state transition and the creation of new sites after BDE-209 sorption [202].

In short, it is of widely concern that the adsorption/desorption of PBDEs on/from soils is highly influenced by the amount and composition of SOM. The hydrophobicity of congeners was proposed to account for their affinity to adsorption sites [202]. PBDEs sorption on soils can be considered irreversible (negligible or no PBDEs recoveries from soils were reported) [199]. Interspecific plant interactions may potentiate the human exposure risk by enhancing PBDEs bioavailability in soils [195]. This may have considerable consequences regarding the long-term fate of PBDEs in soils planted with a multi species of plants.

The levels of total organic carbon exhibited by the soils studied in previous studies (0.09-1.07% [199] and 0.13-0.70% [202]) are similar to the organic contents determined in deposits analyzed during this thesis (0.2-1.0 wt.%). Although the SOM properties were

not known for deposits, it may be advanced that, attending only on the organic content, similar sorption behaviors can be expected on both soil and deposit matrices.

1.2.4 Degradation technologies for PBDEs in waters

1.2.4.1 Overview

Degradation of PBDEs in waters is a research topic really scarcely addressed. In fact, it seems very difficult to carry out experiments in pure water due to the extremely low solubility of PBDEs in this solvent, which significantly enhances any sorption process on container walls or other materials used during the experiments [203]. Additionally, transparency to UVB light and the ability to act as a hydrogen donor are favorable properties of some organic solvents that suggest facile reaction in these solvents [203]. So, the tendency adopted by most researchers was to start by exploring the PBDEs degradation behaviors in other kind of solvents: hexane [159, 203], MeOH [204, 205], mixtures of MeOH/H_2O [206, 207], THF [205, 208, 209], mixtures of THF/H_2O [210-212], ACN [213, 214], acetone/H_2O [215], mixtures of hexane/benzene/acetone [216]. However, care must be taken because the kinetic constants, degradation mechanisms and reaction products may be drastically influenced by the conditions under which the reaction is processed and some predictions concerning real scenarios may clearly fail.

Different approaches are available in the literature for PBDEs degradation in liquids. Proposal technologies are hydrothermal [217] and electrolytic degradation methodologies [206, 209], photocatalysis [208, 212, 213, 218], photolysis [159, 203, 205, 207, 214, 216, 219, 220] and other remediation techniques [204, 210, 211, 215, 221-223]. Figure 1.3 depicts the weight of each methodology (in percentage) for the overall studies found in the literature concerning this research topic; as can be observed, photolysis is the most studied technique.

Concerning the most PBDE congeners investigated, it can be concluded from Figure 1.4 that BDE-209 is the most studied congener followed by BDE-47. A total contribution of only 18% is reserved for the investigation of other PBDEs. It seems that a great concern exists about the BDE-209 degradation behavior in liquid media, driven by the necessity of understand what happens to this congener in the aqueous environment. Even so, BDE-209 is the congener less soluble in water (EPI Suite TM, copyright 2000-2012 Environmental Protection Agency, United States) and, for that reason, it is not expected

that considerable soluble concentrations will be found in the water courses. Additionally, is generally considered to be highly recalcitrant but safe [223].

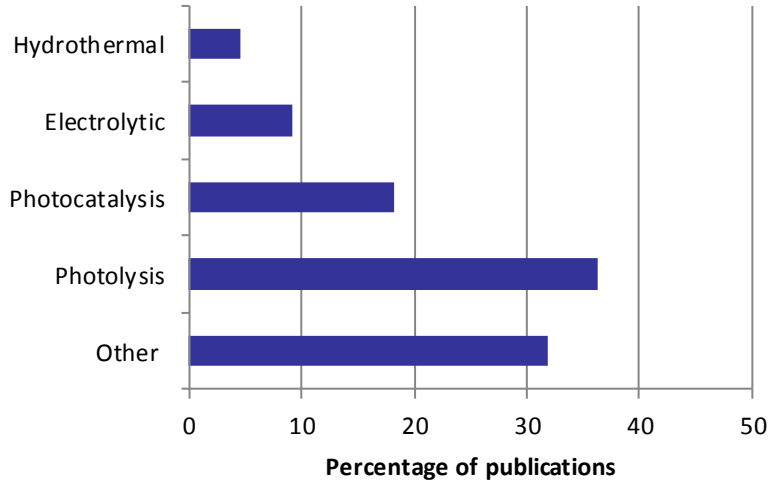

Figure 1.3. Relative contribution of the different degradation technologies used for the treatment of liquids contaminated with PBDEs (search in Scopus data base, from 2003 to 2013).

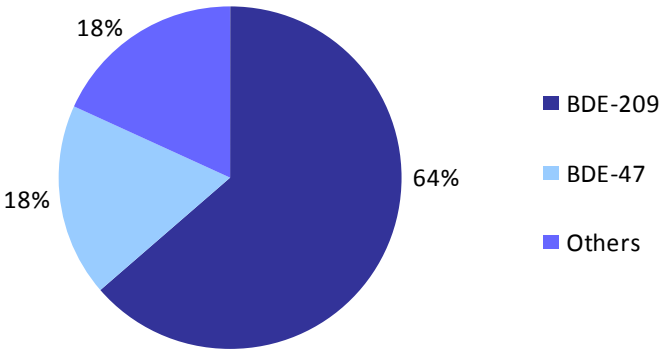

Figure 1.4. Most studied PBDEs congeners (search in Scopus data base, from 2003 to 2013).

On the other hand, BDE-209 is the main congener present in the available deca-BDE commercial mixture [152], and the need to know which lower brominated congeners may

occur in the environment, as a result of BDE-209 decomposition (even at a limit extent), may justify such big investment. Indeed, BDE-209 may be a source of environmentally abundant BDEs (BDEs 47, 99, 100, 154 and 183) [223] and a source of metabolites with high toxicity. Lower PBDEs are actually more persistent, bioaccumulative and toxic [152, 157-159].

Figure 1.5 illustrates the number of studies performed with BDE-209, BDE-47 and other PBDEs using different degradation processes. As demonstrated, hydrothermal and photocatalysis approaches were implemented only for BDE-209 degradation purposes [208, 212, 213, 217, 218]. Electrolytic technique was only tested in order to degrade the two most studied congeners (BDE-209 and BDE-47) [206, 209].

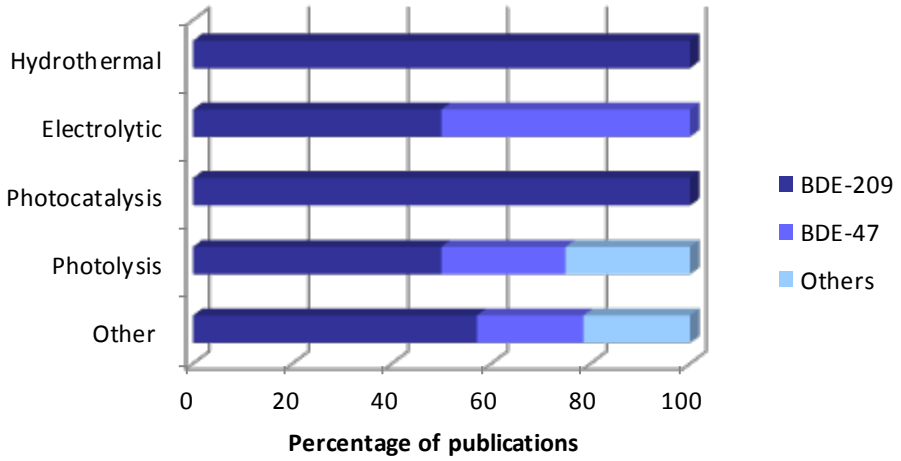

Figure 1.5. Number of publications performed with BDE-209, BDE-47 and others using different degradation processes (search in data base Scopus, from 2003 to 2013).

Another relevant aspect that deserves attention is the initial concentration of the parent compound in PBDEs degradation studies. Most of the available studies are conducted with high initial parent compound concentrations (1-1000 mg/L), fact that is possible due to the high solubility of these compounds in organic solvents, which are always used in the preparation of the starting solutions [203-206, 209-211, 213, 216, 222]. Figure 1.6 shows that around 70% of the studies about PBDEs degradation in liquids are performed starting from concentrations at ppm levels, extremely above of the PBDEs' water solubility. Again, this is another point that contributes to the deviation from real case scenarios, complicating any extrapolation analysis. It is also evident from Figure 1.6 that

the monitorization of PBDEs at lower levels requires highly sensitive methodologies such as GC-ECD and even GC-MS instead of others (LC-UV/DAD). Additionally, concentration procedures may be required at ppb levels prior to the instrumental analysis [214, 217, 220].For simplicity reasons, among the degradation processes above reported, only the photolysis studies were considered for scrupulous analysis.

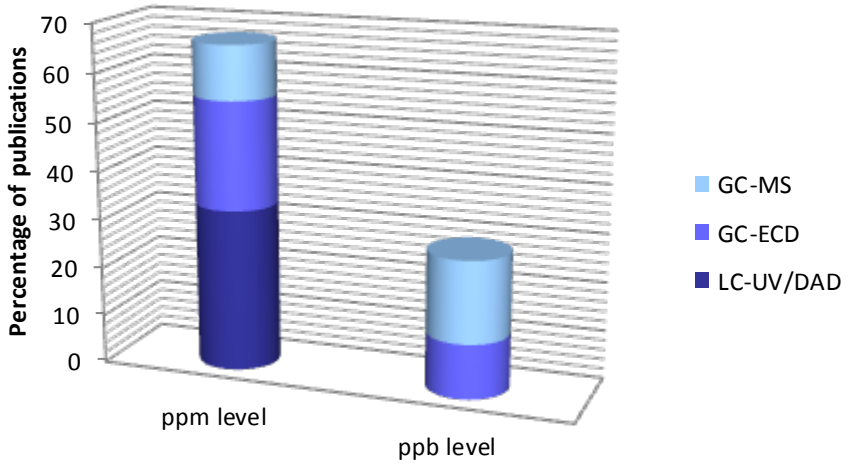

Figure 1.6. Percentage of publications about PBDEs degradation in liquids conducted at ppm and ppb levels and analytical techniques used.

Two reasons were taken into account for this choice: the fact of being the most applied technology in the PBDEs degradation studies and the fact of being explored during this thesis in the particular case of BDE-100 degradation in water (Chapter 7).

1.2.4.2 The particular case of the photolysis process

All studies found about PBDEs photodegradation in liquid mediums are compiled in Table 1.12. As can be seen, the photodegradation of PBDEs typically follows a pseudo-first order kinetic model. The photoreactivity of PBDEs depends on several aspects being one of them the degree of bromination [159, 207]. Generally, higher brominated diphenyl ethers degrade faster than the lowers because the first absorb more and at longer wavelengths, closer to the lamp spectra [159, 207]. On the other hand, HOMO energies (the energy of the highest occupied molecular orbital) increase with increasing number of bromine substituents, except for BDE-100 [159]. So, the increase of the number of bromine substituents leads to an increase of the degradation rate [159].

Table 1.12. Studies found in the literature concerning the photodegradation studies of PBDEs in liquid mediums.

PBDE congeners	Initial Concentration	Matrix	Operating conditions	Taken volumes	Extraction/clean-up	Analytical method	Results and comments	Ref.
BDEs 209, 208, 207, 206, 203, 190, 183, 181, 155, 154, 139, 138, 99, 77, 47	1×10^{-6} M (1 mg/L for BDE-209 and 0.5 mg/L for BDE-47)	MeOH:H_2O (80:20, v/v); MeOH; THF	**Radiation source:** 20 W UV lamp (Philips)	5 mL for solutions in THF; the necessary for injection for other solvents.	Only for samples in THF: 5 mL sample + 10 mL of a mixture of ACN:H_2O (75:25)	HPLC-UV	**Kinetic:** 1st order reaction **Rate constants:** ranging from 0.003 h^{-1} (BDE-47) to 1.44 h^{-1} (BDE-209) in MeOH:H_2O; from 0.004 h^{-1} (BDE-47) to 2.34 h^{-1} (BDE-209) in MeOH; from 0.007 h^{-1} (BDE-47) to 2.99 h^{-1} (BDE-209) in THF. **Degradation products:** lower brominated diphenyl ethers and PBDFs.	[207]
BDE-153	0.8 μg/L	ACN; Distilled water; Seawater	**Radiation source:** 6 W UV-lamp (302 nm) or solar light	100 μL	**For distilled water and seawater:** filtration with $MgSO_4$; wash with 3×250 μL toluene:DCM (1:1, v/v); reduction volume to 25 μL under nitrogen flow and T. **For ACN:** reduction volume to 25 μL under nitrogen flow and T.	HRGC-HRMS	**Kinetic:** 1st order reaction **Rate constants:** 26±6 h^{-1} in ACN; 9±2 h^{-1} in seawater; could not be calculated in distilled water. **Degradation products:** lower brominated PBDEs, 1,2,4,7,8-PeBDF and tetrabrominated 2-hydroxybiphenyls (BDE-153 in ACN); only lower brominated PBDEs (BDE-153 in distilled and sea-waters).	[214]

Table 1.12. Studies found in the literature concerning the photodegradation studies of PBDEs in liquid mediums (continued).

PBDE congeners	Initial Concentration	Matrix	Operating conditions	Taken volumes	Extraction/clean-up	Analytical method	Results and comments	Ref.
BDE-209	2-5 mg/L	Hexane	**Radiation source:** solar light	1 mL	**Not applicable**	GC-μECD (quantification) GC-MS (identification)	**Kinetic:** 1st order reaction **Rate constants:** 6.70 h^{-1} (July 2 of 2003), 4.00 h^{-1} (October 23 of 2003). **Main mechanism**: consecutive reductive debromination **Degradation products:** lower brominated PBDEs (43 BDEs were detected and 21 of them were identified).	[203]
BDEs 28, 47, 99, 100, 153 and 183	10 μg/L	Hexane	**Radiation source:** Hg 500 W filtered with Pyrex glass **Irradiation time:** 40 h	The necessary for injection	**Not applicable**	GC-ECD	**Kinetic:** 1st order reaction **Rate constants:** ranging from 0.10 h^{-1} (BDE-100) to 2.64 h^{-1} (BDE-183) **Main mechanism**: consecutive reductive debromination **Photoreactivity of bromines**: decrease from *ortho* to *para* positions for less brominated PBDEs; no differences were observed for higher brominated congeners. **Degradation products:** lower brominated PBDEs.	[159]

Table 1.12. Studies found in the literature concerning the photodegradation studies of PBDEs in liquid mediums (continued).

PBDE congeners	Initial Concentration	Matrix	Operating conditions	Taken volumes	Extraction/clean-up	Analytical method	Results and comments	Ref.
Deca-BDE	1×10^{-6} M (1 mg/L for BDE-209)	THF MeOH THF/MeOH	**Radiation source:** Fluorescent tube TL 20 W/09N from Philips **Irradiation time:** 100-200 min	500 mL	Evaporation to dryness; reconstitution with 4 mL of *n*-Hexane.	GC-MS (identification and quantification of degradation products)	**Main mechanism**: consecutive reductive debromination, intramolecular elimination of HBr. **Degradation products:** hexa- to nona-BDEs, mono- to penta-BDFs and methoxylated tetra- to penta-BDFs	[205]
BDE-99	3 to 63 μg/L	H_2O Aqueous surfactant solution (Brij 35 and Brij 58)	**Radiation source:** two low-pressure Hg lamps (254 nm, 2.28×10^{-7} Einstein L^{-1} s^{-1}).	4 mL	**LLE** Extraction with hexane (2×); concentration to 1 mL under nitrogen flow at 40 °C for GC-ECD or to 100 μL for GC-MC analysis.	GC-μECD and GC-MS (same samples)	**Kinetic:** pseudo first-order **Rate constants:** ranged from 4.10 to 5.36 h^{-1} in surfactant solutions; 2.20 h^{-1} in H_2O. **Main mechanism:** consecutive reductive debromination or intramolecular elimination of HBr. **Degradation products:** lower brominated PBDEs (mono- to tetra-) and lower brominated PBDFs (mono- to tetra-). **Toxicity/Biodegradability:** PBDFs are more toxic photoproducts.	[219]

Table 1.12. Studies found in the literature concerning the photodegradation studies of PBDEs in liquid mediums (continued).

PBDE congeners	Initial Concentration	Matrix	Operating conditions	Taken volumes	Extraction/clean-up	Analytical method	Results and comments	Ref.
BDE-100	5 μg/L	H_2O (ice and liquid)	**Freezer process:** in a laboratory freezer at -20 °C. **Ice solid samples dimensions:** 6 cm diameter and 0.8 cm height. **Radiation source:** two 8 W low-pressure Hg lamps (254 nm). **Irradiation:** maximum 10 min	22 mL	**HS-SPME** Sample volume – 10 mL Fiber – PDMS Extraction temperature – 100 °C Extraction time – 45 min	GC-MS	**Kinetic:** 1st order reaction **Rate constants:** 10.68 h^{-1} (ice), 9.72 h^{-1} (water) **Main mechanism:** consecutive reductive debromination and intramolecular elimination of HBr. **Degradation products:** lower brominated PBDEs and PBDFs.	[220]
Deca-BDE	100 mg/L	Hexane: benzene: acetone (8:1:1, v/v)	**Radiation source:** Hg lamp (254 nm) and sun light **Irradiation time:** 16 h	5 mL	**Not applicable**	GC-ECD (quantification) GC-MS (identification)	**Main mechanism:** consecutive reductive debromination. **Degradation products:** lower brominated PBDEs (tri- to octa-) and lower brominated PBDFs (mono- to hexa-).	[216]

Notes: ACN – acetonitrile; ECD – electron capture detector; μECD – micro-cell electron capture detector; GC – gas chromatography; HRGC-HRMS – high resolution gas chromatography–mass spectrometry; HS-SPME – headspace solid phase microextraction; LC – liquid chromatography; MeOH – methanol; MS – mass spectrometry detector; THF – tetrahydrofuran; UV – ultraviolet.

BDE-100 fails this rule and is more difficult to degrade than expected due to its stability that is conferred by the specific brominated phenyl ring with a 2,4,6 substitution pattern [159]. Indeed, the position of the substituted bromines is another factor that affects the PBDEs photoreactivity. Fang et al. demonstrated that for lower brominated congeners, bromines at *ortho* position showed higher photoreactivity than those at *para* positions, while for higher brominated PBDEs congeners the difference became insignificant [159]. Beyond the natural PBDEs photoreactivity, the reaction rate can be influenced by other parameters such as the type of the solvent/reaction medium [214, 219, 220] and the intensity and kind of radiation used [205].

Photodegradation of PBDEs generally leads to the formation of lower brominated PBDE congeners by consecutive reductive debromination. Photoproducts with lower bromine content are more persistent and bioavailable than the parent ones [220]. Sequential dehalogenation is often reported as the main mechanism involved in the photodegradation of PBDEs under solar light [203] or UV radiation [159, 205, 207]. However, other relevant degradation pathways may occur and are responsible for the formation of other classes of compounds. One of the most important is the dibenzofuran-type ring closure process via an intermolecular elimination of HBr, which is responsible for the formation of polybrominated dibenzofurans – PBDFs [214, 216, 219, 220]. In fact, it has been widely reported that PBDFs are more toxic compounds than the original ones (PBDEs) [214, 219, 220]. Another possible degradation pathway is the fragmentation to form phenols [205, 216]. Excited degradation by-products may also react with the surrounding solvent. Protic solvents, MeOH and H_2O for example, may lead to the formation of methoxylated or hydroxylated species, respectively [205]. These reactions are responsible for the following findings: MeO-PBDEs, OH-PBDEs, MeO-PBDFs, OH-PBDFs... Nevertheless, the formation of some of these compounds may be unlikely to take place under natural conditions such as MeO-PBDFs [205].

It is finally worth stressing that the degradation pathways as well as the reaction products may be significantly affected by the conditions under which the reaction takes place and experiments under conditions closer to the reality are encouraged (in water and at lower initial concentrations) in order to overcome the great gap concerning this research topic. Preliminary results concerning this new research topic are presented in Chapter 7.

1.3 References

[1] WHO, *Hazards in drinking-water supply and waste management*, in: Health aspects of plumbing, 2006.

[2] J. Fawell and A.D. Hulsmann, *Health effects of chemical contamination of drinking water supplies*, in: Water and Health.

[3] P.H. Gleick, G.H. Wolff, H. Cooley, M. Palaniappan, A. Samulon, E. Lee, J. Morrison and D. Katz, *The World's Water 2006-2007: The Biennial Report on Freshwater Resources*, Island Press, 2006.

[4] P.H. Gleick, *Water and terrorism*, Water policy 8 (2006) 481-503.

[5] SecurEau, http://www.secureau.eu/, retrieved on 05-10-2013.

[6] Y. Picó, G. Font, J.C. Moltó and J. Mañes, *Solid-phase extraction of quaternary ammonium herbicides*, J. Chromatogr. A 885 (2000) 251-271.

[7] Paraquat Information Center, http://paraquat.com/, retrieved on 06-06-2013.

[8] H.J. Beckie, *Herbicide-resistant weed management: focus on glyphosate*, Pest Manag. Sci. 67 (2011) 1037-1048.

[9] T.W. Eubank, D.H. Poston, V.K. Nandula, C.H. Koger, D.R. Shaw and D.B. Reynolds, *Glyphosate-resistant Horseweed (Conyza canadensis) Control Using Glyphosate-, Paraquat-, and Glufosinate-Based Herbicide Programs*, Weed Technol. 22 (2008) 16-21.

[10] D. de Souza, L. Codognoto, S.A.S. Machado and L.A. Avaca, *Electroanalytical determination of the herbicide paraquat in natural water and commercial tea samples with gold electrodes obtained from recordable compact disc*, Anal Lett 38 (2005) 331-341.

[11] I.C. Lopes, D. de Souza, S.A.S. Machado and A.A. Tanaka, *Voltammetric detection of paraquat pesticide on a phthalocyanine-based pyrolitic graphite electrode*, Anal. Bioanal. Chem. 388 (2007) 1907-1914.

[12] N. Mai, X. Liu, W. Wei, S. Luo and W. Liu, *Electrochemical determination of paraquat using a DNA-modified carbon ionic liquid electrode*, Microchim Acta 174 (2011) 89-95.

[13] G.C. Schmitt, C. Paniz, D. Grotto, J. Valentini, K.L. Schott, V.J. Pomblum and S.C. Garcia, *Aspectos gerais e diagnóstico clinicolaboratorial da intoxicação por paraquat*, J. Bras. Patol. Med. Lab. 42 (2006) 235-243.

[14] L.R. Goldfrank and N.E. Flomenbau, *Goldfrank's Toxicological Emergencies*, 6th ed., McGraw-Hill Professional Publishing, 1998.

[15] A.M. Tsatsakis, K. Perakis and E. Koumantakis, *Experience with acute paraquat poisoning in Crete*, Vet. Hum. Toxicol. 38 (1996) 113-117.

[16] C.M. Chen and A.C. Lua, *Lung toxicity of paraquat in the rat*, J. Toxicol. Environ. Health A. 60 (2000) 477-487.

[17] G.R. Sagar, *Uses and Usefulness of Paraquat*, Hum. Exp. Toxicol. 6 (1987) 7-11.

[18] B.G. Stephens and S.K. Moormeister, *Homicidal Poisoning by Paraquat*, Am. J. Forensic Med. Pathol. 18 (1997) 33-39.

[19] C.D. Klaassen, M.O. Amdur and J. Doull, *Casarett and Doull's Toxicology: The basic science of poisons*, Macmillan Publishing Company, New York, 1986.

[20] M.A. El Mhammedi, M. Bakasse and A. Chtaini, *Electrochemical studies and square wave voltammetry of paraquat at natural phosphate modified carbon paste electrode*, J. Hazard. Mater. 145 (2007) 1-7.

[21] R.J. Dinis-Oliveira, F. Remião, H. Carmo, J.A. Duarte, A.S. Navarro, M.L. Bastos and F. Carvalho, *Paraquat exposure as an etiological factor of Parkinson's disease*, NeuroToxicology 27 (2006) 1110-1122.

[22] R. Franco, S. Li, H. Rodriguez-Rocha, M. Burns and M.I. Panayiotidis, *Molecular mechanisms of pesticide-induced neurotoxicity: Relevance to Parkinson's disease*, Chem. Biol. Interact. 188 (2010) 289-300.

[23] M.A. El Mhammedi, M. Bakasse and A. Chtainia, *Square-wave voltammetric determination of paraquat at carbon paste electrode modified with hydroxyapatite*, Electroanal. 19 (2007) 1727-1733.

[24] U.M.F. de Oliveira, J. Lichtig and J.C. Masini, *Evaluation of a nafion coated glassy carbon electrode for determination of paraquat by differential pulse voltammetry*, J. Braz. Chem. Soc. 15 (2004) 735-741.

[25] M. Ibáñez, Y. Picó and J. Mañes, *Improving the solid-phase extraction of 'quat' pesticides from water samples: Removal of interferences*, J. Chromatogr. A 823 (1998) 137-146.

[26] T.M. Chichila and S.M. Walters, *Liquid chromatographic determination of paraquat and diquat in crops using a silica column with aqueous ionic mobile phase*, J. Assoc. Off. Anal. Chem. 74 (1991) 961-967.

[27] Official Journal of the European Union, *Council Directive 98/83/CE*, 1998.

[28] H. Muhamad, B. Ismail, M. Sameni and N. Mat, *Adsorption study of 14C-paraquat in two Malaysian agricultural soils*, Environ. Monit. Assess. 176 (2011) 43-50.

[29] M. Pateiro-Moure, C. Pérez-Novo, M. Arias-Estévez, R. Rial-Otero and J. Simal-Gándara, *Effect of organic matter and iron oxides on quaternary herbicide sorption–desorption in vineyard-devoted soils*, J. Colloid Interface Sci. 333 (2009) 431-438.

[30] M. Pateiro-Moure, C. Pérez-Novo, M. Arias-Estévez, E. López-Periago, E. Martínez-Carballo and J. Simal-Gándara, *Influence of Copper on the Adsorption and Desorption of Paraquat, Diquat, and Difenzoquat in Vineyard Acid Soils*, J. Agric. Food Chem. 55 (2007) 6219-6226.

[31] M. Pateiro-Moure, A. Bermúdez-Couso, D. Fernández-Calviño, M. Arias-Estévez, R. Rial-Otero and J. Simal-Gándara, *Paraquat and Diquat Sorption on Iron Oxide Coated Quartz Particles and the Effect of Phosphates*, J. Chem. Eng. Data 55 (2010) 2668-2672.

[32] U.B. Cheah, R.C. Kirkwood and K.Y. Lum, *Adsorption, Desorption and Mobility of Four Commonly Used Pesticides in Malaysian Agricultural Soils*, Pestic. Sci. 50 (1997) 53-63.

[33] B.V. Tucker, D.E. Pack and J.N. Ospenson, *Adsorption of bipyridylium herbicides in soil*, J. Agric. Food. Chem. 15 (1967) 1005-1008.

[34] K.M. Spark and R.S. Swift, *Effect of soil composition and dissolved organic matter on pesticide sorption*, Sci. Total Environ. 298 (2002) 147-161.

[35] M. Arienzo and A. Buondonno, *Adsorption of paraquat by Terra Rossa soil and model soil aggregates*, Toxicol. Environ. Chem. 39 (1993) 193-199.

[36] W. Amondham, P. Parkpian, C. Polprasert, R.D. Delaune and A. Jugsujinda, *Paraquat Adsorption, Degradation, and Remobilization in Tropical Soils of Thailand*, J. Environ. Sci. Health, Part B 41 (2006) 485-507.

[37] C.C. Ainsworth, J.K. Fredrickson and S.C. Smith, *The effect of sorption on the degradation of aromatic acids and bases*, Washington, DC, 1992.

[38] A. de Keizer, *Adsorption of paraquat ions on clay minerals. Electrophoresis of clay particles.*, Progr. Colloid Polym. Sci. 83 (1990) 118-126.

[39] K. Draoui, R. Denoyel, M. Chgoura and J. Rouquerol, *Adsorption of Paraquat on minerals: A thermodynamic study*, J. Therm. Anal. Calorim. 58 (1999) 597-606.

[40] M. Raupach, W.W. Emerson and P.G. Slade, *The arrangement of paraquat bound by vermiculite and montmorillonite*, J. Colloid Interface Sci. 69 (1979) 398-408.

[41] P.C. Kearney and D.D.V. Kaufman, *Herbicides: chemistry, degradation, and mode of action*, 1st ed., CRC Press, 1988.

[42] M. Fernández, M. Ibáñez, Y. Picó and J. Mañes, *Spatial and Temporal Trends of Paraquat, Diquat, and Difenzoquat Contamination in Water from Marsh Areas of the Valencian Community (Spain)*, Arch. Environ. Contam. Toxicol. 35 (1998) 377-384.

[43] S.D.W. Committee and N.R. Council, *Drinking Water and Health,Volume 1*, The National Academies Press, 1977.

[44] WHO, *Public health response to biological and chemical weapons-WHO guidance*, 2nd ed., Geneva, 2004.

[45] E. Mallat, C. Barzen, R. Abuknesha, G. Gauglitz and D. Barceló, *Fast determination of paraquat residues in water by an optical immunosensor and validation using capillary electrophoresis-ultraviolet detection*, Anal. Chim. Acta 427 (2001) 165-171.

[46] R. Castro, E. Moyano and M.T. Galceran, *On-line ion-pair solid-phase extraction–liquid chromatography–mass spectrometry for the analysis of quaternary ammonium herbicides*, J. Chromatogr. A 869 (2000) 441-449.

[47] O. Núñez, E. Moyano and M.T. Galceran, *Time-of-flight high resolution versus triple quadrupole tandem mass spectrometry for the analysis of quaternary ammonium herbicides in drinking water*, Anal. Chim. Acta 525 (2004) 183-190.

[48] J.C. Marr and J.B. King, *A simple high performance liquid chromatography/ionspray tandem mass spectrometry method for the direct determination of paraquat and diquat in water*, Rapid Commun. Mass Spectrom. 11 (1997) 479-483.

[49] S. Rodriguez-Mozaz, M.J. Lopez de Alda and D. Barceló, *Advantages and limitations of on-line solid phase extraction coupled to liquid chromatography–mass spectrometry technologies versus biosensors for monitoring of emerging contaminants in water*, J. Chromatogr. A 1152 (2007) 97-115.

[50] B. Saad, M.M. Ariffin and M.I. Saleh, *Paraquat sensors containing membrane components of high lipophilicities*, Anal. Chim. Acta 338 (1997) 89-96.

[51] W.H. van der Schalie, R.R. James and T.P. Gargan II, *Selection of a battery of rapid toxicity sensors for drinking water evaluation*, Biosens. Bioelectron. 22 (2006) 18-27.

[52] L.C.S. de Figueiredo-Filho, V.B. dos Santosa, B.C. Janegitz, T.B. Guerreiro, O. Fatibello-Filho, R.C. Faria and L.H. Marcolino-Junior, *Differential pulse voltammetric determination of paraquat using a bismuth-film electrode*, Electroanal. 22 (2010) 1260-1266.

[53] D. de Souza and S.A.S. Machado, *Study of the electrochemical behavior and sensitive detection of pesticides using microelectrodes allied to square-wave voltammetry*, Electroanal. 18 (2006) 862-872.

[54] A. Economou and P.R. Fielden, *Mercury film electrodes: developments, trends and potentialities for electroanalysis*, Analyst 128 (2003) 205-212.

[55] C.D.C. Conceição, R.C. Faria, O. Fatibello and A.A. Tanaka, *Electrocatalytic oxidation and voltammetric determination of hydrazine in industrial boiler feed water using a cobalt phthalocyanine-modified electrode*, Anal. Lett. 41 (2008) 1010-1021.

[56] J. Wang, J.M. Lu, S.B. Hocevar, P.A.M. Farias and B. Ogorevc, *Bismuth-coated carbon electrodes for anodic stripping voltammetry*, Anal. Chem. 72 (2000) 3218-3222.

[57] D. de Souza and S.A.S. Machado, *Electroanalytical study of the paraquat herbicide in aqueous solution by square wave voltammetry using ultramicroelectrodes*, Quím. Nova 26 (2003) 644-647.

[58] D.D. de Souza, S.A.S. Machado and R.C. Pires, *Multiple square wave voltammetry for analytical determination of paraquat in natural water, food, and beverages using microelectrodes*, Talanta 69 (2006) 1200-1207.

[59] D. de Souza and S.A.S. Machado, *Electrochemical detection of the herbicide paraquat in natural water and citric fruit juices using microelectrodes*, Anal. Chim. Acta 546 (2005) 85-91.

[60] T.G. Díaz, A.G. Cabanillas and F. Salinas, *Square-wave and differential pulse oxidative voltammetric determination of diquat and paraquat in alkaline medium*, Electroanal. 12 (2000) 616-621.

[61] L.L.C. Garcia, L.C.S. Figueiredo-Filho, G.G. Oliveira, O. Fatibello-Filho and C.E. Banks, *Square-wave voltammetric determination of paraquat using a glassy carbon electrode modified with multiwalled carbon nanotubes within a dihexadecylhydrogenphosphate (DHP) film*, Sensor. Actuat. B-Chem. 181 (2013) 306-311.

[62] J.M. Zen, S.H. Jeng and H.J. Chen, *Determination of paraquat by square-wave voltammetry at a perfluorosulfonated lonomer/clay-modified electrode*, Anal. Chem. 68 (1996) 498-502.

[63] M.A. El Mhammedi, M. Bakasse, R. Bachirat and A. Chtaini, *Square wave voltammetry for analytical determination of paraquat at carbon paste electrode modified with fluoroapatite*, Food Chem. 110 (2008) 1001-1006.

[64] T.H. Lu and I.W. Sun, *Electrocatalytic determination of paraquat using a nafion film coated glassy carbon electrode*, Talanta 53 (2000) 443-451.

[65] L.B.O. dos Santos, C.M.C. Infante and J.C. Masini, *Development of a sequential injection-square wave voltammetry method for determination of paraquat in water samples employing the hanging mercury drop electrode*, Anal. Bioanal. Chem. 396 (2010) 1897-1903.

[66] A. Walcarius and L. Lamberts, *Square wave voltammetric determination of paraquat and diquat in aqueous solution*, J. Electroanal. Chem. 406 (1996) 59-68.

[67] J.A. Ribeiro, C.A. Carreira, H.J. Lee, F. Silva, A. Martins and C.M. Pereira, *Voltammetric determination of paraquat at DNA-gold nanoparticle composite electrodes*, Electrochim. Acta 55 (2010) 7892-7896.

[68] A.J. Bard, *Electroanalytical Chemistry: A series of advances*, Dekker: New York, 1990.

[69] D. de Souza, S.A.S. Machado and L.A. Avaca, *Square wave voltammetry. Part I: Theoretical aspects*, Quím. Nova 26 (2003) 81-89.

[70] L. Ramaley and M.S. Krause Jr, *Theory of square wave voltammetry*, Anal. Chem. 41 (1969) 1362-1365.

[71] J.H. Christie, J.A. Turner and R.A. Osteryoung, *Square wave voltammetry at the dropping mercury electrode: Theory*, Anal. Chem. 49 (1977) 1899-1903.

[72] M. Lovrić and Š. Komorsky-Lovric, *Square-wave voltammetry of an adsorbed reactant*, J. Electroanal. Chem. 248 (1988) 239-253.

[73] N. Fatouros, J.P. Simonin, J. Chevalet and R.M. Reeves, *Theory of multiple square wave voltammetries*, J. Electroanal.Chem. 213 (1986) 1-16.

[74] D. Krulic, N. Fatouros and J. Chevalet, *Multiple square wave voltammetry: experimental verification of the theory*, J. Electroanal. Chem. 287 (1990) 215-227.

[75] J. Chevalet, G.Y. Champagne, L. Gastonguay, R. Lacasse, M. Ladouceur, N. Fatouros and D. Krulic, *Développement d'instrumentation électroanalytique. Applications aux mesures de faibles concentrations d'espèces électroactives dans divers domaines*, J. Chim. Phys. Phys.-Chim Biol. 93 (1996) 804-817.

[76] P. Ugo, *Trace iron determination by cyclic and multiple square-wave voltammetry at nafion coated electrodes. Application to pore-water analysis*, Electroanal. 13 (2001) 661-668.

[77] L.M. Moretto, J. Chevalet, G.A. Mazzocchin and P. Ugo, *Advances in multiple square wave techniques for ion-exchange voltammetry at ultratrace levels: The europium(III) case*, J. Electroanal. Chem. 498 (2001) 117-126.

[78] L.M. Moretto, B. Brunetti, J. Chevalet and P. Ugo, *Multiple square wave voltammetry of nanomolar and subnanomolar concentrations of europium(III) at polymer-coated electrodes*, Electrochem. Commun. 2 (2000) 175-179.

[79] F.R. Simões, C.M.P. Vaz and C.M.A. Brett, *Electroanalytical Detection of the Pesticide Paraquat by Batch Injection Analysis*, Anal. Lett. 40 (2007) 1800-1810.

[80] L.B.O. dos Santos and J.C. Masini, *Square wave adsorptive cathodic stripping voltammetry automated by sequential injection analysis: Potentialities and limitations exemplified by the determination of methyl parathion in water samples*, Anal. Chim. Acta 606 (2008) 209-216.

[81] L.B.O. dos Santos and J.C. Masini, *Determination of picloram in natural waters employing sequential injection square wave voltammetry using the hanging mercury drop electrode*, Talanta 72 (2007) 1023-1029.

[82] P.C. Schlecht and P.F. O'Connor, *NIOSH Manual of Analytical Methods*, 4th ed., National Institute for Occupational Safety Health, 2003.

[83] R. Castro, E. Moyano and M.T. Galceran, *Determination of quaternary ammonium pesticides by liquid chromatography-electrospray tandem mass spectrometry*, J. Chromatogr. A 914 (2001) 111-121.

[84] R. Castro, E. Moyano and M.T. Galceran, *Ion-trap versus quadrupole for analysis of quaternary ammonium herbicides by LC-MS*, Chromatographia 53 (2001) 273-278.

[85] M.C. Carneiro, L. Puignou and M.T. Galceran, *Comparison of silica and porous graphitic carbon as solid-phase extraction materials for the analysis of cationic herbicides in water by liquid chromatography and capillary electrophoresis*, Anal. Chim. Acta 408 (2000) 263-269.

[86] R. Rial-Otero, B. Cancho-Grande, C. Perez-Lamela, J. Simal-Gándara and M. Arias-Estévez, *Simultaneous determination of the herbicides diquat and paraquat in water*, J. Chromatogr. Sci. 44 (2006) 539-542.

[87] *Simple, sensitive HPLC/UV analysis for paraquat and diquat using high-recovery solid phase extraction and an ultra quat HPLC column*, Restek Corporation, 2005.

[88] M. Ibáñez, Y. Picó and J. Mañes, *Influence of organic matter and surfactants on solid-phase extraction of diquat, paraquat and difenzoquat from waters*, J. Chromatogr. A 727 (1996) 245-252.

[89] J.W. Munch and W.J. Bashe, *Method 549.2 - Determination of diquat and paraquat in drinking water by liquid-solid extraction and high performance liquid chromatography with ultraviolet detection*, U.S. Environmental Protection Agency, Cincinnati, Ohio 45268, 1997.

[90] M. Ibáñez, Y. Picó and J. Mañes, *On-line liquid chromatographic trace enrichment and high-performance liquid chromatographic determination of diquat, paraquat and difenzoquat in water*, J. Chromatogr. A 728 (1996) 325-331.

[91] M. Ibánez, Y. Picó and J. Manes, *On-line determination of bipyridylium herbicides in water by HPLC*, Chromatographia 45 (1997) 402-407.

[92] M. Takino, S. Daishima and K. Yamaguchi, *Determination of diquat and paraquat in water by liquid chromatography/electrospray-mass spectrometry using volatile ion-pairing reagents*, Anal. Sci. 16 (2000) 707-711.

[93] L. Grey, B. Nguyen and P. Yang, *Liquid chromatography-electrospray ionization isotope dilution mass spectrometry analysis of paraquat and diquat using conventional and multilayer solid-phase extraction cartridges*, J. Chromatogr. A 958 (2002) 25-33.

[94] R. Castro, E. Moyano and M.T. Galceran, *Ion-pair liquid chromatography–atmospheric pressure ionization mass spectrometry for the determination of quaternary ammonium herbicides*, J. Chromatogr. A 830 (1999) 145-154.

[95] J.L. Martínez Vidal, A. Belmonte Vega, F.J. Sánchez López and A. Garrido Frenich, *Application of internal quality control to the analysis of quaternary ammonium compounds in surface and groundwater from Andalusia (Spain) by liquid chromatography with mass spectrometry*, J. Chromatogr. A 1050 (2004) 179-184.

[96] V. Taguchi, S.D. Jenkins, P. Crozier and D. Wang, *Determination of diquat and paraquat in water by liquid chromatography-(electrospray ionization) mass spectrometry*, J. Am. Soc. Mass Spectrom. 9 (1998) 830-839.

[97] F. Merino, S. Rubio and D. Pérez-Bendito, *Evaluation and optimization of an on-line admicelle-based extraction-liquid chromatography approach for the analysis of ionic organic compounds*, Anal. Chem. 76 (2004) 3878-3886.

[98] P. Bièvre, *Isotope dilution mass spectrometry: what can it contribute to accuracy in trace analysis?*, Fresenius' J. Anal. Chem. 337 (1990) 766-771.

[99] E. Gelpi, *Advances in Mass Spectrometry*, Wiley, 2001.

[100] K.B. Rundman, *Cast irons*, in: K.H.J. Buschow, R. Cahn, M.C. Flemings, B. Ilschner, E.J. Kramer, S. Mahajan, P. Veyssiere (Eds.) Encyclopedia of Materials: Science and Technology, Pergamon, 2001, pp. 1003-1010.

[101] MAST-Materials Science and Technology, http://matse1.matse.illinois.edu/concrete/prin.html, retrieved on 06-10-2013.

[102] W.R. Sorenson, *Polyvinylchloride*, in: K.H.J. Buschow, R. Cahn, M.C. Flemings, B. Ilschner, E.J. Kramer, S. Mahajan, P. Veyssiere (Eds.) Encyclopedia of Materials: Science and Technology, 2001, pp. 7752-7755.

[103] H.F. Enderle, *Polyethylene: high-density*, in: K.H.J. Buschow, R. Cahn, M.C. Flemings, B. Ilschner, E.J. Kramer, S. Mahajan, P. Veyssiere (Eds.) Encyclopedia of Materials: Science and Technology, 2001, pp. 7172-7180.

[104] F. Echeverría, J.G. Castaño, C. Arroyave, G. Peñuela, A. Ramírez and J. Morató, *Characterization of deposits formed in a water distribution system*, Rev. Chil. Ing. 17 (2009) 275-281.

[105] P. Sarin, V.L. Snoeyink, J. Bebee, W.M. Kriven and J.A. Clement, *Physico-chemical characteristics of corrosion scales in old iron pipes*, Water Res. 35 (2001) 2961-2969.

[106] C.-Y. Peng, G.V. Korshin, R.L. Valentine, A.S. Hill, M.J. Friedman and S.H. Reiber, *Characterization of elemental and structural composition of corrosion scales and deposits formed in drinking water distribution systems*, Water Res. 44 (2010) 4570-4580.

[107] O.M. Zacheus, M.J. Lehtola, L.K. Korhonen and P.J. Martikainen, *Soft deposits, the key site for microbial growth in drinking water distribution networks*, Water Res. 35 (2001) 1757-1765.

[108] M.W. LeChevallier, T.W. Babcock and R.G. Lee, *Examination and characterization of distribution system biofilms*, Appl. Environ. Microbiol. 53 (1987) 2714-2724.

[109] V. Chawla, P.G. Gurbuxani and G.R. Bhagure, *Corrosion of water pipes: a comprehensive study of deposits*, J. Miner. Mater. Charact. Eng. 11 (2012) 479-492.

[110] Z. Tang, S. Hong, W. Xiao and J. Taylor, *Characteristics of iron corrosion scales established under blending of ground, surface, and saline waters and their impacts on iron release in the pipe distribution system*, Corros. Sci. 48 (2006) 322-342.

[111] C.M.C. Infante and J.C. Masini, *Development of a Spectrophotometric Sequential Injection Methodology for Online Monitoring of the Adsorption of Paraquat on Clay Mineral and Soil*, Spectrosc. Lett. 40 (2007) 3-14.

[112] C.M. Lozano, T.P. Ruíz, V. Tomás and E. Yagüe, *Determination of paraquat in biological and environmental samples by a photokinetic method*, Anal. Chim. Acta 209 (1988) 79-86.

[113] M. Pateiro-Moure, E. Martínez-Carballo, M. Arias-Estévez and J. Simal-Gándara, *Determination of quaternary ammonium herbicides in soils: Comparison of digestion, shaking and microwave-assisted extractions*, J. Chromatogr. A. 1196–1197 (2008) 110-116.

[114] T. Pérez-Ruiz, C. Martínez-Lozano, A. Sanz and V. Tomás, *Simultaneous determination of diquat and paraquat residues in various matrices by capillary zone electrophoresis with diode array detection*, Chromatographia 43 (1996) 468-472.

[115] T. Perez-Ruiz and J. Fenoll, *Spectrofluorimetric determination of paraquat by manual and flow injection methods*, Analyst 123 (1998) 1577-1581.

[116] D. Barcel'o, G. Durand and R.J. Vreeken, *Determination of quaternary amine pesticides by thermospray mass spectrometry*, J. Chromatogr. A 647 (1993) 271-277.

[117] J.C. Ingram, G.S. Groenewold, A.D. Appelhans, J.E. Delmore, J.E. Olson and D.L. Miller, *Direct surface analysis of pesticides on soil, leaves, grass, and stainless steel by static secondary ion mass spectrometry*, Environ. Sci. Technol. 31 (1997) 402-408.

[118] M.M. de Andréa, S. Papini and L.E. Nakagawa, *Optimizing microwave-assisted solvent extraction (MASE) of pesticides from soil*, J. Environ. Sci. Health, Part B 36 (2001) 87-93.

[119] V. Lopez Avila, R. Young and N. Teplitsky, *Microwave-assisted extraction as an alternative to Soxhlet, sonication, and supercritical fluid extraction*, J. AOAC Int. 79 (1996) 142-156.

[120] N.K. Hamadi, S. Sri and X.D. Chen, *Adsorption of Paraquat dichloride from aqueous solution by activated carbon derived from used tires*, J. Hazard. Mater. 112 (2004) 133-141.

[121] M. Ruiz, J. Barron-Zambrano, V. Rodilla, A. Szygula and A.M. Sastre, *Paraquat sorption on calcium alginate gel beads*, in: Proceedings of the 4th WSEAS/IASME international conference on Dynamical systems and control, World Scientific and Engineering Academy and Society (WSEAS), Corfu, Greece, 2008, pp. 30-35.

[122] W.-T. Tsai and C.-W. Lai, *Adsorption of herbicide paraquat by clay mineral regenerated from spent bleaching earth*, J. Hazard. Mater. 134 (2006) 144-148.

[123] Y. Seki and K. Yurdakoç, *Paraquat adsorption onto clays and organoclays from aqueous solution*, J. Colloid Interface Sci. 287 (2005) 1-5.

[124] W.T. Tsai, K.J. Hsien, Y.M. Chang and C.C. Lo, *Removal of herbicide paraquat from an aqueous solution by adsorption onto spent and treated diatomaceous earth*, Bioresource Technol. 96 (2005) 657-663.

[125] W.T. Tsai, C.W. Lai and K.J. Hsien, *Adsorption kinetics of herbicide paraquat from aqueous solution onto activated bleaching earth*, Chemosphere 55 (2004) 829-837.

[126] W.T. Tsai, C.W. Lai and K.J. Hsien, *The effects of pH and salinity on kinetics of paraquat sorption onto activated clay*, Colloid Surface A 224 (2003) 99-105.

[127] R. Calvert, *Adsorption-desorption phenomena*, in: R. Hance (Ed.) *Interactions between herbicides and the soil*, Academic Press, European Weed Research Society, 1980, pp. 1-30.

[128] C.H. Giles, T.H. Mac Ewan, S.N. Nakhwa and D. Smith, *Studies in adsorption. Part 11. A system of classification of solution adsorption isotherms, and its use in diagnosis of adsorption mechanisms and measurement of scientific surface area of solids.*, J. Chem. Soc. 786 (1960) 3973-3993.

[129] S. Esplugas, J. Giménez, S. Contreras, E. Pascual and M. Rodríguez, *Comparison of different advanced oxidation processes for phenol degradation*, Water Res. 36 (2002) 1034-1042.

[130] H.J.H. Fenton, *LXXIII.-Oxidation of tartaric acid in presence of iron*, J. Chem. Soc. 65 (1894) 899-910.

[131] J.H. Sun, S.P. Sun, M.H. Fan, H.Q. Guo, L.P. Qiao and R.X. Sun, *A kinetic study on the degradation of p-nitroaniline by Fenton oxidation process*, J. Hazard. Mater. 148 (2007) 172-177.

[132] C. Jiang, S. Pang, F. Ouyang, J. Ma and J. Jiang, *A new insight into Fenton and Fenton-like processes for water treatment*, J. Hazard. Mater. 174 (2010) 813-817.

[133] K. Tennakone and I.R.M. Kottegoda, *Photocatalytic mineralization of paraquat dissolved in water by TiO2 supported on polythene and polypropylene films*, J. Photochem. Photobiol. A-Chem. 93 (1996) 79-81.

[134] E. Moctezuma, E. Leyva, E. Monreal, N. Villegas and D. Infante, *Photocatalytic degradation of the herbicide "Paraquat"*, Chemosphere 39 (1999) 511-517.

[135] M. Kang, *Preparation of TiO2 photocatalyst film and its catalytic performance for 1,1'-dimethyl-4,4'-bipyidium dichloride decomposition*, Appl. Catal. B-Environ. 37 (2002) 187-196.

[136] M.H. Florêncio, E. Pires, A.L. Castro, M.R. Nunes, C. Borges and F.M. Costa, *Photodegradation of Diquat and Paraquat in aqueous solutions by titanium dioxide: evolution of degradation reactions and characterisation of intermediates*, Chemosphere 55 (2004) 345-355.

[137] M.J. Cantavenera, I. Catanzaro, V. Loddo, L. Palmisano and G. Sciandrello, *Photocatalytic degradation of paraquat and genotoxicity of its intermediate products*, J. Photoch. Photobio. A 185 (2007) 277-282.

[138] E. Kanchanatip, N. Grisdanurak, R. Thongruang and A. Neramittagapong, *Degradation of paraquat under visible light over fullerene modified V-TiO2*, Reac. Kinet. Mech. Cat. 103 (2011) 227-237.

[139] P.C. Kearney, J.M. Ruth, Q. Zeng and P. Mazzocchi, *UV ozonation of paraquat*, J.Agric. Food Chem. 33 (1985) 953-957.

[140] R. Andreozzi, A. Insola, V. Caprio and M.G. D'Amore, *Ozonation of 1, 1' dimethyl, 4,4' bipyridinium dichloride (Paraquat) in aqueous solution*, Environ. Technol. 14 (1993) 695-700.

[141] A. Dhaouadi and N. Adhoum, *Heterogeneous catalytic wet peroxide oxidation of paraquat in the presence of modified activated carbon*, Appl. Catal. B-Environ. 97 (2010) 227-235.

[142] A. Dhaouadi and N. Adhoum, *Degradation of paraquat herbicide by electrochemical advanced oxidation methods*, J. Electroanal. Chem. 637 (2009) 33-42.

[143] J.-C. Lee, M.-S. Kim, C. Kim, C.-H. Chung, S. Cho, G. Han, K. Yoon and B.-W. Kim, *Removal of paraquat in aqueous suspension of TiO2 in an immersed UV photoreactor*, Korean J. Chem. Eng. 20 (2003) 862-868.

[144] M.S.F. Santos, A. Alves and L.M. Madeira, *Paraquat removal from water by oxidation with Fenton's reagent*, Chem. Eng. J. 175 (2011) 279-290.

[145] K. D'Silva, A. Fernandes and M. Rose, *Brominated Organic Micropollutants—Igniting the Flame Retardant Issue*, Crit. Rev. Environ. Sci. Technol. 34 (2004) 141-207.

[146] O.I. Olukunle, O.J. Okonkwo, K.K. Kefeni and M. Lupankwa, *Determination of brominated flame retardants in Jukskei River catchment area in Gauteng, South Africa*, Water Sci. Technol. 65 (2012) 743-749.

[147] Q. Xiao, B. Hu, J. Duan, M. He and W. Zu, *Analysis of PBDEs in Soil, Dust, Spiked Lake Water, and Human Serum Samples by Hollow Fiber-Liquid Phase Microextraction Combined with GC-ICP-MS*, J. Am. Soc. Mass Spectr. 18 (2007) 1740-1748.

[148] I. Fulara and M. Czaplicka, *Methods for determination of polybrominated diphenyl ethers in environmental samples - Review*, J. Sep. Sci. 35 (2012) 2075-2087.

[149] M. Polo, G. Gómez-Noya, J.B. Quintana, M. Llompart, C. García-Jares and R. Cela, *Development of a Solid-Phase Microextraction Gas Chromatography/Tandem Mass Spectrometry Method for Polybrominated Diphenyl Ethers and Polybrominated Biphenyls in Water Samples*, Anal. Chem. 76 (2004) 1054-1062.

[150] E. Eljarrat and D. Barceló, *Sample handling and analysis of brominated flame retardants in soil and sludge samples*, Trends Anal. Chem. 23 (2004) 727-736.

[151] C.A. de Wit, *An overview of brominated flame retardants in the environment*, Chemosphere 46 (2002) 583-624.

[152] P.O. Darnerud, G.S. Eriksen, T. Jóhannesson, P.B. Larsen and M. Viluksela, *Polybrominated diphenyl ethers: Occurence, dietary exposure, and toxicology*, Environ. Health Perspect. 109 (2001) 49-68.

[153] Official Journal of the European Union, *Directive 2003/11/EC of the European Parliament and of the Council*, 2003.

[154] A. Möller, Z. Xie, R. Sturm and R. Ebinghaus, *Polybrominated diphenyl ethers (PBDEs) and alternative brominated flame retardants in air and seawater of the European Arctic*, Environ. Pollut. 159 (2011) 1577-1583.

[155] Stockholm Convention, *http://chm.pops.int/Convention/ThePOPs/TheNewPOPs/tabid/2511/Default.aspx*, retrieved on 05-10-2013.

[156] A. Bacaloni, L. Callipo, E. Corradini, P. Giansanti, R. Gubbiotti, R. Samperi and A. Laganà, *Liquid chromatography–negative ion atmospheric pressure photoionization tandem mass spectrometry for the determination of brominated flame retardants in environmental water and industrial effluents*, J. Chromatogr. A 1216 (2009) 6400-6409.

[157] M.L. Hardy, *The toxicology of commercial PBDE flame retardants: DecaBDE, octaBDE, pentaBDE*, Organohalogen. Comp. 47 (2000) 41-44.

[158] R. Millischer, F. Girault, R. Heywood, G. Clarke, D. Hossack and M. Clair, *Decabromobiphenyl: toxicological study*, Toxicol. Eur. Res. 2 (1979) 155-161.

[159] L. Fang, J. Huang, G. Yu and L. Wang, *Photochemical degradation of six polybrominated diphenyl ether congeners under ultraviolet irradiation in hexane*, Chemosphere 71 (2008) 258-267.

[160] C.A. de Wit, M. Alaee and D.G. Muir, *Levels and trends of brominated flame retardants in the Artic*, Chemosphere 64 (2006) 209-233.

[161] K. Hooper and T.A. McDonald, *The PBDEs: An emerging environmental challenge and another reason for breast-milk monitoring programs*, Environ. Health Perspect. 108 (2000) 387-392.

[162] ATSDR, *Health Effects*, in: *Toxicological profile for polybrominated biphenyls and polybrominated diphenyl ethers*, 2004, pp. 57-343.

[163] S.A. Tittlemier, T. Halldorson, G.A. Stern and G.T. Tomy, *Vapor pressures, aqueous solubilities, and Henry's law constants of some brominated flame retardants*, Environ. Toxicol. Chem. 21 (2002) 1804-1810.

[164] E. Braekevelt, S.A. Tittlemier and G.T. Tomy, *Direct measurement of octanol–water partition coefficients of some environmentally relevant brominated diphenyl ether congeners*, Chemosphere 51 (2003) 563-567.

[165] J. Sánchez-Avila, R. Tauler and S. Lacorte, *Organic micropollutants in coastal waters from NW Mediterranean Sea: Sources distribution and potential risk*, Environ. Int. 46 (2012) 50-62.

[166] A.P. Daso, O.S. Fatoki, J.P. Odendaal and O.O. Olujimi, *Occurrence of selected polybrominated diphenyl ethers and 2,2',4,4',5,5'-hexabromobiphenyl (BB-153) in sewage sludge and effluent samples of a wastewater-treatment plant in Cape Town, South Africa*, Arch. Environ. Con. Tox. 62 (2012) 391-402.

[167] B.K. Hope, L. Pillsbury and B. Boling, *A state-wide survey in Oregon (USA) of trace metals and organic chemicals in municipal effluent*, Sci. Total Environ. 417–418 (2012) 263-272.

[168] X. Liu, J. Li, Z. Zhao, W. Zhang, K. Lin, C. Huang and X. Wang, *Solid-phase extraction combined with dispersive liquid–liquid microextraction for the determination for polybrominated diphenyl ethers in different environmental matrices*, J. Chromatogr. A 1216 (2009) 2220-2226.

[169] A.R. Fontana, R.G. Wuilloud, L.D. Martínez and J.C. Altamirano, *Simple approach based on ultrasound-assisted emulsification-microextraction for determination of polibrominated flame retardants in water samples by gas chromatography–mass spectrometry*, J. Chromatogr. A 1216 (2009) 147-153.

[170] A.R. Fontana, M.F. Silva, L.D. Martínez, R.G. Wuilloud and J.C. Altamirano, *Determination of polybrominated diphenyl ethers in water and soil samples by cloud point extraction-ultrasound-assisted back-extraction-gas chromatography–mass spectrometry*, J. Chromatogr. A 1216 (2009) 4339-4346.

[171] N. Fontanals, T. Barri, S. Bergström and J.-Å. Jönsson, *Determination of polybrominated diphenyl ethers at trace levels in environmental waters using hollow-fiber microporous membrane liquid–liquid extraction and gas chromatography–mass spectrometry*, J. Chromatogr. A 1133 (2006) 41-48.

[172] V. Yusà, A. Pastor and M. de la Guardia, *Microwave-assisted extraction of polybrominated diphenyl ethers and polychlorinated naphthalenes concentrated on semipermeable membrane devices*, Anal. Chim. Acta 565 (2006) 103-111.

[173] J. Llorca-Porcel, G. Martínez-Sánchez, B. Álvarez, M.A. Cobollo and I. Valor, *Analysis of nine polybrominated diphenyl ethers in water samples by means of stir bar sorptive extraction-thermal desorption-gas chromatography–mass spectrometry*, Anal. Chim. Acta 569 (2006) 113-118.

[174] A. Zhao, X. Wang, M. Ma, W. Wang, H. Sun, Z. Yan, Z. Xu and H. Wang, *Temperature-assisted ionic liquid dispersive liquid-liquid microextraction combined with high performance liquid chromatography for the determination of PCBs and PBDEs in water and urine samples*, Microchim. Acta 177 (2012) 229-236.

[175] H. Liu, M. Zhang, X. Wang, Y. Zou, W. Wang, M. Ma, Y. Li and H. Wang, *Extraction and determination of polybrominated diphenyl ethers in water and urine samples using*

solidified floating organic drop microextraction along with high performance liquid chromatography, Microchim. Acta 176 (2012) 303-309.

[176] Y. Li, G. Wei, J. Hu, X. Liu, X. Zhao and X. Wang, *Dispersive liquid–liquid microextraction followed by reversed phase-high performance liquid chromatography for the determination of polybrominated diphenyl ethers at trace levels in landfill leachate and environmental water samples*, Anal. Chim. Acta 615 (2008) 96-103.

[177] Y. Li, J. Hu, X. Liu, L. Fu, X. Zhang and X. Wang, *Dispersive liquid-liquid microextraction followed by reversed phase HPLC for the determination of decabrominated diphenyl ether in natural water*, J. Sep. Sci. 31 (2008) 2371-2376.

[178] Y. Li, G. Wei and X. Wang, *Determination of decabromodiphenyl ether in water samples by single-drop microextraction and RP-HPLC*, J. Sep. Sci. 30 (2007) 2698-2702.

[179] X.-H. Zang, Q.-H. Wu, M.-Y. Zhang, G.-H. Xi and Z. Wang, *Developments of Dispersive Liquid-Liquid Microextraction Technique*, Chinese J. Anal. Chem. 37 (2009) 161-168.

[180] H.M. Park, S.M. Hong, M.R. Agustin-Camacho, W. Dirwono and K.B. Lee, *Pressurized liquid extraction for the simultaneous analysis of polychlorinated biphenyls and polybrominated diphenyl ethers from soil by GC-TOF-MS detection*, J. Chromatogr. Sci. 47 (2009) 681-688.

[181] X. Li, J. Huang, W. Zhang, G. Yu, S. Deng and S. Wang, *Determination of 41 polybrominated diphenyl ethers in soil using a pressurised solvent extraction and GC-NCI-MS method*, Int. J. Environ. Anal. Chem. 91 (2011) 1135-1150.

[182] U.R. Thorenz, B.A. Musa Bandowe, J. Sobocka and W. Wilcke, *Method optimization to measure polybrominated diphenyl ether (PBDE) concentrations in soils of Bratislava, Slovakia*, Environ. Pollut. 158 (2010) 2208-2217.

[183] Z. Zhang, M. Shanmugam and S.M. Rhind, *PLE and GC-MS determination of polybrominated diphenyl ethers in soils*, Chromatographia 72 (2010) 535-543.

[184] B. Albero, C. Sánchez-Brunete, E. Miguel, R.A. Pérez and J.L. Tadeo, *Determination of selected organic contaminants in soil by pressurized liquid extraction and gas chromatography tandem mass spectrometry with in situ derivatization*, J. Chromatogr. A 1248 (2012) 9-17.

[185] D. Wang, Z. Cai, J. Guibin, M.H. Wong and W.K. Wong, *Gas chromatography/ion trap mass spectrometry applied for the determination of polybrominated diphenyl ethers in soil*, Rapid Commun. Mass Spectrom. 19 (2005) 83-89.

[186] Z. Cai and G. Jiang, *Determination of polybrominated diphenyl ethers in soil from e-waste recycling site*, Talanta 70 (2006) 88-90.

[187] L. Zhu, B. Ma and X. Liang, *Quantitative analysis of polybrominated diphenyl ethers in earthworms and soil by gas chromatography coupled to ion-trap tandem mass spectrometry*, Rapid Commun. Mass Spectrom. 22 (2008) 394-400.

[188] C. Sánchez-Brunete, E. Miguel and J.L. Tadeo, *Determination of polybrominated diphenyl ethers in soil by ultrasonic assisted extraction and gas chromatography mass spectrometry*, Talanta 70 (2006) 1051-1056.

[189] J. Sun, J. Liu, Q. Liu, G. Qu, T. Ruan and G. Jiang, *Sample preparation method for the speciation of polybrominated diphenyl ethers and their methoxylated and hydroxylated analogues in diverse environmental matrices*, Talanta 88 (2012) 669-676.

[190] Y.-Y. Zhou, C.-Y. Zhang, Z.-G. Yan, K.-J. Li, L. Wang, Y.-B. Xie, F.-S. Li, Z. Liu and J. Yang, *The use of copper(II) isonicotinate-based micro-solid-phase extraction for the analysis of polybrominated diphenyl ethers in soils*, Anal. Chim. Acta 747 (2012) 36-41.

[191] Q. Liu, J. Shi, J. Sun, T. Wang, L. Zeng, N. Zhu and G. Jiang, *Graphene-assisted matrix solid-phase dispersion for extraction of polybrominated diphenyl ethers and their methoxylated and hydroxylated analogs from environmental samples*, Anal. Chim. Acta 708 (2011) 61-68.

[192] J. Zhou, F. Yang, D. Cha, Z. Zeng and Y. Xu, *Headspace solid-phase microextraction with novel sol-gel permethylated-β-cyclodextrin/hydroxyl-termination silicone oil fiber for determination of polybrominated diphenyl ethers by gas chromatography-mass spectrometry in soil*, Talanta 73 (2007) 870-877.

[193] C. Salgado-Petinal, M. Llompart, C. García-Jares, M. García-Chao and R. Cela, *Simple approach for the determination of brominated flame retardants in environmental solid samples based on solvent extraction and solid-phase microextraction followed by gas chromatography–tandem mass spectrometry*, J. Chromatogr. A 1124 (2006) 139-147.

[194] C. Salgado-Petinal, M. Garcia-Chao, M. Llompart, C. Garcia-Jares and R. Cela, *Headspace solid-phase microextraction gas chromatography tandem mass spectrometry for the determination of brominated flame retardants in environmental solid samples*, Anal. Bioanal. Chem. 385 (2006) 637-644.

[195] K.E. Mueller, S.R. Mueller-Spitz, H.F. Henry, A.P. Vonderheide, R.S. Soman, B.K. Kinkle and J.R. Shann, *Fate of Pentabrominated Diphenyl Ethers in Soil: Abiotic Sorption,*

Plant Uptake, and the Impact of Interspecific Plant Interactions, Environ. Sci. Technol. 40 (2006) 6662-6667.

[196] W. Liu, W. Li, J. Hu, X. Ling, B. Xing, J. Chen and S. Tao, *Sorption kinetic characteristics of polybrominated diphenyl ethers on natural soils*, Environ. Pollut. 158 (2010) 2815-2820.

[197] W. Liu, W. Li, B. Xing, J. Chen and S. Tao, *Sorption isotherms of brominated diphenyl ethers on natural soils with different organic carbon fractions*, Environ. Pollut. 159 (2011) 2355-2358.

[198] W. Liu, F. Cheng, W. Li, B. Xing and S. Tao, *Desorption behaviors of BDE-28 and BDE-47 from natural soils with different organic carbon contents*, Environ. Pollut. 163 (2012) 235-242.

[199] Y. Olshansky, T. Polubesova, W. Vetter and B. Chefetz, *Sorption–desorption behavior of polybrominated diphenyl ethers in soils*, Environ. Pollut. 159 (2011) 2375-2379.

[200] M.J. Simpson and P.C.E. Johnson, *Identification of mobile aliphatic sorptive domains in soil humin by solid-state 13C nuclear magnetic resonance*, Environ. Toxicol. Chem. 25 (2006) 52-57.

[201] Y. Drori, Z. Aizenshtat and B. Chefetz, *Sorption of organic compounds to humin from soils irrigated with reclaimed wastewater*, Geoderma 145 (2008) 98-106.

[202] J. Xin, X. Liu, L. Jiang and M. Li, *BDE-47 sorption and desorption to soil matrix in single- and binary-solute systems*, Chemosphere 87 (2012) 477-482.

[203] J. Bezares-Cruz, C.T. Jafvert and I. Hua, *Solar Photodecomposition of Decabromodiphenyl Ether: Products and Quantum Yield*, Environ. Sci. Technol. 38 (2004) 4149-4156.

[204] S. Luo, S. Yang, Y. Xue, F. Liang and C. Sun, *Two-stage reduction/subsequent oxidation treatment of 2,2',4,4'-tetrabromodiphenyl ether in aqueous solutions: Kinetic, pathway and toxicity*, J. Hazard. Mater. 192 (2011) 1795-1803.

[205] A. Christiansson, J. Eriksson, D. Teclechiel and Å. Bergman, *Identification and quantification of products formed via photolysis of decabromodiphenyl ether*, Environ. Sci. Pollut. Res. 16 (2009) 312-321.

[206] J. Su, N. Lu, J. Zhao, H. Yu, H. Huang, X. Dong and X. Quan, *Nano-cubic structured titanium nitride particle films as cathodes for the effective electrocatalytic debromination of BDE-47*, J. Hazard. Mater. 231–232 (2012) 105-113.

[207] J. Eriksson, N. Green, G. Marsh and Å. Bergman, *Photochemical Decomposition of 15 Polybrominated Diphenyl Ether Congeners in Methanol/Water*, Environ. Sci. Technol. 38 (2004) 3119-3125.

[208] C. Sun, J. Zhao, H. Ji, W. Ma and C. Chen, *Photocatalytic debromination of preloaded decabromodiphenyl ether on the TiO2 surface in aqueous system*, Chemosphere 89 (2012) 420-425.

[209] A. Konstantinov, D. Bejan, N.J. Bunce, B. Chittim, R. McCrindle, D. Potter and C. Tashiro, *Electrolytic debromination of PBDEs in DE-83TM technical decabromodiphenyl ether*, Chemosphere 72 (2008) 1159-1162.

[210] Z. Fang, X. Qiu and J. Chen, *Degradation of the polybrominated diphenyl ethers by nanoscale zero-valent metallic particles prepared from steel pickling waste liquor*, Desalination 267 (2011) 34-41.

[211] Z. Fang, X. Qiu and J. Chen, *Debromination of polybrominated diphenyl ethers by Ni/Fe bimetallic nanoparticles: Influencing factors, kinetics, and mechanism*, J. Hazard. Mater. 185 (2011) 958-969.

[212] T. An, J. Chen, G. Li, X. Ding, G. Sheng, J. Fu, B. Mai and K.E. O'Shea, *Characterization and the photocatalytic activity of TiO2 immobilized hydrophobic montmorillonite photocatalysts: Degradation of decabromodiphenyl ether (BDE 209)*, Catal. Today 139 (2008) 69-76.

[213] C. Sun, D. Zhao, C. Chen, W. Ma and J. Zhao, *TiO2-Mediated Photocatalytic Debromination of Decabromodiphenyl Ether: Kinetics and Intermediates*, Environ. Sci. Technol. 43 (2008) 157-162.

[214] S. Rayne, P. Wan and M. Ikonomou, *Photochemistry of a major commercial polybrominated diphenyl ether flame retardant congener: 2,2',4,4',5,5'-Hexabromodiphenyl ether (BDE153)*, Environ. Int. 32 (2006) 575-585.

[215] A. Li, C. Tai, Z. Zhao, Y. Wang, Q. Zhang, G. Jiang and J. Hu, *Debromination of decabrominated diphenyl ether by resin-bound iron nanoparticles*, Environ. Sci. Technol. 41 (2007) 6841-6846.

[216] I. Watanabe and R. Tatsukawa, *Formation of brominated dibenzofurans from the photolysis of flame retardant decabromobiphenyl ether in hexane solution by UV and sun light*, Bull. Environ. Contam. Toxicol. 39 (1987) 953-959.

[217] K. Nose, S. Hashimoto, S. Takahashi, Y. Noma and S.-i. Sakai, *Degradation pathways of decabromodiphenyl ether during hydrothermal treatment*, Chemosphere 68 (2007) 120-125.

[218] K.L. Chow, Y.B. Man, J.S. Zheng, Y. Liang, N.F.Y. Tam and M.H. Wong, *Characterizing the optimal operation of photocatalytic degradation of BDE-209 by nano-sized TiO2*, J. Environ. Sci. 24 (2012) 1670-1678.

[219] X. Li, J. Huang, G. Yu and S. Deng, *Photodestruction of BDE-99 in micellar solutions of nonionic surfactants of Brij 35 and Brij 58*, Chemosphere 78 (2010) 752-759.

[220] L. Sanchez-Prado, K. Kalafata, S. Risticevic, J. Pawliszyn, M. Lores, M. Llompart, N. Kalogerakis and E. Psillakis, *Ice photolysis of 2,2',4,4',6-pentabromodiphenyl ether (BDE-100): Laboratory investigations using solid phase microextraction*, Anal. Chim. Acta 742 (2012) 90-96.

[221] P. Moreira Bastos, J. Eriksson, J. Vidarson and Å. Bergman, *Oxidative transformation of polybrominated diphenyl ether congeners (PBDEs) and of hydroxylated PBDEs (OH-PBDEs)*, Environ. Sci. Pollut. Res. 15 (2008) 606-613.

[222] F. Kastanek, Y. Maleterova, P. Kastanek, J. Rott, V. Jiricny and K. Jiratova, *Complex treatment of wastewater and groundwater contaminated by halogenated organic compounds*, Desalination 211 (2007) 261-271.

[223] Y.-S. Keum and Q.X. Li, *Reductive Debromination of Polybrominated Diphenyl Ethers by Zerovalent Iron*, Environ. Sci. Technol. 39 (2005) 2280-2286.

PART II. PARAQUAT

2 Paraquat quantification in waters*

Abstract

Three analytical methodologies for paraquat dichloride (PQ) identification and quantification in waters were developed and validated in response to different scenarios: a direct injection liquid chromatography with diode array detector (DI-LC-DAD) method for emergency situations, as occurs when there is a suspicion of contamination of drinking water networks; a solid phase extraction liquid chromatography with diode array detector (SPE-LC-DAD) method to control the drinking water quality in accordance with the European Union legislation (maximum of 0.1 μg/L for individual pesticide) and a direct injection liquid chromatography mass spectrometry (DI-LC-MS) method for confirmation purposes and identification of PQ degradation by-products. Limits of detection of 10 μg/L, 0.04 μg/L and 20 μg/L PQ were reached for DI-LC-DAD, SPE-LC-DAD and DI-LC-MS methods, respectively. The PQ analytical response of DI-LC-DAD method was tested in different types of water and in the presence of other species or compounds resulting from the contact of the water with deposits and *Pseudomonas fluorescens* cells that exist in drinking water networks. Additionally, the method response was assessed when a PQ commercial formulation (Gramoxone) was used as PQ source instead of the analytical standard. Recovery percentages after spiking samples of 77, 99 and 101% on average were attained for 0.25, 30 and 80 mg/L of PQ by DI-LC-DAD method, respectively. It was also proved that for concentrations of Fe(II), H_2O_2 and Na_2SO_3 lower than 6.4×10^{-4}, 5.7×10^{-2} and 9.6×10^{-2} M, respectively, no effects are observed in the analytical response of DI-LC-DAD method.

Global uncertainties below 6, 11 and 13% were found for DI-LC-MS, SPE-LC-DAD and DI-LC-DAD, respectively, for the most part of the calibration ranges. All methods proved to be precise, accurate and suitable for the purpose that they were designed.

* Adapted from: Mónica S.F. Santos, Luís M. Madeira and A. Alves, Paraquat quantification in waters, *submitted*, 2013.

2.1 Introduction

The development of analytical methodologies for detection and quantification of PQ in different case scenarios is one of the main goals of this chapter. In particular, it is necessary to develop an analytical methodology to determine the PQ concentration in water matrices in case of a deliberate contamination of a water network. Under such conditions, it is of crucial importance to have a simple and expeditious method to quantify high PQ concentrations with good accuracy and precision, in a short time and using classical equipment, in order to be possible to make the analysis everywhere. Here, a simple DI-LC-DAD is proposed for emergency situations. On the other hand, a more sensitive methodology is also required, such as SPE-LC-DAD, to ensure that PQ levels in drinking water are below the limit recommended by European Union (0.1 μg/L). Since one of the main objectives of the thesis is to develop and implement effective degradation methodologies to treat waters contaminated with chemicals, it is necessary to be able to identify the degradation by-products in order to infer about the toxicity and biodegradability of the generated effluents. Fenton's reaction is an advanced oxidation process which uses H_2O_2 and Fe^{2+} as oxidant and catalyst, respectively, to degrade the organic matter. This degradation process was implemented for the degradation of PQ in waters (Chapter 5). Although acceptable mineralization degrees were reported, a DI-LC-MS method is recommended for confirmation purposes and for identification of some degradation by-products formed during the Fenton's process.

Methods for PQ quantification in waters are already available in the literature and they are similar to the ones proposed here (see section 1.1.1. of Chapter 1). However, it is important to emphasize that none of those studies considered the method validation applied to such different samples: in the presence of deposits, cells, and different types of water, which may represent realistic scenarios in drinking water networks. The analytical response of DI-LC-DAD was also analysed in the presence of Fenton's species which, to the author knowledge, was never ever investigated before.

Additionally, a complete set of validation parameters, including the calculation of the global uncertainty associated to the results in the range of quantification, is presented for all developed methods.

2.2 Experimental Section

2.2.1 Standard solutions and samples

Paraquat dichloride (PQ) PESTANAL® analytical standard (Fluka) was purchased from Sigma-Aldrich (St. Louis, USA). Gramoxone (GMX) with 25.6 wt. % of PQ was kindly supplied by Syngenta Crop Protection, Lda. Heptafluorobutyric acid (HFBA) from Sigma-Aldrich (St. Louis, USA), acetonitrile (HPLC grade) from VWR BDH Prolabo (Fontenay-sous-Bois, France) and methanol (Lichrosolv® hypergrade for liquid chromatography) and water (Lichrosolv® for chromatography) from Merck (Darmstadt, Germany) were used for analysis.

Hydrogen peroxide solution (H_2O_2, 30% v/v), iron (II) sulfate heptahydrate ($FeSO_4$, 99.5%) and anhydrous sodium sulfite (Na_2SO_3, 96%) were purchased from Merck (Darmstadt, Germany) and used in interference tests.

Ammonium chloride (NH_4Cl, 99.9%) from Sigma-Aldrich (St. Louis, USA), methanol (HPLC grade) from VWR BDH Prolabo (Fontenay-sous-Bois, France) and hydrochloric acid (37% for analysis, ACS Merck) were used in solid phase extraction (SPE). The SPE columns were Supelclean™ LC-Si SPE tubes 3 mL from Supelco (Pennsylvania, USA) and Oasis WCX 6 cc cartridge 150 mg from Waters (Dublin, Ireland).

Syringe filters with 0.2 μm PTFE membrane were purchased from VWR (West Chester, USA).

2.2.2 Instrumentation

2.2.2.1 LC-DAD

Chromatographic analysis of PQ by LC-DAD was performed in a Hitachi Elite LaChrom with a L-2130 pump, a L-2200 autosampler and a L-2455 diode array detector (DAD). For PQ concentrations between 0.1 mg/L and 80 mg/L, quantification was done by direct injection of 99 μL in a Purospher® STAR LiChroCART® RP-18 endcapped (240x4 mm, 5 μm) reversed phase column from Merck (Darmstadt, Germany) and using a mobile phase of 80% (v/v) of 10 mM HFBA in water and 20% (v/v) of acetonitrile (ACN), at isocratic conditions, with a flow rate of 1 mL/min. For lower PQ concentrations, the chromatographic separation was achieved by a Chromolith® Performance RP-18e 100-3 (3x4.6 mm) column from Merck (Darmstadt, Germany). The mobile phase used was

composed by 95% of HFBA 10 mM and 5% of ACN at 1 mL/min under isocratic conditions. PQ quantification was done at 259 nm in both cases.

2.2.2.2 LC-MS

Chromatographic analyses were performed using a Varian LC-MS system (Lake Forest, USA) constituted by a ProStar 210 Binary Solvent Delivery Module and a 500-MS LC Ion Trap Mass Spectrometer equipped with an electrospray ionization source (ESI). Data was acquired and processed by Varian MS Workstation Version 6.9 software. A Polaris® C18-A column (50 mm x 2 mm i.d., particle size: 5 µm) in combination with a MetaGuard column Pursuit® C18 (10 mm x 2.0 mm i.d., particle size: 5 µm) were supplied by Varian (Lake Forest, USA). The mobile phase was composed of 5 mM HFBA in water (80%, v/v) and methanol (20%, v/v), running in isocratic conditions. The analyses were done in the positive ion mode. The flow rate was 0.2 mL/min and the injection volume was 10 µL. The MS conditions were optimized during the experimental work, and the final conditions were: µScan average – 3 µscans, drying gas – 20 psi at 400 °C, nebulising gas – 50 psi, multiplier offset – 300 V, needle voltage – 3839 V, capillary voltage – 87 V, RF loading – 77%.

2.2.3 SPE procedure for the SPE-LC-DAD method

In this methodology, one litre of PQ standard (10 µg/L) at pH 9 (adjusted with NaOH) is passed through a cartridge (silica or Oasis WCX waters), where the analyte is retained. After that, 3 mL of a solvent (HCl 0.1 M in methanol, HCl 6 M in methanol or saturated solution of NH_4Cl in methanol) is used to elute paraquat. After solvent evaporation under nitrogen flow, the sample was reconstituted in 1 mL of distilled water and was injected in the HLPC-DAD (enrichment factor is 1000x).

2.2.4 Validation parameters

The validation of the analytical methods and the uncertainty measurement followed the *bottom-up* approach described in the Eurachem CITAC Guide [1] and by other authors [2, 3]. It comprised a first step of in-house validation, where the main parameters were obtained – linearity of the response, limit of detection (LOD) and limit of quantification

(LOQ), precision and accuracy. Precision was assessed by repeatability and intermediate precision for both DI-LC-DAD and DI-LC-MS methods at three PQ concentration levels. Precision of the SPE-LC-DAD method was only evaluated by repeatability at 0.2, 10 and 50 μg/L of PQ. Results were expressed as the coefficient of variation (CV%) of different replicate measurements. Accuracy was investigated by testing the analytical response capability in the presence of other species or compounds. For DI-LC-DAD method a wide range of interference scenarios were considered and, for that reason, a detailed explanation is given in section 2.2.4.1. The accuracy of the SPE-LC-DAD method was determined comparing the PQ contamination level obtained by the calibration curve and the real amount of PQ added to the sample. Concerning the DI-LC-MS method, the accuracy was evaluated by comparing the analytical responses for PQ standards prepared in distilled water and in river water.

The second step of the validation is the estimation of the uncertainty associated to the results, using the other parameters as an assumption that they represented the main sources of uncertainty to the final result.

2.2.4.1 Recovery assays for the DI-LC-DAD method

Recovery assays were performed by the standard addition method at three PQ concentration levels (0.25, 30 and 80 mg/L). Since the developed method should be able to answer in different real scenarios, the analytical response under different water matrices was evaluated: tap water, water after contact with different kind of deposits (herein called S2, S3 and S4), clay and water after cells exposition. The applicability of this method to quantify PQ in waters contaminated with GMX was also evaluated.

2.2.4.1.1 Tap water

Tap water was used to prepare a PQ standard and the analytical response was compared with that obtained when the standard was prepared in distilled water.

2.2.4.1.2 Gramoxone

The analytical response was evaluated when one PQ commercial product (GMX) was added to an aqueous sample. First, a GMX solution was prepared and the analytical

response was obtained. Then, a known amount of PQ analytical standard was added and the recovery was calculated by comparison of the obtained and expected mass of PQ.

2.2.4.1.3 Deposits

The deposit samples (S2, S3 and S4) used in the recovery tests were supplied by Dr. Gabriela Schaule (IWW Water Centre, Germany). The deposits were removed from real cast iron pipes that needed to be replaced. Deposits were submitted to dryness in an oven (till no weight variation has been detected). Then, all deposits were sieved and were kept in dry conditions until the experiments. An extensive physico-chemical characterization of these deposits has been described previously [4] and, for that reason, the nomenclature used in such study was maintained. According to the results obtained in that study, it was possible to classify the S2, S3 and S4 samples as brown, tubercle and white deposits, respectively, being representative of the main classes of deposits formed in drinking water networks [4]. Clay was the other sample used in this test. The main properties of all deposits and clay used are summarized in Table 2.1.

Table 2.1. Physical-chemical composition of the deposits [4] and clay and main characteristics.

	S2	**S3**	**S4**	**Clay**
Deposit classification	Brown	Tubercle	White	----------
ICP-OES analysis (wt.% of the main elements at dry basis)	Fe: 98% Ca: 1%	Fe: 97% P: 1% Mn: 1%	Ca: 97% Fe: 1% Mg: 1%	Al_2O_3: 34% SiO_2: 49%
S_{BET}, m^2/g	5	36	1	Not determined
Surface area (m^2/g)	3.1	19.3	0.2	Not determined
pH_{pzc}, 20 °C	2.6	6.1	9.9	4.8
pH in water, 20 °C	3.3	7.2	9.0	5.3
Main components identified by XRD	lepidocrocite	goethite	calcite ($CaCO_3$)	Not determined
Organic matter content (wt.%)	1.0	1.0	0.2	12

Clay chemical composition was obtained from LNEG (Laboratório Nacional de Energia e Geologia, Portugal) and the particle size was determined by a Coulter Counter LS 230 with small volume model. The pHpzc (point of zero charge) was obtained as for deposits [4].
The organic matter content was determined in a TOC-V_{CSH} apparatus with a solid sample module SSM-5000A. The total surface area was determined by mercury porosimetry.
For recovery assays, a known amount of deposit (300 mg) was put in contact with water (10 mL), at 20 °C in the dark during 24 h (batch conditions). After filtration, the water was used to prepare a PQ standard and the analytical response was compared with that obtained when the standard was prepared in distilled water.

2.2.4.1.4 Cells

A sterile concentrated medium composed by 5.50 g/L of glucose, 2.50 g/L of peptone, 1.25 g/L of yeast extract, 1.88 g/L of KH_2PO_4 and 2.60 g/L of Na_2HPO_4 was inoculated with a culture of *Pseudomonas fluorescens* grown on PCA medium at 37 °C overnight. Cell suspension was incubated overnight at 37 °C on an orbital shaker and, in the next day, they were washed with a phosphate buffer solution under sterile conditions. The optical density of the final suspension was 0.4. Then, the cells were removed by centrifugation and by filtration using a PTFE syringe filter. Recovery tests were performed at three PQ concentration levels by the addition of a known amount of PQ to the filtrate. The analytical responses were compared with that obtained when the same amount of PQ was added to distilled water.

2.2.5 Interference studies of Fenton's species on PQ quantification by DI-LC-DAD

A stock solution of Fe(II) was prepared by dissolving an appropriate amount of $FeSO_4$ in water, adjusting the pH to 3. The Na_2SO_3 and the H_2O_2 were measured directly from the commercial reagents to prepare the standards. First of all, independent solutions of the Fenton's species were injected and the DAD response was analysed. Then, solutions containing both PQ and Fenton's species (individually) were prepared and injected. Two Fe(II) concentrations were considered (3.6×10^{-4} and 6.4×10^{-4} M) and interference tests with this chemical were made for 1, 5 and 80 mg/L of PQ. The interference of Na_2SO_3 and H_2O_2 on the analytical response was assessed for 1, 5, 20, 50, 70 and 80 mg/L of PQ. The

concentrations of Na_2SO_3 (9.6×10^{-3}, 3.9×10^{-2}, 9.6×10^{-2}, 2.0×10^{-1} and 3.4×10^{-1} M) and H_2O_2 (3.4×10^{-2} and 5.7×10^{-2} M) used in interference tests are in accordance with the PQ degradation study by classic Fenton, present in the Chapter 5. The same is applicable to Fe(II) concentrations.

2.3 Results and discussion

2.3.1 Validation of the DI-LC-DAD method for high PQ concentrations

In case of a deliberate contamination, the PQ concentrations in drinking water should be at relatively high levels. So, the goal of this section was to develop an analytical methodology by LC-DAD able to quantify high PQ concentrations in a short time. The applicability of this method was evaluated by testing its response to waters contaminated with paraquat, after being in contact with deposits or cells. These experiments intend to represent the worst case scenario related to the release of some components from these two matrices to the drinking water, during its normal flow in drinking water networks. Additionally, the PQ analytical response obtained with this method was evaluated in the presence of other compounds, as occurred when GMX is used as contamination agent. Finally, the influence of some species (such as Fe(II), H_2O_2 and Na_2SO_3) used in the treatment of paraquat contaminated waters by Fenton's reagent was assessed.

2.3.1.1 Linearity range and limits of detection and quantification

Although the temperature of the analytical column was kept constant during the chromatographic analysis, retention time of the analyte slightly changed (5.7±0.3 min) due to the presence of other compounds/ species, more specifically in real samples. False PQ peak identification was overcome by regular injection of an analytical control standard and by analysis of the herbicide absorption spectrum, which allowed the evaluation of the purity of the peaks obtained.

Calibration was performed by direct injection of ten PQ analytical standards. The linearity range considered was from 0.1 to 80 mg/L of PQ. The calibration curve obtained, when the standards were injected at least twice, and the respective 98% confidence range are presented in Figure 2.1.

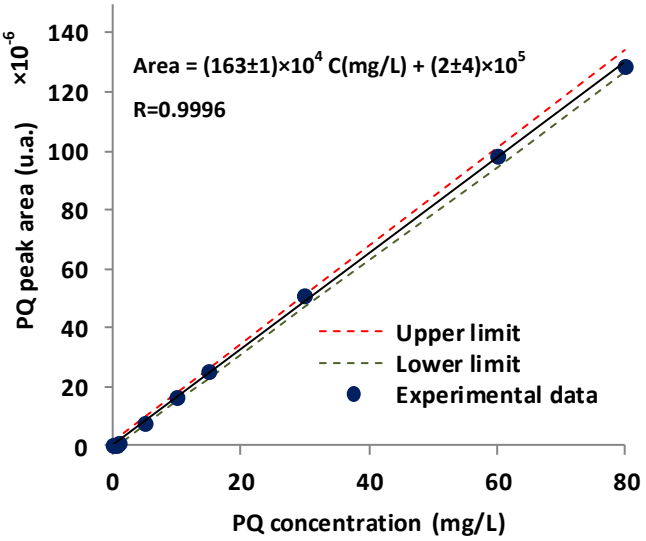

Figure 2.1. Calibration curve for PQ quantification in water by DI-LC-DAD.

The limits of detection and quantification were calculated, based on a Signal Noise to Ratio (S/N) of 3 and 10, and were 0.01 and 0.03 mg/L, respectively. Only one study was found in the literature concerning the direct injection of a PQ standard in a LC-UV and a LOD of 2 mg/L of PQ was obtained [5], which is much higher than the obtained here. To the author´s best knowledge, none study of paraquat quantification in water by DI-LC-DAD was published.

A relative standard deviation of the slope of 0.7% and a correlation coefficient of 0.9996 were obtained. It was also verified that the confidence limits for the interception contains the origin. Those results prove the adequacy of the calibration curve for the purpose of analysis [6].

2.3.1.2 Precision

Precision was evaluated by repeatability and intermediate precision and was expressed as the coefficient of variation (CV%) of different replicate measurements. Repeatability expresses the analytical response variability observed when, at least, six intra-day measurements were performed for a certain standard and under the same conditions. Intermediate precision indicates the analytical response variation observed when one of the factors is changed (in this case the day of injection). The last one was evaluated based

on at least six replicates. Precision was assessed at three PQ concentrations (0.25, 30 and 80 mg/L) and presented in Table 2.2.

Table 2.2. Precision of the DI-LC-DAD method for analytical standards.

	PQ concentration (mg/L)		
n = 6	**0.25**	**30**	**80**
Repeatability (%)	15.5	0.2	0.2
Intermediate Precision (%)	21.0	2.0	1.6

As can be seen, there are higher variations in the response for lower PQ concentrations but, for higher ones the precisions are well below 10%.

2.3.1.3 Accuracy

Accuracy is defined as a measure of the closeness between one analytical result and the true value. This parameter could be assessed comparing the analytical response for a certified reference material with the value indicated by the supplier. Alternatively, this parameter can be evaluated by the standard addition method. By this way, as the name itself mentions, a known amount of PQ is added to a sample and then, the expected and obtained responses are compared. For accuracy assessment, recovery assays were performed at three PQ concentration levels (0.25, 30 and 80 mg/L) and considering different scenarios.

The water into the pipes is constantly in contact with deposits with different compositions depending on the pipe material, water characteristics and region where it is located. Despite of the large heterogeneity of deposits formed along drinking water networks, it is assumed that these deposits may be classified in accordance with the three categories proposed by Echeverría and co-workers (brown, tubercle and white deposits) [7]. For that reason, three different deposits from real drinking water networks, one of each category, were considered for recovery experiments, as well as clay, which were analyzed in Chapter 4. The possibility of some compounds (inorganic and organic) present in these deposits/clay leach to the water phase and interfere in the analytical method response was screening. The same tests were performed with water after being in contact with cells (*Pseudomonas fluorescens*). This was the best available approximation

to represent the effect of the biofilm that grows in drinking water networks. The analytical method response was also evaluated for a different type of water (tap water).

The applicability of the DI-LC-DAD method to quantify PQ in waters, when a PQ commercial formulation (GMX) is used as contamination agent, was also assessed. Although the composition of the commercial mixture was known, the purity in terms of PQ was confirmed by the standard addition method. By this way, increasing amounts of PQ analytical standard were added to a constant amount of GMX [8]. The content of PQ was determined by the interception of the DAD response for the prepared samples with the independent variable axis. It was verified that there are 27±2 mg of PQ per 100 mg of GMX. This result confirms the value supplied by Syngenta, which is 25.6 wt.%.

The recovery values obtained for all referred situations are indicated in Table 2.3.

Table 2.3. Recovery assays of the DI-LC-DAD analytical method.

		PQ concentration (mg/L)		
Recovery (%) (n=3)		**0.25**	**30**	**80**
Tap water		120±3	99±1	100±1
GMX		100±6	101±1	104±1
Deposits	Clay	90±2	95±3	94±4
	S4	109±4	100±1	99±1
	S3	91±6	102±1	107±1
	S2	23±1	95±1	105±1
Cells		6±2	100±1	97±1

Generaly the recovery percentages obtained are acceptable, except for the experiments with S2 deposit and cells at the lowest spiking level. Recoveries on average of 77, 99 and 101% were attained for 0.25, 30 and 80 mg/L of PQ by this method, respectively. The recovery of 23% and 6% respectively for S2 and Cells should be confirmed in future work, but they may be due to the higher global uncertainty associated to results for this concentration level.

2.3.1.4 Estimation of the global uncertainty associated to the DI-LC-DAD method

To evaluate the global uncertainty associated to the quantification of PQ in water by DI-LC-DAD, the *bottom-up* approach was used. This methodology was proposed by the

International Organization for Standardization (ISO) and adopted by EURACHEM/CITAC Guide [1]. The most significant sources of uncertainty that are thought to affect the final result are: the uncertainty associated with the preparation of the standards (U1), to the calibration curve (U2), the uncertainty associated to the precision of the extraction and also of the chromatographic method (U3) and to the accuracy (U4). Description of main contributions and respective calculation formula for the global uncertainty is given in Annex I. The contribution of these four individual uncertainties to the global uncertainty is depicted in Figure 2.2. As illustrated, for PQ concentrations lower than 5 mg/L, the main source of uncertainty is the uncertainty associated to the calibration curve (U2). On the other hand, for higher concentrations of analyte, the accuracy (U4) is the main responsible for the variation of the response. Standard preparation (U1) contributes always with less than 10% for the global uncertainty. Precision (U3) has the same behavior of accuracy (U4): the higher the analyte concentration, the higher the precision and accuracy contributions.

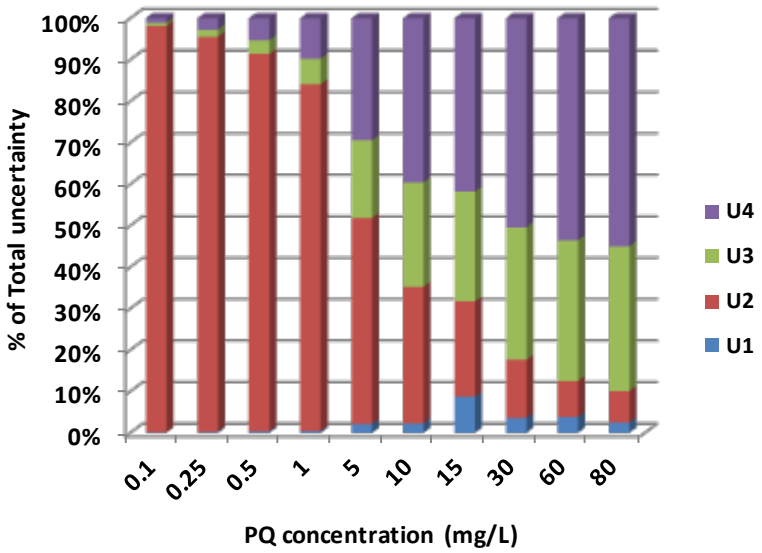

Figure 2.2. Relative weight of each individual source of uncertainty (*bottom-up* approach/EURACHEM) for PQ quantification in waters by DI-LC-DAD.

Global uncertainty below 13% was found for the most part of the calibration range (Figure 2.3). However, when concentrations approach the detection limits of the analytical method, assessed global uncertainty increases and represents more than 100%

of the stated value. For that reason, Figure 2.3 only represents the global uncertainty for paraquat dichloride concentrations higher than 1 mg/L.

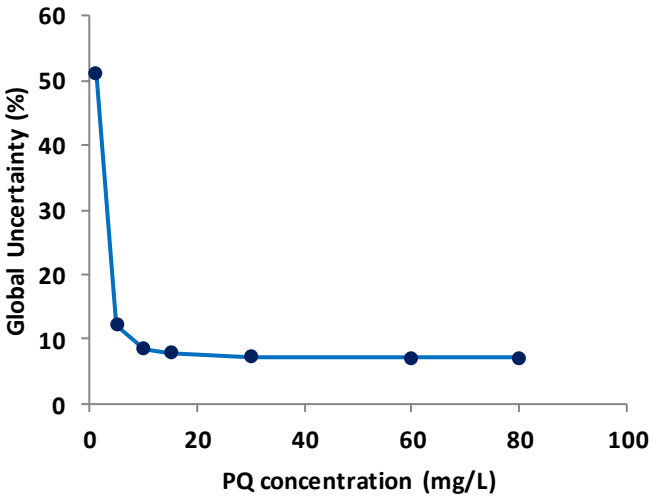

Figure 2.3. Global uncertainty of the analytical methodology for PQ quantification in waters by DI-LC-DAD.

The main advantages of the DI-LC-DAD method are the simplicity and rapidity of the determination, because results may be obtained in few minutes, with good accuracy and precision. The equipment is also common in most analytical laboratories, which is very important in an emergency situation. However some drawbacks should be pointed out:

1) Detection limit (10 μg/L) is higher than maximum legal limit (0.1 μg/L); however in the event of a deliberate contamination this is an excellent method for rapid detection;
2) A significant uncertainty is found near the limit of detection of the method and up to 1 mg/L;
3) Possibility of co-elution of other contaminants and therefore an unequivocal identification of the contaminant cannot be assessed, unless other methods are used for confirmation purposes, as LC-MS.

2.3.1.5 Specificity of the method – study of interferences from Fenton's reaction

This topic is particularly important when water samples have to be analysed following a decontamination procedure using a chemical method, as it happens with the

decontamination by Fenton's reagent, which is presented later (Chapter 5). The interference of chemicals used in the Fenton´s reaction, such as H_2O_2, $FeSO_4$ and Na_2SO_3, on the analytical method response was studied. It was assumed that these species interfere with the measurement of PQ by DI-LC-DAD if the variation of the paraquat peak area was superior to the global uncertainty for the considered PQ contamination level.

It is important to highlight the novelty of this research topic since, up to the author knowledge it was never addressed in any other study reported in open scientific literature.

2.3.1.5.1 Iron salt

The effect of Fe (II) was assessed by evaluating the PQ analytical response in the presence of two $FeSO_4$ concentrations at different PQ contamination levels. Figure 2.4 shows the variation of the PQ peak area in relation to the value achieved for a PQ standard prepared in water.

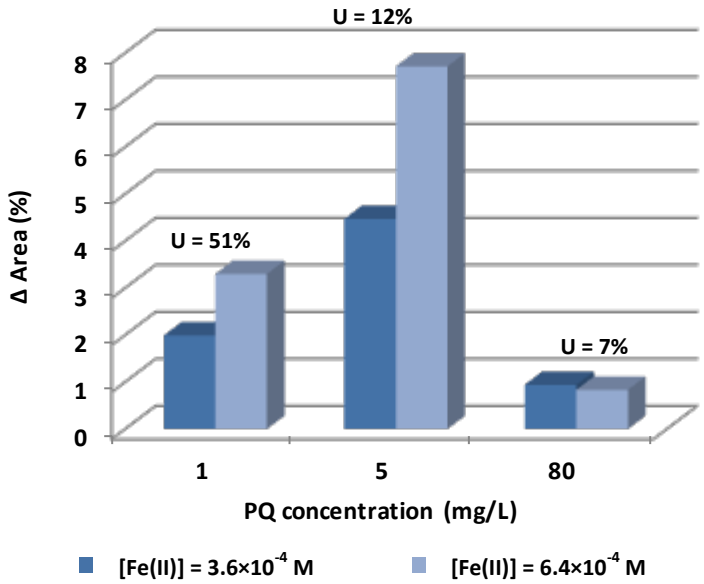

Figure 2.4. Influence of the presence of $FeSO_4$ in paraquat quantification by DI-LC-DAD.

As can be checked from Figure 2.4, variations of the PQ peak area are below the estimated global uncertainty for the correspondent PQ contamination level. For that reason, it can be concluded that there is no influence of the iron salt in the PQ quantification by the proposed method.

2.3.1.5.2 Sodium sulfite and hydrogen peroxide

Regarding the interference of Na_2SO_3, which is added to quench the reaction, it can be observed from Figure 2.5 that it depends on the concentration of this species in solution. The variation of the PQ peak area is below the global uncertainty for the three lower concentrations of Na_2SO_3 (9.6×10^{-3}, 3.9×10^{-2} and 9.6×10^{-2} M). However, for the two higher ones (2.0×10^{-1} and 3.4×10^{-1} M), the variations of the PQ peak area are clearly above the estimated global uncertainty (12% for 5 mg/L of PQ and approximately 7% for higher PQ concentrations). The observed variations are consequence of significant decreases on PQ peak areas in the presence of high concentrations of Na_2SO_3.

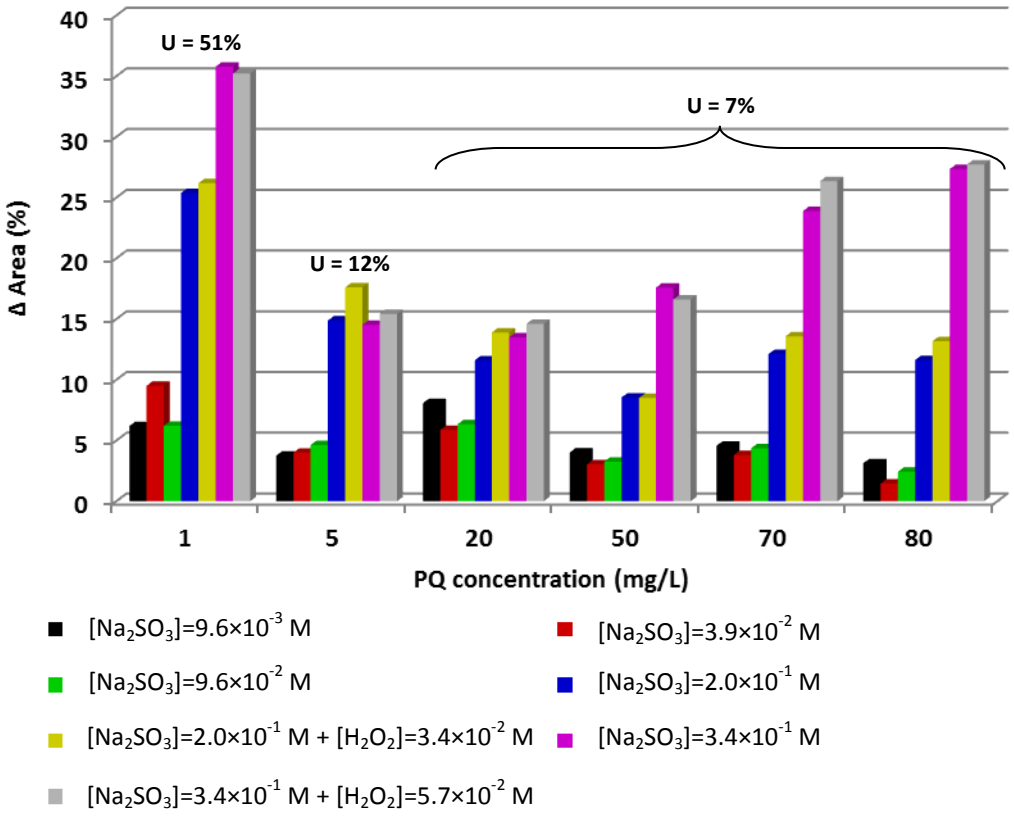

Figure 2.5. Influence of the presence of Na_2SO_3 and H_2O_2 in PQ quantification by DI-LC-DAD.

The interference in the analytical response may be explained by the shift effect, in the maximum wavelength or in the absorbance signal, which a molecule suffers in the presence of other chemical species. The bathochromic or hypsochromic shift is the

change of spectral band position in the absorption spectrum of a molecule to a longer or shorter wavelength, respectively. This can occur because of a change in environmental conditions, for example, or a change in solvent polarity. On the other hand, the hypsochromic shift is the reduction of the intensity of the absorption band.

So, it means that higher concentrations of Na_2SO_3 may interfere with the measurement of PQ concentration in waters by the proposed method. Because of the decrease on the PQ peak area, calibration curves were obtained in the absence and in the presence of the two major concentrations of Na_2SO_3 studied, where influence was verified (Figure 2.6). Figure 2.6 clearly shows that the quantification of PQ in the presence of Na_2SO_3 needs to be corrected by a conversion factor depending on the concentration of this specie.

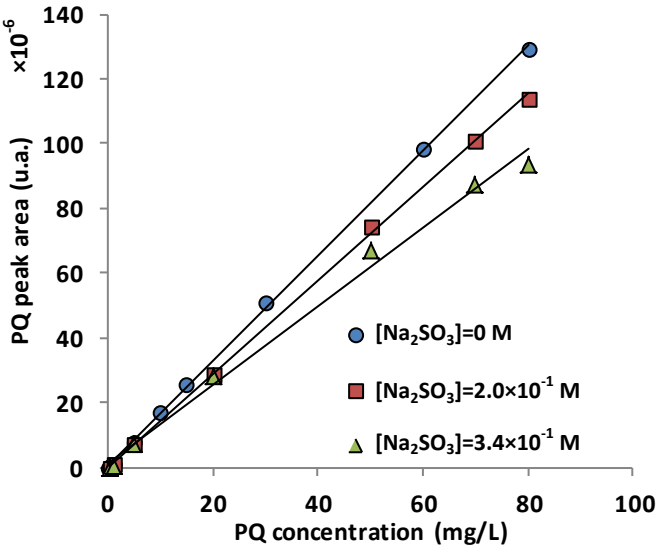

Figure 2.6. Calibration curve for PQ quantification in water and in different concentrations of Na_2SO_3 by DI-LC-DAD.

H_2O_2 is consumed along the Fenton's reaction and its concentration was not monitored along the experiments. Although its concentration was becoming lower with the reaction time, the amount of Na_2SO_3 added to quench the reaction, whenever a sample was withdrawn, was kept constant. The amount of Na_2SO_3 added corresponds to an excess of six times related to the amount of H_2O_2 used in the experiment. So, the best and worst

case scenarios were considered for interference assays with H_2O_2. In other words, the best situation corresponds to a H_2O_2 absence and the worst one to the presence of all H_2O_2 dose added in the experiment at the beginning of the process. For time consuming reasons, only the two higher H_2O_2 concentrations were studied (which corresponds also to the two higher Na_2SO_3 concentrations) because if there were not influence on the analytical response under these conditions it means that there were not at lower H_2O_2 concentration levels. As can be checked from Figure 2.5, the presence of H_2O_2 has no effect on the PQ peak area.

Despite of the interference of high doses of Na_2SO_3 (2.0×10^{-1} and 3.4×10^{-1} M) on the analytical response, is important to highlight that for the optimum PQ degradation conditions ($[Fe^{2+}]_0 = 5.0\times10^{-4}$ M, $[H_2O_2]_0 = 1.6\times10^{-2}$ M and $[Na_2SO_3] = 9.6\times10^{-2}$ M; Chapter 5), there is no influence of Fenton's species on the PQ quantification by DI-HLPC-DAD.

2.3.2 Validation of the SPE-LC-DAD method for low PQ concentrations

As referred before, the DI-LC-DAD method has as disadvantage a limit of detection higher than the EU legislated value (0.1 μg/L). To ensure that PQ in water is lower than the established limit, an analytical methodology was developed to quantify paraquat at low concentrations. For that, it was necessary to optimize a pre-concentration step prior to the injection in the LC-DAD.

2.3.2.1 Extraction technique

Solid phase extraction was the extraction methodology selected for this study because, according to the literature review done in Chapter 1, it has been the most used procedure for clean-up and isolation of PQ from water matrices. Concerning the packing materials used in SPE, it was decided to test silica and a cation exchange resin. Silica was chosen because it is one of the most polar sorbents available for SPE and proved to be a valid option for analysis of quaternary ammonium (QA) compounds like PQ [9-16]. The Oasis WCX sorbent, which is a polymeric reversed-phase, weak ion exchange mixed-mode sorbent, was also considered because it was designed for highly selective sample preparation of strong basic compounds and quaternary amines.

For the experiments with silica, the pH of the PQ aqueous solution was adjusted to 9 before the loading step because it is well known that QA compounds are largely retained

on silica under neutral or slightly basic conditions [9]. It was reported that recoveries for diquat, paraquat and difenzoquat are quite acceptable in the pH 6.5-9.5 range [9]. The same procedure was adopted for Oasis WCX sorbent because, according to the manufacturer, PQ is eluted from this sorbent at low pH (almost 100% for pHs lower than pH 2) [17].

For the elution step, three solvents were considered: HCl 0.1 M in methanol, HCl 6 M in methanol and saturated ammonium chloride in methanol. The acidic eluents were included in the list because as the QA compounds are retained in the sorbent under neutral or slightly basic conditions, it is expected that they will desorb under acidic medium. In particular, hydrochloric acid has been used as eluent in SPE pre-concentration procedures for PQ in waters [10, 11, 14]. Methanol (MeOH) was tested because it is sometimes applied in some eluents to desorb PQ from a wide range of SPE sorbents: silica [10-16], graphitized carbon black [18], resin [19], alumina [20]. On the other hand, MeOH has lower boiling point than water and so, the pre-concentration step of the final extract by solvent evaporation is facilitated. Ammonium compounds such as ammonium sulphate [12, 13, 16, 18], ammonium chloride [19], ammonium formate [21] and ammonium hydroxide [22] have been widely used to elute PQ in SPE. Saturated ammonium chloride is often used as PQ displacement agent in other matrices such as soils [23, 24]. For that reason, saturated ammonium chloride was selected.

The results obtained when 1 L of PQ aqueous solution (10 μg/L) was loaded through silica or Oasis WCX sorbents and the three above-mentioned eluents were used are outlined in Figure 2.7.

The extraction percentages were calculated comparing the analytical response obtained for a 10 mg/L PQ solution with that obtained for the extracted samples. As can be seen, higher extraction percentages are attained when Oasis WCX cartridge was used. As HCl 0.1 M in MeOH is sufficient to obtain acceptable extraction percentages, this solvent was used in the following experiments.

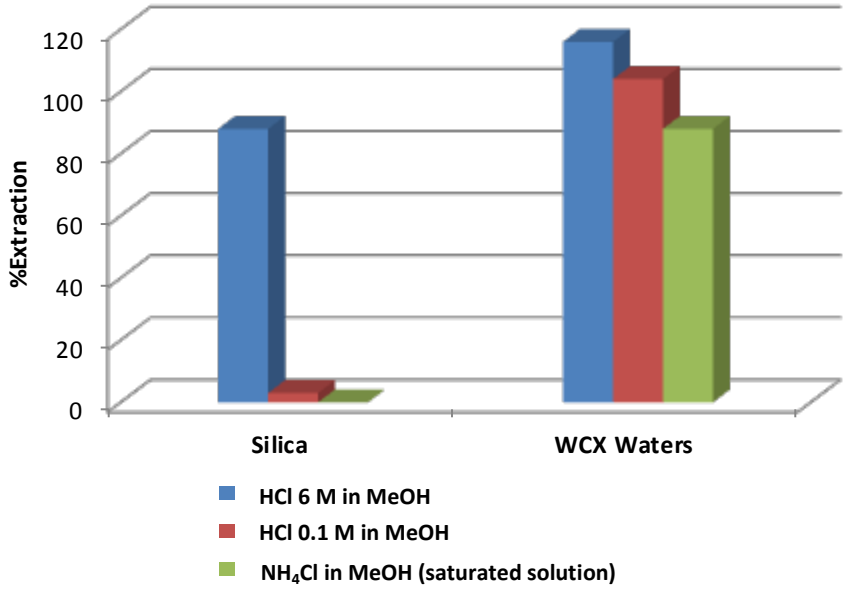

Figure 2.7. Optimization of solid phase extraction methodology.

2.3.2.2 Quantitative analysis

The calibration curve was carried out at seven concentration levels, in the range of 0.1 to 50 μg/L of PQ. Good linearity was obtained in the concentration range studied (R = 0.9989). Quantitative parameters were obtained from the calibration curve and are indicated in Table 2.4. The limits of detection and quantification were calculated based on a Signal Noise to Ratio (S/N) of 3 and 10 and are 0.04 and 0.1 μg/L, respectively.

Table 2.4. Quantitative parameters obtained from PQ analysis in water by SPE-LC-DAD.

Parameters	**SPE-LC-DAD**
Calibration curve[a]	$A = (94\pm1)\times10^{4}\ C\ (\mu g/L) + (-2\pm3)\times10^{5}$
Range of linearity (μg/L)	0.1 – 50
Correlation coefficient (R)	0.9989
LOD (μg/L)[b]	0.04
LOQ (μg/L)[c]	0.1

[a] A is PQ peak area and C is the concentration in μg/L; [b] Limit of detection; [c] Limit of quantification.

The LOD of 0.04 μg/L of PQ is of the same order of magnitude [13, 15, 16, 18] or lower [12, 14, 22] than the values reported in other studies of the literature.

The relative standard deviation of the slope was 1.5% and the correlation coefficient of the calibration curve was 0.9989. It was also verified that the confidence limits for the interception contains the origin (b-sb<0<b+sb). Again, and according to these results, it can be concluded that the calibration curve is adequate for the purpose of this analysis [6].

2.3.2.3 Precision and accuracy

Precision was evaluated by six consecutive injections of extracts obtained from the concentration of PQ analytical standards by SPE. The precision was inspected at three PQ concentration levels and the results, expressed as relative standard deviation, were 8.9, 1.4 and 0.5% for 0.2, 10 and 50 μg/L, respectively.

Accuracy of this methodology was estimated comparing the PQ concentration level obtained from the calibration curve with the expected concentration determined by the real amount added to the water. This parameter was evaluated at two PQ concentration levels – 10 and 50 μg/L. Recoveries were on average 84 and 101% for 10 and 50 μg/L levels, respectively.

2.3.2.4 Estimation of the global uncertainty associated to the SPE-LC-DAD method

The global uncertainty associated to the quantification of PQ in water by SPE-LC-DAD was also estimated by the *bottom-up* approach/EURACHEM [1]. From Figure 2.8, it can be seen that the uncertainty associated to the calibration curve (U2) represents the main source of uncertainty, particularly for lower PQ concentration levels. For higher PQ concentrations, the weight of the uncertainty associated to the precision (U3) for the overall uncertainty is comparable to that attained for the uncertainty associated to the calibration curve (U2). The uncertainties associated with the preparation of the standards (U1) and accuracy (U4) increase for higher PQ contamination degrees, but minimal relative individual contributions to the total uncertainty were estimated.

As shown in Figure 2.9, the lower the concentration level, the higher is the uncertainty associated to the results.

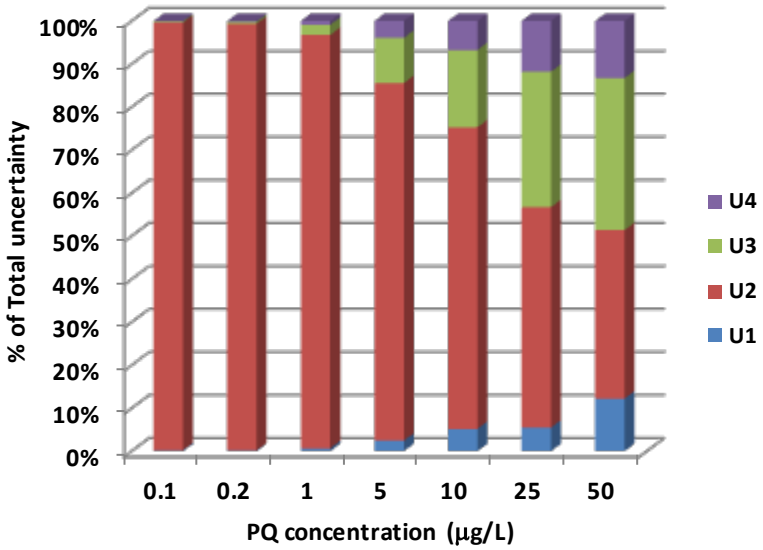

Figure 2.8. Relative weight of each individual source of uncertainty (*bottom-up* approach/EURACHEM) for PQ quantification in waters by SPE-LC-DAD.

Global uncertainty below 11% was found for PQ concentrations higher than 5 µg/L (Figure 2.9). However, in the vicinity of the LOD of the analytical method, assessed global uncertainty increases and represents more than 100% of the stated value. For that reason, Figure 2.9 only represents the global uncertainty for PQ concentrations higher than 1 µg/L.

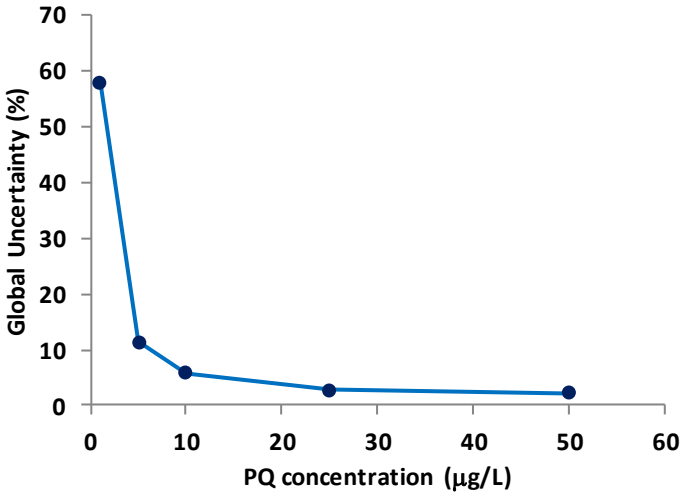

Figure 2.9. Global uncertainty of the analytical methodology for PQ quantification in waters by SPE-LC-DAD.

2.3.3 Validation of the DI-LC-MS method for confirmation purposes

A drawback of the LC–DAD methods is the impossibility of the unequivocal identification of the contaminants/ oxidation by-products. The solution is to use an alternative method for confirmation purposes. That is to say, in the event of detecting a possible contamination by the rapid method (LC–DAD), a confirmation needs to be done by LC–MS.

Paraquat may be analysed by direct injection in LC–MS in less than 5 minutes. This is the main advantage, besides the fact that it is the only method that imparts an unequivocal identification of the detected analyte, although the equipment is extremely expensive and its use is reserved to high-skilled and trained technicians.

2.3.3.1 Solvents/ Mobile phase selection

Charged quaternary amines, such as paraquat, exhibit little retention on C18 or other alkyl stationary phases and therefore a mobile phase modifier (ion-pairing reagent) needs to be added to increase the interactions between paraquat and the stationary phase, providing the necessary retention and resolution. For compatibility with MS detection, however, a volatile mobile phase is needed and, therefore, low concentrations of HFBA effectively shield the positive charges of paraquat, increasing interactions between the quaternary amines and the stationary phase.

2.3.3.2 MS optimization procedures

The optimization of MS is achieved in three steps: mass, ionization source and chromatographic optimization.

Firstly, a PQ standard solution (5 mg/L) was direct-infused in the electrospray mass spectrometer. This procedure allowed obtaining the mass fragmentation pattern of PQ, as well as, the parent ion. The most abundant peaks were the singly charged molecular ion $[M]^{+\bullet}$ (*m/z* 186) and the deprotonated molecule $[M\text{-}H]^{+}$ (*m/z* 185). The highest predominant ion which results from the fragmentation of $[M\text{-}H]^{+}$ was the $[M\text{-}CH_3]^{+}$ (*m/z* 171) one.

The mass optimization was carried out by evaluating the MS response when the capillary voltage, the needle voltage and the RF loading were changing at a time while the others were kept constant (single factor-at-a-time approach). The value which gave the best

single factor-at-a-time MS response was considered the optimal condition for the parameter under study. Finally, for the best individual conditions the excitation amplitude CID was set. The shield voltage was set at 600 V, according to the manufacturer. The optimal values for each parameter are compiled in Table 2.5.

The optimal condition for the temperature of the drying gas, as well as, the best drying and nebulization gas pressures were determined by direct injection of a PQ standard solution (5 mg/L) in combination with the mobile phase (0.2 mL/min). The mobile phase was 50% HFBA 5 mM and 50% MeOH. Again, the best conditions represent the best individual MS responses by varying each parameter at a time (Table 2.5).

Table 2.5. Optimal mass spectrometry conditions for PQ determination.

Ionization mode	**Capillary voltage (V)**	**Needle voltage (V)**	**RF loading (%)**	**$T_{drying\ gas}$ (°C)**	**$P_{drying\ gas}$ (psi)**	**$P_{nebulization\ gas}$ (psi)**	**Excitation amplitude CID (V)**
positive	87	3839	77	400	20	50	1.36

The drying and the nebulization gas pressures are related to the flow rate of the mobile phase. Typically, values between 0.2-0.3 mL/min for the flow rate of the mobile phase were used in LC-MS analysis. Therefore, according to the manufacturer' reference values, the nebulization gas pressure should be higher than 40 psi and the drying gas pressure should range from 15 to 45 psi.

To optimize the chromatographic conditions, a PQ analytical standard (5 mg/L) was injected in a C18 column, under the conditions optimized previously. The influence of the amount of methanol in the mobile phase on the LC-MS response was studied. The maximum MS response was attained when 20% of MeOH and 80% of HFBA 5 mM were used. Under these conditions, the retention time for PQ was 4.7 min.

2.3.3.3 Linearity and limits of detection and quantification

The calibration curve for determination of PQ in water by LC–MS was obtained with ten PQ analytical standards (from 0.1 to 10 mg/L). The analytical standards were directly injected in the LC-MS, at least twice, with a coefficient of variation in the range of 1.9 - 9.4%. The calibration curve and the respective 98% confidence range are presented in

Figure 2.10. The quantitative information about the method developed in LC–MS is presented in Table 2.6.

As observed in the other proposed methods, LC-MS method is also suitable to be applied in a quality control laboratory because the relative standard deviation of the slope is lower than 5%, the correlation coefficient is higher than 0.995 and the confidence limits for the interception contains the origin (b-sb<0<b+sb) [6].

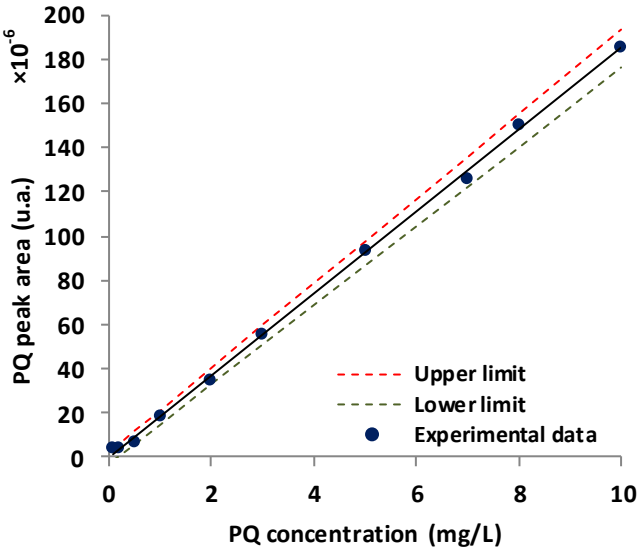

Figure 2.10. Calibration curve for PQ quantification in water by DI-LC-MS.

Table 2.6. Quantitative parameters obtained from PQ analysis in water by DI-LC-MS.

Parameters	**LC-MS**
Calibration curve[a]	$A = (185\pm2)\times10^5\ C\ (mg/L) + (-6\pm9)\times10^5$
Range of linearity (mg/L)	0.1 – 10
Correlation coefficient (R)	0.9991
LOD (mg/L)[b]	0.02
LOQ (mg/L)[c]	0.06

[a] A is PQ peak area and C is the concentration in mg/L; [b] Limit of detection; [c] Limit of quantification.

The limits of detection and quantification were determined based on a Signal Noise to Ratio (S/N) of 3 and 10 and were 20 and 60 μg/L, respectively. Similar LODs (7-25 μg/L) were found in the literature for DI-LC-MS methods [25-27].

2.3.3.4 Precision and accuracy

Precision of the PQ analytical method by LC-MS was assessed by repeatability and intermediate precision. Repeatability was determined by six consecutive injections of three PQ analytical standards (0.2, 5 and 10 mg/L). The intermediate precision was evaluated for the same PQ concentration levels and corresponds to the injection of each standard in three days. The results expressed as relative standard deviation are shown in Table 2.7.

Table 2.7. Analytical method precision for analytical standards.

	PQ concentration (mg/L)		
	0.2	**5**	**10**
Repeatability (%) (n=6)	5.3	4.0	3.8
Intermediate Precision (%) (n=3)	12.9	5.9	6.4

Accuracy was evaluated comparing the analytical response for a standard prepared in distilled water with that obtained for a standard prepared in river water (Rio Ave). This parameter was assessed in triplicate at three PQ concentrations: 0.2, 5 and 10 mg/L. Recoveries were 94±10, 101±11 and 96±7 for 0.2, 5 and 10 mg/L of PQ.

2.3.3.5 Estimation of the global uncertainty associated to the LC-MS method

The global uncertainty associated to the results obtained by the proposed LC-MS method was estimated by the *bottom-up* approach/EURACHEM. Figure 2.11 depicts the contribution of each individual source of uncertainty for the overall uncertainty. As demonstrated, the uncertainty of a result is mainly dependent on the uncertainty associated to the calibration curve (U2) for low PQ concentrations. However, this source of uncertainty contributes only with 12% to the total uncertainty at high PQ concentration degrees while the uncertainties associated to precision (U3) and accuracy (U4) with around 80-85%. The uncertainty associated to the preparation of the standards (U1) is minimal in the overall range of concentrations.

The global uncertainty for all PQ linearity range (0.1 to 10 mg/L) is illustrated in Figure 2.12.

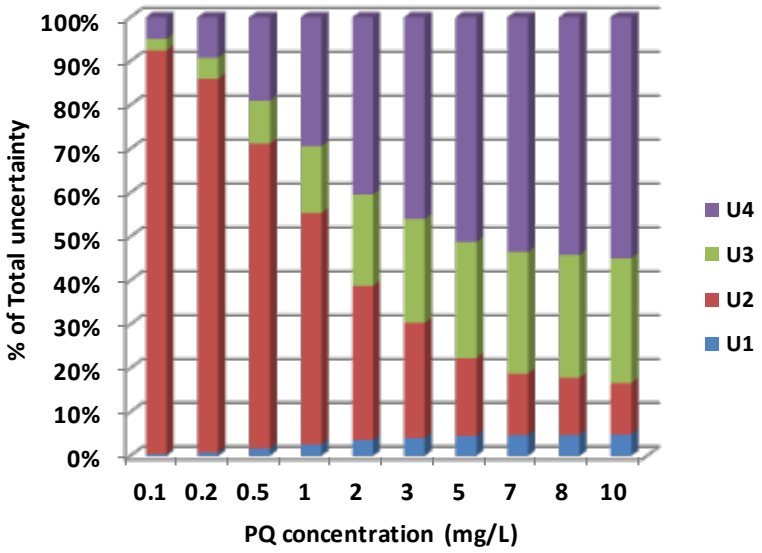

Figure 2.11. Relative weight of each individual source of uncertainty (*bottom-up* approach/EURACHEM) for PQ quantification in waters by DI-LC-MS.

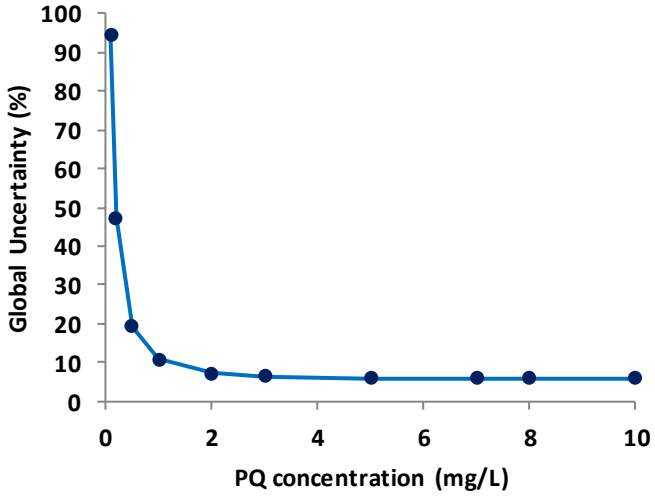

Figure 2.12. Global uncertainty of the analytical methodology for PQ quantification in waters by DI-LC-MS.

As observed in Figure 2.12, the global uncertainty is around 6% for PQ concentrations higher than 3 mg/L (the most part of the linearity range). For lower concentrations, the global uncertainty associated to the results increase exponentially. In short, this method proved to be reliable for confirmation of PQ in waters at concentrations above 20 μg/L.

2.4 Conclusions

The three analytical methods presented in this chapter were successfully validated as *bottom-up* for PQ analysis in waters. LODs of 10 μg/L, 0.04 μg/L and 20 μg/L of PQ were reached for DI-LC-DAD, SPE-LC-DAD and DI-LC-MS methods, respectively. Precision was evaluated for all methods and it was verified that for medium and higher PQ concentrations, the variations in the response are well below 10% (typically the acceptable error). The DI-LC-DAD method proved to be accurate in the presence of other species or compounds resulting from the contact of the water with deposits and cells, from the PQ commercial formulation (GMX) and from other types of water. Recoveries on average of 77, 99 and 101% were attained for 0.25, 30 and 80 mg/L of PQ by DI-LC-DAD method, respectively. It was also shown that for concentrations of Fe(II), H_2O_2 and Na_2SO_3 lower than 6.4×10^{-4}, 5.7×10^{-2} and 9.6×10^{-2} M, respectively, no effects are observed in the analytical response of the DI-LC-DAD method. It is important to highlight that for the optimum PQ degradation conditions ($[Fe^{2+}]_0 = 5.0\times10^{-4}$ M, $[H_2O_2]_0 = 1.6\times10^{-2}$ M and $[Na_2SO_3] = 9.6\times10^{-2}$ M; Chapter 5), there is no influence of Fenton's species on the PQ quantification by this method. Average recoveries of 93 and 97% were obtained for SPE-LC-DAD and DI-LC-MS methods, respectively, which account for they accuracy.

For all methods, the global uncertainty increase with the decrease of PQ concentration. Global uncertainties of 6 to 13% were obtained for PQ concentrations higher than 5 mg/L (linearity of 0.1 to 80 mg/L of PQ) by DI-LC-DAD, 5 μg/L (linearity of 0.1 to 50 μg/L of PQ) by SPE-LC-DAD and higher than 1 mg/L (linearity of 0.1 to 10 mg/L of PQ) by DI-LC-MS.

All methods proved to be precise, accurate and suitable for the purpose that they were designed.

2.5 References

[1] S.L.R. Ellison, M. Rosslein and A. Williams, *Eurachem/ Citac Guide- Quantification uncertainty in analytical measurement*, EURACHEM/ CITAC, UK, 2000.

[2] N. Ratola, J. Amigo and A. Alves, *Levels and Sources of PAHs in Selected Sites from Portugal: Biomonitoring with Pinus pinea and Pinus pinaster Needles*, Arch. Environ. Contam. Toxicol. 58 (2010) 631-647.

[3] S. Teixeira, C. Delerue-Matos, A. Alves and L. Santos, *Fast screening procedure for antibiotics in wastewaters by direct HPLC-DAD analysis*, J. Sep. Sci. 31 (2008) 2924-2931.

[4] C. Oliveira, M.S.F. Santos, F.J. Maldonado-Hódar, G. Schaule, A. Alves and L.M. Madeira, *Use of pipe deposits from water networks as novel catalysts in paraquat peroxidation*, Chem. Eng. J. 210 (2012) 339-349.

[5] P.C. Schlecht and P.F. O'Connor, *NIOSH Manual of Analytical Methods*, 4th ed., National Institute for Occupational Safety Health, 2003.

[6] J.C. Miller and J.N. Miller, *Statistics for analytical chemistry*, 2nd ed., Ellis Horwood, Chichester-England, 1988.

[7] F. Echeverría, J.G. Castaño, C. Arroyave, G. Peñuela, A. Ramírez and J. Morató, *Characterization of deposits formed in a water distribution system*, Rev. Chil. Ing. 17 (2009) 275-281.

[8] D.C. Harris, *Quantitative Chemical Analysis*, 6th ed., W.H. Freeman, New York, 2003.

[9] Y. Picó, G. Font, J.C. Moltó and J. Mañes, *Solid-phase extraction of quaternary ammonium herbicides*, J. Chromatogr. A 885 (2000) 251-271.

[10] J.L. Martínez Vidal, A. Belmonte Vega, F.J. Sánchez López and A. Garrido Frenich, *Application of internal quality control to the analysis of quaternary ammonium compounds in surface and groundwater from Andalusia (Spain) by liquid chromatography with mass spectrometry*, J. Chromatogr. A 1050 (2004) 179-184.

[11] R. Castro, E. Moyano and M.T. Galceran, *Ion-pair liquid chromatography–atmospheric pressure ionization mass spectrometry for the determination of quaternary ammonium herbicides*, J. Chromatogr. A 830 (1999) 145-154.

[12] M. Ibáñez, Y. Picó and J. Mañes, *On-line liquid chromatographic trace enrichment and high-performance liquid chromatographic determination of diquat, paraquat and difenzoquat in water*, J. Chromatogr. A 728 (1996) 325-331.

[13] M. Ibáñez, Y. Picó and J. Mañes, *Influence of organic matter and surfactants on solid-phase extraction of diquat, paraquat and difenzoquat from waters*, J. Chromatogr. A 727 (1996) 245-252.

[14] M.C. Carneiro, L. Puignou and M.T. Galceran, *Comparison of silica and porous graphitic carbon as solid-phase extraction materials for the analysis of cationic herbicides in water by liquid chromatography and capillary electrophoresis*, Anal. Chim. Acta 408 (2000) 263-269.

[15] R. Rial-Otero, B. Cancho-Grande, C. Perez-Lamela, J. Simal-Gándara and M. Arias-Estévez, *Simultaneous determination of the herbicides diquat and paraquat in water*, J. Chromatogr. Sci. 44 (2006) 539-542.

[16] M. Ibáñez, Y. Picó and J. Mañes, *Improving the solid-phase extraction of 'quat' pesticides from water samples: Removal of interferences*, J. Chromatogr. A 823 (1998) 137-146.

[17] H. White, *Sample preparation strategies for water analysis*, Waters Corporation, 2007.

[18] M. Ibánez, Y. Picó and J. Manes, *On-line determination of bipyridylium herbicides in water by HPLC*, Chromatographia 45 (1997) 402-407.

[19] L. Grey, B. Nguyen and P. Yang, *Liquid chromatography-electrospray ionization isotope dilution mass spectrometry analysis of paraquat and diquat using conventional and multilayer solid-phase extraction cartridges*, J. Chromatogr. A 958 (2002) 25-33.

[20] F. Merino, S. Rubio and D. Pérez-Bendito, *Evaluation and optimization of an on-line admicelle-based extraction-liquid chromatography approach for the analysis of ionic organic compounds*, Anal. Chem. 76 (2004) 3878-3886.

[21] O. Núñez, E. Moyano and M.T. Galceran, *Time-of-flight high resolution versus triple quadrupole tandem mass spectrometry for the analysis of quaternary ammonium herbicides in drinking water*, Anal. Chim. Acta 525 (2004) 183-190.

[22] J.W. Munch and W.J. Bashe, *Method 549.2 - Determination of diquat and paraquat in drinking water by liquid-solid extraction and high performance liquid chromatography with ultraviolet detection*, U.S. Environmental Protection Agency, Cincinnati, Ohio 45268, 1997.

[23] B.V. Tucker, D.E. Pack and J.N. Ospenson, *Adsorption of bipyridylium herbicides in soil*, J. Agric. Food. Chem. 15 (1967) 1005-1008.

[24] T. Perez-Ruiz and J. Fenoll, *Spectrofluorimetric determination of paraquat by manual and flow injection methods*, Analyst 123 (1998) 1577-1581.

[25] R. Castro, E. Moyano and M.T. Galceran, *Ion-trap versus quadrupole for analysis of quaternary ammonium herbicides by LC-MS*, Chromatographia 53 (2001) 273-278.

[26] R. Castro, E. Moyano and M.T. Galceran, *On-line ion-pair solid-phase extraction–liquid chromatography–mass spectrometry for the analysis of quaternary ammonium herbicides*, J. Chromatogr. A 869 (2000) 441-449.

[27] R. Castro, E. Moyano and M.T. Galceran, *Determination of quaternary ammonium pesticides by liquid chromatography-electrospray tandem mass spectrometry*, J. Chromatogr. A 914 (2001) 111-121.

3 Paraquat quantification in deposits from drinking water networks*

Abstract

The aim of this work was to develop an expedite analytical methodology to evaluate the contamination level of paraquat in deposits from drinking water networks. This is a completely new work since, to the author knowledge, no other study has been focused on this matter. Three deposits representative of those typically found in drinking water networks were used: two iron-based – S2 and S3, and a calcium rich one – S4. The analytical method consists of an easy and fast extraction step, using a saturated ammonium chloride solution, followed by direct injection in a liquid chromatography with diode array detection (LC-DAD). A matrix-matched calibration was performed for paraquat, in the range of 5 to 193 μgPQ/g deposit, and a limit of detection of 0.1 μgPQ/g deposit was reached. The good percentages of recovery (90-101% on average) and the low relative standard deviations for repeated analyses observed for PQ-S3 system (3, 4 and 2% for 20, 80 and 160 μgPQ/g deposit, respectively) enable a reliable quantification of paraquat, even at the lowest contamination levels. The developed analytical methodology can also be extended for diquat and proved to be also suitable for paraquat quantification in different types of deposits.

3.1 Introduction

In case of an accidental or deliberated contamination event, deposits from drinking water networks may represent crucial zones of chemicals accumulation. Although sorption studies of PQ on representative deposits from drinking water networks (Chapter 4) suggested that it is unlikely that this chemical may adsorb on such materials, during the normal water distribution [1], other situations should be taken into account. In fact, in case of stagnancy of the fluid for a very long period of time (in tanks or pipes in case of a consumption break) or low water flow (e.g. during the night), this compound may adsorb

* Adapted from: Mónica S.F. Santos, Luís M. Madeira and A. Alves, Paraquat quantification in deposits from drinking water networks, *submitted*, 2013.

on deposits. On the other hand, adsorption on loose deposits that are transported with the flowing water is much more likely to occur [1]. Therefore, it is imperative to develop an analytical methodology able to quantify paraquat/diquat (PQ/DQ) in deposits formed in the pipe walls. Ultimately, the quantification of PQ and DQ in deposits may have particular impact and interest for society, since deposits may be used as an indirect measure of the water quality and degree of pollution. Indeed, whenever a cleaning or maintenance procedure is scheduled the deposits may be considered for analyses with this purpose in mind.

Many approaches have been described for PQ and DQ extractions from solid matrices as soils, food crops and plants. Since they have tendency to interact strongly with various surfaces via hydrogen, ionic and π-π bonds, their extraction typically involves a refluxing/digestion step with acid, for periods of several hours, to destroy the structure and release the herbicides from it [2]. As explained with more detail in section 1.1.2– Chapter 1, the traditional refluxing or digestion techniques (in acidic medium) are the ones most reported for extraction of PQ from soils, but the microwave-assisted technique (also implemented in acidic conditions) has gained popularity due to the shorter extraction times, less solvent quantities and sample amounts required. However, these techniques may be not suitable to be applied for other pesticides analysis because, typically, they are not stable under these very acidic conditions [3]. On the other hand, the release of chemicals by matrix structure destruction provides little or no information on their adsorption status [3]. This can be a relevant aspect in the context proposed here, since it is important to have an idea of the degree of interaction between chemicals and deposits; in other words, if they have tendency to be released from them by simple contact with “clean water”.

This chapter intends to diminish the great lack of information about analytical methodologies able to quantify compounds in deposits formed along drinking water networks, developing a methodology for PQ as case-study (and extensible for DQ). To the author best knowledge, no other study is available on this matter. The simple and inexpensive method proposed here consists of a fast and easy extraction step, which uses small sample and solvent amounts. Furthermore, a complete set of validation parameters is presented, including the calculation of the global uncertainty associated to the results in the range of quantification.

3.2 Experimental section

3.2.1 Reagents and working solutions

Paraquat dichloride PESTANAL® analytical standard 99.2% (Fluka) and Diquat dibromide monohydrate PESTANAL® analytical standard were purchased from Sigma-Aldrich (St. Louis, USA). Heptafluorobutyric acid (HFBA) was from Sigma-Aldrich and acetonitrile (ACN) and methanol (MeOH) HPLC grade were from VWR BDH Prolabo (Poole, UK). Syringe filters with 0.2 μm PTFE membrane were purchased from VWR (West Chester, USA) and granular anhydrous calcium chloride (93%) and ammonium chloride (99.9%) from Sigma-Aldrich.

Stock solutions (1 g/L) of PQ and DQ were prepared in distilled water by solubilizing a known amount of the correspondent dried salt. The saturated ammonium chloride solution was prepared mixing 40 g of ammonium chloride salt with 100 mL of distilled water at 20 °C.

3.2.2 Deposits

The analytical methodology developed in this work was applied to three deposits representative of those typically found in drinking water distribution systems [4, 5]. Deposits (S2, S3 and S4) from Germany and Netherlands drinking water networks were kindly supplied by the IWW Water Centre (Mülheim an der Ruhr, Germany) and were already well characterized in previous published works [1, 5]. For simplicity, the nomenclature used before was kept here: S2 and S3 are iron-rich materials and S4 is a calcium rich deposit. Those deposits were collected from old cast iron pipes that needed replacement. They were dried in an oven until no weight variation was detected, before being sieved and kept dry until the experiments. Only particles sized between 38 and 64 μm were used in this work.

3.2.3 Equipment and operating conditions

The amounts of PQ and DQ extracted from deposits were measured by direct injection of 99 μL of the liquid phase in a Hitachi Elite LaChrom HPLC (Darmstadt, Germany) equipped with a L-2130 pump, a L-2200 autosampler and a L-2455 diode array detector (DAD). The chromatographic separation was achieved by a Purospher® STAR LiChroCART® RP-18 endcapped (240×4 mm, 5 μm) reversed phase column, supplied by VWR (West Chester,

USA), using gradient elution. The mobile phase is composed by a 10 mM HFBA aqueous solution and ACN. Initial gradient conditions were set at 100% HFBA 10 mM for 5 min, and then the organic phase was increased to 20% v/v during 5 min and kept for 15 min. Finally, it was returned to 100% HFBA after 5 min and kept for 10 min. The spectra were recorded from 220 to 400 nm, but PQ and DQ quantifications, with retention times of 16.2 and 16.0 min, were performed at 259 and 310 nm, respectively.

3.2.4 Spiking of deposits with PQ/DQ

In order to have samples contaminated with different PQ/DQ concentrations, 0.5 g of deposit was put in contact with 10 mL of a PQ/DQ solution of known concentration for 24 h at 20 °C. After that, the liquid and solid phases were separated by centrifugation in a Hettich Rotofix 32A Centrifuge – Kirchlengern, Germany (10 min, 4000 rpm). The PQ or DQ amount remaining in the liquid phase was measured by LC-DAD and the difference between the amounts at the beginning and at the end of the adsorption experiment allowed the calculation of the amount transferred to the solid phase (amount of pesticide adsorbed to the deposit).

3.2.5 Extraction procedure for the analytical determination

After PQ or DQ spiking, the deposit was freeze-dried in a lyophilizer for 12 h. After that, several amounts of extraction solvent were added to the contaminated deposit and the mixture was kept under agitation during several periods at 20 °C. A parametric study was performed in order to improve the extraction efficiency. The parameters considered in this study were: the type/nature of extraction solvent, the volume of extraction solvent and the extraction time.

3.2.6 Validation

The validation of the analytical method, including the uncertainty measurement, followed the *bottom-up* approach described in the EURACHEM CITAC Guide [6], and by other authors [7, 8]. Description of main contributions and respective calculation formula for the global uncertainty is given in Annex I. It comprised a first step of in-house validation, where the main parameters were obtained – linearity of the response, limit of detection (LOD) and limit of quantification (LOQ), precision and accuracy. The precision of the

method was evaluated extracting independent contaminated deposits at different contamination levels. Results were expressed as the coefficient of variation (CV%) of different replicate measurements. Accuracy was evaluated comparing the contamination level obtained by the calibration curve and the real amount of PQ/DQ adsorbed to the deposits. This parameter was evaluated at different degrees of contamination and for different systems.

The second step was evaluated by the estimation of the uncertainty of the results, using the other validation parameters as an assumption that they represented the main sources of uncertainty to the final result.

3.3 Results and discussion

This work comprised a previous optimization of the extraction technique for S3 deposit contaminated with PQ, followed by the validation of the analytical methodology, with special care to the estimation of the global uncertainty associated to the results. S3 was selected for method development over S2 and S4 given its higher PQ adsorption capacity, as demonstrated in a previous study [1]. Even so, the method response was also evaluated for the other two deposits (S2 and S4). Additionally, the analytical methodology developed for PQ was extended to the quantification of DQ, using S3 deposit as a case-study.

3.3.1 Optimization of the extraction technique

3.3.1.1 Effect of extraction solvent type

As explained before, no study about PQ quantification in deposits formed along drinking water networks was found in literature. So, the selection of the extraction solvents used to remove PQ from the deposits was based on the available information for soil matrices, which may however have a higher load of organic constituents. Additionally, a detailed study previously performed by our research group, about PQ adsorption on typical deposits, was taken into consideration [1]. In such work it was demonstrated that, although morphologically similar, soils and deposits could be very different in terms of PQ adsorption. It was concluded that the interactions between PQ and the deposits are extremely weak when compared to the interactions established in the major PQ-clay and PQ-soil systems found in the literature [1]. Two major factors were pointed out as the

main contributors for such observation: the lower organic fraction exhibited by deposits (around 1 wt.% or less) and their lower clay mineral content. Therefore, water and a saturated ammonium chloride solution were selected to study the extraction solvent, because, according to Tucker and co-workers [9], these solvents were able to remove the unbound PQ and the loosely bonded to a soil, respectively. Methanol is sometimes also applied to extract PQ from soils [10, 11] and, for that reason, was included in the list of solvents tested. The calcium chloride solution (0.01 M) was also selected since it is often chosen to remove PQ from soil, although to an extremely low extent due to the strong interactions established between analyte and adsorbent [12-14].

An S3 deposit (0.5 g) was spiked with paraquat (350 μgPQ/gS3) and was extracted with 10 mL of extraction solvent for 24 h at 20 ◦C. Then, a "clean" S3 deposit was extracted under the same conditions and the final extract was spiked with the same amount of paraquat added previously (350 μgPQ/gS3). The analytical responses for both were compared to calculate the extraction percentage.

As shown in Figure 3.1a, the saturated ammonium chloride solution is the solvent with higher extraction capability (95±10%) followed by the calcium chloride solution (29±1%). Water and MeOH exhibited very low desorption percentages when compared to the other solvents. These results indicated that, according to the classification given by Tucker et al. [9], PQ is loosely bound to S3 because a simple ion exchange process is sufficient to remove almost all the analyte. Since water leads to extremely low desorption percentages, it is important to highlight that it is unlikely that PQ desorbs from S3 by simple contact with "clean" water, as occurs in a normal drinking water flow, after the contamination front has passed through.

Therefore, the following experiments were carried out using saturated ammonium chloride solution as extraction solvent.

3.3.1.2 Effect of extraction solvent volume

The objective here was to use the lowest solvent volume possible, without compromising the extraction efficiency. The lower the extraction solvent volume, the higher the PQ concentration in the final extracts and, consequently, the lower the limit of detection reached. The volumes tested were 1, 2, 4, 6, 8 and 10 mL of saturated ammonium chloride solution. Volumes below 1 mL were not considered because there was not

enough extract for subsequent LC analysis. As seen in Figure 3.1b, the extraction percentage is almost not affected by the solvent volume in the range of volumes studied.

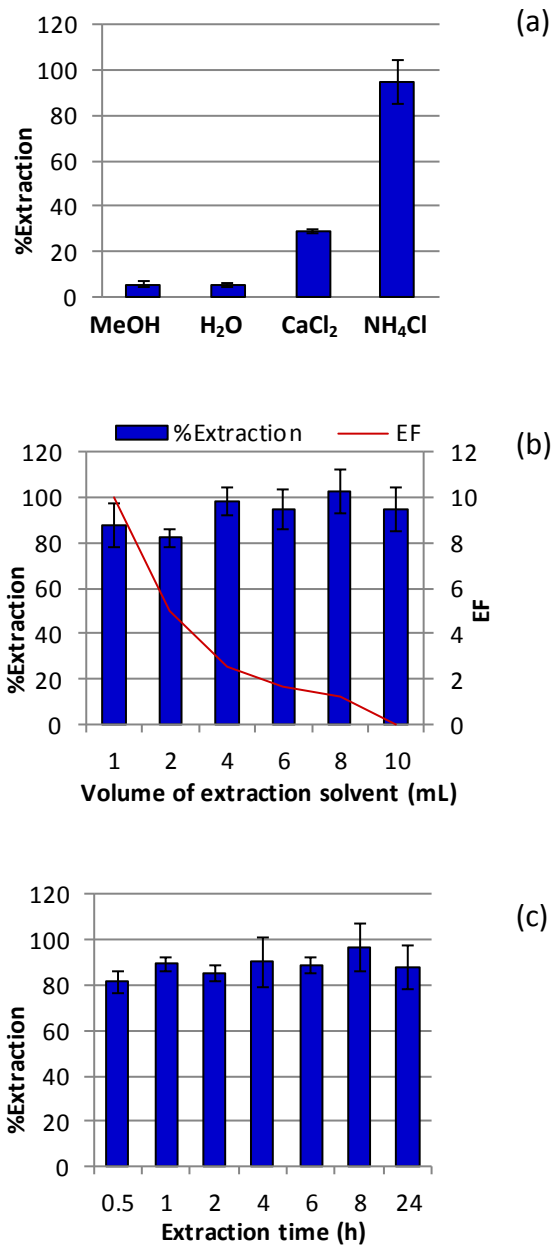

Figure 3.1. Effect of some parameters on the percentage of PQ extraction from S3 deposit and on the enrichment factor (EF): (a) Effect of extraction solvent type – 0.5 g S3, 10 mL of extraction solvent, 24 h, 20 °C; (b) Effect of extraction solvent volume – 0.5 g S3, saturated ammonium chloride solution, 24 h, 20 °C and (c) effect of extraction time – 0.5 g S3, 1 mL saturated ammonium chloride solution, 20 °C. Error bars correspond to standard deviation.

This means that the lowest volume tested (1 mL) is enough to displace almost all PQ molecules. On the other hand, the lower the extraction solvent volume the higher the enrichment factor (EF). Experiments at higher PQ contamination levels were also carried out and the same tendency was observed (although the amount of PQ increases for the same volume). The worst case scenario corresponds to the higher paraquat contamination level because the extraction with saturated ammonium chloride solution consists in the replacement of paraquat molecules by ammonium chloride ones. So, if a certain amount of extraction solvent is sufficient to displace all paraquat molecules (at high contamination levels) it is assumed that no problems exist at lower contamination levels. Thus, the solvent volume used in the following experiments was 1 mL.

3.3.1.3 Effect of the extraction time

The time of analysis is an important aspect if the analytical method is designed to be applied either for environment monitoring or degradation/sorption studies. Additionally, this is a crucial point, for instance, to obtain a fast response after a suspicion of contamination. Thus, extraction times of 0.5, 1, 2, 4, 6, 8 and 24 h were tested. According to the results shown in Figure 3.1c, after 30 min of contact 82±5% of PQ is extracted from the deposit. An increase of the time of contact apparently does not lead to an increase on the PQ extraction percentage, or it is marginal. This indicates that this simple and fast extraction process has a great advantage over other time-consuming processes in use and mentioned in the introduction section.

3.3.2 Quantitative analysis

3.3.2.1 Interference studies

The interference studies were performed to evaluate the effect of the presence of other species in the solution, resulting from the contact between extraction solvent and deposit, on the analytical response for PQ and DQ. With this in mind, the contamination and extraction procedures were also conducted without PQ/DQ addition in the contamination step (blank). After that, spiked tests were carried out and correspond to the addition of known amounts of analyte to this final extract (spiked blanks). The analytical response obtained for each spiked blank was compared with the correspondent standard prepared in distilled water. The tests were carried out at different concentration

levels and the results are presented in Figure 3.2. The final extract (blank) was also injected directly into the LC-DAD and none of the target compounds were detected in the original matrices. As can be checked from Figure 3.2, the analytical responses achieved for all spiked blanks (experiments denoted as PQ-S2, PQ-S3, PQ-S4 and DQ-S3 in Figure 3.2) are statistically equivalent to those obtained for standards prepared in water (experiments denoted as PQ-water and DQ-water in Figure 3.2). It was concluded that the analytical response is not affected by the presence of other species in solution.

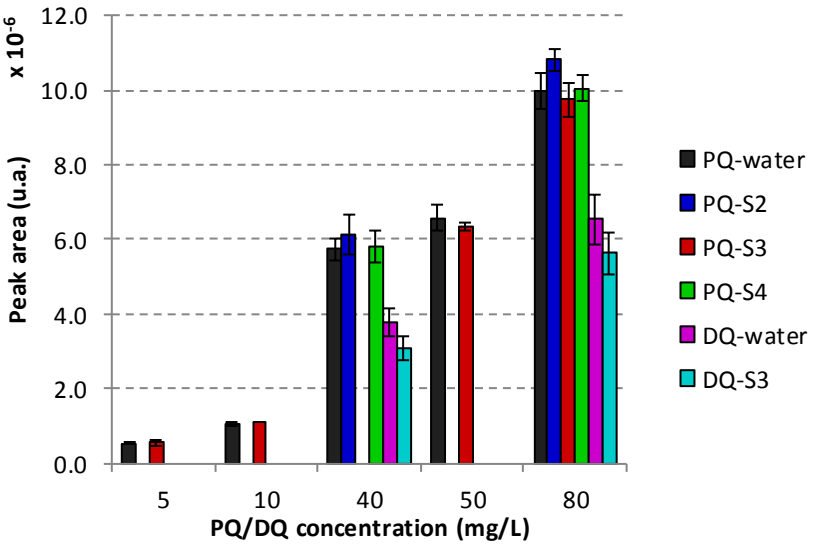

Figure 3.2. Interference studies in the paraquat and diquat quantification.

3.3.2.2 Linearity and limits of detection and quantification

Calibration was performed for PQ by LC-DAD using 7 S3 spiked samples (from 5 to 193 μgPQ/gS3), extracted as mentioned in the previous sections (Figure 3.3). The correlation coefficient (R=0.996) and the linearity tests revealed a good performance for the linearity. The LOD and LOQ calculated based on a signal-to-noise-ratio of 3 and 10 were 0.1 and 0.4 μgPQ/gS3, respectively.

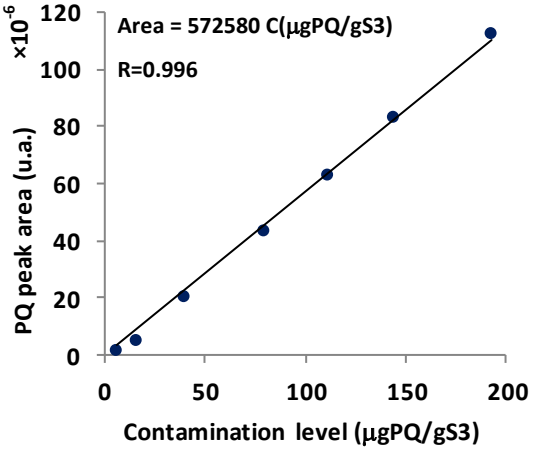

Figure 3.3. Calibration curve obtained for PQ-S3 system by LC-DAD.

3.3.2.3 Precision and Accuracy

The intermediate precision was evaluated at three PQ spiking levels – 20, 80 and 160 μgPQ/gS3. Intermediate precision, as expressed here, corresponds to the relative standard deviation (RSD%) observed when six independent samples, for each contamination level, were extracted and injected in the same day under the same conditions. Average precision was 3, 4 and 2% for 20, 80 and 160 μgPQ/gS3.

Accuracy was assessed comparing the contamination level obtained from the calibration curve and the amount of PQ adsorbed on the deposit. Recoveries were 90±1%, 97±2% and 101±1% for 20 μgPQ/gS3, 80 μgPQ/gS3 and 160 μgPQ/gS3, respectively.

The good recovery results and the low RSDs observed enable a reliable quantification of PQ in the tested samples, even at the lowest contamination level assessed.

3.3.2.4 Estimation of the global uncertainty associated to the results

It was assumed that there are four main sources responsible for the overall uncertainty of the results [6]: uncertainty associated with the preparation of the standards (U1), uncertainty associated with the calibration curve (U2), uncertainty associated to the precision of the extraction and also of the chromatographic method (U3) and the uncertainty associated to the accuracy (U4). The contribution of each source is depicted in Figure 3.4a.

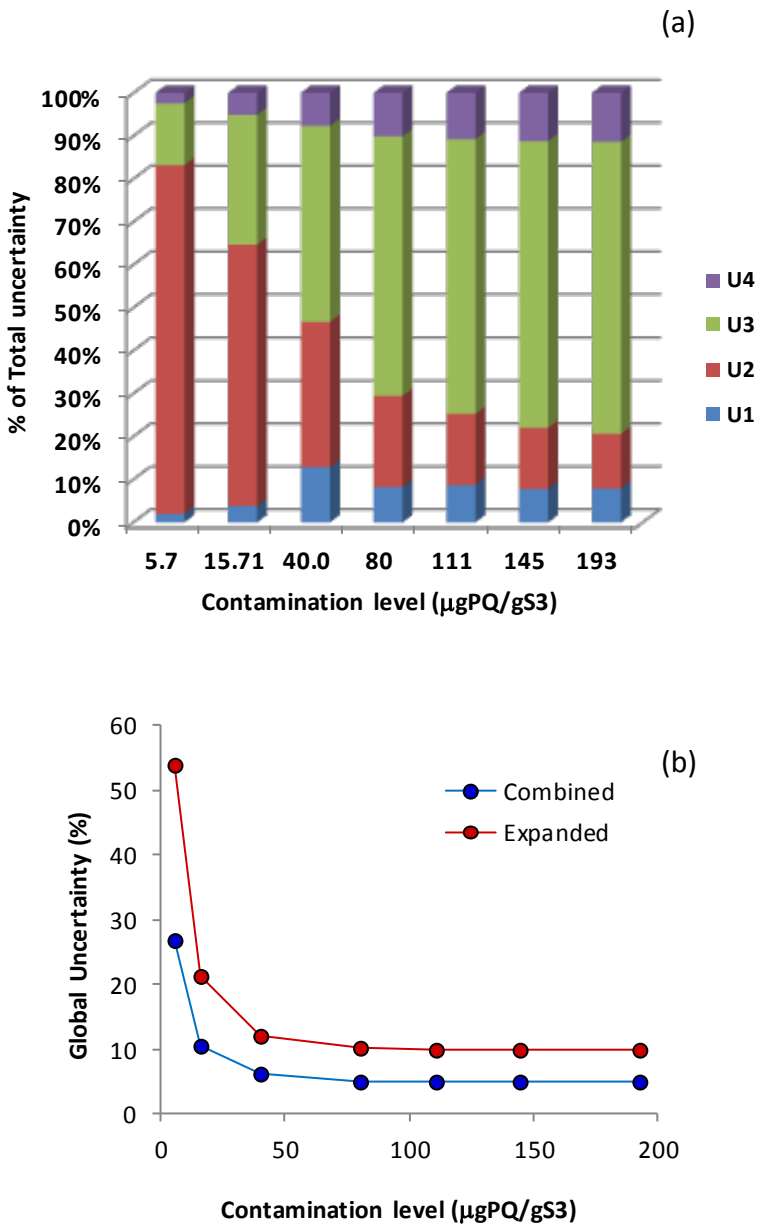

Figure 3.4. (a) Contribution of each source of uncertainty to the global uncertainty for different PQ contamination levels and (b) combined and expanded global uncertainty for PQ analysis in the S3 deposit.

As observed, the most significant uncertainty source at low contamination levels corresponds to the uncertainty associated with the calibration curve. On the other hand, an increase on the weight of the uncertainty of precision (U3) and accuracy (U4) is evident for the highest contamination levels. Both combined and expanded uncertainties were determined for each point of the calibration curve (Figure 3.4b). The combined uncertainty corresponds to the standard uncertainty and, as the name implies, was calculated from the combination of the overall uncertainty sources, as described in the

bottom-up approach of the EURACHEM CITAC Guide [6]. The expanded was obtained multiplying the combined uncertainty by a coverage factor of two, which provides a level of confidence of approximately 95% [8]. The values for the expanded uncertainty are between 10 and 54%, when the concentration ranges from 193 to 5 μgPQ/gS3. It is clearly evident that the uncertainty increases significantly when approaching the LODs (lower contamination levels), being around 10% for PQ concentration above 40 μgPQ/gS3.

3.3.3 Paraquat quantification in different deposits

The robustness of the method was also evaluated testing its response capability when different kind of deposits spiked with PQ were used. For that, two other deposits were also considered (S2 and S4). The tests with S2 were made in triplicate at three PQ contamination levels (40, 80 and 160 μgPQ/gS2). As can be seen from Table 3.1, the extraction percentages obtained for S2 (around 30%) were much lower than those achieved for S3 (Figure 3.1). However, the method remains precise and the recovery was not affected even using a different deposit (Table 3.1). A limit of detection of 0.6 μgPQ/gS2 was estimated for PQ-S2 system. In this case a matrix-matched calibration is recommended for PQ quantification. For S4, four PQ contamination levels were considered (80, 120, 160 and 200 μgPQ/gS4). Here, the experiments were also carried out in triplicate and the results were compiled in Table 3.1.

Table 3.1. Extraction percentages, precision and recovery for PQ-S2 and PQ-S4 systems.

System	Contamination level (μg/g)	%Extraction	Precision (RSD%)	Recovery (%)
PQ-S2 (n=3)	40	31±5	16	95±7
	80	27±3	10	93±1
	160	32±2	7	99±3
PQ-S4 (n=3)	80	32±3	9	101±4
	120	50±4	9	98±5
	160	66±3	5	97±4
	200	72±4	6	97±5

In this case, it can be observed that the extraction percentage is dependent on the degree of contamination (ranged from 32 to 72%). Actually, plotting the four points it can be observed that the representation follows a linear tendency but, the trendline crosses the

x-axis at 63 μgPQ/gS4 (data not shown). When 0.5 g of S4 is put in contact with 1 mL of a saturated ammonium chloride solution contaminated with increasing amounts of PQ until equilibrium is established, a Langmuir isotherm was obtained and the calculated PQ maximum adsorption capacity was precisely 63 μgPQ/gS4. This means that the extraction methodology used is not suitable for the PQ-S4 system at levels below 63 μgPQ/gS4, otherwise PQ will remain in the solid phase. Nevertheless, this analytical method is still very useful for calcium rich deposits (like S4 sample) because, in case of a deliberate or accidental contamination, much higher PQ contamination levels are plausible (400 μgPQ/gS4 at 20 °C and 550 μgPQ/gS4 at 4 °C) [1]. Additionally, the method proved to be very precise and accurate (Table 3.1). Again, a matrix-matched calibration will have to be performed to quantify PQ.

Generally, this simple analytical methodology proved to be suitable for the quantification of PQ/DQ in different kind of deposits whenever the extraction percentages were taken into account.

3.3.4 Suitability of the extraction methodology for Diquat

The applicability of the developed analytical methodology for DQ quantification in S3 contaminated deposits was also evaluated. For that, S3 samples were contaminated with DQ and then submitted to the same extraction procedure developed previously for PQ. This study was performed at three different contamination levels (9, 76 and 154 μgDQ/gS3) and in triplicate. The average extraction percentages were on average 82±15%. Mean precision was 5, 3 and 2% for 9, 76 and 154 μgDQ/gS3, respectively. The accuracy was again assigned to the difference observed between real contamination and that determined from the calibration curve. Recoveries were 95%, 114% and 107% for 9, 76 and 154 μgDQ/gS3 contamination degrees, respectively.

Being simple and fast, this method constitutes an excellent approach for PQ/DQ monitoring in deposits from drinking water networks, namely for sorption/degradation studies or even for risk assessment purposes.

3.4 Conclusions

An analytical methodology able to quantify PQ and DQ in deposits from drinking water networks was developed for the first time. This simple and inexpensive method consists in a fast and easy extraction step which requires small sample and solvent amounts. Concerning the optimization of the extraction procedure, the best conditions correspond to the use of 1 mL of a saturated ammonium chloride solution as solvent for 30 min for each 0.5 g of deposit. A limit of detection of 0.1 μgPQ/gS3 was obtained for PQ-S3 system with the expanded uncertainty ranging from 10-54% for concentrations between 193 and 5 μgPQ/gS3, respectively. The method was also successfully applied to the DQ quantification in the S3 deposit. Additionally, precision and accuracy was verified when applied to different kinds of deposits (S2 and S4), but the correspondent extraction percentages must be taken into account to obtain the PQ/DQ contamination level.

This methodology can be easily implemented in a quality control laboratory and, due to its simple and expedite nature proves to be a good first approach to PQ/DQ quantification in deposits from drinking water distribution systems.

3.5 References

[1] M.S.F. Santos, G. Schaule, A. Alves and L.M. Madeira, *Adsorption of paraquat herbicide on deposits from drinking water networks*, Chem. Eng. J. 229 (2013) 324-333.

[2] D.S. Kolberg, D. Mack, M. Anastassiades, M. Hetmanski, R. Fussell, T. Meijer and H.J. Mol, *Development and independent laboratory validation of a simple method for the determination of paraquat and diquat in potato, cereals and pulses*, Anal. Bioanal. Chem. 404 (2012) 2465-2474.

[3] T.R. Roberts, J.S. Dyson and M.C.G. Lane, *Deactivation of the Biological Activity of Paraquat in the Soil Environment: a Review of Long-Term Environmental Fate*, J. Agric. Food Chem. 50 (2002) 3623-3631.

[4] F. Echeverría, J.G. Castaño, C. Arroyave, G. Peñuela, A. Ramírez and J. Morató, *Characterization of deposits formed in a water distribution system*, Rev. Chil. Ing. 17 (2009) 275-281.

[5] C. Oliveira, M.S.F. Santos, F.J. Maldonado-Hódar, G. Schaule, A. Alves and L.M. Madeira, *Use of pipe deposits from water networks as novel catalysts in paraquat peroxidation*, Chem. Eng. J. 210 (2012) 339-349.

[6] S.L.R. Ellison, M. Rosslein and A. Williams, *Eurachem/ Citac Guide- Quantification uncertainty in analytical measurement*, EURACHEM/ CITAC, UK, 2000.

[7] N. Ratola, L. Martins and A. Alves, *Ochratoxin A in wines-assessing global uncertainty associated with the results*, Anal. Chim. Acta 513 (2004) 319-324.

[8] S. Teixeira, C. Delerue-Matos, A. Alves and L. Santos, *Fast screening procedure for antibiotics in wastewaters by direct HPLC-DAD analysis*, J. Sep. Sci. 31 (2008) 2924-2931.

[9] B.V. Tucker, D.E. Pack and J.N. Ospenson, *Adsorption of bipyridylium herbicides in soil*, J. Agric. Food. Chem. 15 (1967) 1005-1008.

[10] M. Pateiro-Moure, E. Martínez-Carballo, M. Arias-Estévez and J. Simal-Gándara, *Determination of quaternary ammonium herbicides in soils: Comparison of digestion, shaking and microwave-assisted extractions*, J. Chromatogr. A. 1196–1197 (2008) 110-116.

[11] G. Strachan, J.A. Whyte, P.M. Molloy, G.I. Paton and Porter, *Development of Robust, Environmental, Immunoassay Formats for the Quantification of Pesticides in Soil*, Environ. Sci. Technol. 34 (2000) 1603-1608.

[12] M. Pateiro-Moure, C. Pérez-Novo, M. Arias-Estévez, R. Rial-Otero and J. Simal-Gándara, *Effect of organic matter and iron oxides on quaternary herbicide sorption–desorption in vineyard-devoted soils*, J. Colloid Interface Sci. 333 (2009) 431-438.

[13] M. Pateiro-Moure, C. Pérez-Novo, M. Arias-Estévez, E. López-Periago, E. Martínez-Carballo and J. Simal-Gándara, *Influence of Copper on the Adsorption and Desorption of Paraquat, Diquat, and Difenzoquat in Vineyard Acid Soils*, J. Agric. Food Chem. 55 (2007) 6219-6226.

[14] K.M. Spark and R.S. Swift, *Effect of soil composition and dissolved organic matter on pesticide sorption*, Sci. Total Environ. 298 (2002) 147-161.

4 Adsorption of paraquat herbicide on deposits from drinking water networks*

Abstract

Although forbidden in Europe, paraquat dichloride (PQ) is still largely used worldwide as herbicide. Therefore, the hypothesis of an accidental or deliberate contamination of drinking water distribution systems (DWDS) may be posed. The interactions between PQ and three typical deposits (S2, S3 and S4 deposits) from DWDS were investigated in order to understand the fate of this chemical in such systems in case of contamination. Additionally, these materials can be valorized as adsorbents in wastewater treatment applications. The effect of stirring speed, adsorbent dose, initial PQ concentration and temperature on the adsorption kinetics was evaluated. Good adherence was observed between experimental data and both kinetic (pseudo-second order) and equilibrium (Langmuir) models. The interaction between PQ and the deposits is extremely weak when compared to those established in the PQ-clay system, where irreversible sorption was observed. It was found that S2 and S3 may represent potential adsorbents regarding the treatment of PQ-contaminated waters.

4.1 Introduction

Most water distribution networks have a buildup of particles in the walls – deposits. Depending on the material used in the network construction and several water quality parameters, deposits with different properties and characteristics may be formed [1, 2]. In spite of this large heterogeneity, typically they are classified in three main representative groups: brown, tubercle and white deposits [3]. According to Echeverría et al. [3], brown deposits are constituted by aluminosilicates and humic acids, tubercle deposits are mostly mixtures of magnetite, goethite and in some cases lepidocrocite, and white deposits are formed by calcite, aluminosilicates and quartz. There are several

* Adapted from: Mónica S.F. Santos, Gabriela Schaule, A. Alves and Luís M. Madeira, Adsorption of paraquat herbicide on deposits from drinking water networks, *Chemical Engineering Journal* 229, 324-333, 2013.

studies about PQ adsorption on clays and soils (Chapter 1) but, up to the author knowledge, there are no studies regarding the sorption of PQ on deposits typically found in DWDS. Although often compared to soils, deposits found in drinking water networks may be very distinct. The main objective of this chapter is to evaluate the interaction between PQ and the deposits found in a DWDS, which is of crucial importance to understand the behavior and fate of PQ in aquatic systems. Besides, it would allow exploring the use of such materials, often discarded upon pipes cleaning/maintenance operations, as low-cost adsorbents for the treatment of PQ contaminated waters. For that, three real deposits, representative of drinking water networks, were collected from an old water distribution system in Germany and the Netherlands.

4.2 Experimental Section

4.2.1 Pesticides and chemicals

Paraquat dichloride PESTANAL® analytical standard (Fluka) was purchased from Sigma-Aldrich (St. Louis, USA). Heptafluorobutyric acid (HFBA) was from Sigma-Aldrich (St. Louis, USA), and acetonitrile (HPLC grade) from VWR BDH Prolabo (Poole, UK). Granular anhydrous calcium chloride was obtained from Sigma-Adrich (St. Louis, USA).

4.2.2 Deposits and other materials

The deposits samples (S2, S3 and S4) used in the adsorption studies were taken from a real DWDS. The deposits were removed from cast iron pipes that needed to be replaced. Deposits were submitted to drying in an oven (till no weight variation has been detected). Then, all deposits were sieved and were kept in dry conditions until the experiments. An extensive physical-chemical characterization of these deposits has been described previously [4] and, for that reason, the nomenclature used previously was maintained. In the same study, and according to the results obtained, it was possible to classify the S2, S3 and S4 samples as brown, tubercle and white deposits, respectively.

Clay was the other adsorbent used in this work. Its chemical composition was obtained from LNEG (Laboratório Nacional de Energia e Geologia, Portugal) and the particle size was determined by a Coulter Counter LS 230 with small volume model. The pHpzc (point of zero charge) was obtained as for deposits [4].

The organic matter content was determined in a TOC-V_{CSH} apparatus with a solid sample module SSM-5000A. The total surface area was determined by mercury porosimetry.

The main properties of all adsorbents used are summarized in Table 4.1.

Table 4.1. Physical-chemical composition of the real deposits [4] and clay.

	S2	**S3**	**S4**	**Clay**
Deposit classification	Brown	Tubercle	White	----------
ICP-OES analysis (wt.% of the main elements at dry basis)	Fe: 98% Ca: 1%	Fe: 97% P: 1% Mn: 1%	Ca: 97% Fe: 1% Mg: 1%	Al_2O_3: 34% SiO_2: 49%
S_{BET}, m^2/g	5	36	1	Not determined
Surface area (m^2/g)	3.1	19.3	0.2	Not determined
pH_{pzc}, 20 ºC	2.6	6.1	9.9	4.8
pH in water, 20 ºC	3.3	7.2	9.0	5.3
Main components identified by XRD	lepidocrocite	goethite	calcite ($CaCO_3$)	Not determined
Organic matter content (wt.%)	1.0	1.0	0.2	12

4.2.3 Adsorption experiments with suspended particles (clay, or from real "loose deposits")

A paraquat solution of 1 g/L was prepared by dissolving an appropriate amount of paraquat dichloride salt in distilled water. The adsorbent ("loose deposit" from drinking water pipes or clay particles) was first put in contact with 10 mL of distilled water to obtain stable conditions (for example constant pH). After that the contamination was done adding fixed volumes of 1 g/L paraquat solution. The experiments were performed at fixed stirring speed, temperature and pH. Stirring was ensured by a multi-positions magnetic stirrer from Velp Scientific (583 rpm – position 7 – unless otherwise stated). It is important to emphasize that all adsorption experiments with clay and deposits samples were performed at different pH values since they have different equilibrium pH in water. The aqueous phase of the contaminated samples was analyzed along time by direct injection-liquid chromatography with diode array detector (DI-LC-DAD) for the

determination of the PQ concentration (kinetic experiments). In equilibrium experiments, the concentration of PQ in the liquid phase was determined at the beginning (t = 0) and after equilibrium has been reached. All experiments were performed in duplicate and each sample was analyzed twice by DI-LC-DAD, to guarantee the reproducibility of the results. A maximum coefficient of variation (CV%) of 15% was obtained for duplicates during the experiments.

4.2.4 Desorption experiments

Firstly, 0.5 g of S3 and S4 deposits were contaminated with 10 mL of a 50 mg/L paraquat solution during 24 h. After this time, even if the equilibrium stage has not been achieved, the solid and liquid phases were separated by centrifugation (4000 rpm; 10 min). Then, the liquid phase was analyzed by DI-LC-DAD and the contaminated deposits were dried in a freeze-dry during 5 h. Afterwards, 10 mL of 0.01 M $CaCl_2$ was added to the contaminated samples and after 24 h the supernatant was analyzed by DI-LC-DAD. The process was repeated three times (total of four steps).

4.2.5 Analytical methods

Paraquat in aqueous phase was analyzed by DI-LC-DAD (Hitachi Elite LaChrom System – Darmstadt, Germany). The chromatographic separation was achieved by a Purospher® STAR LiChroCART® RP-18 endcapped (240×4 mm, 5 μm) reversed phase column from Merck (Darmstadt, Germany), using a mobile phase of 80% (v/v) of 10 mM HFBA in water and 20% (v/v) of acetonitrile, at isocratic conditions, with a flow rate of 1 mL/min. The calibration curve for PQ in water was performed by direct injection of 10 standards, from 0.1 to 80 mg/L of PQ. The coefficient of determination obtained was 0.9996 and the linearity tests revealed an excellent fitness for the linearity. A detection limit of 0.01 mg/L was reached. Precision (expressed in terms of coefficient of variation) was on average 8% and recovery was on average 77, 99 and 101% for 0.25, 30 and 80 mg/L of PQ (Chapter 2).

4.3 Results and discussion

4.3.1 Adsorption kinetics

Simple kinetic models (such as pseudo-first and pseudo-second order) [5-7] were considered to describe the experimental results of PQ adsorption over pipe deposits and

clay. By performing mass balances to the liquid phase in the batch vessel, assuming first and second order kinetics for the driving force term, equations 4.1 and 4.2 are obtained, respectively.

$$-\frac{dn}{dt} = -V\frac{dC}{dt} = k_1 w(C - C_e) \quad 4.1$$

$$-\frac{dn}{dt} = -V\frac{dC}{dt} = k_2 w(C - C_e)^2 \quad 4.2$$

In these equations, n is the mass of PQ in the liquid phase (mg), V is the volume of the liquid phase (L), C the PQ concentration in the liquid phase (mg/L), C_e the PQ concentration in the liquid phase at equilibrium stage (mg/L), w is the mass of adsorbent (g), t is the time of contact (min) and k_1 and k_2 the adsorption kinetic constants of first (L/g/min) and second order (L^2/min/g/mg), respectively.

Integrating equations 4.1 and 4.2 between the initial instant and time t, taking into account the initial condition (i.e., for t = 0 C = C_0), equations 4.3 and 4.4 are obtained, respectively.

$$\ln\left(\frac{C - C_e}{C_0 - C_e}\right) = -k_1\frac{w}{V}t \quad 4.3$$

$$C = C_e + \frac{V(C_0 - C_e)}{V + k_2 wt(C_0 - C_e)} \quad 4.4$$

On the other hand, equation 4.5 represents the relationship between the PQ concentration in the liquid (C) and solid phase (q), which represents the mass conservation equation (PQ removal from the liquid phase is transferred to the solid). Substituting all concentration of PQ in the liquid phase for the ones in the solid phase, equations 4.3 and 4.4 are transformed into equations 4.6 and 4.7, respectively:

$$q = \frac{(C_0 - C)V}{w} \quad 4.5$$

$$q = q_e\left(1 - \exp\left(-k_1 \frac{w}{V} t\right)\right) \quad 4.6$$

$$q = \frac{q_e{}^2 \left(\frac{w}{V}\right)^2 k_2 t}{1 + q_e \left(\frac{w}{V}\right)^2 k_2 t} \quad 4.7$$

In these equations, q (mg/g) and q_e (mg/g) stand for the PQ concentration in the solid at time t and in the equilibrium, respectively.

The parameters of equations 4.6 and 4.7 were determined by fitting the models to the experimental data by a non-linear regression analysis. Equation 4.8 was used as a criterion to evaluate which model better describes the experimental results. This mathematic/model selection criterion (MSC) has been used for similar purposes [8, 9]. It takes into account not only the correlation between the experimental data and the theoretical results but also the number of parameters of the model. Therefore, it gives higher values both for models that fit better and for models with less number of parameters.

$$MSC = \ln\left[\frac{\sum_{t=1}^{m}(C_t - \overline{C_t})^2}{\sum_{t=1}^{m}(C_t - C_{tcal})^2}\right] - \frac{2p}{m} \quad 4.8$$

In equation 4.8, m is the number of experimental points, p is the number of fitting parameters, $\overline{C_t}$ is the mean of the experimental PQ concentration and C_{tcal} is the PQ concentration obtained from the model.

Preliminary results indicated that the deposits have different adsorption capacities and, for that reason, depending on the adsorbent considered, different conditions were used. The results obtained are compiled in Table 4.2 and shown in Figure 4.1 to Figure 4.3. To compare the adsorption of PQ on deposits with the adsorption on clay, some experiments were made with this last adsorbent. Both first and second order kinetic models exhibit good adherence to the experimental results.

Table 4.2. Kinetic parameters for adsorption of PQ on deposits and clay.

Adsorbent Material	$[PQ]_0$ (mg/L)	[Adsorbent] (g/L)	T (°C)	Adsorption models					
				Pseudo first order model			Pseudo second order model		
				q_e (mg/g)	k_1 (L/(g min))	*MSC*	q_e (mg/g)	k_2 (L^2/(g min mg))	*MSC*
Clay	5	0.3	20	5.9±0.3	2.0±0.3	1.49	6.2±0.2	2.2±0.7	2.22
S2	20	3	20	5.1±0.2	$(2.3\pm0.2)\times10^{-4}$	3.36	6.0±0.4	$(1.4\pm0.3)\times10^{-5}$	3.48
	20	3	4	6.1±0.2	$(2.7\pm0.3)\times10^{-4}$	2.73	6.8±0.3	$(1.9\pm0.6)\times10^{-5}$	2.86
	35	3	20	5.8±0.3	$(2.0\pm0.3)\times10^{-4}$	2.60	6.4±0.6	$(1.2\pm0.3)\times10^{-5}$	2.94
	50	3	20	5.9±0.4	$(4\pm1)\times10^{-4}$	2.41	6.6±0.8	$(1.9\pm0.8)\times10^{-5}$	2.50
S3	50	7	20	4.9±0.2	$(1.3\pm0.2)\times10^{-4}$	1.94	5.7±0.4	$(4\pm1)\times10^{-6}$	2.02
	50	7	4	6.4±0.3	$(1.6\pm0.3)\times10^{-4}$	2.43	7.3±0.4	$(4\pm1)\times10^{-6}$	2.87
	60	7	20	7.1±0.7	$(9\pm1)\times10^{-5}$	2.65	8.0±3.0	$(2\pm1)\times10^{-6}$	2.72
	70	7	20	7.90±0.08	$(1.7\pm0.1)\times10^{-4}$	4.85	9.2±0.1	$(3.1\pm0.2)\times10^{-6}$	5.04
S4	5	7	20	0.23±0.01	$(3.0\pm0.8)\times10^{-3}$	1.70	0.25±0.01	$(4\pm1)\times10^{-3}$	2.16
	5	7	4	0.47±0.02	$(1.0\pm0.4)\times10^{-2}$	1.34	0.47±0.02	$(8\pm4)\times10^{-3}$	1.88
	10	7	20	0.29±0.01	$(8\pm3)\times10^{-3}$	2.20	0.30±0.01	$(7\pm2)\times10^{-3}$	2.71
	15	7	20	0.362±0.007	$(1.3\pm0.2)\times10^{-2}$	3.12	0.373±0.003	$(7.7\pm0.6)\times10^{-3}$	4.55

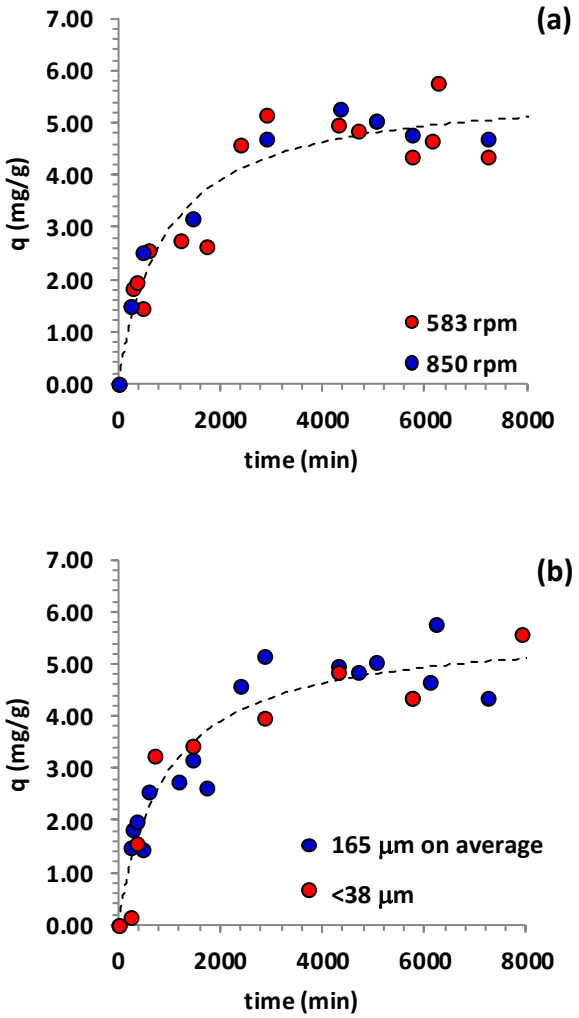

Figure 4.1. Effect of stirring speed **(a)** and particle size **(b)** on the adsorption of PQ on S3 deposit; (a**)** 50 mg/L PQ, 7 g/L S3, 20 ^{o}C, average particle diameter of 165 µm and pH = 7.2; (b) 50 mg/L PQ, 7 g/L S3, 20 ^{o}C, stirring speed of 583 rpm and pH = 7.2. Dashed line corresponds to the pseudo-second order fitted model.

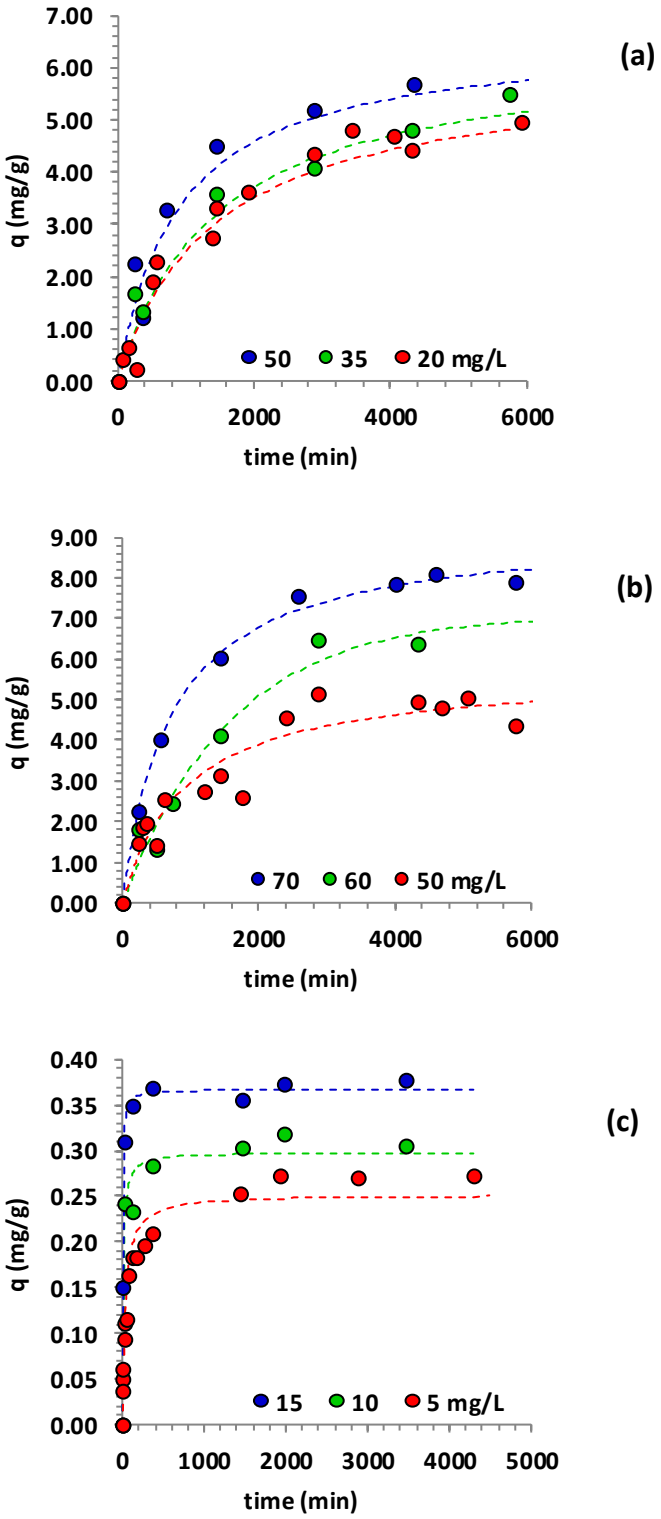

Figure 4.2. Effect of the initial PQ concentration on the adsorption of PQ on different pipe deposits: **(a)** S2 – 3 g/L S2, 20 ^{o}C, 583 rpm and pH = 3.3 (a); **(b)** S3 – 7 g/L S3, 20 ^{o}C, 583 rpm and pH = 7.2; **(c)** S4 – 7 g/L S4, 20 ^{o}C, 583 rpm and pH = 9.0. Dashed lines correspond to the pseudo-second order fitted model.

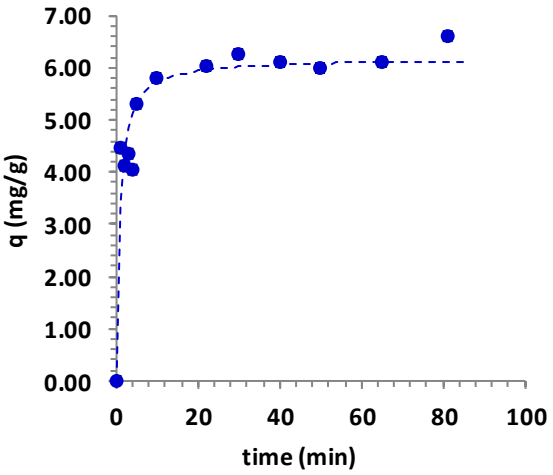

Figure 4.3. Adsorption of PQ on clay – 0.3 g/L clay, 5 mg/L PQ, 20 ^{o}C, 583 rpm and pH = 5.3. Dashed line corresponds to the pseudo-second order fitted model.

However, according to the MSC values obtained for each situation it is evident that the PQ adsorption on real deposits and clay follows a second order kinetic model. These results are in accordance with literature since the most part of studies about adsorption of PQ in different adsorbents indicate that the pseudo-second order kinetic model is the one that describes better the experimental data [10-14]. The first main difference that should be highlighted among the adsorbents used is related to the time needed to reach the equilibrium state. Although different conditions were used, it can be observed that the adsorption kinetics of PQ on real deposits is much lower than on clay (in real deposits it takes days to reach equilibrium while for clay only a few minutes are needed – cf. Figure 4.1 to Figure 4.3). This behavior could be related to the fast and strong interaction between PQ and clay minerals and/or the organic matter, as reported by other authors in previous studies [12, 15-18]. In other words, the solid state organic fraction and the clay mineral content in a solid sample are considered the major factors governing the sorption of PQ [17].

The strong adsorption associated to the relatively high organic matter content is related to the negative adsorption surface predominantly exhibited by the soil organic matter and the delocalized positive charge displayed by PQ ion [17]; clay is the material with higher organic matter content (Table 4.1). In case of adsorbents with high clay content the interactions established with PQ could be of hydrogen bonds type (as C-H…O bonding) as a result of the presence of activated C-H bond from the methyl groups in quat

structure and the oxygens of the siloxane surface of silicate clay [19]. The strong binding of PQ to clays is evidenced by the little amount of PQ desorbed from them when $CaCl_2$, ammonium chloride or water were used as extraction solvents [15, 16]. In section 2.3.3 some desorption experiments done with clay also confirm these results. It is expected that much lower organic matter content exists in deposits found in water distribution systems networks. Indeed, the three representative deposits studied here have less than 1% (w/w) of organic matter (Table 4.1). Since Fe oxides dictate the net electrical charge as well as the electric potential of the soils, here, these elements could play an important role in the overall sorption [15]. As can be checked from Table 4.2, the kinetic constants obtained for S2 and S3 are very close (which also have similar iron contents – Table 4.1) and a slightly higher value was achieved for S4.

4.3.1.1 Parameters affecting external and internal mass transfer: effect of the stirring speed and particle diameter

The external mass transfer coefficient increases as the stirring speed increases until a value after which this coefficient remains constant [20]. Under such conditions, resistances in the film should be neglected. To evaluate the effect of the stirring speed, two experiments were performed for each deposit, at 583 rpm and 850 rpm (positions 7 and 10 in the multiple positions stirrer, respectively). For brevity reasons, only the results obtained for S3 deposit are presented. The results are plotted in Figure 4.1 and the dashed line corresponds to the pseudo-second order kinetic model (fitted to the experiment at 583 rpm). It is observed that when stirring speeds is increased from 583 to 850 rpm, the PQ adsorption seems not to be influenced. Additionally, in the same figure it is possible to observe the effect of S3 particle diameter in the PQ adsorption process (dp<38 μm and average particle diameter of 165 μm). As can be checked from Figure 4.1, the particle diameter has no effect on the kinetics, which means that no internal mass transfer resistance exists. Besides, in the subsequent experiments the stirring speed was kept at 583 rpm (thus ensuring external mass transfer resistance is also absent).

4.3.1.2 Effect of initial paraquat concentration

The influence of the PQ concentration, at the beginning of the process, in the adsorption process is shown in Figure 4.2 for all pipe deposits. As can be seen, a decrease on the

adsorption rate is evidenced along the contact time until the equilibrium is reached, which is due to the decrease of the mass transfer driving force; actually, for the duration of the experiments herein shown, equilibrium is only reached for deposit S4. In the range of concentrations studied, it is seen that when the initial PQ concentration increases, the initial adsorption rate is also increased, as evidenced by the higher slope at initial times for all deposits. Additionally, the amount adsorbed at the equilibrium conditions also seems to increase for higher concentrations of PQ at the beginning of the process.

4.3.1.3 Effect of the temperature

The effect of temperature on the PQ adsorption was studied at 4 and 20 °C. The minimum temperature chosen is very close to that find in drinking water systems of colder European countries [21]. On the other hand, temperatures above 20 °C were not considered because they are not usually to occur. In addition, the World Health Organization recommends that drinking water temperatures should be kept outside the range of 25-50 °C and preferably 20-50 °C because higher water temperatures enhances the growth of microorganisms [22].

The effect of temperature on the PQ adsorption by real deposits was investigated by comparing the amount of PQ adsorbed as a function of time at the above-refereed temperatures. The results are indicated in Figure 4.4. As shown, the amount of herbicide adsorbed at equilibrium conditions increases with decreasing temperature, because this is an exothermic process. The results obtained are in-line with others found in the literature about PQ sorption in spent and treated diatomaceous earth [23] and in activate bleaching earth [10].

4.3.2 Adsorption isotherms

The adsorption isotherms of PQ on deposits were obtained by plotting the amount of PQ adsorbed in the solid after equilibrium has been reached (q_e, mg/g) against the herbicide remaining dose in the liquid phase, also at equilibrium (C_e, mg/L).

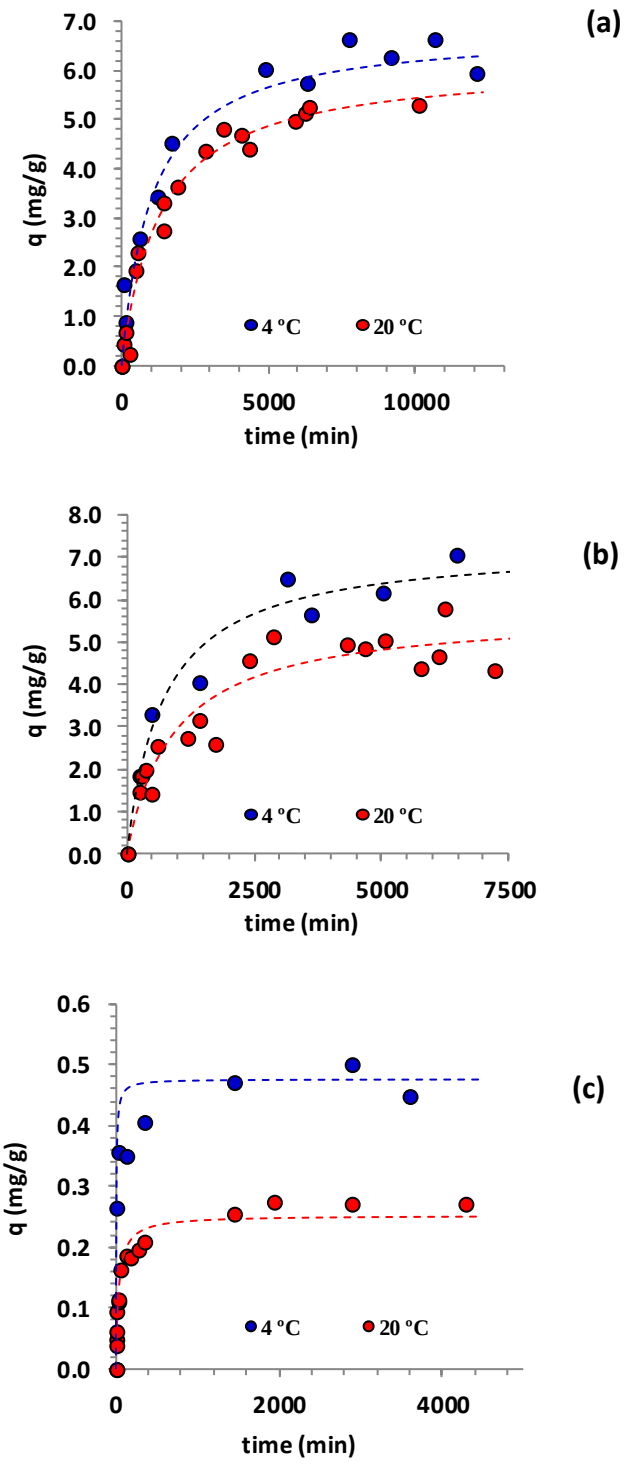

Figure 4.4. Temperature effect in the kinetic adsorption of PQ on different pipe deposits: **(a)** S2 – 20 mg/L PQ; 3 g/L S2, 583 rpm and pH = 3.3 (a); **(b)** S3 – 50 mg PQ/7 g S3, 583 rpm and pH = 7.2; **(c)** S4 – 5 mg PQ/7 g S4, 583 rpm and pH = 9.0. Dashed lines correspond to the pseudo-second order fitted model.

The fit of Langmuir, Freundlich and Temkin isotherms (equations 4.9, 4.10 and 4.11, respectively) to the experimental results and their applicability were investigated and the results are indicated in Figure 4.5 and Table 4.3; other models were also tested, like the Langmuir-Freundlich, but the lack of fit led us to not include them here (for brevity reasons).

$$q_e = \frac{q_{\max} K_L C_e}{1 + K_L C_e} \qquad 4.9$$

In equation 4.9, K_L is the Langmuir adsorption equilibrium constant (L/mg) and $q_{\max}$ the monolayer capacity (mg/g).

$$q_e = K_f C_e^{1/n} \qquad 4.10$$

In equation 4.10, K_f stands for the adsorption equilibrium constant (mg/g/(mg/L)$^{1/n}$) and n is the Freundlich constant.

$$qe = \frac{RT}{b} \ln(ACe) \qquad 4.11$$

While A is the Temkin isotherm constant (L/mol), b is the Temkin constant related to heat of sorption (Jg/mol^2), R is the gas constant (8.314 J/mol/K) and T is the absolute temperature (K).

All models describe well the experimental results but, taking into consideration the values obtained for the MSC (Table 4.3), the Langmuir equation gives in most cases better adherence between the theoretical and experimental data than the others.

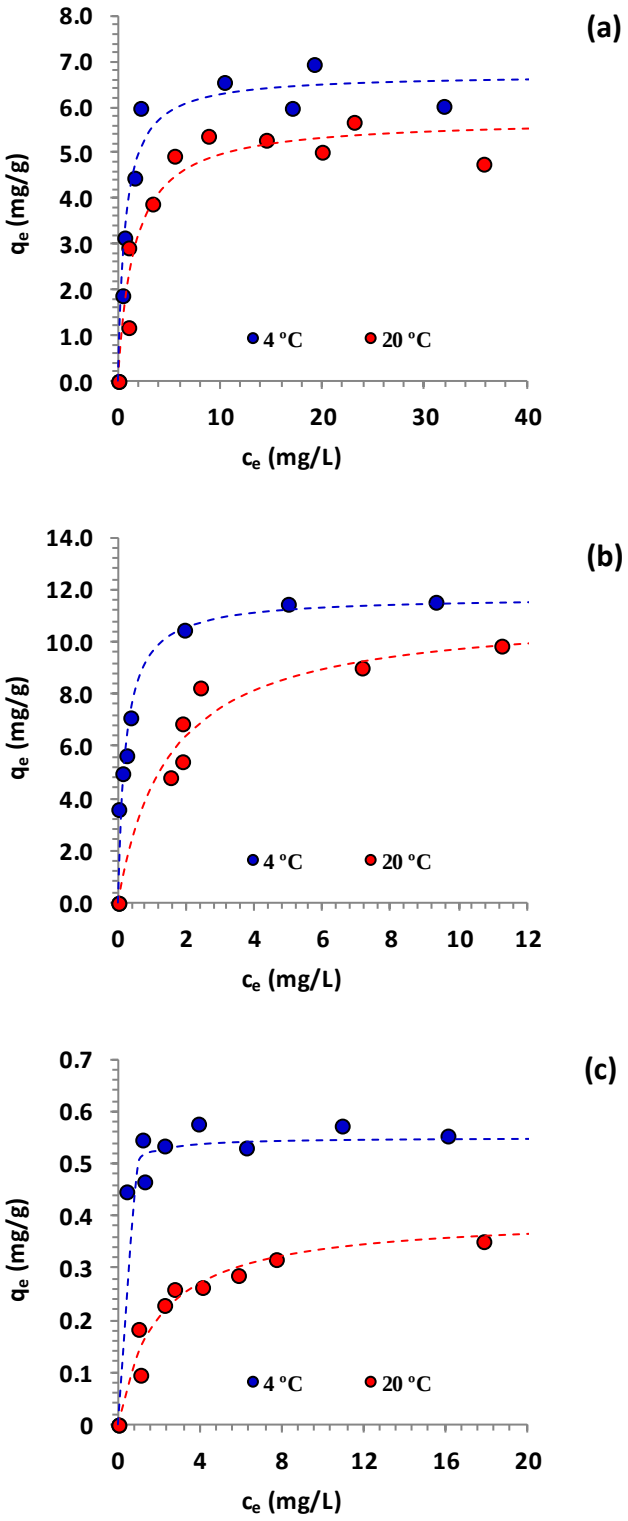

Figure 4.5. Temperature effect in the adsorption isotherm of PQ on different pipe deposits: **(a)** S2 – 3 g/L S2, 583 rpm and pH = 3.3 (a); **(b)** S3 – 7 g/L S3, 583 rpm and pH = 7.2; **(c)** S4 – 7 g/L S4, 583 rpm and pH = 9.0. Lines represent fit by Langmuir model.

Table 4.3. Parameters of adsorption isotherms for PQ on deposits and clay.

Adsorbent Material	T (°C)	Langmuir isotherm			Freundlich isotherm			Temkin isotherm		
		q_{max} (mg/g)	K_L (L/mg)	*MSC*	K_f (mg/g/(mg/L)$^{1/n}$)	*n*	*MSC*	*A* (L/mol)	*b* (Jg/mol^2)	*MSC*
Clay	**20**	**8.6±0.3**	**2.4±0.6**	**3.27**	**5.9±0.4**	**6±1**	**2.73**	**(4±1)×10^7**	**(50±9)×10^7**	**3.13**
S2		**5.7±0.4**	**0.6±0.2**	**2.07**	**2.8±0.5**	**5±2**	**1.30**	**(5±2)×10^6**	**(7±2)×10^8**	**1.52**
S3		**11±1**	**0.7±0.2**	**2.35**	**5.3±0.6**	**3.8±0.9**	**2.06**	**(20±7)×10^5**	**(30±7)×10^7**	**2.29**
S4		**0.40±0.02**	**0.52±0.09**	**2.81**	**0.18±0.02**	**4.6±0.6**	**2.22**	**(3±1)×10^6**	**(10±1)×10^9**	**3.91**
S2	**4**	**6.7±0.3**	**1.4±0.3**	**2.70**	**3.9±0.5**	**6±2**	**1.48**	**(20±8)×10^6**	**(7±2)×10^8**	**1.75**
S3		**12±1**	**5±2**	**1.62**	**8.2±0.7**	**5±1**	**1.51**	**(4±1)×10^7**	**(40±9)×10^7**	**1.60**
S4		**0.55±0.01**	**11±3**	**3.32**	**0.50±0.02**	**26±12**	**2.93**	**(3±2)×10^{16}**	**(4±2)×10^{10}**	**2.95**

The observation is consistent with other several studies which demonstrate that Langmuir model describes well the adsorption isotherms of PQ on clays [24], iron oxide coated quartz particles [25] and on calcium alginate gel beads [13]. Despite of the Langmuir isotherm has been derived assuming a finite number of uniform adsorption sites and the absence of lateral interaction between adsorbed species, this model has been successfully applied to describe the adsorption of a wide range of chemicals in soils [26-30]. The lack of information concerning PQ adsorption on deposits from DWDS justifies the comparison made with soils due to their similarity.

As can be observed in Table 4.3, and focusing on the Langmuir model data, the PQ adsorption capacity increases when the temperature decreases from 20 to 4 °C due to the exothermicity of the adsorption process. On the other hand, the isotherms obtained for real deposits indicated that S4 has a much lower PQ adsorption capacity (only 0.40 mg/g against 5.7 and 11 mg/g for S2 and S3, respectively, at 20 °C). This may be associated to the PQ interactions with the main metal ions present in each sample. Mbuk et al. [31] studied the translocation of some metal ions to subsurface soils and concluded that, when a soil is treated with PQ, as it happens in agriculture soils that are exposed to this herbicide, the leaching of metal ions such as Fe (II) and Mn (II) is suppressed. They suggested that PQ may have an ability to form complexes with these metal ions preventing its release towards the liquid phase. Sebiomo et al. [32] also confirmed such behavior for Fe (II) and also concluded that a significant leaching of Ca (II) is observed when the soils are treated with PQ. A few years ago, Jang et al. [33] demonstrated that the competition between calcium and cooper affected seriously the calcium alginate capacity for copper adsorption. More recently, Ruiz et al. [13] studied the PQ adsorption on calcium alginate gel beads and concluded that as adsorption of PQ proceeds, the calcium leached increases and a competition for the binding sites between both is observed. In short, this may suggest that PQ compete with Ca (II) for the binding sites and, for that reason, when this element is in large quantities in the adsorbent (as is the case of S4 sample – cf. Table 4.1), only few sites are available for PQ uptake. Additionally, if some calcium release occurs when the adsorbent is put in contact with PQ, a competition between both starts and the PQ adsorption is compromised. Besides the Fe (II) and Mn (II) that may contribute to the enhancement of PQ adsorbed at the equilibrium, as observed in S3 sample, the presence of phosphate may also represent

another factor for such result. The presence of phosphate ions leads to a more negative adsorbent surface facilitating the adsorption of positively charged compounds like PQ [25]. Another relevant point for the PQ adsorption capacities may be the textural properties. It is worth noting that the adsorption capacities follow the trend of the BET surface areas – Table 4.1 and Table 4.3.

Comparing the PQ adsorption capacities of the deposits (Table 4.3) with those of other adsorbents (Chapter 1 – section 1.1.3), it can be inferred that brown and tubercle deposits (S2 and S3, respectively) may be potential adsorbents for the treatment of PQ contaminated waters. Indeed, although slow adsorption kinetic constants were pointed out for these materials, they are a good alternative to other expensive adsorbents for the treatment of PQ contamination waters. On the other hand, taking into account the contact time needed to reach significant PQ adsorption amounts and the extreme conditions employed (high adsorbent dosage), it may be advanced that, in case of a drinking water contamination, it is unlikely that PQ would adsorb to the deposits attached in the pipe networks since here, much lower contact time and surface area available for adsorption are observed, unless there is a stagnancy of the fluid for a very long period of time. On the other hand, adsorption in loose deposits that are transported with the flowing water is much more likely to occur. Further experiments in a pilot loop are encouraged to support such preliminary conclusions.

In sum, if a deliberate or accidental drinking water contamination occurs with PQ the main concern will be related to the drinking water decontamination. Two works about decontamination of water polluted with PQ by oxidation with Fenton's reagent were already carried out, showing that this advanced oxidation process is feasible and effective using as catalyst either sulfate iron [34] or the iron rich deposits (brown) [4].

4.3.3 Desorption studies

In order to compare the strength of adsorption between PQ and clays and real deposits some desorption experiments were conducted with clay, S3 and S4 adsorbents. Concerning the samples S3 and S4, Figure 4.6 depicts the results of the sequential PQ desorption percentages when calcium chloride solution was employed as extraction solvent.

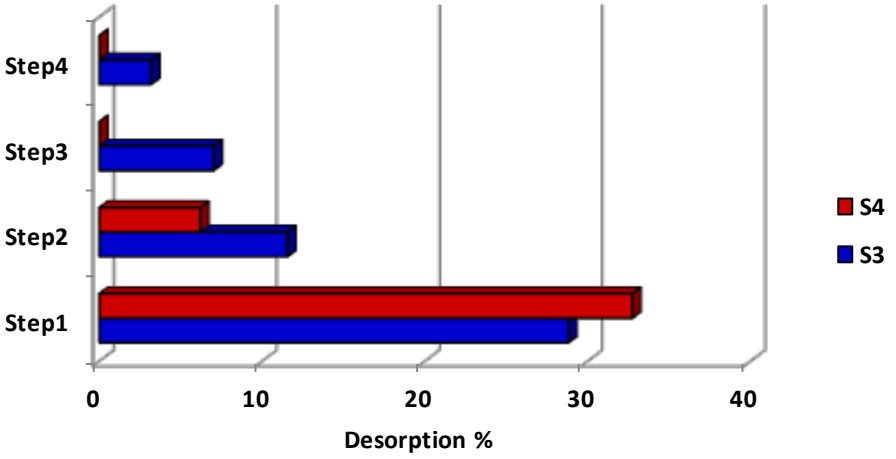

Figure 4.6. Variation of PQ desorption percentage in successive extractions of deposits with $CaCl_2$.

Calcium chloride solution was selected as extraction solvent because is typically used to assess the ability of calcium to displace PQ [15, 18]. Additionally, PQ extraction with calcium chloride solution is frequently considered as a measure of the PQ binding extent on soil matrix [15]. As can be observed, 29% and 33% of PQ is removed from S3 and S4, respectively, after the first step. Desorption percentages successively decrease in subsequent extractions with calcium chloride solution. A global PQ desorption percentage of 51% and 39% was respectively attained for S3 and S4 deposits, after 4 successive extractions with $CaCl_2$ solution. The desorption percentages are much higher than those found in the literature for PQ adsorption in soils. For example, Spark and Swift [17] concluded that negligible desorption of PQ from soils (in the absence or presence of increased content of soluble fulvic) was obtained when an aqueous solution of 0.01 M $CaCl_2$ was used as extraction solvent. Pateiro-Moure et al. [18] also studied the ability of $CaCl_2$ to desorb PQ from two vineyard acid soils and no more than one percent of PQ desorption was attained. More recently, Pateiro-Moure et al. [15] also reported the strong binding of PQ to some vineyard-devoted soils and, consequently, its low desorption percentages when calcium chloride was used as extraction solvent (it ranged from 2.1-2.4% and 10.5-14.3% at 100 and 200 mg/g of PQ, respectively). The differences observed may again be related to the higher clay and organic matter contents exhibited by soil samples. In fact, a lot of desorption experiments were conducted to evaluate the

extraction capability of some solvents to remove PQ from clay. The solvents tested were water and aqueous solutions of calcium chloride (0.01 M), saturated ammonium chloride, hydrochloric acid and diquat. No PQ desorption or negligible PQ removal was attained using the listed solvents (data not shown). Only under extremely hard conditions (reflux with concentrate sulfuric acid at 148 °C during 3h) around 70% of PQ was extracted from clay.

These results show that the interaction between PQ and the deposits is extremely weak when compared to the interactions established in the major PQ-clay and PQ-soil systems found in the literature. The results also suggest that these materials may be partially regenerated guaranteeing their reuse in other cycles of adsorption.

4.4 Conclusions

It was demonstrated that the adsorption of PQ in pipe deposit samples is an exothermic process. The kinetic data obtained for deposits were well described by a pseudo-second order kinetic model and revealed that the adsorption process is much slower than the one observed for PQ-clay system, which may be related to the clay and organic matter contents of these materials. Additionally, desorption experiments indicated that PQ is strongly adsorbed on clay but relatively high PQ desorption percentages were attained when $CaCl_2$ solution was used as extraction solvent in S3 (51%) and S4 (39%) adsorbents. Maximum PQ adsorption Langmuir capacities of 8.6, 5.7, 11 and 0.40 mg/g were achieved at 20 °C for clay, S2, S3 and S4 samples, respectively.

It was found that deposits S2 (brown deposit) and S3 (tubercle deposit) proved to be good adsorbents, and potential alternatives to other expensive materials, for the treatment of PQ contaminated waters.

4.5 References

[1] P. Sarin, V.L. Snoeyink, J. Bebee, W.M. Kriven and J.A. Clement, *Physico-chemical characteristics of corrosion scales in old iron pipes*, Water Res. 35 (2001) 2961-2969.

[2] C.-Y. Peng, G.V. Korshin, R.L. Valentine, A.S. Hill, M.J. Friedman and S.H. Reiber, *Characterization of elemental and structural composition of corrosion scales and deposits formed in drinking water distribution systems*, Water Res. 44 (2010) 4570-4580.

[3] F. Echeverría, J.G. Castaño, C. Arroyave, G. Peñuela, A. Ramírez and J. Morató, *Characterization of deposits formed in a water distribution system*, Rev. Chil. Ing. 17 (2009) 275-281.

[4] C. Oliveira, M.S.F. Santos, F.J. Maldonado-Hódar, G. Schaule, A. Alves and L.M. Madeira, *Use of pipe deposits from water networks as novel catalysts in paraquat peroxidation*, Chem. Eng. J. 210 (2012) 339-349.

[5] V. Vadivelan and K.V. Kumar, *Equilibrium, kinetics, mechanism, and process design for the sorption of methylene blue onto rice husk*, J. Colloid Interface Sci. 286 (2005) 90-100.

[6] Z. Reddad, C. Gerente, Y. Andres and P. Le Cloirec, *Adsorption of Several Metal Ions onto a Low-Cost Biosorbent: Kinetic and Equilibrium Studies*, Environ. Sci. Technol. 36 (2002) 2067-2073.

[7] K.K.H. Choy, G. McKay and J.F. Porter, *Sorption of acid dyes from effluents using activated carbon*, Resour. Conserv. Recycl. 27 (1999) 57-71.

[8] H. Akaike, *An information criterion (AIC)*, Math. Sci. 14 (1976) 5-9.

[9] L. Brandão, D. Fritsch, L.M. Madeira and A.M. Mendes, *Kinetics of propylene hydrogenation on nanostructured palladium clusters*, Chem. Eng. J. 103 (2004) 89-97.

[10] W.T. Tsai, C.W. Lai and K.J. Hsien, *Adsorption kinetics of herbicide paraquat from aqueous solution onto activated bleaching earth*, Chemosphere 55 (2004) 829-837.

[11] W.-T. Tsai and C.-W. Lai, *Adsorption of herbicide paraquat by clay mineral regenerated from spent bleaching earth*, J. Hazard. Mater. 134 (2006) 144-148.

[12] W.T. Tsai, C.W. Lai and K.J. Hsien, *The effects of pH and salinity on kinetics of paraquat sorption onto activated clay*, Colloid Surface A 224 (2003) 99-105.

[13] M. Ruiz, J. Barron-Zambrano, V. Rodilla, A. Szygula and A.M. Sastre, *Paraquat sorption on calcium alginate gel beads*, in: Proceedings of the 4th WSEAS/IASME international conference on Dynamical systems and control, World Scientific and Engineering Academy and Society (WSEAS), Corfu, Greece, 2008, pp. 30-35.

[14] N.K. Hamadi, S. Sri and X.D. Chen, *Adsorption of Paraquat dichloride from aqueous solution by activated carbon derived from used tires*, J. Hazard. Mater. 112 (2004) 133-141.

[15] M. Pateiro-Moure, C. Pérez-Novo, M. Arias-Estévez, R. Rial-Otero and J. Simal-Gándara, *Effect of organic matter and iron oxides on quaternary herbicide sorption–desorption in vineyard-devoted soils*, J. Colloid Interface Sci. 333 (2009) 431-438.

[16] B.V. Tucker, D.E. Pack and J.N. Ospenson, *Adsorption of bipyridylium herbicides in soil*, J. Agric. Food. Chem. 15 (1967) 1005-1008.

[17] K.M. Spark and R.S. Swift, *Effect of soil composition and dissolved organic matter on pesticide sorption*, Sci. Total Environ. 298 (2002) 147-161.

[18] M. Pateiro-Moure, C. Pérez-Novo, M. Arias-Estévez, E. López-Periago, E. Martínez-Carballo and J. Simal-Gándara, *Influence of Copper on the Adsorption and Desorption of Paraquat, Diquat, and Difenzoquat in Vineyard Acid Soils*, J. Agric. Food Chem. 55 (2007) 6219-6226.

[19] Z.Y. Hseu, S.H. Jien and S.F. Cheng, *Sorption of Paraquat on Clay Components in a Taiwan's Oxisol*, J. Environ. Sci. Health, Parte B 38 (2003) 441-449.

[20] S.D.W. Committee and N.R. Council, *Drinking Water and Health,Volume 1*, The National Academies Press, 1977.

[21] R. Koskinen, T. Ali-Vehmas, P. Kämpfer, M. Laurikkala, I. Tsitko, E. Kostyal, F. Atroshi and M. Salkinoja-Salonen, *Characterization of Sphingomonas isolates from Finnish and Swedish drinking water distribution systems*, J. Appl. Microbiol. 89 (2000) 687-696.

[22] World Health Organization, *Guidelines for Drinking-water Quality* 2011.

[23] W.T. Tsai, K.J. Hsien, Y.M. Chang and C.C. Lo, *Removal of herbicide paraquat from an aqueous solution by adsorption onto spent and treated diatomaceous earth*, Bioresource Technol. 96 (2005) 657-663.

[24] Y. Seki and K. Yurdakoç, *Paraquat adsorption onto clays and organoclays from aqueous solution*, J. Colloid Interface Sci. 287 (2005) 1-5.

[25] M. Pateiro-Moure, A. Bermúdez-Couso, D. Fernández-Calviño, M. Arias-Estévez, R. Rial-Otero and J. Simal-Gándara, *Paraquat and Diquat Sorption on Iron Oxide Coated Quartz Particles and the Effect of Phosphates*, J. Chem. Eng. Data 55 (2010) 2668-2672.

[26] M.I. Al-Wabel, G. Abdel-Nasser, A.M. Al-Turki and M.H. El-Saeid, *Behavior of Atrazine and Malathion Pesticides in Soil: Sorption and Degradation Processes*, J. Applied Sci. 10 (2010) 1740-1747.

[27] E. Loffredo and N. Senesi, *The role of humic substances in the fate of anthropogenic organic pollutants in soil with emphasis on endocrine disruptor compounds*, in: I. Twardowska, H.E. Allen, M.M. Haggblom, S. Stefaniak (Eds.) *Viable Methods of Soil and Water Pollution Monitoring, Protection and Remediation*, 2006, pp. 69-92.

[28] M. Schmidt, J. Halvorson, J. Gonzalez and A. Hagerman, *Kinetics and binding capacity of six soils for structurally defined hydrolyzable and condensed tannins and related phenols*, J. Soils Sediments 12 (2012) 366-375.

[29] J. Germán-Heins and M. Flury, *Sorption of Brilliant Blue FCF in soils as affected by pH and ionic strength*, Geoderma 97 (2000) 87-101.

[30] J. Mead, *A comparison of the Langmuir, Freundlich and Temkin equations to describe phosphate adsorption properties of soils*, Aust. J. Soil Res. 19 (1981) 333-342.

[31] R.O. Mbuk, R. Sha'Ato and N.N. Nkpa, *The role of paraquat and glyphosate in translocation of metal ions to subsurface soils*, Pak. J. Anal. Environ. Chem. 10 (2009) 19 - 24.

[32] A. Sebiomo, V.W. Ogundero and S.A. Bankole, *The impact of four herbicides on soil minerals*, Res. J. Environ. Earth Sci. 4 (2012) 617 - 624.

[33] L.K. Jang, W. Brand, M. Resong, W. Mainieri and G.G. Geesey, *Feasibility of using alginate to absorb dissolved copper from aqueous media*, Environ. Prog. 9 (1990) 269-274.

[34] M.S.F. Santos, A. Alves and L.M. Madeira, *Paraquat removal from water by oxidation with Fenton's reagent*, Chem. Eng. J. 175 (2011) 279-290.

5 Paraquat Removal from Water by Oxidation with Fenton's Reagent*

Abstract

Fenton's reaction, an advanced oxidation process (AOP), was studied for paraquat degradation purposes. A parametric study was conducted and the variables considered were the temperature, the pH and the initial iron, hydrogen peroxide and paraquat concentrations, the latter in the range 50-200 mg/L. Under the optimum conditions (T =30 ºC, $[Fe^{2+}]_0$ = 5.0×10^{-4} M, $[H_2O_2]_0$ = 1.6×10^{-2} M, and pH_0 = 3.0, for $[PQ]_0$ = 100 mg/L), complete paraquat degradation and 40% of mineralization were reached after 4 h of reaction (batch reactor). Gramoxone commercial product revealed a slower initial rate of degradation than the paraquat analytical standard, probably due to the parallel consumption of the hydroxyl radicals by other organic compounds. A semi-empirical kinetic model was proposed to simulate the paraquat dichloride concentration histories under a wide range of conditions; the adequacy of the model was statistically checked and also validated by comparison with some additional experiments. The biodegradability and toxicity of the final oxidation products were assessed. Preliminary experiments concerning the degradation of PQ in water by photo-Fenton process indicated that 96% of the chemical was mineralized after only 1 h of reaction (T =30 ºC, $[Fe^{2+}]_0$ = 5.0×10^{-4} M, $[H_2O_2]_0$ = 1.6×10^{-2} M, and pH_0 = 3.0, for $[PQ]_0$ = 100 mg/L).

5.1 Introduction

When contaminated water is removed from the pipes, after an accidental or deliberate contamination, it should be treated before further disposal. Only few studies were found in the open access literature concerning the treatment of waters contaminated with paraquat (PQ) (Chapter 1, section 1.1.4). Most of the publications correspond to the photocatalytic degradation of PQ using TiO_2-based photocatalysts. Although advantages are recognized in the use of such semiconductor for degradation purposes, it should be

* Adapted from: Mónica S.F. Santos, A. Alves and Luís M. Madeira, Paraquat removal from water by oxidation with Fenton's reagent, *Chemical Engineering Journal* 175, 279-290, 2011.

emphasized that such removal technology could be very expensive, since TiO_2 needs ultraviolet light to be activated [1]. Other degradation methodologies were also applied for the degradation of PQ in waters but some of them exhibited relatively low PQ degradation performance [2] or may represent expensive alternatives [3, 4]. Dhaouadi and Adhoum [5], studied the PQ degradation performance of three electrochemical advanced oxidation processes (anodic oxidation (AO), electro-fenton (EFe) and photo-electro-Fenton (PEF)) and compared them with that obtained for classic Fenton (CFe). Although CFe led to the highest removal rate at the initial stage of the process, they concluded that CFe has significantly lower oxidative ability as compared to the other processes, due to the poor final degradation efficiency attained [5]. However, the main variables responsible for the efficacy of the CFe process were not studied (as it was performed for the other processes) and this result may be related to the insufficient oxidant dose (H_2O_2) used in the experiment. Therefore, an optimized classic Fenton process could potentially lead to comparable PQ degradation efficiencies. Up to the author knowledge, there are no other studies reported concerning PQ degradation by the homogeneous Fenton's process.

In this chapter, a detailed parametric study was done to evaluate the pesticide degradation performance by this AOP, in order to assess and understand the effect of each individual operating condition in the degradation performance. Such study allows overcoming the limitations reported in previous works and optimizing process performance. Additionally, a kinetic model was developed to simulate the PQ degradation performance under a wide range of conditions. The establishment of a good model is of crucial importance for reactor design and scale-up. Some experiments were also performed to access the response capability of the proposed model for other conditions. The mineralization degree was measured along the reaction for all performed experiments and the toxicity and biodegradability of the final oxidation products were evaluated.

5.2 Experimental section

5.2.1 Reagents

Paraquat dichloride PESTANAL® analytical standard 99.2% (Fluka) was purchased from Sigma Aldrich (St. Louis, USA) and Gramoxone with 25.6 wt. % of PQ was gently supplied

from Syngenta Crop Protection, Lda. Hydrogen peroxide solution (30% v/v), iron (II) sulfate heptahydrate (99.5%), iron (III) sulfate x hydrate (76%) and anhydrous sodium sulfite were purchased from Merck (Darmstadt, Germany). Sulfuric acid (96%) from José M. Vaz Pereira, Lda (Lisboa, Portugal) and sodium hydroxide (98.7%) from José Manuel Gomes dos Santos, Lda (Odivelas, Portugal) were utilized. Heptafluorobutyric acid (HFBA) was from Sigma Aldrich, and acetonitrile (HPLC grade) from Prolabo. Syringe filters with 0.2 μm PTFE membrane were purchased from VWR (West Chester, USA).

5.2.2 Standards preparation

A PQ stock solution of analytical standard was prepared by dissolving 100 mg of PQ analytical standard in 100 mL of distilled water. Analytical PQ solutions of 50 mg/L (1.9×10^{-4} M), 100 mg/L (3.9×10^{-4} M) and 200 mg/L (7.8×10^{-4} M) were prepared by dilution of the previous stock solution. Gramoxone is a concentrated commercial solution (SL) of PQ, 25.6 wt. %. A PQ solution of 100 mg/L (3.9×10^{-4} M) was prepared in distilled water from Gramoxone commercial product. PQ solutions were stored at 4 °C in polypropylene containers.

5.2.3 Analytical methods

The samples collected along the reaction (see section 5.2.4) were analyzed, in order to quantify the PQ degradation, by direct injection-liquid chromatography-diode array detector (DI-LC-DAD). Chromatographic analysis of PQ was performed by direct injection of 99 μL in a Hitachi Elite LaChrom HPLC equipped with a L-2130 pump, a L-2200 autosampler and a L-2455 diode array detector (DAD). The chromatographic separation was achieved by a Purospher® STAR LiChroCART® RP-18 endcapped (240×4 mm, 5 μm) reversed phase column supplied by VWR, using a mobile phase of 80% (v/v) of 10 mM HFBA in water and 20% (v/v) of acetonitrile, at isocratic conditions, with a flow rate of 1 mL/min. The spectra were recorded from 220 to 400 nm and the PQ quantification, at the retention time of 5.7±0.3 min, was performed at 259 nm. The PQ degradation in water was quantified by direct injection liquid chromatography with diode array detector (DI-LC-DAD); this means that no concentration procedure was employed. The analytical method was developed and the main validation parameters were obtained. The calibration curve for PQ in water was performed by direct injection of 10 standards, from 0.1 to 80 mg/L of

PQ. The coefficient of determination obtained was 0.9996 and the linearity tests revealed an excellent fitness for the linearity. A detection limit of 0.01 mg/L was reached. Precision was evaluated by the repeatability of six injections of the same analytical standard, being the coefficient of variation (CV%) extremely low (0.2% for 30 and 80 mg/L standards, respectively).

Mineralization degree was assessed by total organic carbon (TOC) analyses, with a TC/TOC analyzer (Shimadzu 5000A analyzer), using the standard method 5310 D [6]. Total organic carbon was calculated by subtracting inorganic carbon to the total carbon. For that a calibration curve for total carbon and inorganic carbon was obtained from 5 to 100 mg/L. A limit of detection of 0.27 mg/L and 0.63 mg/L was attained for total carbon and inorganic carbon, respectively. TOC values reported represent the average of at least two measurements; in most cases each sample was injected three times, validation being performed by the apparatus only if CV is smaller than 2%.

5.2.4 Oxidation with Fenton's reagent

All Fenton experiments were carried out in a stirred jacketed batch reactor with 300 mL of capacity. A PQ solution (250 mL) was prepared and placed into the reactor. The Huber thermostatic bath (Polystat CC1 unit) was turned on and the desired temperature (± 1 °C) was kept constant by recycling water through the reactor jacket. After the temperature stabilization, pH was adjusted to the desired value, by adding small amounts of 2 M H_2SO_4 or NaOH aqueous solutions. To measure the solution temperature and pH, a thermocouple and a pH electrode (WTW, SenTix 41 model), connected to a pH-meter from WTW (model Inolab pH Level 2), were used. To start the oxidation process, the solid iron salt and the hydrogen peroxide were added to the reactor. Degradation assays were run up to 240 min and periodically samples of 10 mL were taken from the reactor and the remaining H_2O_2 eliminated by adding excess Na_2SO_3 (in order to instantaneously stop the reaction). Subsequently, these samples were filtered with a PTFE syringe filter, if required diluted, and analyzed as described before – section 5.2.3.

The effect of various operating parameters was systematically studied by changing one of them while the others were kept constant. The parameters tested were: initial pH (in the range 2.0 – 5.0), H_2O_2 concentration (from 1.6×10^{-3} to 5.7×10^{-2} M), Fe^{2+} concentration (1.0×10^{-4} – 5.0×10^{-4} M), initial PQ concentration (1.9×10^{-4} – 7.8×10^{-4} M), temperature

(10.0 – 70.0 °C), and catalyst source ($FeSO_4.7H_2O$ or $Fe_2(SO_4)_3.\chi H_2O$). After, two assays were done to access if a gradual addition of H_2O_2 is better than the whole oxidant addition in the beginning of the experiment. Beyond this, the best conditions found were tested in a PQ commercial product degradation, with 25.6 wt. % of PQ, to verify possible matrix interferences.

Some experiments were run in duplicate; in these replicates, the variations in the PQ concentration were within the analytical uncertainty.

5.2.5 Biodegradability and Toxicity of Fenton's reaction effluents

Biodegradability and toxicity of PQ solution and its oxidation products were evaluated by respirometry using a WTW InoLab 740 sensor. This was only made for one experiment with relatively low hydrogen peroxide concentration (T= 30.0 °C, pH_0 = 3, $[Fe^{2+}] = 5.0\times10^{-4}$ M, $[PQ]_0 = 3.9\times10^{-4}$ M, $[H_2O_2] = 6.5\times10^{-3}$ M) and taking the sample after 25 h to guarantee that no oxidant remained in the solution, because it interferes with the analysis. Other common methods used to quench the reaction interfered either with this method, or with PQ stability (e.g. hydrolysis at high pH). The sample biodegradability was determined by comparing the Oxygen Uptake Rate (OUR) obtained when the bacteria consortium was fed with the oxidation sample (OUR_{Sample}) with that obtained with a completely biodegradable standard (acetic acid, $OUR_{Acetic\ acid\ I}$) equation 5.1. To access the sample's toxic character, acetic acid was fed a second time to the activated sludge that had previously contacted with the pollutants ($OUR_{Acetic\ acid\ II}$) and the OUR value obtained compared to that of $OUR_{Acetic\ acid\ I}$ – equation 5.2. The bacteria consortium was obtained from an aeration tank of Rabada WWTP (Santo Tirso – Portugal) – 700 mg/L in volatile suspended solids.

$$\%Biodegradability = \left(\frac{OUR_{Sample}}{OUR_{Acetic\ acid\ I}} \right) \times 100 \qquad 5.1$$

$$\%Toxicity = \left(\frac{OUR_{Acetic\ acid\ I} - OUR_{Acetic\ acid\ II}}{OUR_{Acetic\ acid\ I}} \right) \times 100 \qquad 5.2$$

This approach, based on the oxygen uptake rate, is often used to evaluate the biodegradability and toxicity of aqueous samples [7-10].

5.2.6 Oxidation by Photo-Fenton

The experiments were performed in a 1000 mL glass immersion photochemical reactor which is equipped with an UV-visible lamp, located axially and held in a quartz immersion tube. The radiation source was a 150 W medium-pressure mercury vapor lamp (Heraeus TQ 150), whose more intense line is at 366 nm (Figure 5.1).

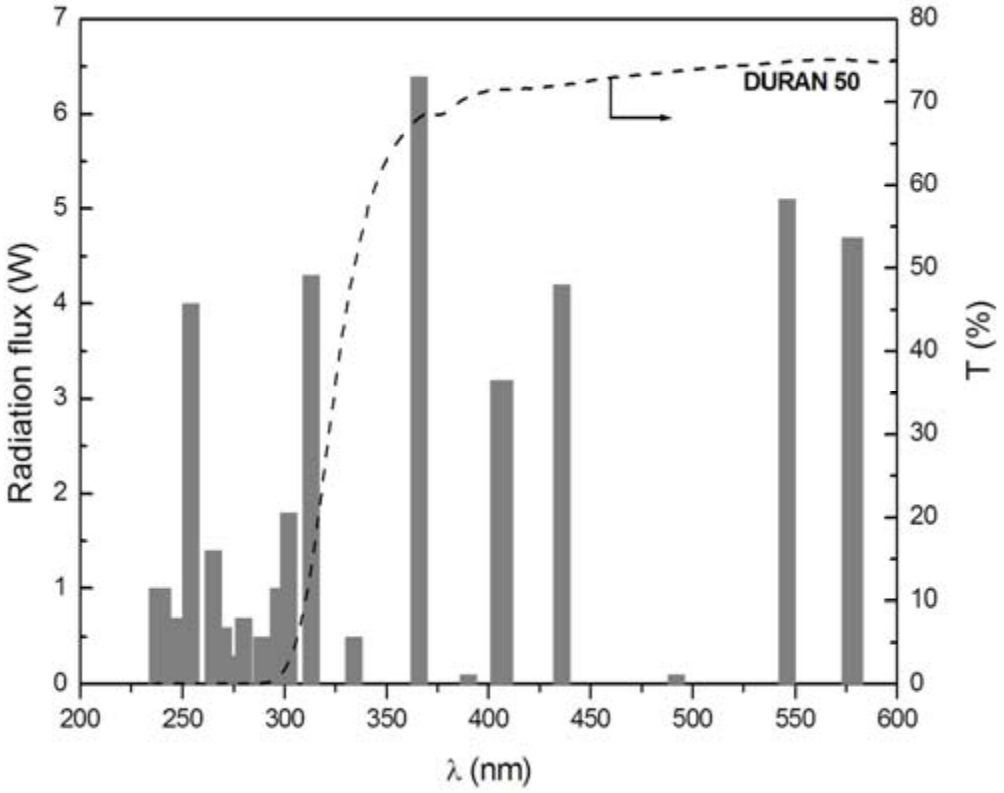

Figure 5.1. Emission spectrum of a 150 W medium-pressure mercury vapor lamp from Heraeus.

After the charge of the photochemical reactor with 800 mL of PQ solution (100 mg/L), the pH was adjusted to 3 as described previously and the temperature was set at 30 °C. Then, the lamp was introduced coaxially in the reactor and the iron ($[Fe^{2+}]_0$ = 5.0×10^{-4} M) and hydrogen peroxide ($[H_2O_2]_0$ = 1.6×10^{-2} M) were immediately added. It is worth noting that the lamp was switched on before 15 min of the beginning of the reaction to

guarantee constant photonic flux. The temperature of the reaction was kept at 30 °C by the water cooling jacket placed around the radiation source. Samples were withdrawn regularly and analyzed by DI-LC-DAD for PQ monitoring and by TOC for mineralization degree assessment.

5.3 Results and Discussion

5.3.1 Parametric study of the variables affecting the Fenton's reaction

To assess the effect of each parameter on PQ degradation performance, a parametric study was conducted, changing one variable at a time. Before that some control experiments were done to confirm the PQ stability and the absence of adsorption to the reactor/containers in the conditions employed (data not shown). It was also observed that hydrogen peroxide alone (without iron catalyst) is not capable to degrade PQ.

5.3.1.1 Effect of the temperature

The effect of temperature in the PQ degradation by Fenton's reagent was examined changing the temperature between 10.0 and 70.0 °C, while keeping the H_2O_2 concentration, the Fe^{2+} dose, the pH_0 and the initial PQ concentration constant (Figure 5.2). The temperature increase has a positive effect on the PQ degradation and on the TOC removal, as expected and predicted by the Arrhenius' law (rate constants increase exponentially with temperature, as shown below). However, as observed in Figure 5.2a, when the temperature is increased from 50.0 to 70.0 °C there is only a minor impact on the degradation rate, which is attributed to the thermal decomposition of H_2O_2 at high temperatures [11, 12]. Figure 5.2 shows that nearly all the initial PQ present in the reactor was degraded after 60 min, at 70.0 °C.

On the other hand, 60% of the organic matter was totally mineralized into CO_2 and H_2O, after 240 min. Longer reaction times, particularly at lower temperatures (e.g. 50.0 °C), could result in better performances. At low temperatures the degradation slows down considerably, particularly at 10.0 °C.

In the subsequent experiments the temperature was set to 30.0 °C because of the smaller energy consumption in real practice and because there was only a slight improvement in PQ degradation for temperatures above 30.0 °C. Besides, this is the temperature of reference in related studies.

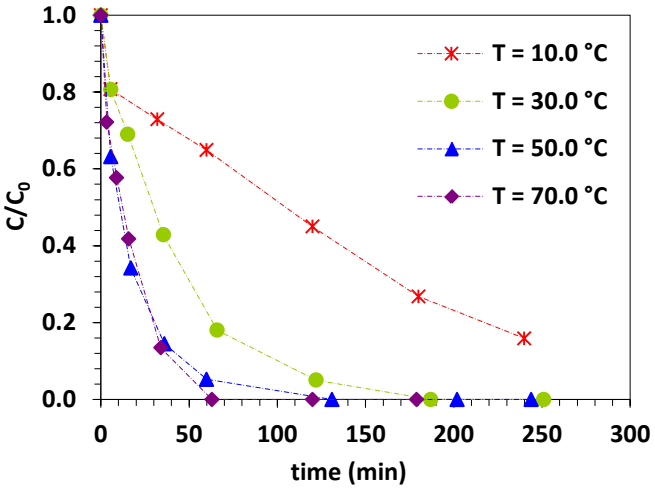

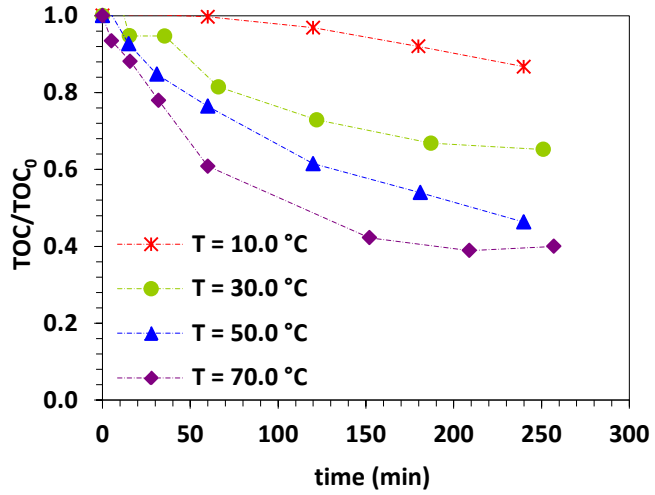

Figure 5.2. Temperature effect on the PQ concentration evolution (a) and on the TOC removal (b) as a function of time ($[H_2O_2]_0$ = 3.4×10^{-2} M, $[Fe^{2+}]_0$ = 5.0×10^{-4} M, pH_0 = 3.0 and $[PQ]_0$ = 3.9×10^{-4} M). Dashed lines are merely illustrative of the data trend.

5.3.1.2 Effect of iron salt concentration

The relationship between PQ degradation (a) and TOC removal (b) with the initial Fe^{2+} concentration is shown in Figure 5.3 For the lowest catalyst dose employed (1.0×10^{-4} M), both the parent compound degradation and mineralization proceed at low rate.

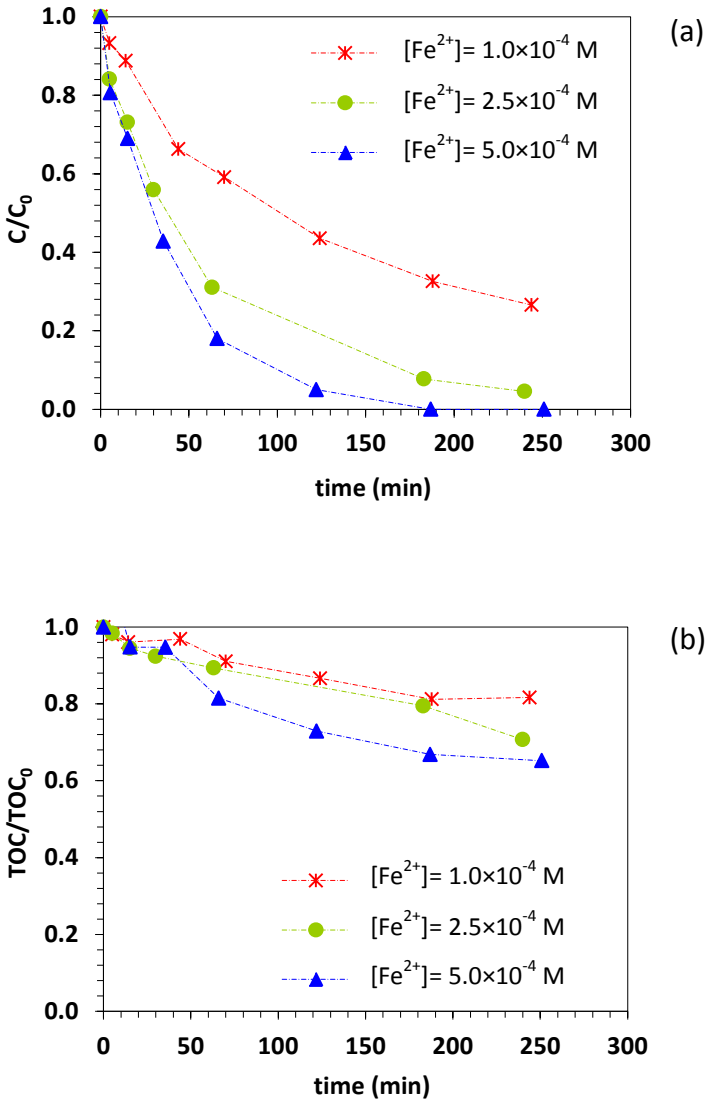

Figure 5.3. Fe^{2+} concentration effect on the PQ degradation (a) and on the TOC removal (b) as a function of time (T = 30.0 °C, pH_0 = 3.0, $[H_2O_2]_0 = 3.4\times10^{-2}$ M, and $[PQ]_0 = 3.9\times10^{-4}$ M). Dashed lines are merely illustrative of the data trend.

As expected, raising the Fe^{2+} concentration above this value has a positive effect on both the PQ and mineralization degradation rates because the salt acts as catalyst in the process. For the highest iron concentration studied (5.0×10^{-4} M) complete PQ decomposition (within the analytical uncertainties) is reached after 180 min (Figure 5.3a), and 35% is converted into CO_2 and H_2O after the same time (Figure 5.3b). Iron (II) concentrations higher than 5.0×10^{-4} M were not considered because iron precipitation occurs.

5.3.1.3 Effect of the H_2O_2 concentration

To assess the H_2O_2 concentration effect on the PQ degradation, some experiments were done by changing this parameter while keeping the others constants (T= 30.0 °C, pH_0 = 3, $[Fe^{2+}]$ = 5.0×10^{-4} M, $[PQ]_0$ = 3.9×10^{-4} M). Five hydrogen peroxide concentrations were tested, in the range 1.6×10^{-3} M – 5.7×10^{-2} M, as shown in Figure 5.4. This range corresponds to $[H_2O_2]/[Fe(II)]$ and $[H_2O_2]/[PQ]$ molar ratios between ca. 3 – 114 and 4 – 146, respectively. According to Dhaouadi and Adhoum [5], the stoichiometric amount of hydrogen peroxide required for complete PQ mineralization corresponds to a molar ratio of 31, so values clearly below and above this ratio were tested.

Figure 5.4a indicates that there is an optimum H_2O_2 concentration (ca. 6.5×10^{-3} – 1.6×10^{-2} M). For the lowest H_2O_2 concentration, 1.6×10^{-3} M, and although a rapid initial PQ degradation was observed, the herbicide concentration remains constant after 30 min of reaction because all hydrogen peroxide is consumed. This is also observed after 180 min of reaction for an initial dose of 6.5×10^{-3} M. Increasing the initial H_2O_2 concentration, the initial PQ degradation rate decreases, and for a H_2O_2 dose of 5.7×10^{-2} M, the initial PQ degradation rate is the smallest one. Hydrogen peroxide is the source of hydroxyl radicals responsible for the organic matter degradation; so, increasing the initial H_2O_2 concentration should increase the PQ degradation, but this is not verified. The reason for such behavior resides in the scavenging effect that becomes more significant at high hydrogen peroxide doses [11, 13, 14] and/or to the fact that the oxidant species are preferentially consumed in the oxidation of PQ by-products rather than in the parent compound. In fact, as shown in Figure 5.4b, the highest mineralization occurs for the higher hydrogen peroxide dose (5.7×10^{-2} M). This means that for maximizing TOC removal it is necessary to add more hydrogen peroxide than for simple PQ decomposition.

This is normal because it is easier to decompose PQ into intermediate compounds than the latter into CO_2 and H_2O. For $[H_2O_2]_0$ = 1.6×10^{-2} M, 95% of PQ is degraded after 120 min but for the same time only 27% of PQ is totally mineralized into CO_2 and H_2O (a value of 38% was reached after 240 min).

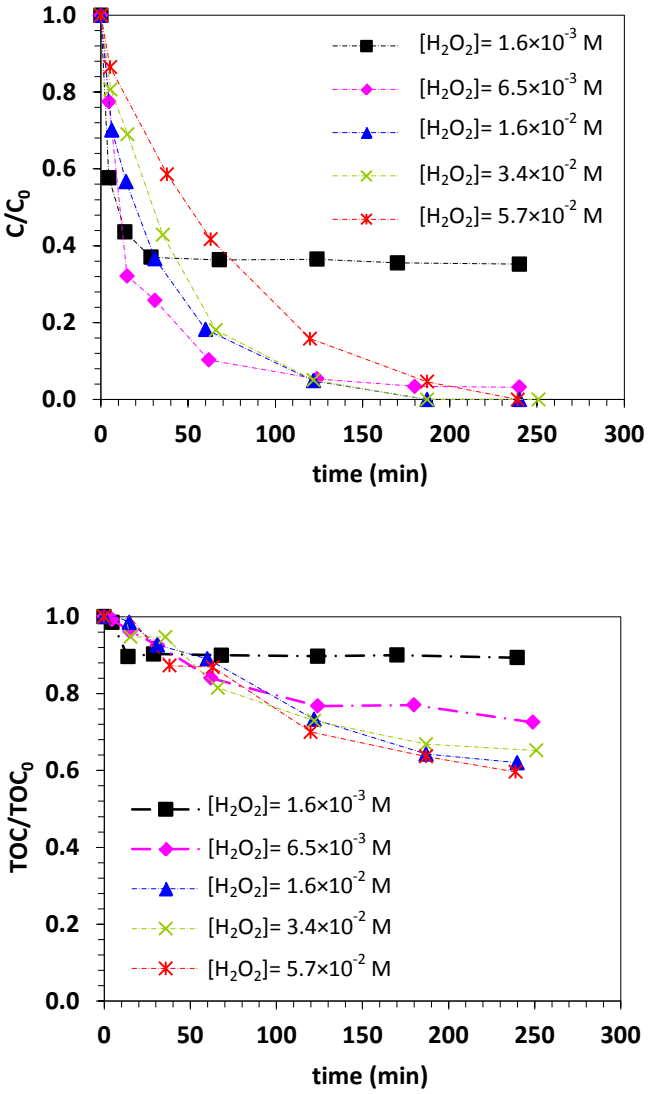

Figure 5.4. H_2O_2 concentration effect on the PQ degradation (a) and on the TOC removal (b) as a function of time (T = 30.0 °C, pH_0 = 3.0, $[Fe^{2+}]_0 = 5.0\times10^{-4}$ M, and $[PQ]_0 = 3.9\times10^{-4}$ M). Dashed lines are merely illustrative of the data trend.

5.3.1.4 Effect of the initial pH

The pH of the medium plays an important role in the Fenton's chemistry and thus in the oxidation process [15]. There are several studies indicating that the best removal efficiencies of organic compounds are obtained at pH values between 3.0 and 3.5 [16-18]. The PQ decomposition under different pH conditions was studied over a range of initial

pH from 2.0 to 5.0 (Figure 5.5). The results show that the highest PQ degradation is attained for pH_0 of 3.0 (Figure 5.5a).

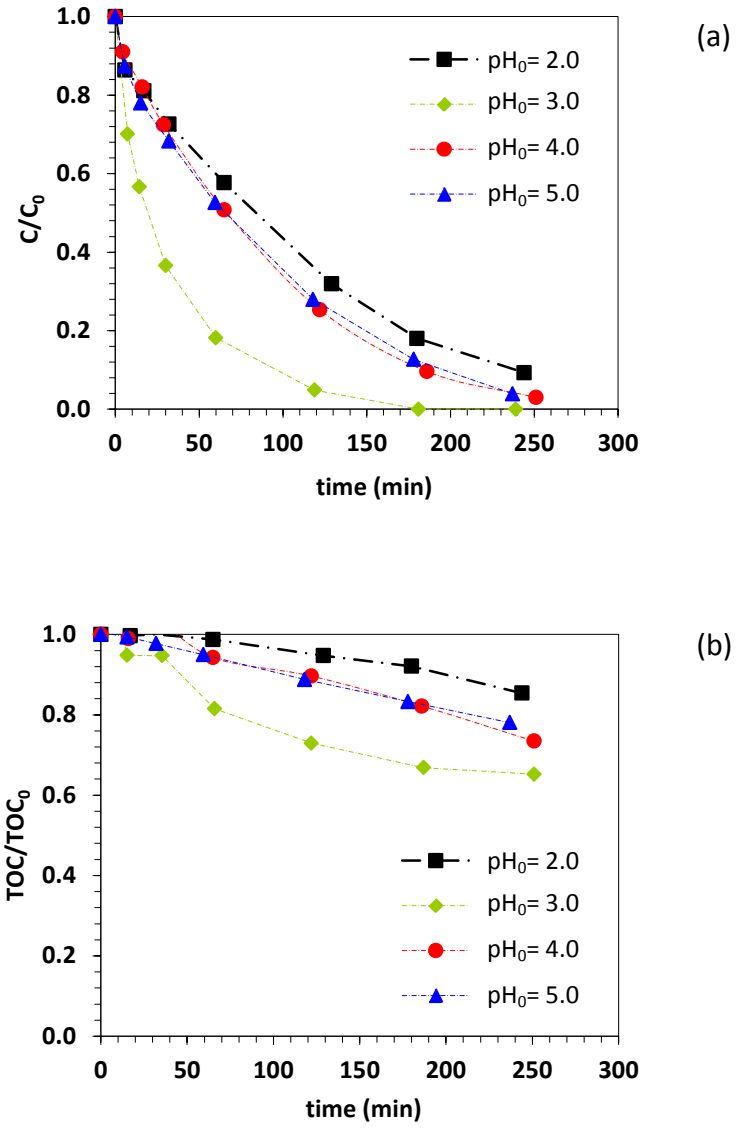

Figure 5.5. Initial pH effect on the PQ degradation (a) and on the TOC removal (b) as a function of time (T = 30.0 °C, $[Fe^{2+}]_0$ = 5.0×10^{-4} M, $[H_2O_2]_0$ = 1.6×10^{-2} M, and $[PQ]_0$ = 3.9×10^{-4} M). Dashed lines are merely illustrative of the data trend.

This is mainly caused by the fact that when pH is higher than 3, ferrous and ferric oxyhydroxides are formed which inhibit the reaction between Fe^{2+} and H_2O_2 and thus the

hydroxyl radicals production. In addition, hydrogen peroxide stability is also smaller at high pH values. However, in the employed conditions, even at an initial pH of 5 the pesticide was effectively degraded, although at a much slower rate than at pH_0 = 3. The decrease of the pH along reaction time, reaching values around 3, justifies these results. On the other hand, at lower pHs excessive H^+ reacts with H_2O_2 to produce $H_3O_2^+$, which is stable and cannot react with iron (II) to form the $HO^\bullet$ species. Additionally, hydroxyl radicals can also be scavenged by excessive H^+. Figure 5.5b demonstrates that pH 3 is also the best condition for TOC removal.

5.3.1.5 Effect of iron salt source

Figure 5.6 depicts the effect of using a Fe^{2+} or Fe^{3+} salt on the PQ degradation performance, at different pH values. As represented, a higher initial PQ degradation rate is observed with iron (II) than with iron (III), particularly for pH_0 = 2.0 (Figure 5.6a). The main reason for this is that ferrous ions (II) react very quickly with hydrogen peroxide to produce large amounts of hydroxyl radicals (see equation 1.1 of Chapter 1 and corresponding rate constant), which can then react rapidly with the parent compound. This is the reason for the sudden decrease of the PQ concentration for short reaction times – so-called Fe^{2+}/H_2O_2 stage. Ferric ions produced can then react with H_2O_2 to produce hydroperoxyl radicals and restore ferrous ions (equations 1.6 and 1.7 of Chapter 1); the rate of oxidation in the second stage (Fe^{3+}/H_2O_2 stage) is slower than in the first one due to the slow production of Fe^{2+} from Fe^{3+}. Because the reaction in which Fe^{2+} is converted into Fe^{3+} is very fast, the first stage is short and afterwards the process enters into a so-called pseudo steady-state, wherein iron is mainly in the 3+ oxidation state [12, 19]. The same behavior is observed in Figure 5.6b, which represents the PQ degradation at pH_0 = 3 when Fe(II) or Fe(III) were used.

Due to the interest of avoiding acidification of the waters/wastewaters to be treated, the same study was conducted at pH 5, as demonstrated in Figure 5.6c. In the first 120 min of reaction, degradation catalyzed by Fe(III) is again slightly slower, due to the low extension of the reaction between Fe^{3+} and hydrogen peroxide.

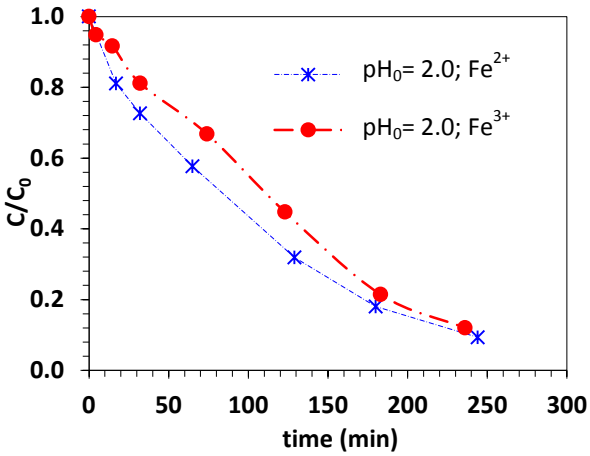

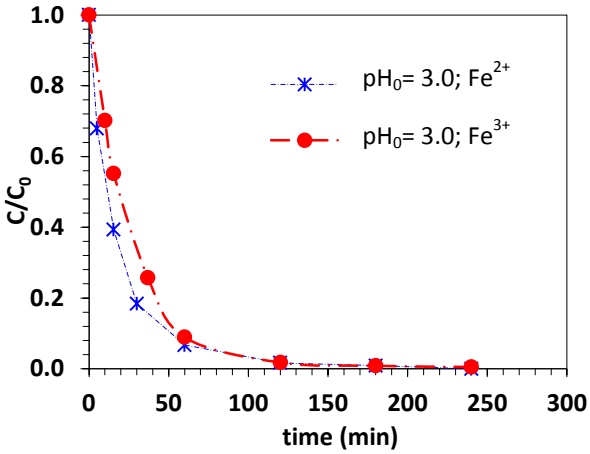

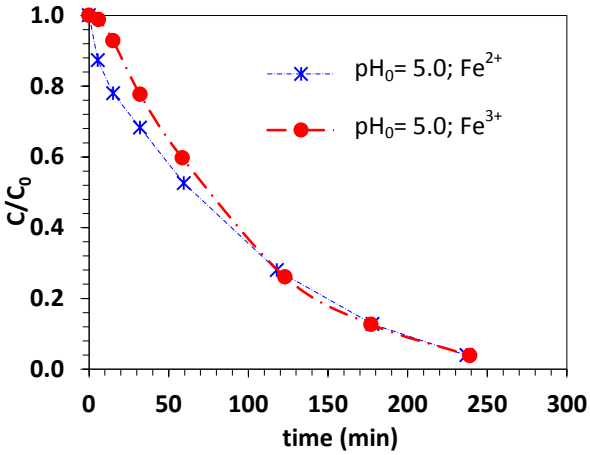

Figure 5.6. Iron salt effect on the PQ degradation at pH_0 = 2 (a), pH_0 = 3 (b) and at pH_0 = 5 (c) as a function of time (T = 30.0 °C, $[Fe^{2+}$ or $Fe^{3+}]_0$ = 5.0×10^{-4} M, $[H_2O_2]_0$ = 1.6×10^{-2} M, $[PQ]_0$ = 3.9×10^{-4} M). Dashed lines are merely illustrative of the data trend.

On the other hand, in the reaction catalyzed by iron (II) the decline of PQ concentration is faster due to the quick hydroxyl radicals production, as mentioned above. After 120 min of reaction, the rate of PQ degradation is nearly the same for both iron salts tested.

5.3.1.6 Effect of the initial paraquat concentration

As expected, for the lowest PQ concentration the degradation level is higher because the same hydrogen peroxide quantity is used to degrade less pesticide; so, after 2 h all PQ has been degraded to levels below the detection limit for $[PQ]_0 = 1.9\times10^{-4}$ M (Figure 5.7a). For initial PQ concentrations of 3.9×10^{-4} M and 7.8×10^{-4} M the time for complete conversion progressively increases. It is noteworthy that the fraction of the initial parent compound converted at a given time is smaller for an initial dose of 7.8×10^{-4} M, although the amount converted is higher. The mineralization degree is also smaller for higher initial PQ concentrations (Figure 5.7b).

5.3.1.7 Effect of the mode of oxidant addition

To assess the influence of a gradual hydrogen peroxide addition on PQ degradation, three experiments were done. In the first case the hydrogen peroxide was added once at time zero of the reaction, which lasted 4 h (experiments described up to now, mentioned as 0.4 mL in Figure 5.8). In the second case 1/2 of the overall hydrogen peroxide quantity was added at time zero and the remaining peroxide was divided in equal doses and was added after 1, 2 and 3 hours of reaction (experiment denoted as 0.19 mL + 3 × 0.07 mL in Figure 5.8). The third case corresponds to the addition of equal hydrogen peroxide quantities after 0, 1, 2 and 3 hours of reaction (denoted as 4 × 0.1 mL). The results indicate that the PQ degradation rate is higher for the third case, being the lowest for the first one. This means that the more divided is the hydrogen peroxide addition the better, because in this way the scavenging effects are not as significant as when all H_2O_2 is added at once (equation 1.3 of Chapter 1) is favored by high H_2O_2 concentrations). Ideally, the oxidant should be added continuously, transforming the batch reactor into a semi-continuous one. This approach was also suggested by other authors [20, 21] as a way of more efficient peroxide usage. It is also beneficial for better temperature management,

because for wastewaters containing a huge organic load, the exothermic nature of the oxidation reactions can compromise process efficiency and safety.

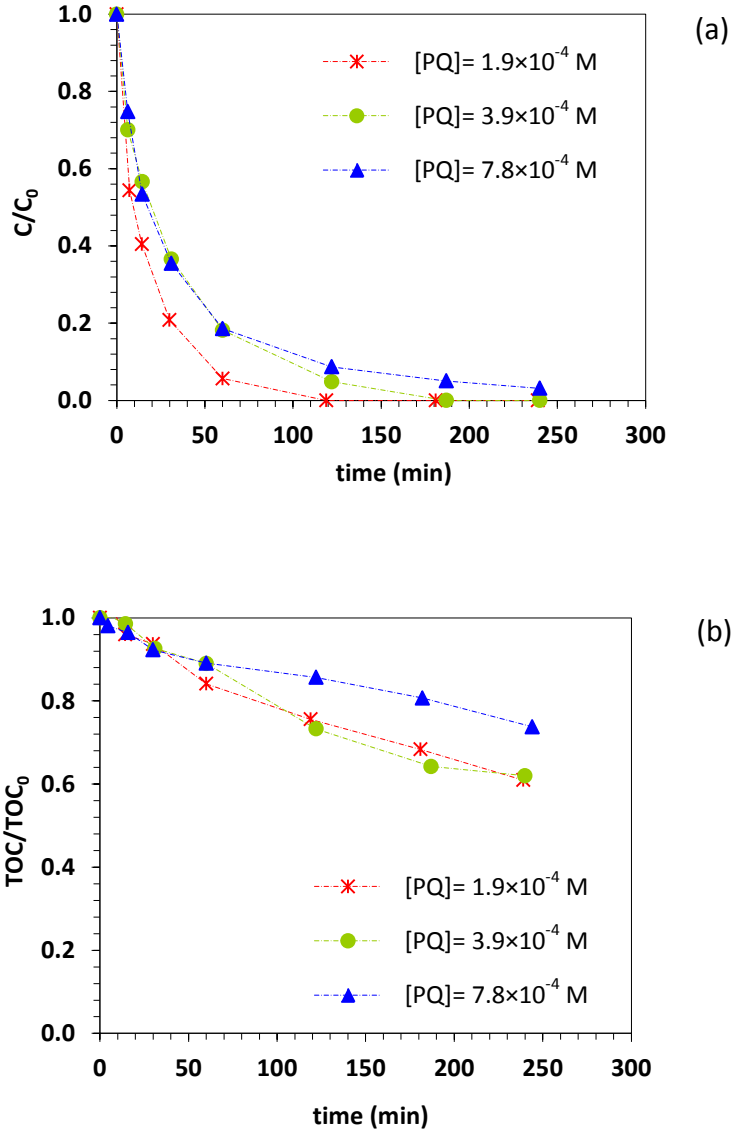

Figure 5.7. Initial PQ concentration effect on the PQ degradation (a) and on the TOC removal (b) as a function of time (T = 30.0 °C, $[Fe^{2+}]_0$ = 5.0×10^{-4} M, $[H_2O_2]_0$ = 1.6×10^{-2} M, and pH_0 = 3.0). Dashed lines are merely illustrative of the data trend.

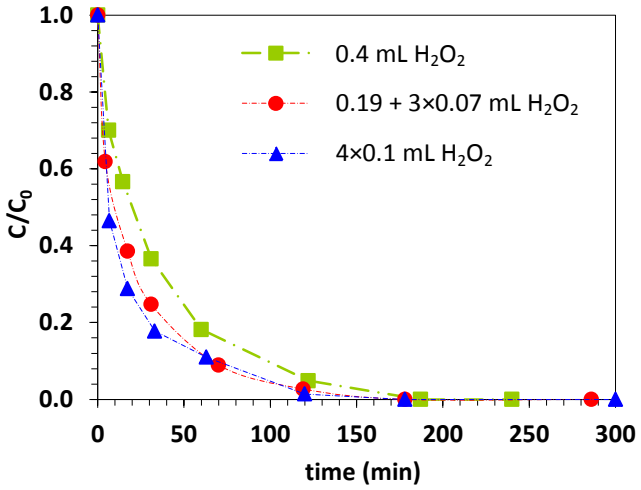

Figure 5.8. Mode of hydrogen peroxide addition effect on the PQ degradation (T = 30.0 °C, $[Fe^{2+}]_0$ = 5.0×10^{-4} M, $[H_2O_2]_T$ = 1.6×10^{-2} M, $[PQ]_0$ = 3.9×10^{-4} M and pH_0 = 3.0). Dashed lines are merely illustrative of the data trend.

5.3.2 Commercial paraquat degradation under optimal conditions

The "best" conditions found through the parametric study were tested for Gramoxone (commercial paraquat) degradation. In both experiments (with the analytical and commercial product) the same initial PQ concentration was employed. The commercial product degradation rate is lower (Figure 5.9), most probably due to the presence of other organic compounds that also consume the hydrogen peroxide/hydroxyl radicals. TOC results indicated that 27% of gramoxone and 38% of PQ analytical standard were mineralized after 323 min and 240 min, respectively (data not shown). This suggests that the analytical pesticide is easier to degrade than the commercial product but is important to realize that the initial total organic carbon is higher for the second case.

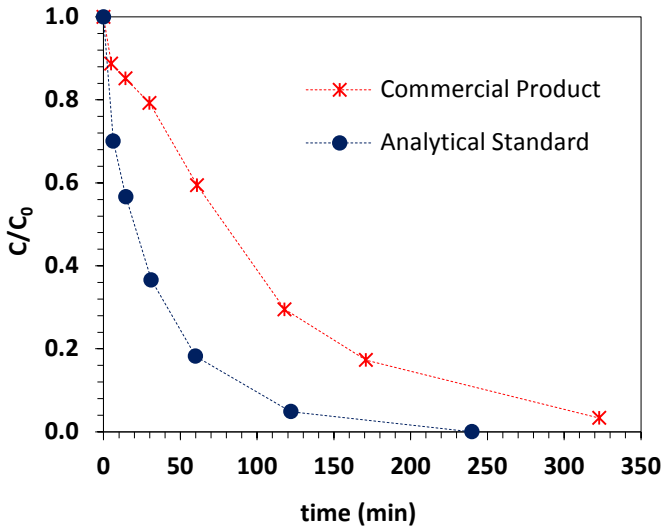

Figure 5.9. Gramoxone commercial PQ vs. analytical standard degradation as a function of time (T = 30.0 ºC, $[Fe^{2+}]_0$ = 5.0×10^{-4} M, $[H_2O_2]_0$ = 1.6×10^{-2} M, $[PQ]_0$ = 3.9×10^{-4} M and pH_0 = 3.0). Dashed lines are merely illustrative of the data trend.

5.3.3 Kinetic model for paraquat degradation with the Fenton's process

To describe the transient pesticide concentration in this complex process, tens of ordinary differential equations are required (equations 1.1 to 1.7 of Chapter 1 are merely a simplification of the set of reactions involved). Besides, rate constants reported in the literature differ from work to work, and in some cases temperatures are not provided (authors simply mention that the work was done at room temperature). In addition, an extreme sensibility of the results to some rate constants was found. Therefore, we decided to look for a different approach, aiming to find a simple kinetic equation, even if there is no phenomenological explanation behind. This macroscopic or engineering approach is however still very useful if one is able to describe and predict the parent compound degradation in a wide range of conditions, and has recently deserved the attention of some researchers [22-25]. This is commonly done in the field of reaction engineering, for reactor design and scale-up (by using empirical power-law rate equations, etc.). For that purpose the model proposed by Behnajady et al. [24] was applied:

$$\frac{C}{C_0} = 1 - \frac{t}{m + bt} \qquad 5.3$$

where C is the parent compound concentration (M) at time t (min), C_0 is the initial parent compound concentration (M) and m and b are two characteristic constants. According to the authors, the physical meaning of the term m can be understood by taking the derivative of equation 5.3:

$$\frac{dC/C_0}{dt} = \frac{-m}{(m+bt)^2} \qquad 5.4$$

and applying the limit when $t \to 0$, one gets:

$$\left(\frac{dC/C_0}{dt}\right)_{t\to 0} = -\frac{1}{m} \qquad 5.5$$

As can be seen, $1/m$ is proportional to the initial decay rate of PQ (in a homogeneous liquid phase batch reactor, $r_o = -\left(\frac{dC}{dt}\right)_{t\to 0}$); so, the higher $1/m$, the faster is the initial decay rate of PQ (for the same initial PQ concentration), as illustrated in Figure 5.10.

On the other hand, when $t \to \infty$, equation 5.3 yields:

$$\frac{1}{b} = 1 - \left(\frac{C}{C_0}\right)_{t\to\infty} \qquad 5.6$$

This means that parameter $1/b$ is related with the maximum oxidation degree attained (Figure 5.10).

To determine the m and b terms for each experiment, equation 5.3 was linearized:

$$\frac{t}{1-C/C_0} = m + bt \qquad 5.7$$

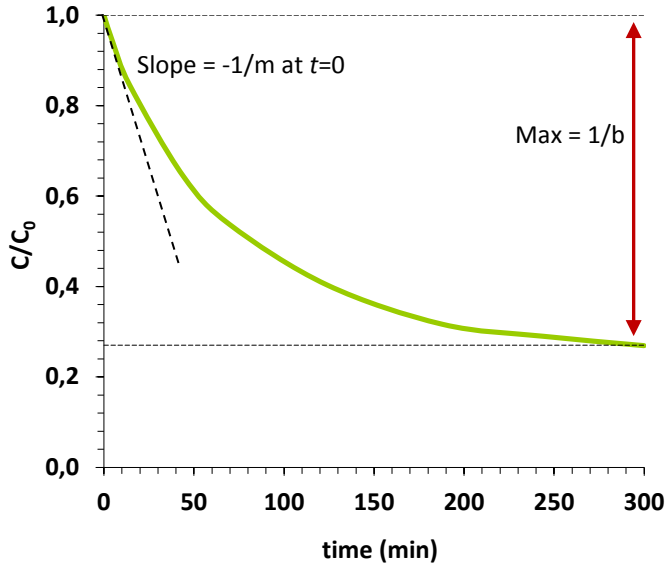

Figure 5.10. Physical meanings of m and b terms of the Behnajady et al. [24] model.

In Figure 5.11 an example of that linearization is depicted, which provides directly the parameters required.

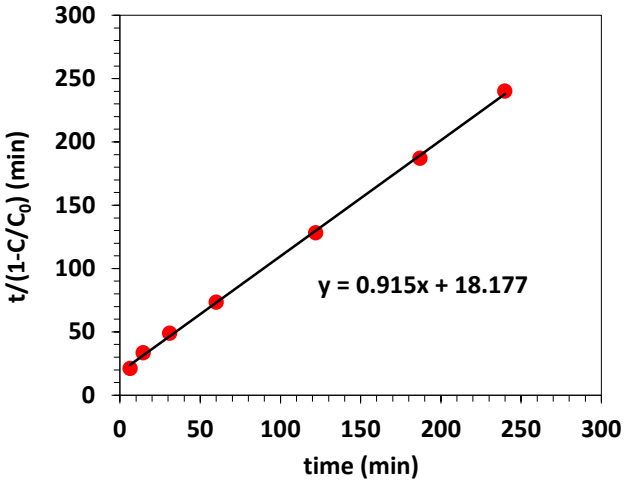

Figure 5.11. Linearization of the kinetic model (equation 5.7) for one experiment (pH_0 = 3.0; $[PQ]_0 = 3.9\times10^{-4}$ M; $[H_2O_2]_0 = 1.6\times10^{-2}$ M; $[Fe(II)]_0 = 5.0\times10^{-4}$ M and T = 30.0 °C).

All m and b terms obtained for the experiments with the Fe^{2+}/H_2O_2 process are compiled in Table 5.1.

Table 5.1. Condition employed in all the experiments done and obtained *m* and *b* parameters for each case (equation 5.7).

pH_0	$[PQ]_0$ (M)	$[H_2O_2]_0$ (M)	$[Fe^{2+}]_0$ (M)	T (°C)	m (min)	b	R^2
3.0	3.9×10^{-4}	3.4×10^{-2}	5.0×10^{-4}	**10**	99.9	0.8	0.996
				30	27.1	0.9	0.994
				50	10.0	0.9	0.998
				70	10.0	0.9	0.998
3.0	3.9×10^{-4}	3.4×10^{-2}	**1.0×10^{-4}**	30	92.4	1.0	0.978
			2.5×10^{-4}		36.4	0.9	0.996
			5.0×10^{-4}		27.1	0.9	0.994
3.0	3.9×10^{-4}	**1.6×10^{-3}**	5.0×10^{-4}	30	3.1	1.5	1.000
		6.5×10^{-3}			10.7	1.0	0.999
		1.6×10^{-2}			18.2	0.9	0.999
		3.4×10^{-2}			27.1	0.9	0.994
		5.7×10^{-2}			49.6	0.8	0.983
3.0	**1.9×10^{-4}**	1.6×10^{-2}	5.0×10^{-4}	30	8.3	1.0	0.999
	3.9×10^{-4}				18.2	0.9	0.999
	7.8×10^{-4}				16.3	1.0	0.999
2.0	3.9×10^{-4}	1.6×10^{-2}	5.0×10^{-4}	30	91.2	0.7	0.980
3.0					18.2	0.9	0.999
4.0					82.0	0.7	0.996
5.0					61.4	0.8	0.967

For each single experiment a very good agreement to equation 5.7 was obtained, with coefficients of determination in the range 0.967 – 1.000.

As shown in Table 5.1, the term m decreases when increasing the temperature (but only up to 50.0 °C) or the iron concentration, because at higher temperatures or Fe^{2+} doses the initial reaction rate is faster (as mentioned above $1/m$ is directly proportional to the initial parent compound decay rate). At temperatures above 50.0 °C the thermal decomposition of hydrogen peroxide might be the reason for the constant PQ oxidation rate. On the other hand, data from Table 5.1 allow concluding that the initial reaction rate is inversely proportional to the initial H_2O_2 dose (for the reasons discussed above, *cf.* section 5.3.1.3) and is higher for increasing PQ concentrations (one should notice that

$r_o \ \alpha \frac{1}{m} \times C_0$). When changing the pH, smaller *m* values are obtained at the optimum pH of 3.0, for the reasons also described before.

Regarding parameter b, which is inversely related to the maximum oxidation degree, Table 5.1 shows that it is nearly independent of the temperature, catalyst dose or pesticide concentration (this means that for long enough reaction times, the parent compound removal fraction is approximately the same). Better oxidation degrees are reached at an initial pH of 3.0 and for higher oxidant dosages. Actually, and as mentioned above, if the H_2O_2 concentration is low a fraction of the pesticide will remain in solution without being oxidized.

With the objective of trying to relate the parameters m and b from Table 5.1 with the experimental conditions (P_i) of each series of experiments, simple power-law type equations (or Arrhenius reaction rate dependency from temperature) were tested. With such monotonous equations one can predict the values of the parameters (and inherently the oxidation performances) at intermediate conditions, within the range of the fitting. Therefore, whenever and optimum in the m or b parameters versus experimental conditions was obtained (e.g. for data at different pH) or the trend was not persistent over the all range, the ranges in this global model were limited (temperatures only up to 50.0 °C were employed, as well as $C_{H_2O_2} \geq 6.5 \times 10^{-3} M$, with data at pH_0 = 3.0).

The power-law type equations for parameters m and b can be linearized, yielding:

$$\log\left(\frac{1}{m}\right) = Xi + Yi \ \log(Pi) \qquad 5.8$$

$$\log\left(\frac{1}{b}\right) = Zi + Wi \ \log(Pi) \qquad 5.9$$

where Xi and Zi are characteristic constants, while Yi and Wi are the apparent orders; Pi refers to the parameter studied in each series of experiments (initial concentration of oxidant, catalyst or PQ – $[H_2O_2]_0$, $[Fe(II)]_0$ or $[PQ]_0$, respectively). The dependency of $1/m$ from temperature (Arrhenius equation) in linearized form is as follows:

$$\ln\left(\frac{1}{m}\right) = Ji - \frac{Ea}{R}\frac{1}{T} \qquad 5.10$$

where Ea is the apparent activation energy for PQ degradation, R the ideal gas constant ant T the absolute temperature; Ji is a constant.

Figure 5.12 to Figure 5.15 show an example of the correlation between the m and b constants and the experimental conditions, in particular the initial hydrogen peroxide concentration and temperature.

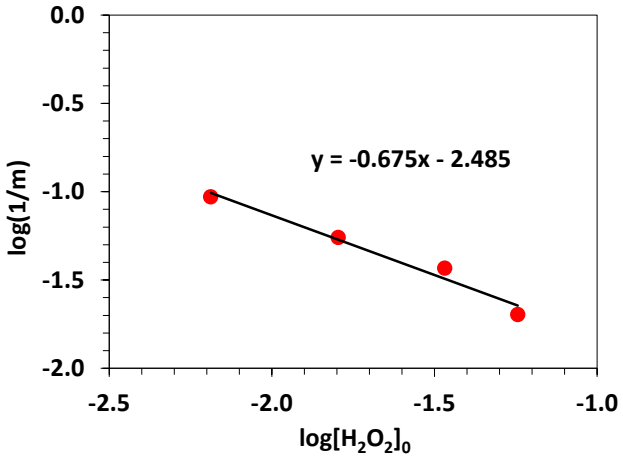

Figure 5.12. Relation between the initial hydrogen peroxide concentration and the inverse of the term m (equation 5.8).

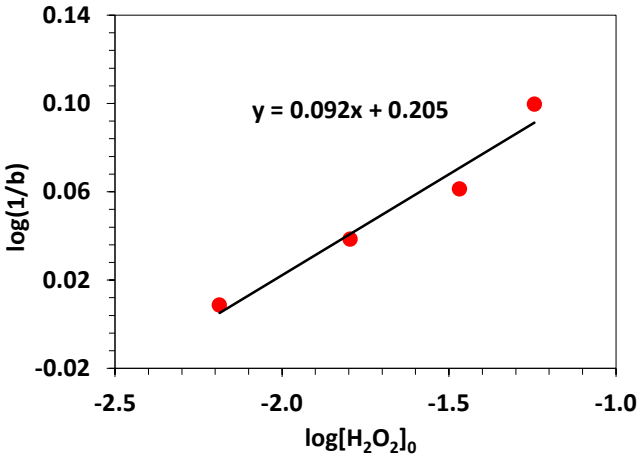

Figure 5.13. Relation between the initial hydrogen peroxide concentration and the inverse of the term b (equation 5.9).

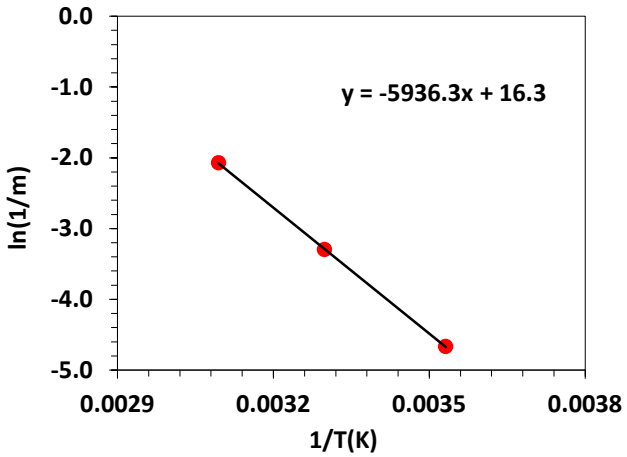

Figure 5.14. Relation between the inverse of the absolute temperature and the inverse of the term m (equation 5.10).

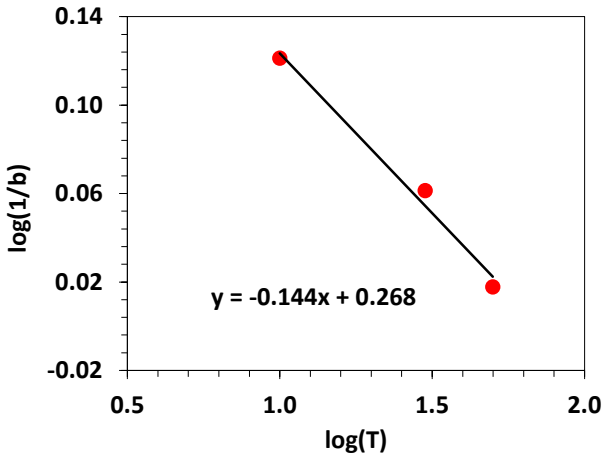

Figure 5.15. Relation between the absolute temperature and the inverse of the term b (equation 5.9).

From the slopes of these fittings (and similar ones for the other parameters), it was possible to obtain the estimated apparent order dependencies (Table 5.2), assuming power-law equations:

$$m = MC_{PQ_0}^{a} C_{H_2O_{2_0}}^{b} C_{Fe(II)_0}^{c} \exp\left(\frac{Ea}{RT}\right) \qquad 5.11$$

$$b = BC_{PQ_0}^{a'} C_{H_2O_{2_0}}^{b'} C_{Fe(II)_0}^{c'} T^{d'} \quad 5.12$$

where M and B are constants, the exponents a, b, c, a', b', c' and d' represent the apparent reaction orders, and Ea is the apparent activation energy for PQ degradation.

While for m significant dependencies (but lower than 1) were obtained, for b the apparent orders are much less significant - cf. Table 5.2.

By combining equation 5.3 with equations 5.11 and 5.12 one has a single function that allows predicting pesticide decay curves at any conditions, within the ranges of this study. All these parameters were then determined by non-linear regression (minimizing the sum of the square residues between experimental C/C_0 data and computed C/C_0 values). As a first estimative the values from Table 5.2 were used. The following results were obtained:

$$m = 2\times10^{-6} C_{PQ_0}^{0.6} C_{H_2O_{2_0}}^{0.8} C_{Fe(II)_0}^{-0.6} \exp\left(\frac{5925}{T}\right) \quad 5.13$$

$$b = 0.08\ C_{PQ_0}^{-0.03} C_{H_2O_{2_0}}^{-0.11} C_{Fe(II)_0}^{-0.14} T^{0.2} \quad 5.14$$

Table 5.2. Estimative apparent order dependency of parameters *m* and *b* on the oxidant, catalyst and parent compound concentrations and the absolute temperature – equations 5.11 and 5.12.

a	*a'*	*b*	*b'*	*c*	*c'*	*d'*	*Ea* (kJ/mol)
0.48	0.006	0.68	-0.09	-0.77	-0.09	0.14	59.4

The comparisons of the model prediction vs. the experimental responses are given in Figure 5.16. As shown, the model fits quite well the experimental data. The ANOVA test was employed to evaluate the adequacy of the model [26]. The *F*-ratio value obtained for the normalized PQ concentration ($F_{1,74}$ = 6770.56) is much higher than the Fisher's *F*-value ($F_{1,74}$ = 3.97), thus supporting the adequacy of the model (variations that occur in the response are associated to the model, not to random errors). To access the model response capability under different conditions than those considered, some experiments

were conducted in the range (Figure 5.17a) and out of the range (Figure 5.17b) considered in the kinetic study. Figure 5.17 indicates that the simple developed model reasonably predicts the PQ degradation by classic dark Fenton's reagent at different conditions. The same can be concluded from Figure 5.18 in which the parity plot shows that there are no significant differences between the data used in the kinetic model (average absolute deviation of only 2.5%) and the data used in and out of the range considered in the kinetic study (average absolute deviations of 4.1 and 6.3%, respectively).

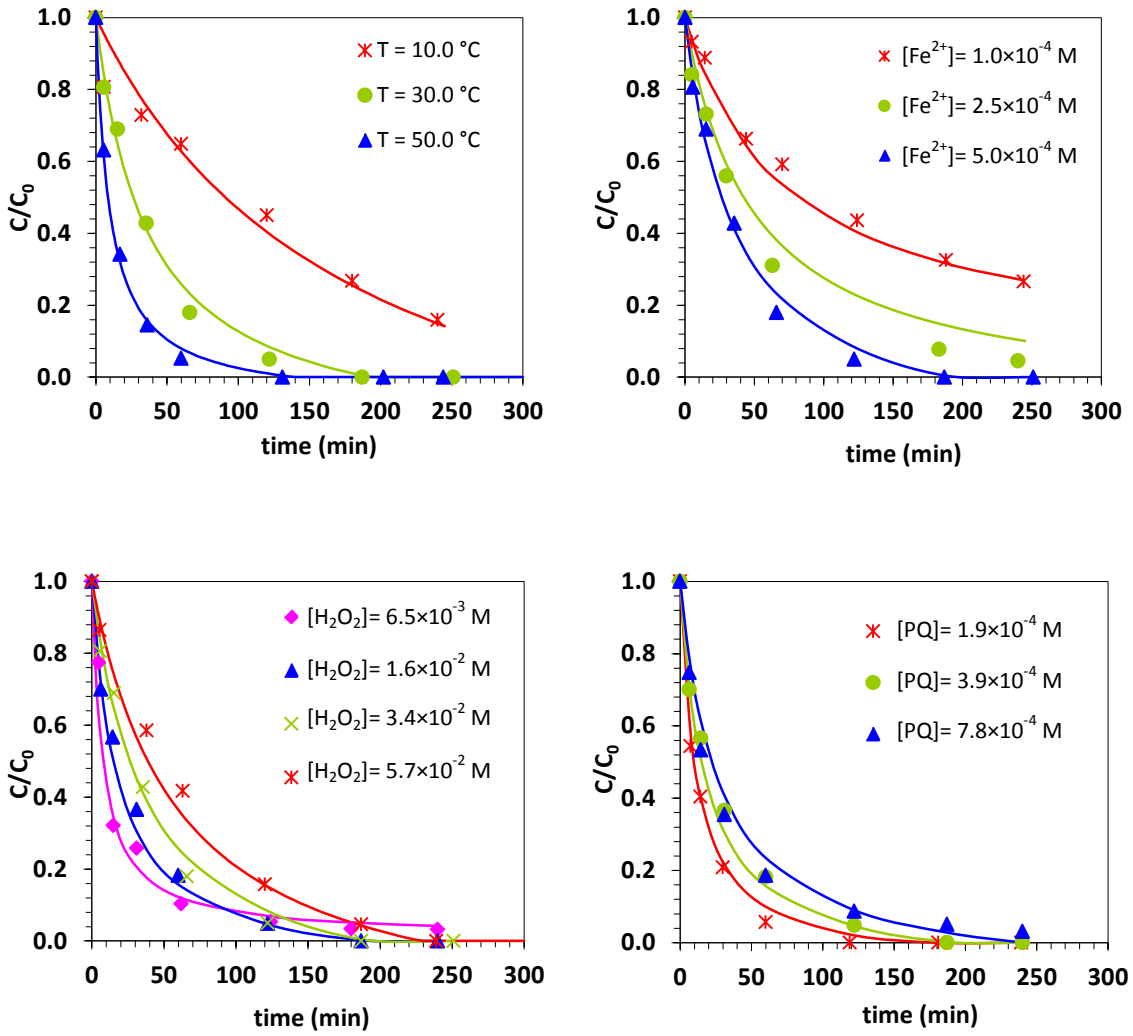

Figure 5.16. Comparison of the experimental data with the model predictions by equations 5.3, 5.13 and 5.14 - continuous lines.

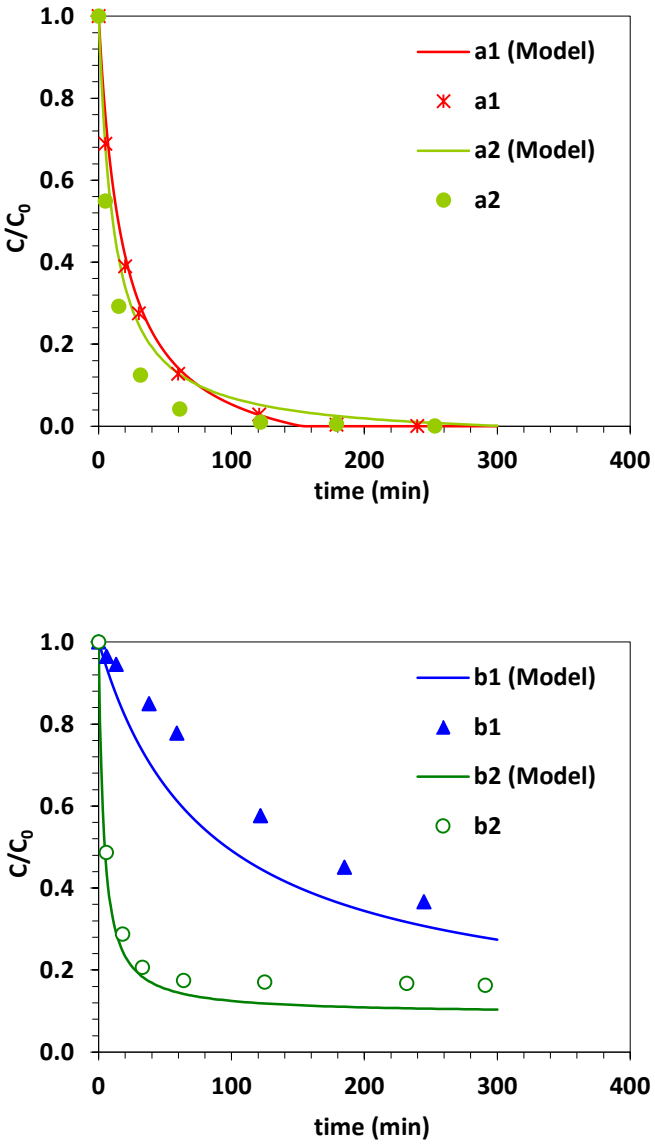

Figure 5.17. Assessment of the model response (continuous lines) for two different experiments conducted under conditions (a) within the range considered in the parametric study [a1 - ($[H_2O_2]_0$= 3.4x10^{-2} M, $[Fe(II)]_0$= 5.0x10^{-4} M, $[PQ]_0$= 3.9x10^{-4} M, pH_0= 3 and T= 40 ºC); a2 - ($[H_2O_2]_0$= 1.0x10^{-2} M, $[Fe(II)]_0$= 5.0x10^{-4} M, $[PQ]_0$= 3.9x10^{-4} M, pH_0= 3 and T= 30 ºC)] and (b) out of the range of conditions considered in the parametric study [b1 - ($[H_2O_2]_0$= 3.4x10^{-2} M, $[Fe(II)]_0$= 8.0x10^{-5} M, $[PQ]_0$= 3.9x10^{-4} M, pH_0=3 and T= 30 ºC); b2 - ($[H_2O_2]_0$= 3.0x10^{-3} M, $[Fe(II)]_0$= 5.0x10^{-4} M, $[PQ]_0$= 3.9x10^{-4} M, pH_0=3 and T= 30 ºC)].

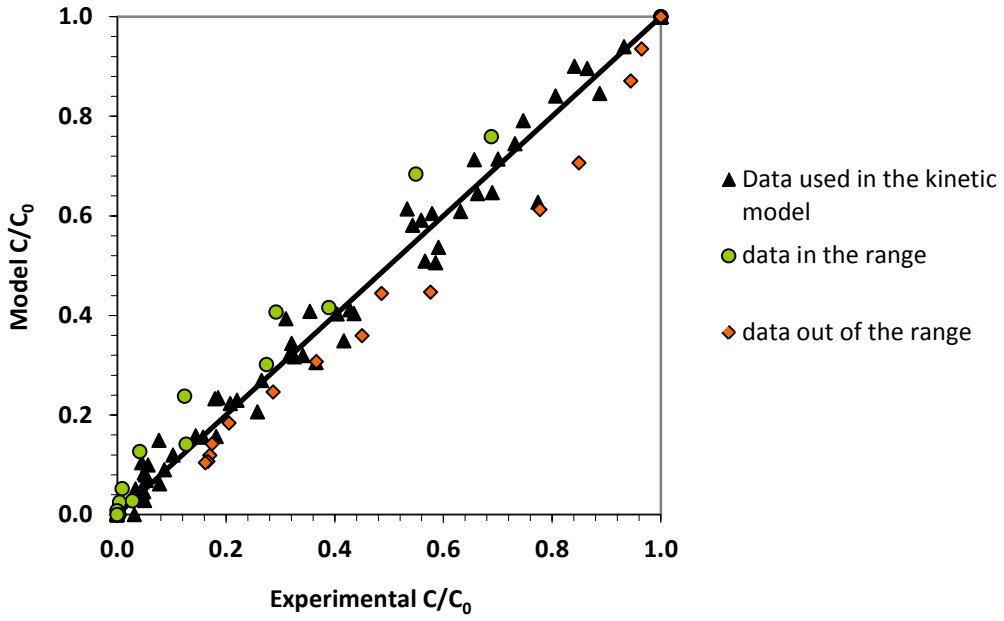

Figure 5.18. Parity plot comparing data used in the kinetic model and data gathered in and out of the range considered to develop the model.

5.3.4 Biodegradability and toxicity of oxidation products

The biodegradability of the effluent sample, withdrawn after 25 h of chemical treatment, was assessed by respirometry (cf. equation 5.1). It is important to highlight that a very low oxidant dose was employed in this experiment (for the reasons mentioned in section 5.2.5), thus clearly far from the optimal oxidation conditions. A value of 43% was obtained, which is smaller than that obtained for the 3.9×10^{-4} M PQ solution (80 %). The respiration rates obtained for PQ solution and for the effluent after 25 h of reaction were 18.1 and 12.3 g O_2/(kg_{VSS} . h), respectively. These values indicate that both samples are still biodegradable, because are higher than 10 g O_2/ (kg_{VSS} . h) [27]. The toxicity of the parent compound and of the sample after 25 h of reaction is 70 and 73%, respectively (cf. equation 5.2).

The evaluation of the toxicity of the effluents generated from the treatment of waters contaminated with PQ by Fenton´s reagent was undertaken in close collaboration with Eng. Rúben Ribeiro as part of his integrated master thesis [28]. The work was focused on the detection and identification of degradation by-products by LC-DAD and LC-MS techniques. Three degradation products, resulting from the treatment of PQ-

contaminated waters by Fenton's reagent, were detected and identified after 4 h of reaction and correspond to oxalic acid, isonicotinic acid and 4-carboxy-1-methylpyridinium ion (T =30 °C, $[Fe^{2+}]_0$ = 5.0×10^{-4} M, $[H_2O_2]_0$ = 1.6×10^{-2} M, and pH_0 = 3.0, for $[PQ]_0$ = 100 mg/L). The degradation pathway that may be involved in the process is depicted in Figure 5.19.

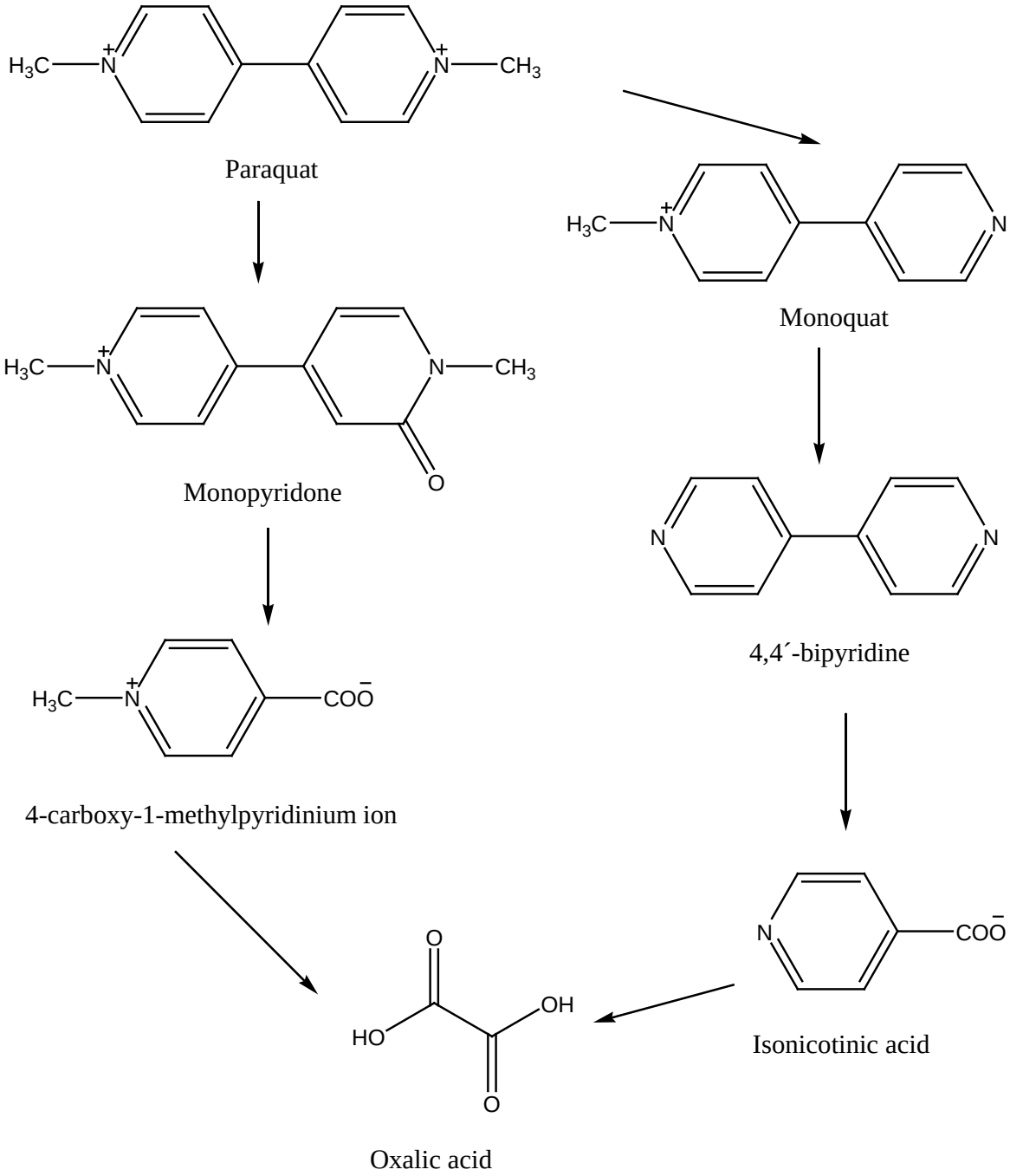

Figure 5.19. Proposed pathway for PQ degradation during classic Fenton (adapted from [2]).

The organic carbon remaining after such 4 h of reaction is 60% of the initial PQ (40% mineralization). From this, it was estimated that 61% corresponds to the identified products (oxalic acid, isonicotinic acid and 4-carboxy-1-methylpyridinium ion). Additionally, five other molecular ions were detected in the LC-MS (*m/z* 201, 265, 267, 283 and 291), but none was matched to chemical structures. Toxicity values of oxalic acid, isonicotinic acid and PQ were compared and it was concluded that both degradation products are less toxic than the parent compound.

5.3.5 Preliminary experiments using photo-Fenton reaction

To verify how much the use of UV-Vis light improves the PQ degradation, a test using the same optimal conditions as for classic Fenton reaction (T =30 °C, $[Fe^{2+}]_0$ = 5.0×10^{-4} M, $[H_2O_2]_0$ = 1.6×10^{-2} M, and pH_0 = 3.0, for $[PQ]_0$ = 100 mg/L) was performed in the presence of the radiation emitted by a 150 W medium-pressure mercury vapor lamp (Heraeus TQ-150). Figure 5.20 shows a very fast PQ degradation by the photo-Fenton process, as only five minutes are needed to degrade 99% of the pesticide.

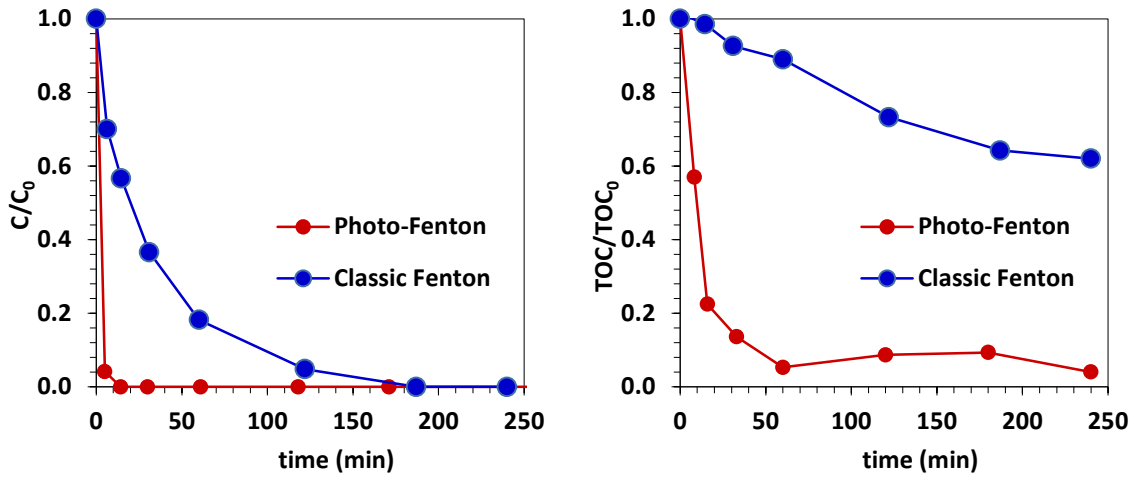

Figure 5.20. Treatment of PQ-contaminated waters by photo-Fenton (T =30 °C, $[Fe^{2+}]_0$ = 5.0×10^{-4} M, $[H_2O_2]_0$ = 1.6×10^{-2} M, and pH_0 = 3.0, for $[PQ]_0$ = 100 mg/L): (a) PQ degradation and (b) mineralization degree along time.

TOC removal is also very high when compared with the classic Fenton process. In the photo-Fenton process 96% of PQ is totally mineralized into carbon dioxide and water after only one hour of reaction. Longer reaction time did not lead to any improvement in

the mineralization degree, evidencing that either there is no more oxidant available or the products formed are refractory towards degradation by this AOP.

5.4 Conclusions

In the present chapter, a detailed parametric study was performed to evaluate the effect of temperature, H_2O_2 concentration, Fe^{2+} concentration, pH, iron source and PQ concentration on the pesticide degradation by dark Fenton's reagent.

Under optimum conditions (T =30 °C, $[Fe^{2+}]_0 = 5.0\times10^{-4}$ M, $[H_2O_2]_0 = 1.6\times10^{-2}$ M, and pH_0 = 3.0, for $[PQ]_0$ = 100 mg/L) all the initial PQ present in the reactor was degraded after 4 h and 40% of the organic matter was totally mineralized into CO_2 and H_2O. It was estimated that 61% of the remaining organic carbon after 4 h of reaction was identified (oxalic acid, isonicotinic acid and 4-carboxy-1-methyl pyridinium ion), being two of them less toxic than PQ. The PQ present in the Gramoxone commercial product had a lower degradation performance due to the presence of other organic compounds. A simple model was developed and applied to the results, fitting quite well the experimental data (on average only a 2.5 % of absolute deviation was obtained). Some experiments were performed out of the range considered in the parametric study and the model also predicts reasonably the PQ concentration profiles in the batch oxidation experiments.

The photo-Fenton process proved to be an attractive alternative to classic Fenton: much higher initial PQ degradation rate and 96% of mineralization degree after 1 h of reaction were reached.

5.5 References

[1] U.G. Akpan and B.H. Hameed, Parameters affecting the photocatalytic degradation of dyes using TiO2-based photocatalysts: a review, J. Hazard. Mater. 170 (2009) 520-529.

[2] P.C. Kearney, J.M. Ruth, Q. Zeng and P. Mazzocchi, UV ozonation of paraquat, J.Agric. Food Chem. 33 (1985) 953-957.

[3] R. Andreozzi, A. Insola, V. Caprio and M.G. D'Amore, Ozonation of 1, 1' dimethyl, 4,4' bipyridinium dichloride (Paraquat) in aqueous solution, Environ. Technol. 14 (1993) 695-700.

[4] A. Dhaouadi and N. Adhoum, Heterogeneous catalytic wet peroxide oxidation of paraquat in the presence of modified activated carbon, Appl. Catal. B-Environ. 97 (2010) 227-235.

[5] A. Dhaouadi and N. Adhoum, Degradation of paraquat herbicide by electrochemical advanced oxidation methods, J. Electroanal. Chem. 637 (2009) 33-42.

[6] A.D. Eaton, L.S. Clesceri, A.E. Greenberg and M.A.H. Franson, Standard methods for the examination of water and wastewater, 20th ed., American Public Health Association, Washington, DC, 1998.

[7] R.C. Martins, N. Amaral-Silva and R.M. Quinta-Ferreira, Ceria based solid catalysts for Fenton's depuration of phenolic wastewaters, biodegradability enhancement and toxicity removal, Appl. Catal. B-Environ. 99 (2010) 135-144.

[8] A. Guisasola, J.A. Baeza, J. Carrera, C. Casas and J. Lafuente, An off-line respirometric procedure to determine inhibition and toxicity of biodegradable compounds in biomass from an industrial WWTP, Water Sci Technol. 48 (2004) 267-275.

[9] I.S. Kim, J.C. Young and S. Kim, Development of monitoring methodology to fingerprint the activated sludge processes using oxygen uptake rate, Environ. Eng. Res. 6 (2001) 251-259.

[10] N.-C. Shang, Y.-H. Yu, H.-W. Ma, C.-H. Chang and M.-L. Liou, Toxicity measurements in aqueous solution during ozonation of mono-chlorophenols, J. Environ. Manage. 78 (2006) 216-222.

[11] I. Gulkaya, G. Surucu and F. Dilek, Importance of H2O2/Fe2+ ratio in Fenton's treatment of a carpet dyeing wastewater, J. Hazard. Mater. 136 (2006) 763-769.

[12] J.H. Ramirez, F.M. Duarte, F.G. Martins, C.A. Costa and L.M. Madeira, Modelling of the synthetic dye Orange II degradation using Fenton’s reagent: From batch to continuous reactor operation, Chem. Eng. J. 148 (2009) 394-404.

[13] C. Jiang, S. Pang, F. Ouyang, J. Ma and J. Jiang, A new insight into Fenton and Fenton-like processes for water treatment, J. Hazard. Mater. 174 (2010) 813-817.

[14] J.H. Sun, S.H. Shi, Y.F. Lee and S.P. Sun, Fenton oxidative decolorization of the azo dye Direct Blue 15 in aqueous solution, Chem. Eng. J. 155 (2009) 680-683.

[15] M.L. Kremer, The Fenton Reaction. Dependence of the Rate on pH, J. Phys. Chem. A 107 (2003) 1734-1741.

[16] C.S.D. Rodrigues, L.M. Madeira and R.A.R. Boaventura, Optimization of the azo dye Procion Red H-EXL degradation by Fenton's reagent using experimental design, J. Hazard. Mater. 164 (2009) 987-994.

[17] F.J. Rivas, V. Navarrete, F.J. Beltrán and J.F. García-Araya, Simazine Fenton's oxidation in a continuous reactor, Appl. Catal. B-Environ. 48 (2004) 249-258.

[18] T.D. Waite, Challenges and opportunities in the use of iron in water and wastewater treatment, Rev. Environ. Sci. Biotechnol. 1 (2002) 9-15.

[19] J.H. Ramirez, C.A. Costa and L.M. Madeira, Experimental design to optimize the degradation of the synthetic dye Orange II using Fenton's reagent, Catal. Today 107–108 (2005) 68-76.

[20] D.A. Saltmiras and A.T. Lemley, Degradation of Ethylene Thiourea (ETU) with Three Fenton Treatment Processes, J. Agric. Food Chem. 48 (2000) 6149-6157.

[21] S.G. Poulopoulos, M. Nikolaki, D. Karampetsos and C.J. Philippopoulos, Photochemical treatment of 2-chlorophenol aqueous solutions using ultraviolet radiation, hydrogen peroxide and photo-Fenton reaction, J. Hazard. Mater. 153 (2008) 582-587.

[22] J. Herney-Ramirez, A.M.T. Silva, M.A. Vicente, C.A. Costa and L.M. Madeira, Degradation of Acid Orange 7 using a saponite-based catalyst in wet hydrogen peroxide oxidation: Kinetic study with the Fermi's equation, Appl. Catal. B-Environ. 101 (2011) 197-205.

[23] D. Nichela, M. Haddou, F. Benoit-Marquié, M.-T. Maurette, E. Oliveros and F.S. García Einschlag, Degradation kinetics of hydroxy and hydroxynitro derivatives of benzoic acid by fenton-like and photo-fenton techniques: A comparative study, Appl. Catal. B-Environ. 98 (2010) 171-179.

[24] M.A. Behnajady, N. Modirshahla and F. Ghanbary, A kinetic model for the decolorization of C.I. Acid Yellow 23 by Fenton process, J. Hazard. Mater. 148 (2007) 98-102.

[25] C. Zaror, C. Segura, H. Mansilla, M.A. Mondaca and P. Gonzalez, Kinetic study of Imidacloprid removal by advanced oxidation based on photo-Fenton process, Environ. Technol. 31 (2010) 1411-1416.

[26] D.C. Montgomery and G.C. Runger, Applied statistics and probability for engineers, 2nd ed., John Wiley Sons, New York, 1999.

[27] M. Henze, P. Harremoës, J.l.C. Jansen and E. Arvin, Wastewater treatment: biological and chemical processes, 2nd ed., Springer-Verlag, Berlin, 1997.

[28] Rúben Lopes Casal Ribeiro, Deteção de subprodutos resultantes da degradação do pesticida paraquato por oxidação química, Tese de Mestrado Integrado em Engenharia Química, Faculdade de Engenharia da Universidade do Porto, 2012.

PART III. BDE-100

6 Nanogram per liter level determination of PBDEs in water by a simple DLLME-GC-MS method[1]

Abstract

Dispersive liquid-liquid microextraction (DLLME) is an extraction procedure gaining popularity in the last years due to the easiness of operation, enabling a high enrichment factor, low cost and low consumption of organic solvents. This extraction method, prior to gas chromatography with mass spectrometry detection (GC-MS), was optimized for the analysis of polybrominated diphenyl ethers (PBDEs) in aqueous samples. These were extracted with chlorobenzene (extraction solvent) and acetonitrile (dispersive solvent), allowing an enrichment factor of about 469 for BDE-100. The calibration curve for BDE-100 was linear in the range of 0.005-10 μg/L, with an average reproducibility of 12% (relative standard deviation – RSD%). The limit of detection (LOD), calculated by the signal-to-noise ratio, was 0.5 ng/L for BDE-100 and the recovery ranged from 91-107% for all spiked samples. Overall uncertainty was concentration-dependent, reaching high values near the limit of quantification and decreasing up to 7% for concentrations higher than 1 μg/L of BDE-100. The dispersive liquid-liquid microextraction combined with gas chromatography with mass spectrometry detection (DLLME-GC-MS) method could be successfully applied to the determination of other PBDEs in water samples.

6.1 Introduction

Analytical methods for PBDEs in waters are complex and laborious, due to the necessity of using a pre-concentration step in the extraction procedure. This pre-concentration step is always needed in order to reach LODs low enough to determine the ultra-trace levels at which PBDEs are present in water (normally within the ng/L or low μg/L range) [1-3]. The analytical methods found in the literature for PBDEs quantification in water matrices are

[1] Adapted from: Mónica S.F.Santos, José Luís Moreira, Luís M. Madeira and Arminda Alves, Nanogram per liter level determination of PBDEs in water by a simple DLLME-GC-MS method, *submitted*, 2013.

presented with more detail in Chapter 1 – section 1.2.1. Although advantages are recognized to each of the described methods, some drawbacks are also pointed out. For instance some methods are rather laborious, increasing the time of analysis [4-6], while others present lower precision [7, 8], as reported by [9, 10], or require higher sample volumes (up to 1.5 L) [6, 11, 12]. Finally, carry-over phenomena have also been pointed as a disadvantage for stir bar sorptive extraction (SBSE) and headspace solid-phase microextraction (HS-SPME) [5, 13].

Therefore, the proposed analytical methodology intends to overcome some lacks concerning the determination of PBDEs at nanogram per litter level by using DLLME as a quick and easy extraction step, that requires few sample volume, hyphenated to mass spectrometry detection. Additionally, this method intends to constitute a quick and reliable approach for identification and quantification of PBDEs in case of a deliberate or accidental contamination (emergency situations). On the other hand, this study presents for the first time a complete set of validation parameters, including the calculation of the global uncertainty associated to the results in the range of quantification.

6.2 Experimental Section

6.2.1 Reagents

2,4,4'-tribromodiphenyl ether (BDE-28, 50 mg/L in isooctane), 2,2´,4,4'-tetrabromodiphenyl ether (BDE-47, 50 mg/L in isooctane), 2,2',3,4',4-pentabromodiphenyl ether (BDE-85, 50 mg/L in isooctane), 2,2',4,4',5-pentabromodiphenyl ether (BDE-99, 50 mg/L in isooctane), 2,2',4,4',6-pentabromodiphenyl ether (BDE-100, 50 mg/L in isooctane), 2,2',4,4',5,5'-hexabromodiphenyl ether (BDE-153, 50 mg/L in isooctane), 2,2',4,4',5,6'-hexabromodiphenyl ether (BDE-154, 50 mg/L in isooctane), 2,2',3,4,4',5',6-heptabromodiphenyl ether (BDE-183, 50 mg/L in isooctane) were obtained from Sigma-Aldrich (St. Louis, USA). Distilled water was used for standards preparation. Acetonitrile (ACN), acetone (AC) and methanol (MeOH) of LC-MS grade were obtained from VWR (Porto, Portugal). Chlorobenzene (CB) of analytical grade and dichloromethane (DCM) for pesticide residue analysis were purchased from VWR (Porto, Portugal). Carbon tetrachloride (CTC) and chloroform (CF) were p.a. from Merck (Darmstadt, Germany). 1,1,2,2-Tetrachloroethane (TCE) was reagent grade from Sigma-Aldrich (St. Louis, USA).

6.2.2 Standard solutions and samples

Stock solutions were prepared by evaporating an appropriate amount of each analytical standard under a gentle nitrogen flow. Then, the residue was redissolved in acetonitrile. Aqueous standard solutions were prepared daily by evaporating an appropriate amount of stock solution, under nitrogen flow, and resuspending the residue in 25 mL of water. A calibration curve with 12 BDE-100 standards extracted by DLLME, as further described, was obtained from 0.005 to 10 μg/L.

Three different types of water samples were used to validate the application of the analytical methodology: a natural river water (collected from Sousa River), tap water (from our laboratory located at the Northern region of Portugal, a relatively hard water, pH = 6.90, TOC = 2.3 mg/L) and a mineral water (commercial water with pH = 6.39, TOC = 1.1 mg/L).

All types of water were filtered (VWR quantitative filter papers with particle retention between 5-10 μm – West Chester, USA) and stored in amber glass bottles, at -20 °C, protected from light until they were processed. Preliminary tests did not reveal any retention in the filters used.

6.2.3 Instrumentation

PBDEs were analyzed by a Varian 4000 GC-MS Chromatograph. The mass spectrometer was operated in the electronic impact ionization (EI) mode. The temperatures for the injector, trap, transfer line and manifold were held respectively at 290 °C, 200 °C, 250 °C and 50 °C. A DB-5MS column was used (30 m x 0.25 mm ID x 0.25 μm film thickness – Walnut Creek, CA, USA) and the oven temperature was programmed as follows: initial 60 °C for 2 min, rate of 30 °C/min to 250 °C, then 5 °C/min until 300 °C and held for 8 min. The injected volume was 1 μL and a 701N Hamilton syringe was used. Carrier gas was Helium (99.9999 %) at 1 mL/min flowrate. Monitoring ions in the selected ion-monitoring mode (SIM) are listed in Table 6.1. The identification of the compounds was done by comparison of the retention times with those obtained for standard solutions directly injected. All PBDEs were injected separately under the optimized conditions described below.

Table 6.1. Retention time, quantification and qualifier ions for each PBDE by GC-MS.

PBDEs	Class	Retention time (min)	Quantification ion (*m/z*)	Qualifier ion (*m/z*)
BDE-28	Tri-BDE	10.720	248 + 408	246
BDE-47	Tetra-BDE	12.513	326 + 486	328
BDE-85	Penta-BDE	15.954	406 + 564	404
BDE-99	Penta-BDE	14.829	406 + 566	404
BDE-100	Penta-BDE	14.227	406 + 566	564
BDE-153	Hexa-BDE	17.459	484 + 644	486
BDE-154	Hexa-BDE	16.480	484	644
BDE-183	Hepta-BDE	20.473	564 + 724	562

6.2.4 DLLME procedure

Extractions were performed in 50 mL plastic screw-cap test tubes with conical bottom. An aqueous sample (25 mL) was extracted with given volumes of different dispersive and extraction solvents; optimized conditions were 1 mL of ACN and 80 μl of CB. The mixture was centrifuged for 5 min at 4000 rpm in a Hettich Rotofix 32A Centrifuge. The sedimented-phase was collected with a syringe and was injected in the GC-MS.

6.2.5 Validation parameters

Precision was evaluated by extracting 3 independent standards at 3 concentration levels: 0.01, 1 and 10 μg/L and 3 independent spiked samples (tap water, drinking water and river water) at three concentration levels: 0.01, 1 and 10 μg/L.

Accuracy was evaluated by standard addition using tap, drinking and river waters spiked with BDE-100 at the same 3 concentration levels.

6.3 Results and discussion

This work comprised a previous optimization of the extraction method by DLLME, followed by the validation of the analytical methodology, with special care to the estimation of the global uncertainty associated to the results.

6.3.1 Optimization of DLLME

The effect of some critical parameters on the DLLME performance was investigated, among them the kind and volume of extraction and dispersive solvents, extraction time and salt addition. For such purpose, BDE-100 was selected as a model compound to evaluate in which manner the extraction process was affected by such parameters. So, all results obtained in this section were carried out from aqueous solutions containing 1 μg/L of BDE-100. The final conditions were afterwards applied to the others PBDEs. To better understand the effects of the above-mentioned parameters on DLLME performance, enrichment factors (EF) and extraction recoveries ($\%ER$) were determined:

$$EF = C_{sed} / C_0 \quad (6.1)$$

$$\%ER = (C_{sed} V_{sed}) / (C_0 V_{aq}) \times 100 \quad (6.2)$$

where C_0 and V_{aq} are the BDE concentration and volume of aqueous solution samples and C_{sed} and V_{sed} the BDE concentration and volume of the sedimented-phase.

All experiments were performed in triplicate and injected in the GC-MS at least twice.

6.3.1.1 Effect of extraction and dispersive solvents

The kind of extraction and dispersive solvent is crucial in the extraction efficiency by DLLME [10]. The extraction solvent must display high extraction capability for the analytes, higher density than water, good chromatographic behavior and low water solubility [10, 14, 15]. Typically, halogenated hydrocarbons are used due to their high density [10]. On the other hand, the selection of the dispersive solvent should take into account its miscibility both in water and in the extraction solvent. The commonly used dispersive solvents include methanol, ethanol, acetonitrile, acetone and tetrahydrofuran [10]. Usually, the selection of extraction and dispersive solvents is made separately but the result may be compromised. In this study, this selection was made jointly to determine which set of solvents leads to a higher extraction efficiency. Therefore, the combinate effect of four extraction solvents (CTC, CB, DCM and CF) and three dispersive solvents (AC, MeOH and ACN) on DLLME performance was studied. TCE was also tested as extraction solvent with acetonitrile but this set of solvents proved to be aggressive for

some components of the equipment used, such as the GC injection syringe, and therefore was discarded.

The experiments were performed using 1 mL of dispersive solvent containing 100 μL of extraction solvent (Table 6.2).

Table 6.2. Analytical responses and extraction recoveries obtained when different extraction and dispersive solvents were used on DLLME technique.

	CB			CTC		
	ACN	**MeOH**	**AC**	**ACN**	**MeOH**	**AC**
Area	$(25\pm2)\times10^4$	$(27\pm1)\times10^4$	$(22\pm1)\times10^4$	$(15\pm1)\times10^4$	$(18\pm2)\times10^4$	$(17\pm2)\times10^4$
%ER	75±3	71±4	73±2	63±5	77±6	70±8

The analytical responses obtained for the extracted samples were compared to those obtained for standards prepared in the same solvent. Dichloromethane and chloroform were automatically discarded because the formation of two phases was not observed under the conditions employed and using the mentioned dispersive solvents. Although similar extraction recoveries were attained for both extraction solvents (CTC and CB), chlorobenzene was chosen because it gave higher analytical response. This last point is very important specifically in the quantification of tracer compounds like PBDEs. On the other hand, CTC leads to higher variation coefficients and has lower boiling point which could represent a relevant source of error.

Yanyan Li et al. [15] used TCE and acetonitrile as extraction and dispersive solvents, respectively. This set of solvents led to higher extraction efficiencies (extraction recovery of around 103%) but, injections were made manually in the liquid chromatography (LC) due to the aggressive character of the solvent mixture, which may contribute to the decrease of the precision. The same problem arose when this organic solvent was also applied joint with tetrahydrofuran (dispersive solvent) for BDE-209 determination in water samples [14].

Concerning the dispersive solvent, although chlorobenzene showed good results when combined with acetone, higher reproducibility was obtained with acetonitrile, probably due to less leaks of solvent evaporation and therefore this was the selected dispersive solvent, combined with the extraction solvent - chlorobenzene.

6.3.1.2 Effect of the extraction solvent volume

To examine the effect of the chlorobenzene volume on the extraction process performance, BDE-100-containing aqueous samples were submitted to the same DLLME procedure by using 1 mL of acetonitrile containing different volumes of chlorobenzene (80, 100, 150 and 200 μL). Chlorobenzene volumes below 80 μL were not considered because a minimum safety volume of 40 μL was set for the sedimented-phase. Figure 6.1a depicts the extraction recovery and the enrichment factor versus chlorobenzene volume, respectively. As shown in Figure 6.1a, the enrichment factor decreased as the chlorobenzene volume increases. Indeed, higher chlorobenzene volumes lead to higher volumes of sedimented-phase (data not shown) and consequently, lower target compound concentrations and lower enrichment factors (Figure 6.1a).

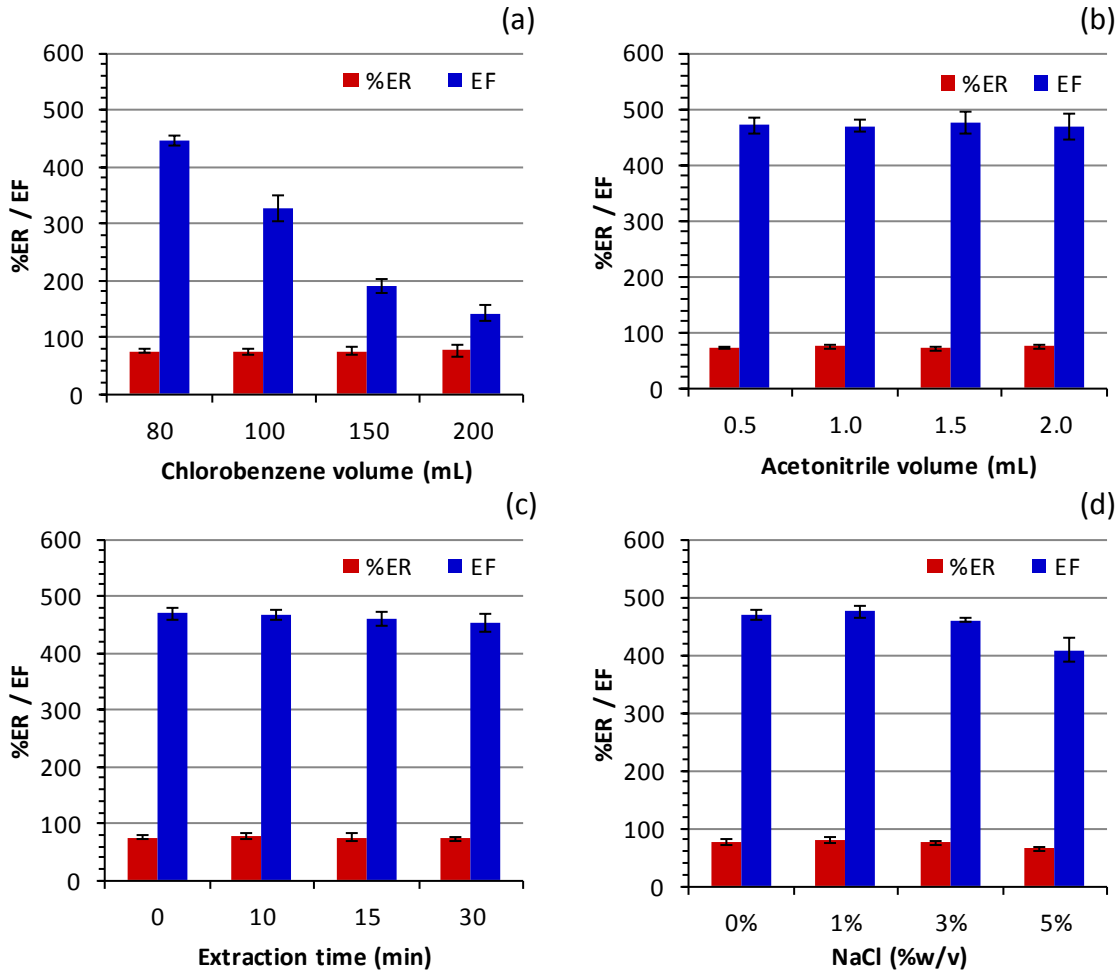

Figure 6.1. Effect of chlorobenzene volume (a), acetonitrile volume (b), extraction time (c) and salt addition (d) on the enrichment factor and extraction recovery for BDE-100.

On the other hand, the extraction recovery is not affected by the volume of extraction solvent used. The same behavior has been observed by other authors which implemented DLLME technique to determine a huge number of target compounds in different matrices [10, 14-16]. Therefore, 80 μL of chlorobenzene was selected as the optimum volume.

6.3.1.3 Effect of dispersive solvent volume

The dispersive solvent is directly responsible for the formation of the cloudy solution and, by this way, its volume may compromise the degree of dispersion of the extraction solvent in the aqueous phase [10]. To evaluate the effect of dispersive solvent volume, the experimental conditions included the use of 0.5, 1, 1.5 and 2 mL of acetonitrile, containing 80 μL of chlorobenzene. The results show that either the extraction recovery or the enrichment factor were not significantly affected by the volume of acetonitrile (Figure 6.1b). Other authors have found an optimum value of dispersive solvent volume but, different sample volumes were used (5 mL instead 25 mL) for the same dispersive solvent volumes tested here [14-17]. So, within the range of the volumes used in this study, the same tendency was not found and therefore, 1 mL of acetonitrile was chosen for the subsequent experiments because it conducts to more precise results (lower coefficient of variation).

6.3.1.4 Effect of extraction time

In DLLME, the extraction time is defined as the interval between the injection of the extraction and dispersive solvents mixture and the centrifugation step. One remarkable advantage of this extraction technique is the short time needed to transfer the analyte from the aqueous phase to the organic one and thus, the equilibrium stage [10]. It is important to study this parameter because the extraction time can influence significantly the extraction efficiency [18]. The extraction recoveries obtained from aqueous solutions submitted to the same DLLME procedure and different extraction times (0, 5, 10, 15 and 30 min) are shown in the Figure 6.1c.

As observed, the extraction time has no impact on the extraction efficiency within the interval of time selected. Longer times were not considered, because the aim is to obtain a rapid extraction with acceptable efficiency. Thus, the most time-consuming step is the centrifuging, which lasts about 5 min. This is an important aspect since it marks the great

advantage of this extraction technique against the others presented in the Chapter 1– section 1.2.1. Similar results were also achieved by other researchers [14-16], meaning that the mass transfer is very fast, occurring during the injection of the solvents/start-up of the centrifuge.

6.3.1.5 Effect of salt addition

The increase of the aqueous sample ionic strength by salt addition may cause opposite consequences on the recovery. Firstly, the increase of the ionic strength can lead to a decrease of analyte and extraction solvent solubilities in the aqueous phase, which may contribute to the increase on the extraction process recovery [10]. However, the volume of sedimented-phase increases by increasing ionic strength and thus, the analyte concentration decreases [10]. The ionic strength was evaluated adding sodium chloride to the aqueous solution in the range between 0 and 5%(w/v). Under such conditions it was not observed any significant salt addition effect on the DLLME performance (Figure 6.1d). Similar results were already obtained by other authors [6, 19, 20]. Consequently, the following experiments were performed without the addition of salt.

6.3.2 Quantitative analysis

Quantitative analysis of contaminants as BDE-100, or ultra-trace contaminants in water samples, is usually necessary for different objectives. The most important is to allow the monitoring of waters in different environmental media (rivers, lakes, drinking and tap water, etc) and for that, the main purpose of the validation is to obtain the lowest quantification limit possible. However, other objectives include the quantification of the contaminants for degradation studies, or other, where normally higher concentrations are used. In this case, it is acceptable to reach somewhat higher quantification limits, but the limiting factor is the available sample volume, because most of the time, batch experiments are used and samples have to be taken along the time. Therefore, analytical methods have to be able to quantify the contaminants at low levels, using low sample volumes. In these cases, the estimation of the uncertainty of the results plays an important role, because models will be constructed. The combination of low quantification limits with low sample volume will have an impact in the uncertainty of the results.

The validation of the analytical method, including the uncertainty measurement, followed the *bottom-up* approach described in EURACHEM CITAC Guide [21] and by the authors elsewhere [22, 23]. Description of main contributions and respective calculation formula for the global uncertainty is in Annex I. It comprised a first step of in-house validation, where the main parameters were obtained – linearity of the response, using standards extracted in the same mode as samples, LOD and LOQ (limit of quantification), precision and accuracy. The second step was the estimation of the uncertainty of the results, using the validation parameters as assumption that those represented the main sources of uncertainty of final result.

6.3.2.1 Response linearity and detection and quantification limits

Calibration was performed for BDE-100 by DLLME-GC-MS using the 12 standards extracted in the same conditions as the samples (from 0.005 to 10 μg/L). The correlation coefficient (R=0.9997) and the linearity tests revealed a good performance for the linearity. The LOD and LOQ were calculated based on a signal-to-noise-ratio of 3 and 10, and they were found to be 0.5 and 2 ng/L, respectively. Comparing with other techniques, whose results are reported in the Introduction, the obtained LOD is lower or, at least, of the same order of magnitude.

6.3.2.2 Precision and Accuracy

The precision was evaluated by repeatability and intermediate precision at three BDE-100 concentration levels – 0.01, 1 and 10 μg/L. Repeatability corresponds to the RSD% observed when one sample is injected six times in the same day under the same conditions. Repeatability expressed as RSD% was 7, 5 and 3% for 0.01, 1 and 10 μg/L. Intermediate precision was analyzed extracting three independent standards (ultrapure water) and spiked samples (drinking, tap and river water) at three concentration levels (Table 6.3). Average precision, expressed as relative standard deviation, was 12% for standards and 13%, 12% and 10% for spiked drinking, tap and river waters, respectively.

Accuracy was evaluated by the percentage of recovery for spiked samples (drinking, tap and river waters) because nor reference materials, neither interlaboratory or proficiency studies were available. Recoveries were on an average higher than 91% and lower than 107% for all spiked sample considered (Table 6.3).

Table 6.3. Precision and recoveries obtained for BDE-100 standards and spiked water samples.

	Precision (RSD%) (n=3)			Recovery (%) (n=3)		
	0.01 μg/L	1 μg/L	10 μg/L	0.01 μg/L	1 μg/L	10 μg/L
Standard	18	10	8	-----	-----	-----
Spiked drinking water	20	6	13	96±19	107±6	88±12
Spiked tap water	19	6	11	114±22	103±6	105±11
Spiked river water	11	14	4	82±9	110±16	82±3

The good recovery results and the low RSDs observed enable an accurate evaluation of the BDE-100 in the tested samples, even at the lowest level assessed.

The analytical response for standards prepared in ultrapure water was compared to the response obtained for spiked drinking, tap and river waters at the same concentration levels. It was observed that the analytical response is almost independent of the type of water used, meaning that there is no matrix effect.

6.3.2.3 Estimation of the global uncertainty associated to the results

The four uncertainty sources that were judged more important in the contribution for the overall uncertainty of results were uncertainty associated with the preparation of the standards (U1), the calibration curve (U2), the precision of the extraction and also of the chromatographic method (U3) and uncertainty associated to the accuracy (U4).

Figure 6.2a shows the contribution of each uncertainty source for the overall uncertainty. As can be seen, the uncertainty associated with the calibration curve is the most significant contribution at lower concentrations, showing the importance of this estimation. For higher concentrations, the uncertainty of precision and accuracy exhibit more importance for the global uncertainty. From Figure 6.2b, it can be observed that the uncertainty decreases from 11 to 7% for BDE-100 concentration from 0.5 to 10 μg/L, which is acceptable and normally obtained with other methods.

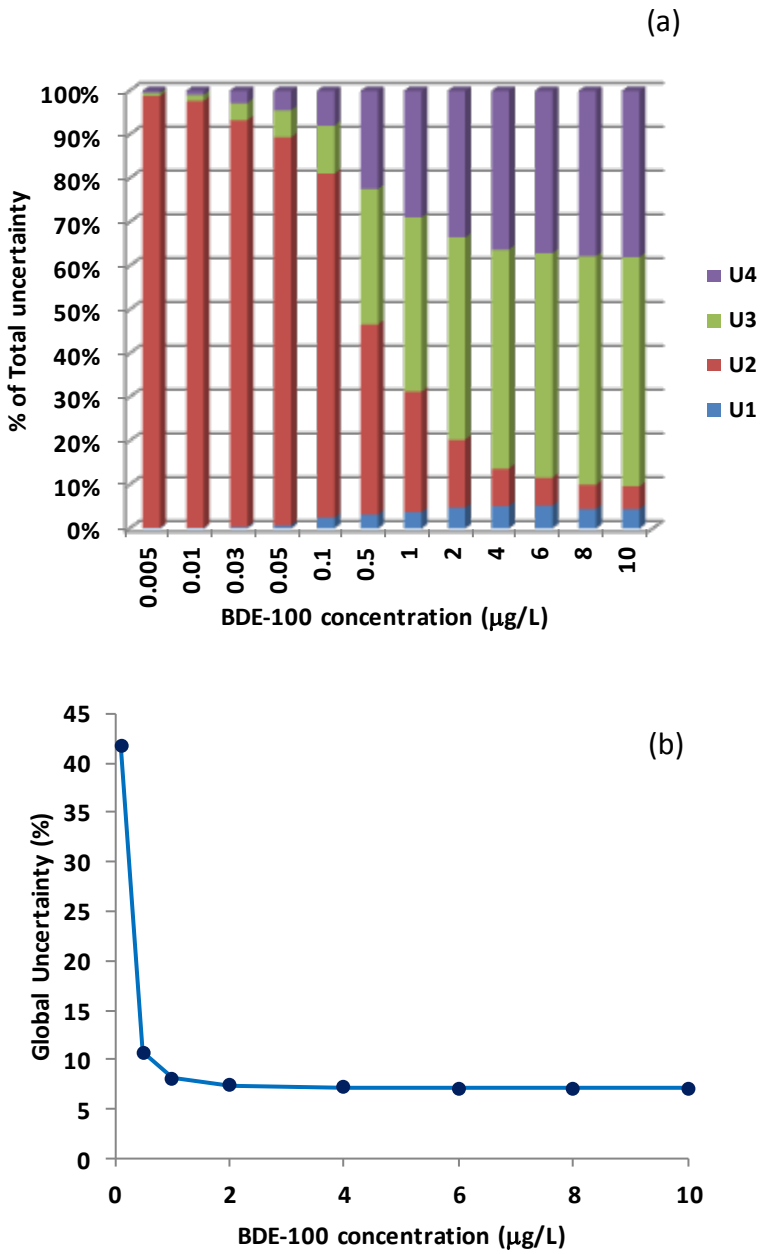

Figure 6.2. Contribution of each source of uncertainty to the total uncertainty – U1: standards preparation, U2: calibration curve, U3: precision and U4: accuracy (a) and global uncertainty (b) for BDE-100 analysis in water by DLLME-GC-MS.

However, care must be taken when considering the results for concentrations lower than 0.5 µg/L because much higher uncertainty may be found, which is typical of trace analysis and most authors do not evaluate the global uncertainty in the vicinity of the quantification limit [23, 24].

6.3.3 Suitability of the extraction methodology to other PBDEs

The applicability of the developed analytical methodology (DLLME-GC-MS) for other PBDEs quantification in water matrices was also evaluated. The PBDEs selected are the most environmentally dominant congeners [25]. Firstly, the extraction recovery was determined for each PBDE at two concentration levels – 1 and 10 μg/L (Table 6.4).

Table 6.4. Extraction recoveries, precision and estimated LOQ for all PBDEs by DLLME-GC-MS.

	%ER (n=3)		Precision (RSD%) (n=3)		Estimated LOQ
	1 μg/L	10 μg/L	1 μg/L	10 μg/L	(ng/L)
BDE-28	71±6	69±7	11	12	10
BDE-47	70±6	69±6	12	13	30
BDE-85	72±9	78±6	12	12	93
BDE-99	72±7	77±5	12	9	27
BDE-100	76±7	73±5	12	10	2
BDE-153	66±6	73±5	13	11	73
BDE-154	69±8	68±4	14	11	23
BDE-183	63±7	70±5	8	9	113

For that, aqueous solutions prepared from a mixture of all PBDEs were submitted to DLLME, under conditions optimized in the last section. Figure 6.3 shows an example of a chromatogram obtained, where it can be observed good separation of compounds and high resolution. As can be seen, and despite of the extraction optimization being performed based only on the DLLME performance for BDE-100 quantification, good and similar extraction recoveries were attained for the other PBDEs. On the other hand, it can be observed that the extraction efficiency of BDE-100 is not affected by the presence of the other congeners. These results prove that such extraction methodology can be successfully applied for the other PBDEs and it seems that the extraction efficiency of individual PBDEs is similar both when they are alone or together in the sample. In terms of quantitative analysis, the precision was evaluated by extracting three independent standard solutions at the same two concentration levels (1 and 10 μg/L). The results expressed as RSD% are compiled in Table 6.4. Again, it can be advanced that the method

remains precise, even when it was applied to a mixture of PBDEs. Estimated LOQs were calculated based on a signal-to-noise-ratio of 10 (Table 6.4). As observed from Table 6.4 the method proposed here, beyond successful applied for all PBDEs considered, allows reaching lower or comparable quantification limits of those existing in the literature (with more complex or time consuming extraction techniques).

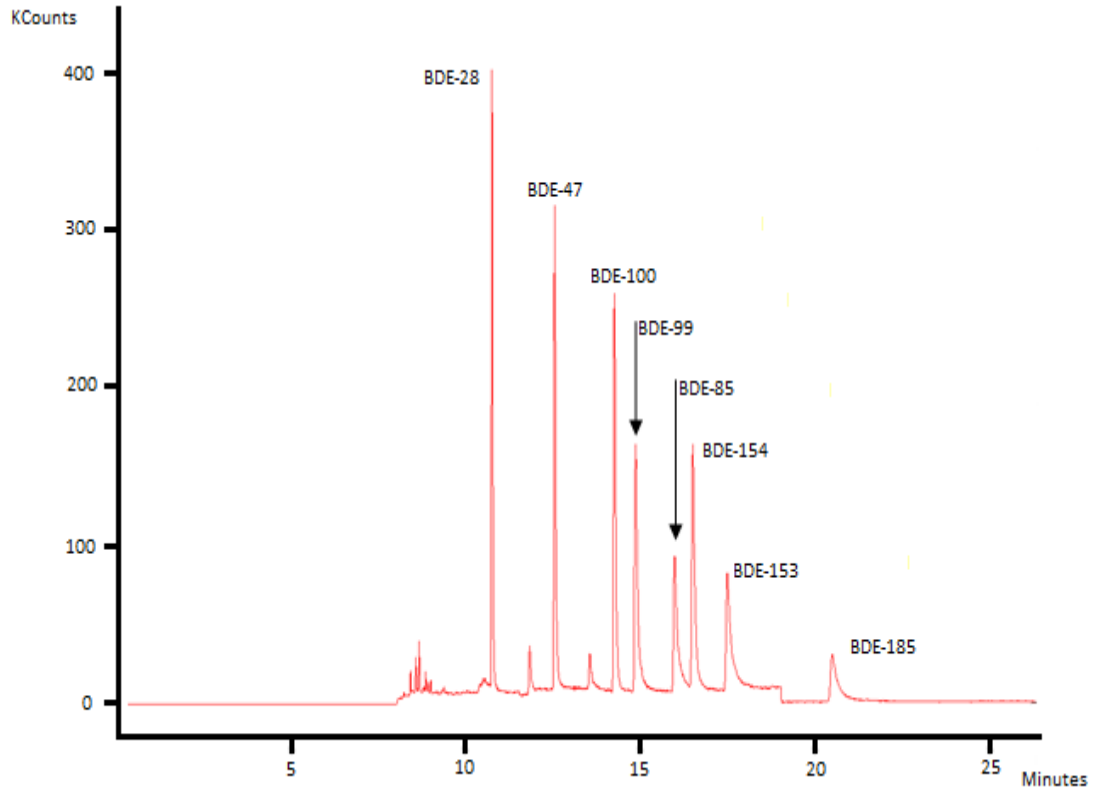

Figure 6.3. Chromatogram of a standard solution of PBDEs at individual concentration of 1 μg/L.

6.4 Conclusions

A method by DLLME-GC-MS has been described for the determination of PBDEs in water samples. Additionally, the global uncertainty of the results was assessed for the first time, which is important especially for low concentration levels, where most uncertainty sources are extremely significant. The LOQ for BDE-100 was 2 ng/L and acceptable precision (12% for standards and 13%, 12% and 10% for spiked drinking, tap and river waters, respectively) and accuracy (91-107% of percentage of recovery for all spiked samples) were obtained. The uncertainty decreased from 11% to 7% when concentration

of BDE-100 increases from 0.5 μg/L to 10 μg/L. Similar extraction recoveries were achieved when the developed method was applied to the other PBDEs. The precision remains satisfactory (average 11%) even, when mix standards with all PBDEs were analyzed. Lower or comparable LOQs to those reported in literature were obtained with this cheap, fast and easy to implement method for PBDEs quantification in water (2-113 ng/L).

6.5 References

[1] J. Sánchez-Avila, R. Tauler and S. Lacorte, Organic micropollutants in coastal waters from NW Mediterranean Sea: Sources distribution and potential risk, Environ. Int. 46 (2012) 50-62.

[2] A.P. Daso, O.S. Fatoki, J.P. Odendaal and O.O. Olujimi, Occurrence of selected polybrominated diphenyl ethers and 2,2',4,4',5,5'-hexabromobiphenyl (BB-153) in sewage sludge and effluent samples of a wastewater-treatment plant in Cape Town, South Africa, Arch. Environ. Con. Tox. 62 (2012) 391-402.

[3] B.K. Hope, L. Pillsbury and B. Boling, A state-wide survey in Oregon (USA) of trace metals and organic chemicals in municipal effluent, Sci. Total Environ. 417–418 (2012) 263-272.

[4] A.R. Fontana, M.F. Silva, L.D. Martínez, R.G. Wuilloud and J.C. Altamirano, Determination of polybrominated diphenyl ethers in water and soil samples by cloud point extraction-ultrasound-assisted back-extraction-gas chromatography–mass spectrometry, J. Chromatogr. A 1216 (2009) 4339-4346.

[5] J. Llorca-Porcel, G. Martínez-Sánchez, B. Álvarez, M.A. Cobollo and I. Valor, Analysis of nine polybrominated diphenyl ethers in water samples by means of stir bar sorptive extraction-thermal desorption-gas chromatography–mass spectrometry, Anal. Chim. Acta 569 (2006) 113-118.

[6] X. Liu, J. Li, Z. Zhao, W. Zhang, K. Lin, C. Huang and X. Wang, Solid-phase extraction combined with dispersive liquid–liquid microextraction for the determination for polybrominated diphenyl ethers in different environmental matrices, J. Chromatogr. A 1216 (2009) 2220-2226.

[7] Q. Xiao, B. Hu, J. Duan, M. He and W. Zu, Analysis of PBDEs in Soil, Dust, Spiked Lake Water, and Human Serum Samples by Hollow Fiber-Liquid Phase Microextraction Combined with GC-ICP-MS, J. Am. Soc. Mass Spectr. 18 (2007) 1740-1748.

[8] N. Fontanals, T. Barri, S. Bergström and J.-Å. Jönsson, Determination of polybrominated diphenyl ethers at trace levels in environmental waters using hollow-fiber microporous membrane liquid–liquid extraction and gas chromatography–mass spectrometry, J. Chromatogr. A 1133 (2006) 41-48.

[9] A.R. Fontana, R.G. Wuilloud, L.D. Martínez and J.C. Altamirano, Simple approach based on ultrasound-assisted emulsification-microextraction for determination of polibrominated flame retardants in water samples by gas chromatography–mass spectrometry, J. Chromatogr. A 1216 (2009) 147-153.

[10] X.-H. Zang, Q.-H. Wu, M.-Y. Zhang, G.-H. Xi and Z. Wang, Developments of Dispersive Liquid-Liquid Microextraction Technique, Chinese J. Anal. Chem. 37 (2009) 161-168.

[11] V. Yusà, A. Pastor and M. de la Guardia, Microwave-assisted extraction of polybrominated diphenyl ethers and polychlorinated naphthalenes concentrated on semipermeable membrane devices, Anal. Chim. Acta 565 (2006) 103-111.

[12] A. Bacaloni, L. Callipo, E. Corradini, P. Giansanti, R. Gubbiotti, R. Samperi and A. Laganà, Liquid chromatography–negative ion atmospheric pressure photoionization tandem mass spectrometry for the determination of brominated flame retardants in environmental water and industrial effluents, J. Chromatogr. A 1216 (2009) 6400-6409.

[13] M. Polo, G. Gómez-Noya, J.B. Quintana, M. Llompart, C. García-Jares and R. Cela, Development of a Solid-Phase Microextraction Gas Chromatography/Tandem Mass Spectrometry Method for Polybrominated Diphenyl Ethers and Polybrominated Biphenyls in Water Samples, Anal. Chem. 76 (2004) 1054-1062.

[14] Y. Li, J. Hu, X. Liu, L. Fu, X. Zhang and X. Wang, Dispersive liquid-liquid microextraction followed by reversed phase HPLC for the determination of decabrominated diphenyl ether in natural water, J. Sep. Sci. 31 (2008) 2371-2376.

[15] Y. Li, G. Wei, J. Hu, X. Liu, X. Zhao and X. Wang, Dispersive liquid–liquid microextraction followed by reversed phase-high performance liquid chromatography for the determination of polybrominated diphenyl ethers at trace levels in landfill leachate and environmental water samples, Anal. Chim. Acta 615 (2008) 96-103.

[16] M. Rezaee, Y. Assadi, M.-R. Milani Hosseini, E. Aghaee, F. Ahmadi and S. Berijani, Determination of organic compounds in water using dispersive liquid–liquid microextraction, J. Chromatogr. A 1116 (2006) 1-9.

[17] A. Zhao, X. Wang, M. Ma, W. Wang, H. Sun, Z. Yan, Z. Xu and H. Wang, Temperature-assisted ionic liquid dispersive liquid-liquid microextraction combined with high performance liquid chromatography for the determination of PCBs and PBDEs in water and urine samples, Microchim. Acta 177 (2012) 229-236.

[18] R. Sousa, V. Homem, J.L. Moreira, L.M. Madeira and A. Alves, Optimisation and application of dispersive liquid-liquid microextraction for simultaneous determination of carbamates and organophosphorus pesticides in waters, Anal. Method 5 (2013) 2736-2745.

[19] P. Liang, J. Xu and Q. Li, Application of dispersive liquid-liquid microextraction and high-performance liquid chromatography for the determination of three phthalate esters in water samples, Anal. Chim. Acta 609 (2008) 53-58.

[20] R.R. Kozani, Y. Assadi, F. Shemirani, M.R.M. Hosseini and M.R. Jamali, Part-per-trillion determination of chlorobenzenes in water using dispersive liquid-liquid microextraction combined gas chromatography-electron capture detection, Talanta 72 (2007) 387-393.

[21] S.L.R. Ellison, M. Rosslein and A. Williams, Eurachem/ Citac Guide- Quantification uncertainty in analytical measurement, EURACHEM/ CITAC, UK, 2000.

[22] N. Ratola, L. Martins and A. Alves, Ochratoxin A in wines-assessing global uncertainty associated with the results, Anal. Chim. Acta 513 (2004) 319-324.

[23] S.L. Silva, A. Alves and L. Santos, Uncertainty Measurement of Chlorophenols and PCBs Analyzed in Aqueous Media by SPME-GC-ECD, J. Chromatogr. Sci. 47 (2009) 103-109.

[24] H.-B. Moon, M. Choi, J. Yu, R.-H. Jung and H.-G. Choi, Contamination and potential sources of polybrominated diphenyl ethers (PBDEs) in water and sediment from the artificial Lake Shihwa, Korea, Chemosphere 88 (2012) 837-843.

[25] Y.-W. Qiu, G. Zhang, L.-L. Guo, G.J. Zheng and S.-Q. Cai, Bioaccumulation and historical deposition of polybrominated diphenyl ethers (PBDEs) in Deep Bay, South China, Mar. Environ. Res. 70 (2010) 219-226.

7 Preliminary results on the degradation of BDE-100 in waters by photolysis and photo-Fenton*

Abstract

The work presented in this chapter is related to the BDE-100 degradation in waters by advanced oxidation processes. Two technologies were considered in this study (direct photolysis and photo-Fenton) and, for the first time, degradation experiments were designed to treat waters contaminated with BDE-100 without adding organic solvents (which are commonly employed to help solubilization in water and/or to work with higher initial concentrations).

Photolysis proved to be an effective process to degrade BDE-100 in waters. Actually, almost complete BDE-100 degradation (92%) was achieved after 6 h of irradiation (1.6×10^{-6} Einstein/s), which is a very interesting result with regard to those available in the literature. Photo-Fenton was also tested in the treatment of waters contaminated with BDE-100, which constitutes another innovation of the present work. However, results on this topic are still preliminary.

7.1 Introduction

BDE-100 degradation in liquid phase is a quite new research topic since, up to the author knowledge, no more than three studies were published. Two of them are based on degradation studies by direct photolysis [1, 2] and the other on a remediation process with zerovalent iron [3]. The polybrominated diphenyl ethers (PBDEs) degradation studies, including BDE-100, have been developed and optimized in the presence of organic solvents. The rationale for conducting the experiments under such conditions is two-fold. First, the use of organic solvents, even at low doses, allows using contaminated solutions with high PBDEs concentrations because the solubility of PBDEs increases. Second, the degradation process is facilitated because the tendency for PBDEs to adsorb to surfaces, such as container walls, decreases significantly in the presence of organic

* Adapted from: Mónica S.F. Santos, Arminda Alves and Luís M. Madeira, Preliminary results on the degradation of BDE-100 in waters by photolysis and photo-Fenton, *paper in preparation*, 2013.

solvents. However, care must be taken because the performances reached, degradation mechanisms and reaction products may be drastically influenced by the conditions under which the reaction is processed and some predictions concerning real scenarios may fail.
In this chapter and for the first time, a degradation methodology by direct photolysis will be implemented to treat waters contaminated with concentrations of BDE-100 close to the limit of solubility of such congener in water, without the presence of organic solvents. Additionally, some preliminary results concerning the degradation of BDE-100 in waters by photo-Fenton will be discussed. It is important to highlight that this advanced oxidation process was never addressed in the open scientific literature in this context.

7.2 Experimental Section

7.2.1 Reagents

2,2',4,4',6-pentabromodiphenyl ether (BDE-100, 50 mg/L in isooctane) was obtained from Sigma-Aldrich (St. Louis, USA). Acetonitrile (ACN) of LC-MS grade and chlorobenzene (CB) of HPLC grade were purchased from VWR (Fontenay-sous-Bois, France). Hydrogen peroxide solution (30% v/v), iron (II) sulfate heptahydrate (99.5%) and anhydrous sodium sulfite were from Merck (Darmstadt, Germany). Sulfuric acid (96%) from VWR BDH Prolabo (Fontenay-sous-Bois, France) and sodium hydroxide (98.7%) from José Manuel Gomes dos Santos, Lda (Odivelas, Portugal) were utilized.
Potassium ferrioxalate from Strem Chemicals (Newburyport-Massachusetts, USA), 1,10-Phenantroline analytical reagent from VWR BDH Prolabo (Fontenay-sous-Bois, France), sodium acetate (≥99.0%) from sigma-Aldrich (St. Louis, USA) and Vert Cibacrone T3G-E from Ciba-Geigy (Delhi, India) were used in actinometry experiments.

7.2.2 Standard solutions

Stock solutions of BDE-100 were prepared by evaporating an appropriate amount of the analytical standard under a gentle nitrogen flow. Then, the residue was redissolved in acetonitrile. Aqueous standard solutions of BDE-100 (50 μg/L) were prepared daily by evaporating an appropriate amount of stock solution, under nitrogen flow, and resuspending the residue in 25 mL of distilled water at pH 3.

7.2.3 Photocatalytic reactor and light source

The radiation source was a 150 W medium-pressure mercury vapor lamp (Heraeus TQ-150), whose emission spectrum is shown in Figure 7.1.

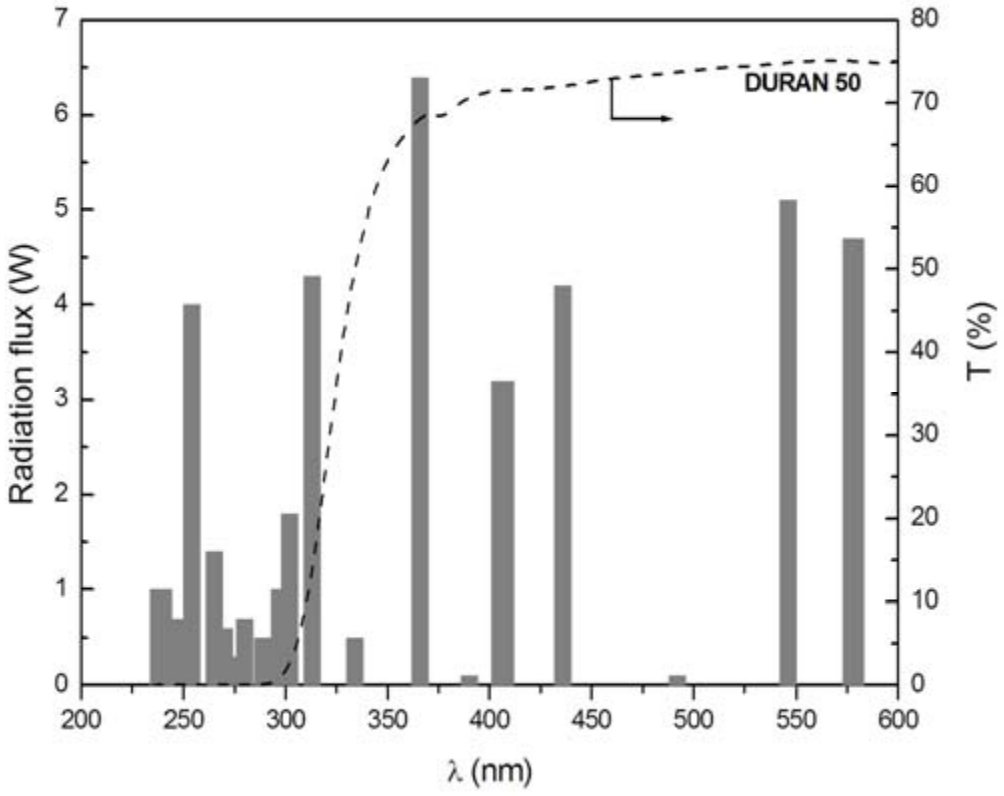

Figure 7.1. Emission spectrum of a 150 W medium-pressure mercury vapor lamp from Heraeus.

This lamp has a polychromatic emission in the range from 250 to 650 nm wavelength, but the most important emission line is at 366 nm. The intensity of incident light was measured for this wavelength (366 nm) by actinometry [4]. The potassium ferrioxalate is the most commonly used chemical actinometer to determine the photonic flux of a radiation source emitting in the UV spectral region [5]. For that reason, this actinometer was selected over others for the experiments.

A potassium ferrioxalate solution ($K_3Fe(C_2O_4)_3$) with a concentration of 6×10^{-3} M was prepared in 10% H_2SO_4 1 N. After that, 25 mL (V_1) of this solution was put in each of two 50 mL polypropylene (PP) flasks. One flask was maintained in dark conditions and the other was submitted to irradiation for 5 min. One should note that the lamp was switched on before 15 min of the irradiation period to guarantee constant photonic flux. After 5

min, 1 mL (V_2) of the irradiated solution was added to a 25 mL (V_3) volumetric flask, where 2 mL of 1,10-phenantroline (1 g/L) and 1 mL of a buffer constituted by sodium acetate (0.6 N) and sulfuric acid (0.36 N) were already placed. The same procedure was done for the non-irradiated solution. To ensure complete complexation between Fe^{2+} ions and 1,10-Phenantroline ($Fe(phen)_3^{2+}$), the final samples were left for one hour in the dark, after which the absorbances at 510 nm were measured by molecular absorption spectroscopy. The number of Fe^{2+} ions formed during the irradiation process is given by equation 7.1 [6]:

$$N_{Fe^{2+}} = \frac{N_A V_1 V_3 \Delta Abs_{510}}{10^3 V_2 \varepsilon_{510} b} \qquad 7.1$$

where N_A is the Avogadro´s constant, ΔAbs_{510} corresponds to the optical difference in absorbance between the irradiated solution and that taken in the dark at 510 nm, ε_{510} is the molar absorptivity for the complex $Fe(phen)_3^{2+}$ at 510 nm, b is the path length in cm, V_1 is the irradiated volume, V_2 is the aliquot of the irradiated solution taken for the determination of the ferrous ions (Fe^{2+}) and V_3 is the final volume after complexation with 1,10-phenantroline (all in cm^3).

The photonic flux (φ) emitted by the TQ-150 W lamp at 366 nm is determined by equation 7.2 [6]:

$$\varphi = \frac{N_{Fe^{2+}}}{\phi_\lambda t} \qquad 7.2$$

where ϕ_λ is the quantum yield of Fe^{2+} production at the irradiation wavelength of 366 nm and t is the time of irradiation.

The dependence of the quantum yield of production of Fe^{2+} from potassium ferrioxalate on the irradiation wavelength has been extensively studied. The recommended value for 366 nm, obtained by different methods, is 1.21 [7].

When necessary, the photon flux was controlled by using a quartz-glass jacket around the light source with dye solutions of different concentrations flowing inside of it. This strategy was already adopted by other authors [8].

7.2.4 Degradation experiments

7.2.4.1 Photolysis

BDE-100 aqueous solutions of 50 μg/L (25 mL) were irradiated in 50 mL PP flasks placed 5 cm from the lamp. The experiments were made at room temperature (25±3 °C) under agitation. The irradiation procedure was repeated as many times as the necessary to obtain the required irradiation times for each sample and build up the degradation kinetic curves. After the irradiation period, the aqueous samples (25 mL) were extracted with 1 mL of acetonitrile and 80 μL of chlorobenzene, according to the dispersive liquid-liquid microextraction (DLLME) procedure explained before (Chapter 6). The mixture was centrifuged for 5 min at 4000 rpm in a Hettich Rotofix 32A Centrifuge. The sedimented-phase was collected with a syringe and was analyzed by gas chromatography-mass spectrometry (GC-MS).

7.2.4.2 Classic dark Fenton

A stock solution of Fe^{2+} (7.5×10^{-3} M) was prepared by dissolving an appropriate amount of $FeSO_4$ in water, adjusting the pH to 3. This solution was re-prepared on a weekly base. A stock solution of H_2O_2 (2.5×10^{-1} M) was also prepared by diluting a certain volume of the commercial reagent in distilled water. Since hydrogen peroxide is very unstable, the stock solution was divided in small doses and each one was stored in a separated amber glass flask at 2-4 °C. Each flask was only open once and for a unique experiment.

The Fenton's reaction experiments were carried out in 50 mL PP flasks, at room temperature (25±3 °C) and in the dark. For that, appropriate amounts of oxidant (H_2O_2) and catalyst (Fe^{2+}) were added to 25 mL of BDE-100 aqueous solutions (50 μg/L; pH= 3.0) in 50 mL PP tubes. The reaction proceeded under agitation for a preset time, after which an excess of Na_2SO_3 was added to quench the degradation process; this substance reacts instantaneously with the remaining H_2O_2 stopping the degradation process. Afterwards, samples from different reaction times were extracted by DLLME and injected in the GC-MS.

7.2.4.3 Photo-Fenton

For photo-Fenton experiments, 25 mL of a BDE-100 aqueous solution (50 μg/L; pH= 3.0) was put in a 50 mL PP flask. Then, appropriate amounts of H_2O_2 and $FeSO_4$ stock solutions were added to the flask and the irradiation of the solution started (t=0). The reaction proceeds for a certain period under agitation and at room temperature (25±3 °C). The procedure was repeated for different times of irradiation in order to have a degradation curve for BDE-100 along time.

Finally, the irradiated samples were submitted to DLLME after quenching the reaction by the addition of an excess of Na_2SO_3. The final extract was analyzed by GC-MS for BDE-100 monitoring purposes.

7.2.5 Analytical methods

Samples from degradation experiments were analyzed by a Varian 4000 GC-MS Chromatograph after DLLME extraction procedure. The mass spectrometer was operated in the electronic impact ionization (EI) mode. The temperatures for the injector, trap, transfer line and manifold were held respectively at 290 °C, 200 °C, 250 °C and 50 °C. A DB-5MS column was used (30 m x 0.25 mm ID x 0.25 μm film thickness – Walnut Creek, CA, USA) and the oven temperature was programmed as follows: initial 60 °C for 2 min, rate of 30 °C/min to 250 °C, then 5 °C/min until 300 °C and held for 8 min. The injected volume was 1 μL and a 701N Hamilton syringe was used. Carrier gas was Helium (99.9999 %) at 1 mL/min flowrate. The quantifier and qualifier ions were *m/z* 406+566 and *m/z* 564, respectively, in the selected ion-monitoring mode (SIM). The identification of BDE-100 was done by comparison of the retention time with that obtained for standard solution directly injected.

Samples from actinometry experiments were analysed in a JASCO V-530 UV-Vis Spectrophotometer.

7.3 Results and discussion

7.3.1 Degradation by photolysis

The degradation of BDE-100 in water by photolysis was studied at different light intensities. First, solutions of BDE-100 (50 μg/L) were directly irradiated by a 150 W medium-pressure vapor lamp placed inside a quartz jacket, where water circulation was

promoted by a Huber Thermostatic bath (Polystat CC1 unit). Then, the water flowing through the quartz jacket was substituted by two different concentrations of a dye (Vert Cibacrone T3G-E).

The light intensity, i.e. the photonic flux for the three situations was measured at 366 nm by potassium ferrioxalate actinometry, as described in section 7.2.3. The radiation intensities are listed in Table 7.1.

Table 7.1. Intensity of incident light, for different dye concentrations, determined by potassium ferrioxalate actinometry at 366 nm.

	Photonic flux	
Dye concentration (mg/L)	photons/s	Einstein/s
0	9.7×10^{17}	1.6×10^{-6}
270	4.1×10^{16}	6.8×10^{-8}
930	7.8×10^{14}	1.3×10^{-9}

As can be checked from Table 7.1, the Vert Cibacrone T3G-E has the ability of absorbing light, reducing the intensity of the incident radiation.

The effect of the photonic flux on the BDE-100 degradation in water is depicted in Figure 7.2.

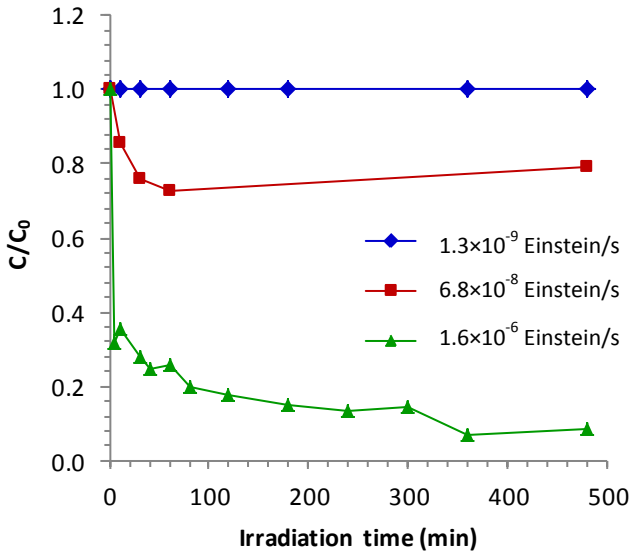

Figure 7.2. BDE-100 degradation in water by photolysis using different light intensities ($[BDE\text{-}100]_0$= 50 μg/L; pH_0= 3.0 and T=25±3 °C).

As demonstrated in Figure 7.2, the intensity of the light is an important factor on the BDE-100 degradation by this methodology. None BDE-100 degradation was attained for a photonic flux of 1.3×10^{-9} Einstein/s, which means that the dye concentration used in the experiment was high enough to absorb the remaining radiation that could lead to BDE-100 degradation. For the maximum light intensity (lower dye concentration in the jacket), nearly 80% of BDE-100 was degraded after 80 min of reaction, reaching 92% after 6 h. However, a very quick decay was observed in only 5 min of reaction time.

Up to the author knowledge, there are only three studies about degradation of BDE-100 in liquid phase [1-3]. The first study was published in 2005 and was focused in the degradation of six polybrominated diphenyl ethers (BDEs 7, 28, 47, 66, 100 and 209) with zerovalent iron [3]. It was shown that around 65% of the initial BDE-100 concentration was converted after only 40 days of reaction ($[BDE\text{-}100]_0$ = 50 mg/L in ethyl acetate, Iron = 5 g/mL, T = 30 ºC) [3]. Later, Fang et al. (2008) studied the degradation of other six PBDE congeners (BDEs 28, 47, 99, 100, 153 and 183) in hexane under ultraviolet irradiation [1]. It was reported that 55% of the initial BDE-100 was degraded after 8 h of irradiation ($[BDE\text{-}100]_0$ = 10 μg/L in hexane, 500 W mercury lamp) [1]. They also demonstrated that BDE-100 exhibits lower photodegradation rates than the expected ones due to its bromine substitution pattern [1]. In 2012, Sanchez-Prado et al. investigated the degradation of BDE-100 in ice solid samples and in aqueous solutions (containing small amounts of isooctane) using an artificial UV light source [2]. Concerning the aqueous solutions, 79% of BDE-100 degradation was recorded after exposition to UV light during 10 min ($[BDE\text{-}100]_0$ = 5 μg/L in ethyl acetate, two 8 W low-pressure mercury lamps – 254 nm) [2].

As demonstrated, besides the very scarce information concerning the BDE-100 degradation in liquid phase, the results from the available studies are very distinct. The differences could be attributed to the nature of the removal technology applied and to the different reaction conditions implemented, including UV light sources, initial concentrations of BDE-100 and photolytic matrices in photodegradation studies. However, it can be advanced that the degradation methodology proposed here conducts to attractive results in terms of BDE-100 degradation rates.

Even so, the great advantage of this study over the others available in the literature is the fact that this is applicable to waters without the presence of organic solvents. The others

were based on the degradation of BDE-100 in organic solvents [1] or in aqueous solutions prepared from organic solvent solutions [2, 3]. This is particularly important, namely in water contamination events.

As occurred with BDE-100, dye molecules may also be degraded by exposition to the light. For that reason, the dye concentration was monitoring along the BDE-100 degradation process to ensure that the intensity of light was as constant as possible. Where necessary, the dye concentration was adjusted to the desired value adding an appropriate amount of dye. Figure 7.3 shows the evolution of the dye concentration during the reaction.

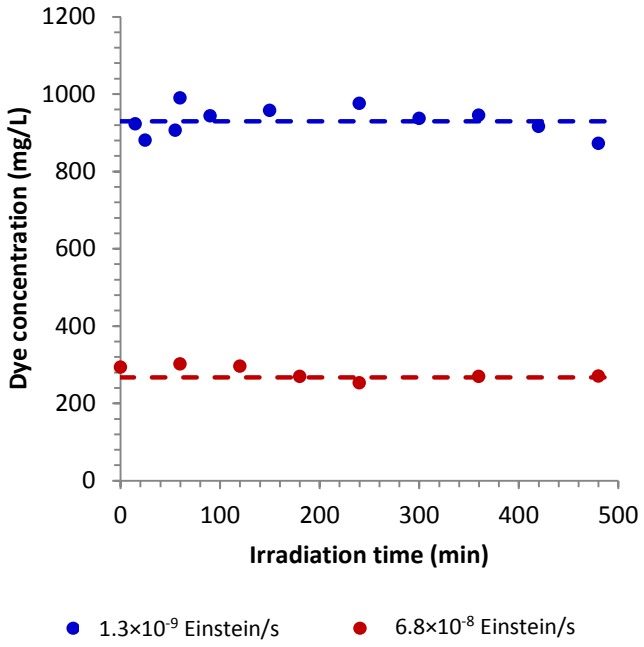

Figure 7.3. Dye concentration along the degradation of BDE-100 by photolysis.

As can be checked from Figure 7.3, the dye concentrations were approximately constant during the degradation experiments so, a constant photonic flux was ensured.

7.3.2 Degradation by Fenton and photo-Fenton

To accelerate the process, the suitability of using a photo-Fenton methodology to degrade BDE-100 in waters was evaluated. As referred previously in the introduction section (Chapter 1), no other study was found in the literature concerning the application of photo-Fenton, or even, classic Fenton, on the degradation of PBDEs in waters.

Due to the lack of information, the starting amounts of H_2O_2 and Fe^{2+} used in the photo-Fenton experiments were estimated by a relation established with other chemical well

studied by our research team (Paraquat dichloride – PQ). PQ was effectively degraded in water by classic Fenton under the following conditions: $[Fe^{2+}]_0 = 5.0\times10^{-4}$ M and $[H_2O_2]_0 = 1.6\times10^{-2}$ M (Chapter 5). For constant ratios of [compound]/$[Fe^{2+}]$ and [compound]/$[H_2O_2]$, it was estimated that the concentrations of Fe^{2+} and H_2O_2 should be 1×10^{-7} M and 4×10^{-6} M, respectively, for an initial BDE-100 concentration of 50 μg/L. Since the degradation profile is highly dependent on the chemical and also on its initial concentration (beyond other factors), a 3000× over estimation was applied to the above written concentrations. The initial estimated values for the concentrations of Fe^{2+} and H_2O_2 were 3×10^{-6} M and 1×10^{-4} M, respectively.

Figure 7.4 illustrates the BDE-100 degradation profile in water by photolysis ($[BDE\text{-}100]_0$ = 50 μg/L, 1.6×10^{-6} Einstein/s) and photo-Fenton ($[BDE\text{-}100]_0$ = 50 μg/L, $[H_2O_2]_0 = 1\times10^{-4}$ M; $[Fe^{2+}]_0 = 3\times10^{-6}$ M, 1.6×10^{-6} Einstein/s) processes.

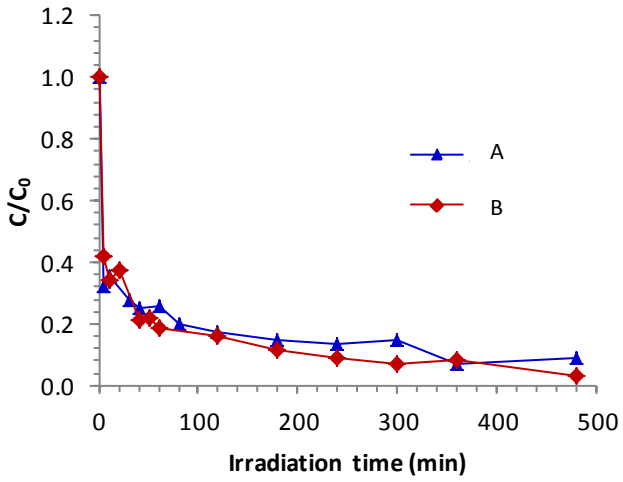

Figure 7.4. BDE-100 degradation in water by photolysis (A – $[BDE\text{-}100]_0$ = 50 μg/L, 1.6×10^{-6} Einstein/s) and photo-Fenton (B – $[BDE\text{-}100]_0$ = 50 μg/L, $[H_2O_2]_0 = 1\times10^{-4}$ M, $[Fe^{2+}]_0 = 3\times10^{-6}$ M, 1.6×10^{-6} Einstein/s).

As displayed in Figure 7.4, no significant differences were obtained for the degradation of BDE-100 in water by the two processes. Two reasons may be pointed out to justify that behavior: the light intensity is too strong to observe any difference caused by the additional use of peroxide and Fe^{2+} doses; or none BDE-100 degradation results by the action of such H_2O_2 and Fe^{2+} amounts. So, it was decided to double the amounts of H_2O_2 and Fe^{2+} in the photo-Fenton process (Figure 7.5).

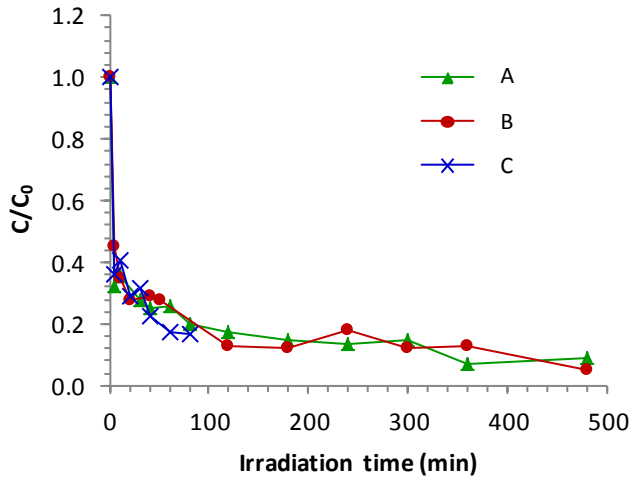

Figure 7.5. BDE-100 degradation in water by photolysis (A – $[BDE\text{-}100]_0$ = 50 μg/L, 1.6×10^{-6} Einstein/s) and photo-Fenton (B – $[BDE\text{-}100]_0$ = 50 μg/L, $[H_2O_2]_0 = 2\times10^{-4}$ M, $[Fe^{2+}]_0 = 3\times10^{-6}$ M, 1.6×10^{-6} Einstein/s; C – $[BDE\text{-}100]_0$ = 50 μg/L; $[H_2O_2]_0 = 1\times10^{-4}$ M, $[Fe^{2+}]_0 = 6\times10^{-6}$ M, 1.6×10^{-6} Einstein/s).

Again, even at double concentrations, no effects were observed in the BDE-100 degradation effectiveness by photo-Fenton. Indeed, a classic Fenton experiment was performed at nearly the same conditions as the implemented in photo-Fenton methodologies ($[BDE\text{-}100]_0$ = 50 μg/L, $[H_2O_2]_0 = 2\times10^{-4}$ M, $[Fe^{2+}]_0 = 3\times10^{-6}$ M) and none BDE-100 degradation was attained (data not shown). This means that higher concentrations of oxidant and catalyst must be taken into account to study the influence of the main parameters on the overall process and to implement an effective degradation approach for BDE-100 in waters. The possibility of the occurrence of scavenging effects due to the use of excessive oxidant and catalyst doses is another possible explanation for these results, which has still to be clarified.

7.4 Conclusions

The treatment of waters contaminated with concentrations of BDE-100 close to the limit of solubility in water was ensured by direct photolysis. As expected, the degradation efficiency is highly dependent on the intensity of the radiation. For the maximum light intensity tested (1.6×10^{-6} Einstein/s), nearly 68% of BDE-100 was degraded after 5 min of reaction reaching 92% after 6 h. This result is very attractive when compared to those

achieved in the few existing studies about BDE-100 degradation in liquid phases. On the other hand, it was tested for the first time the degradation of BDE-100 in waters by photo-Fenton. Additional experiments must be done to obtain conclusive results.

7.5 References

[1] L. Fang, J. Huang, G. Yu and L. Wang, Photochemical degradation of six polybrominated diphenyl ether congeners under ultraviolet irradiation in hexane, Chemosphere 71 (2008) 258-267.

[2] L. Sanchez-Prado, K. Kalafata, S. Risticevic, J. Pawliszyn, M. Lores, M. Llompart, N. Kalogerakis and E. Psillakis, Ice photolysis of 2,2',4,4',6-pentabromodiphenyl ether (BDE-100): Laboratory investigations using solid phase microextraction, Anal. Chim. Acta 742 (2012) 90-96.

[3] Y.-S. Keum and Q.X. Li, Reductive Debromination of Polybrominated Diphenyl Ethers by Zerovalent Iron, Environ. Sci. Technol. 39 (2005) 2280-2286.

[4] Chemical Actinometry, in: M. Montalti, A. Credi, L. Prodi, M.T. Gandolfi (Eds.) Handbook of Photochemistry, CRC Press, 2006, pp. 601-616.

[5] H.J. Kuhn, S.E. Braslavsky and R. Schmidt, Chemical actinometry (IUPAC technical report), Pure Appl. Chem. 76 (2004) 2105-2146.

[6] Cláudia Sofia Castro Gomes da Silva, Processos avançados de oxidação fotoquímica na descoloração de soluções aquosas fortemente coradas, Tese de Mestrado, Faculdade de Engenharia da Universidade do Porto, 2003.

[7] C.G. Hatchard and C.A. Parker, A New Sensitive Chemical Actinometer. II. Potassium Ferrioxalate as a Standard Chemical Actinometer, Proc. R. Soc. Lond. A 235 (1956) 518-536.

[8] C.G. Silva and J.L. Faria, Effect of key operational parameters on the photocatalytic oxidation of phenol by nanocrystalline sol-gel TiO2 under UV irradiation, J. Mol. Catal. A: Chem. 305 (2009) 147-154.

PART IV. GENERAL CONCLUSIONS AND FUTURE WORK

8 Conclusions

The knowledge obtained during this work aimed to contribute to the definition of an appropriate strategy for rapidly restore the use of drinking water networks after a deliberate or accidental chemical contamination.

The work was focused in two chemicals (paraquat and BDE-100) which were considered as potential candidates of being used in the framework of EU project SecurEau.

Since the drinking water should be the first matrix to suffer the effects of the contamination event, different analytical methodologies were developed and validated in order to identity and quantify the target compounds in this matrix.

For paraquat, three analytical methodologies were implemented due to the need: to have a quick response in emergency situations, as occurs when there is a suspicion of contamination of drinking water networks (DI-LC-DAD); to ensure that PQ concentration in water is below the limit recommended by European Union for pesticides (SPE-LC-DAD) and to the need of an unequivocal identification of PQ and its degradation by-products after treatment of contaminated waters, e.g. with Fenton's reagent (DI-LC-MS). Concerning the DI-LC-DAD method, it was developed for relatively high PQ concentrations (mg/L level), as expected to be found in contamination events. The DI-LC-DAD method proved to be accurate in different circumstances which may represent realistic scenarios in drinking water networks: in the presence of other species or compounds resulting from the contact of the water with deposits and cells, from the PQ commercial formulation Gramoxone (in case of being used as contamination agent instead of the analytical standard) and from other types of water. Additionally, it was also shown that this method is reliable for analyses of PQ in samples from decontamination procedures by Fenton's reagent. Indeed, under the optimum conditions to degrade PQ in waters by Fenton's reagent ($[Fe^{2+}]_0 = 5.0\times10^{-4}$ M, $[H_2O_2]_0 = 1.6\times10^{-2}$ M and $[Na_2SO_3] = 9.6\times10^{-2}$ M; Chapter 5), no effect of Fenton's species (Fe(II), H_2O_2 and Na_2SO_3) were noticed on the PQ quantification by DI-LC-DAD. The limit of detection of this method was of 10 μg/L of PQ, which is much lower than other similar alternatives published, and the global uncertainty, evaluated by *bottom-up* approach, was below 13% for the most part of the calibration range. SPE-LC-DAD, designed for the screening of low PQ concentrations in water, presents a limit of detection of 0.04 μg/L, which is below the value recommended by

European Union (0.1 μg/L). DI-LC-MS method proved to be reliable for confirmation of PQ in waters at concentrations above 20 μg/L. Global uncertainties of 11 and 6% were obtained for PQ concentrations higher than 5 μg/L (linearity of 0.1 to 50 μg/L of PQ) by SPE-LC-DAD and higher than 1 mg/L (linearity of 0.1 to 10 mg/L of PQ) by DI-LC-MS, respectively. All methods proved to be precise, accurate and suitable for the purpose that they were designed.

Concerning the other chemical, BDE-100, only one analytical methodology was developed by DLLME-GC-MS. Herein, it was not possible to develop an analytical methodology for high concentrations of BDE-100 and using classic equipment since its solubility in water is extremely small and its quantification requires more sensitive equipment or extraction procedures. Despite of this, a simple and quick extraction procedure, such as DLLME extraction was selected over others to diminish as much as possible the time of analysis for this method. Optimization of DLLME was performed for BDE-100 and recoveries ranged from 91 to 107%. Although the method was only optimized and validated for BDE-100, it proved suitable for the quantification and identification of other environmentally abundant PBDEs (BDE 28, 47, 85, 99, 153, 154 and 183). Similar extraction recoveries were achieved and the precision remained satisfactory (average 11%) even when mix standards with all PBDEs were analyzed. Limits of quantification between 2 ng/L (BDE-100) and 113 ng/L (BDE-183) were reported for this cheap, fast and easy method.

Another point that should not be neglected is the interaction of the chemical compounds with the deposits formed in the pipe walls. Indeed, these interactions will define the accumulation and dispersion of the contamination along the drinking water networks. The adsorption of PQ in three different deposits (S2, S3 and S4) representative of those found in drinking water distribution systems was studied. The PQ adsorption on such deposits is a relatively slow process (it takes days to reach the equilibrium) and follows a pseudo-second order kinetic model. The adsorption capacities depend on the PQ interactions with the main metal ions present in each deposit and on their textural properties. PQ competes with Ca(II) for the same binding sites and, for that reason, S3 deposit (calcium rich) has low PQ adsorption capacity. On the other hand, the presence of Fe(II) and Mn (II) in the deposits improves the PQ adsorption capacity because it has the ability to form complexes with these two metal ions. Additionally, the presence of phosphate ions leads to a more negative adsorbent surface facilitating the adsorption of

positively charged compounds like PQ. Maximum PQ adsorption Langmuir capacities of 5.7, 11 and 0.40 mg/g were achieved at 20 ºC for S2 (iron rich deposit), S3 (iron rich deposit) and S4 samples (calcium rich deposit), respectively. It was also found that deposits S2 (brown deposit) and S3 (tubercle deposit) can be good adsorbents, and potential alternatives to other expensive materials, for the treatment of PQ contaminated waters. Concerning the desorption process, relatively high PQ desorption percentages were attained when $CaCl_2$ solution was used as extraction solvent in S3 (51%) and S4 (39%) contaminated samples, which means that the interaction between PQ and deposits is not so strong as those reported for soils and clays. On the other hand, taking into account the contact time needed to reach significant PQ adsorption amounts and the extreme conditions employed (high adsorbent dosage and batch conditions), it may be advanced that, in case of a drinking water contamination, it is unlikely that PQ would adsorb to the deposits attached in the pipe networks since here, much lower contact time and surface area available for adsorption are observed. However, other situations should be taken into account. In fact, in case of stagnancy of the fluid for a very long period of time (in tanks or pipes in case of a consumption break) or low water flow (e.g. during the night), this compound may adsorb on pipe deposits. On the other hand, adsorption on loose deposits that are transported with the flowing water is much more likely to occur.

Another objective of this thesis was to develop an analytical method for PQ quantification in such deposits. This was a challenging task since it is a completely new research topic and the method should deal with the problem of a great heterogeneity of the matrix of interest. A simple and inexpensive method was developed and comprises a fast and easy extraction step using a saturated ammonium chloride solution. A limit of detection of 0.1 μgPQ/gS3 was obtained for PQ-S3 system with the expanded uncertainty ranging from 10-54% for concentrations between 193 and 5 μgPQ/gS3, respectively. The application of this method to the quantification of PQ in the other two representative deposits (S2 and S4) implies the consideration of the correspondent extraction percentage. The method also proved to be suitable for the quantification of diquat in the S3 deposit.

Finally, degradation experiments were performed for both chemicals in water, ultimately aiming to contribute to the implementation of efficient cleaning procedures for the treatment of contaminated waters. Concerning PQ, the dark classic Fenton was successfully implemented to degrade the pesticide in waters. Under the optimum

conditions (T =30 °C, $[Fe^{2+}]_0$ = 5.0×10^{-4} M, $[H_2O_2]_0$ = 1.6×10^{-2} M, and pH_0 = 3.0, for $[PQ]_0$ = 100 mg/L) complete PQ degradation and 40% of mineralization are reached after 4 h of reaction. Additionally, it was proved that the final effluent is less toxic than the original one. For the same conditions, the PQ commercial formulation (Gramoxone) exhibited lower degradation performance due to the presence of other organic compounds. A semi-empirical model was also developed to predict the PQ degradation profile under selected conditions. This simple model was statistically checked and validated fitting quite well the experimental data in a wide range of conditions. The photo-Fenton process proved to gather some advantages over classic Fenton in the treatment of waters contaminated with PQ: much higher degradation rate and 96% of mineralization after 1 h of reaction are reached.

The treatment of waters contaminated with BDE-100 concentrations close to its water solubility, and without using organic solvents, was ensured by direct photolysis. Attractive results were achieved by using this technology since nearly 68% of BDE-100 was degraded after 5 min of reaction reaching 92% after 6 h ($[BDE\text{-}100]_0$ = 50 μg/L and 1.6×10^{-6} Einstein/s). Photo-Fenton methodology was, for the first time, tested for the treatment of waters contaminated with BDE-100, but additional experiments must be done to obtain conclusive results.

In sum, this work allowed the development of analytical methodologies for quantification and identification of two key chemicals in waters in emergency situations, as those that may occur when there is a suspicion of contamination in water networks. It also allowed the validation and implementation of an analytical methodology for PQ quantification in deposits formed in the pipe walls, which was never ever published in the open scientific literature, even for other chemicals. This thesis also aimed at contributing to better understand the fate of PQ in the drinking water networks. Indeed, it can be advanced that if a deliberate or accidental contamination occurs with such pesticide, the main concern will be related to the drinking water decontamination. Both classic Fenton and photo-Fenton processes proved to be feasible and effective advanced oxidation technologies for the treatment of waters polluted with PQ. The valorization of the iron-rich deposits from drinking water networks as adsorbents for the treatment of waters contaminated with PQ is another remarkable contribution of this work, as well as their potential use as catalysts in these advanced oxidation processes.

9 Future work

Much more has still to be done concerning surveillance and protection procedures against deliberate or accidental contamination of drinking water networks. Indeed, any contribution for this wide, diverse and delicate research area seems to be always insufficient to answer all the questions addressed to real attack situations on our precious drinking water.

So, I will indicate only some suggestions for future work that result from this thesis work:

- To study the interaction between BDE-100 and the deposits from drinking water networks;
- To develop an analytical methodology to quantify BDE-100 in such deposits;
- To evaluate the interaction between the two chemicals considered and biofilms;
- To develop analytical methods for the quantification of both chemicals in biofilms;
- To optimize the degradation of BDE-100 in water by photo-Fenton process;
- To identify degradation by-products resulting from the degradation of BDE-100 by photolysis and photo-Fenton processes;
- To extend this study to other chemicals;
- To design and implement a methodology using sensors able to provide an early warning of intrusion.

ANNEX

Annex I – Estimation of the global uncertainty associated to the analytical results

Global uncertainty (U) is expressed as follows [1]:

$$U = \sqrt{U1^2 + U2^2 + U3^2 + U4^2}$$

where,

$U1$ is the uncertainty associated with the preparation of the standards (it was estimated using the error propagation law for the different dilution steps from the stock standard solution):

$$U1 = U_{st} = \sqrt{\sum_i \left(\frac{\Delta mi}{mi} \right)}$$

Δ*mi* – error associated to the measurement equipment; *mi* – measured value.

$U2$ is the uncertainty associated with the calibration curve (it was calculated for the different concentration levels of the standards):

$$U2 = \frac{sx_o}{x_o} = \frac{1}{x_o} \frac{s_{y/x}}{a} \sqrt{\frac{1}{m} + \frac{1}{n} + \frac{(yo - \bar{y})^2}{a^2 \sum_i (x_i - \bar{x})^2}}$$

sx_o – standard deviation of the concentration; x_o – concentration; a – slope; m – number of replicates performed; n – number of standards to build the calibration curve; y_o – *y* values calculated by the calibration curve from *x* values; $\bar{y}$ – average of y_i values (experimental values); x_i – concentration of standards used in the calibration curve; $\bar{x}$ – average of x_i values.

$U3$ is the uncertainty associated with the precision of the extraction and also of the chromatographic method (it was estimated as the worse result of RSD % for each concentration level):

$$U3 = \frac{s}{y_{med}\sqrt{n}}$$

s – standard deviation of precision assays; y_{med} – average of the area values obtained for each concentration; n – number of assays.

$U4$ is the uncertainty associated with the accuracy (it was calculated as the average % of recovery obtained within all the experiments):

$$U4 = \frac{s(\eta)}{\sqrt{n}}$$

$s(\eta)$ – relative standard deviation of the average percent recovery; n – number of assays.

References

[1] S.L.R. Ellison, M. Rosslein and A. Williams, *Eurachem/ Citac Guide- Quantification uncertainty in analytical measurement*, EURACHEM/ CITAC, UK, 2000.